



TOGETHER
for a sustainable future

OCCASION

This publication has been made available to the public on the occasion of the 50th anniversary of the United Nations Industrial Development Organisation.



TOGETHER
for a sustainable future

DISCLAIMER

This document has been produced without formal United Nations editing. The designations employed and the presentation of the material in this document do not imply the expression of any opinion whatsoever on the part of the Secretariat of the United Nations Industrial Development Organization (UNIDO) concerning the legal status of any country, territory, city or area or of its authorities, or concerning the delimitation of its frontiers or boundaries, or its economic system or degree of development. Designations such as “developed”, “industrialized” and “developing” are intended for statistical convenience and do not necessarily express a judgment about the stage reached by a particular country or area in the development process. Mention of firm names or commercial products does not constitute an endorsement by UNIDO.

FAIR USE POLICY

Any part of this publication may be quoted and referenced for educational and research purposes without additional permission from UNIDO. However, those who make use of quoting and referencing this publication are requested to follow the Fair Use Policy of giving due credit to UNIDO.

CONTACT

Please contact publications@unido.org for further information concerning UNIDO publications.

For more information about UNIDO, please visit us at www.unido.org

RESTRICTED

17235

DP/ID/SER.A/1122
23 January 1989
ORIGINAL: ENGLISH

CHINA NATIONAL TECHNICAL DEVELOPMENT CENTRE OF GEARS

DP/CPR/85/015/11-01

THE PEOPLE'S REPUBLIC OF CHINA

Technical report : Rating, optimum design and computer aided
design of gears and gear systems *

Prepared for the Government of the People's Republic of China
by the United Nations Industrial Development Organization,
acting as executing Agency for the United Nations Development Programme

Based on the work of E. William Jones
UNIDO Expert

Backstopping officer : H. Seidel, Engineering Industries Branch

United Nations Industrial Development Organization
Vienna

* This document has not been edited.

TABLE OF CONTENTS

	page
1. INTRODUCTION	1
1. LECTURES SERIES	1
3. ORGANIZATION OF ZRIME	5
4. FACILITIES FOR GEAR WORK	7
5. RESEARCH AND TECHNICAL SERVICE	16
6. CONSULTING ACTIVITIES	17
7. VISIT TO SICHUAN GEARBOX PLANT	18
8. CONCLUSIONS	19
APPENDIX : Participants in lectures on Gears CAD	21
LECTURE 1 : Computer aided design : steady state and kinematic simulation	25
LECTURE 2 : Predicting the performance of dynamic mechanical systems	77
LECTURE 3 : Torsional vibrations	129
LECTURE 4 : An introduction to the finite Element method	171
LECTURE 5 : Metal failures in transmissions	209
LECTURE 6 : A review of AGMA 218.01, AGMA standard for rating the pitting resistance and bending strength of spur and helical involute gear teeth	226
LECTURE 7 : Gear CAD	235

1. INTRODUCTION:

The purpose of this project is to introduce the status and trends in gear rating, optimum design and the computer aided design of gears and gear systems and to provide assistance in the development of a computer aided design system for high speed gears and gear systems. This will be accomplished by presenting a series of lectures to engineers and educators in China, by providing assistance to engineers developing a CAD system for gears , and by suggesting advisory opinions on aspects of research works, gear rating and optimum design.

2. LECTURE SERIES:

The lecture series to be given at ZRIME consists of seven different, but related, topics. The titles of the lectures are:

- A. Computer Aided Design: Steady State and Kinematic Simulation
- B. Predicting the Performance of Dynamic Mechanical Systems
- C. Torsional vibrations
- D. An Introduction to the Finite Element Method
- E. Metal Failures in Transmissions
- F. A Review of AGMA 218.01 , AGMA Standard for Rating the Pitting Resistance and Bending Strength of Spur and Helical Involute Gear Teeth
- G. Gear CAD

After the lectures are completed, demonstrations and training sessions are provided for three groups of about 20 persons. These sessions use an IBM-XT 286 computer to provide experience with the following software:

A. Gear Design Software by Geartech Software, Inc.:

1. GEARCALC:

Evaluates maximum capacity gear set with minimum volume and weight. Allows designer to select tooth numbers and addendum modification based on the application.

2. AGMA 218.01 :

Verifies compressive stress, bending stress, and gear life for the design from GEARCALC.

3. SCORING+:

Verifies the probably of wear and scoring for the design from GEARCALC by evaluating flash temperatures, sliding velocities, and elasto-hydrodynamic film thickness.

B. Mini TK solver:

Solves linear and non-linear systems of equations. It is a mathematical "tool box" from Universal Technical Systems, Inc.

C. GEARFORC:

Evaluates gear tooth forces and bearing reactions for a shaft supported by two bearings and carrying any number of external gears.

D. FOURBAR:

Evaluates the positions and velocities of points on a fourbar mechanism. Graphical output of the positions is given to illustrate setup of graphics code.

E. INERTIA:

Evaluates the mass moment of inertia, weight, and torsional spring rate for a stepped rotor system.

F. VEHICLE SIMULATION:

Evaluates the displacement versus time of a vehicle dynamic model with a three speed, shiftable transmission.

G. OPTIMUM:

Optimization method for multivariable, non-linear, constrained problem using the complex method.

This program is a modification of Dr.G.H.Michaud's work to evaluate sensitivity studies and provide graphical output. It evaluates the variables to give the maximum or the minimum value of the objective function and the graphical sensitivity study shows how the optimum value changes with each variable.

H. FRAME:

Evaluates the reactions and deflections of a structure using the plane frame element. The frame finite element has three degrees of freedom at each of its two nodes: X, Y and θ .

One major theme of the first four lectures is to provide a course in computer aided design methods including modeling of dynamic systems.

Most of the examples are selected for gear systems in order to show the relevance. The torsional vibration analysis and finite element analysis are important CAD methods. An example evaluating the internal tooth dynamics is not explicitly presented, but the numerical integration method, the process of creating an equivalent mass-elastic system, and the FEM for evaluating the varying tooth stiffness are covered. Hence, the fundamentals for evaluating internal gear tooth forces are explained.

One major theme of the last three lectures is to show the development of the AGMA 218.01 standard for gear design relative to fundamentals and the experiences by the American gear Manufacturing Association's members.

The lectures were attended by 72 engineers from 34 different industries and institutions representing all areas of the nation. Their names and affiliations are listed in Appendix A. This list indicates the broad interest in this project. The three interpreters were experts:

Mr. Jia Sun
Senior Engineer of Materials, Hot Processing
Department
Zhengzhou Research Institute of Mechanical
Engineering

Vice Director

Gear Research Institute

Mechanical Engineering Department,

Shanghai University of Technology

Professor Zongying Ou

Dalian Institute of Technology

Department of Mechanical Engineering

Director of Mechanical Design Division

A copy of these lectures is attached to this report for reference.

3. ORGANIZATION OF ZRIME:

The Zhengzhou Research Institute of Mechanical Engineering has three research divisions and one design division:

A. Mechanical Strength and Vibrations Division.

.Structural Analysis

.Fatigue and Fracture

.Strain measurement

B. Hot Processing Division.

.Foundry

.Forging

.Welding

C. Electrical and Mechanical Design Division

.This group designs products for commercial production

This division has five departments:

1. Fundamental Technology Department.

.Basic research topics:

gear rating, lubrication

life prediction

gear CAD

new developments

2. Technical Developments Department.

.The goal is to assist the Government with the development of new products per the Five Year Plan, and to develop needed equipment or assist in selecting foreign equipment.

3. Materials and Heat Treating Department.

.Conduct research on domestic materials including Carburizing, Nitriding and Induction hardening.

4. Gear Manufacturing Research Department.

.Conduct research on gear manufacturing methods including honing, shaving, grinding and hobbing.

5. Technical Services Department.

.Conducts national symposiums and seminars, develops the China gear standards, publishes a bimonthly gear journal, represents China on the International Standards Organization committee TC-60, represents China on IFTOM. (and will host the Fall IFTOM.

meeting at ZRIME), provides headquarters for the China Mechanical Transmission Society which is a branch of the China Mechanical Engineering Society.

The National Center for Quality Control of Gears is also located at ZRIME. This group inspects the quality of gears in the factories and reports their findings in order to correct any deficiencies and assure the quality of the Nation's gear products.

ZRIME has approximately 900 employees and about 45% are engineers. The Gear Division has 155 employees and 115 are engineers.

Each division has a Chief Engineer. The divisions are relatively independent and self supporting. The divisions coordinate their efforts to provide mutual support through the Director of the Gear Division Mr. Wang.

4. FACILITIES FOR GEAR WORK:

In order to indicate the capability of the Gear Division and the National Center for Quality Control of Gears, some of the equipment and facilities are listed below.

This list is not complete.

1. Pfauter hobbing machine

- 1.25 meters maximum diameter

2. China made hobbing machine

1.5 meters maximum diameter

3. China made hobbing machine

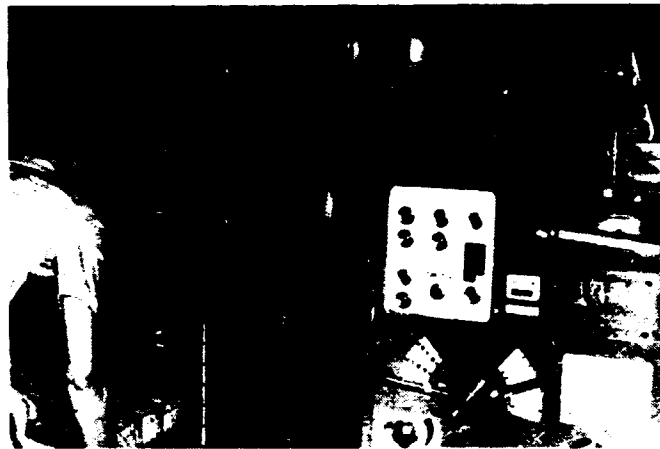
2.0 meters maximum diameter can cut large modules.

4. MAAG Shaper SH75K

700mm max. diameter

320mm max. stroke

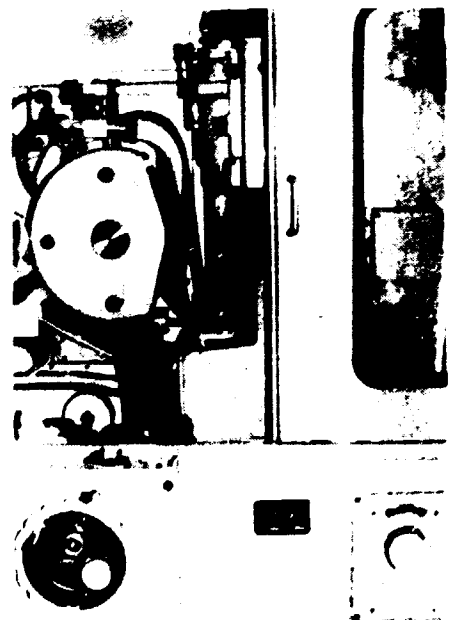
Quality: DIN 4, AGMA 12-13



5. Shanghai gear grinder

320mm max. diameter

5 max. module



上海机床厂

6. MAAG Grinder SD62

620 mm max. diameter

15 max module

Quality: DIN 4, AGMA 12-13



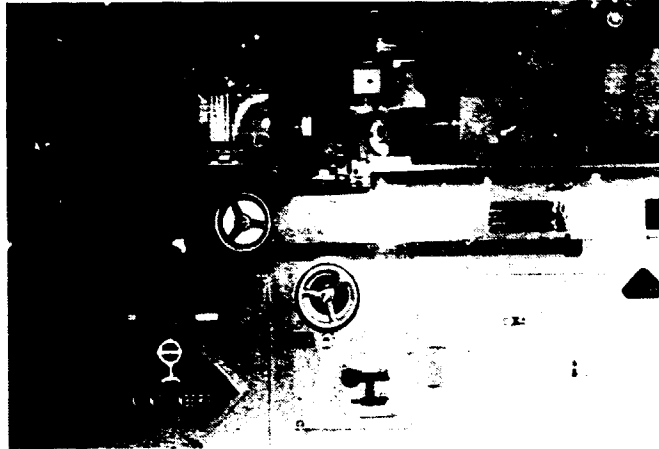
7. Controls for wear and lubrication test



8. Klingelnberg Hob Grinder

300 mm max. diameter

Quality: AAA



9. Klingelnberg Tester

(used with MAAG SD62 Grinder)

1.2 m max. diameter



10. Klingelberg machine to check accuracy of hob.
300 mm max. hob diameter

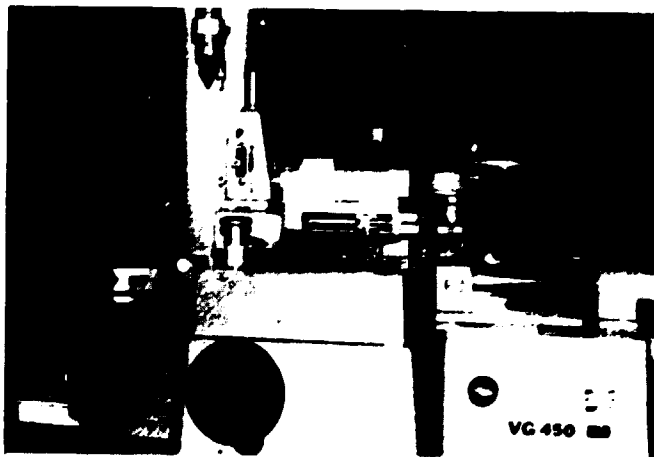


11. Klingelberg machine SP90 to inspect cylindrical
and spirol bevel gears is on order.

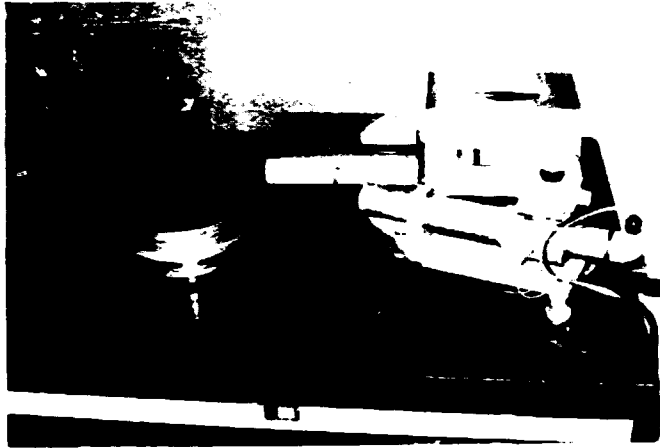
900 mm max. diameter

12. VG450 for checking profile of master gears,
450 mm max. diameter

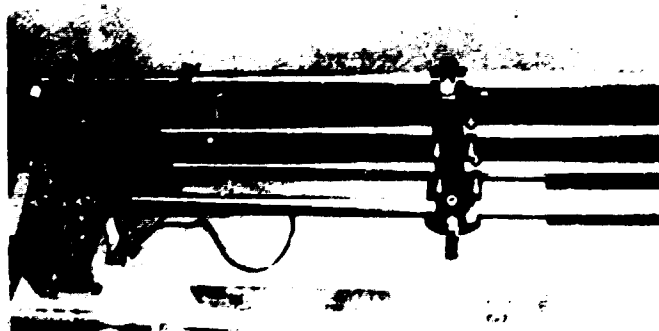
Quality: AGMA 13 or higher



3. Concentricity measurement-laser
0.5 arc second accuracy



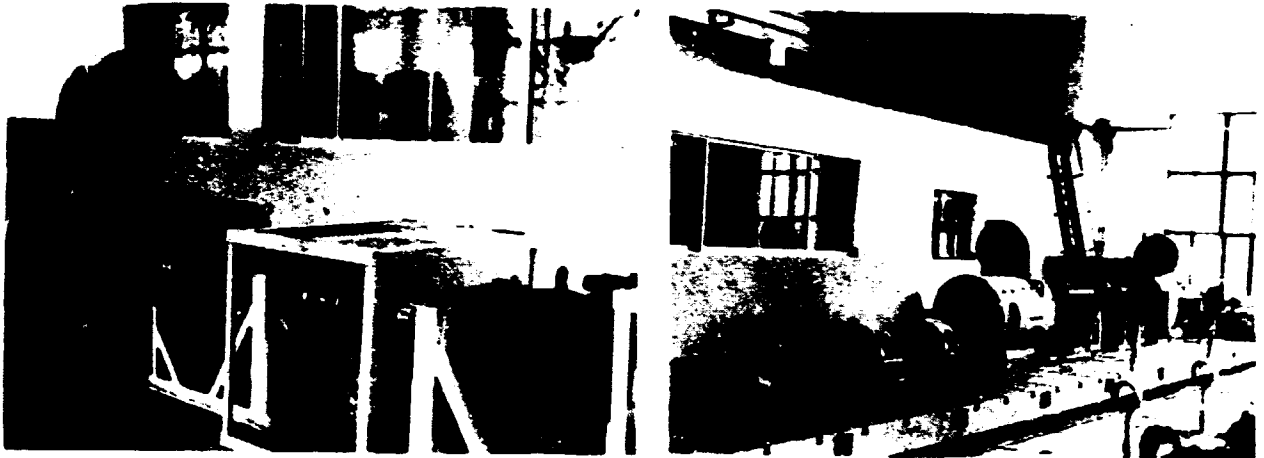
14. Goulder Mikron machine to check profile of
large turbine gears
10 module maximum
1 m minimum diameter



15. Four Square Test Stand:

250 Kw max. power

Computer control is on order. Measures noise, vibration, torque, efficiency, and oil temperature for a complete assembled gear system.



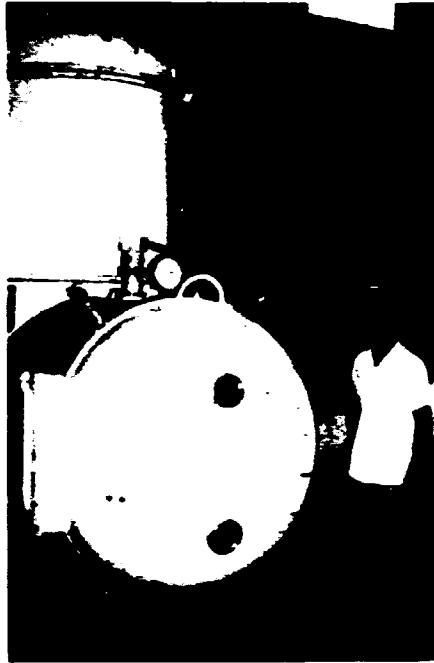
16. Four Square Test Stands:

Four test stands with 150 mm center distance and four with 100 mm center distance.

For test of lubrication, scoring and wear. Size of wear particles in oil, vibrations, and dynamic loads are monitored.



17. Plasma carbonitride heat treating
500 mm max. diameter



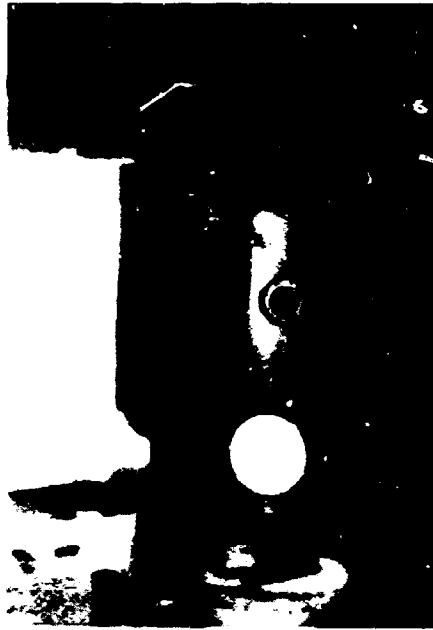
18. Gas carburizing heat treatment
1.2 m max. diameter
2.4 m max. width
4 mm case depth is achieved



19. Plasma Nitride heat treating

Ring gear, 900 mm max. diameter

2.3 m max. width



20. B&K Noise and Vibration instruments for measurement in field by portable system and tape recorder. Analysis of data by FFT on main computer.
21. Computer facilities include an IBM 4381 with connected terminals, a large design terminal, and a Calcomp plotter. Seven IBM PC computers are in the Gear Division.
22. The ADINA finite element code is used.

5. RESEARCH AND TECHNICAL SERVICE:

The gear research and the technical service provided by ZRIIE are important to the development of the Nation as it strives to provide transportation, food and energy to the citizens. The fundamental research on gear materials which are manufactured and processed within the Nation is necessary to establish the life and reliability of these materials. The life and reliability of gears depends on the material in addition to all of the machining and heat processing operations which are used to manufacture the gear.

The basic research on gear life, heat treating and new materials will be beneficial to China and to the world. The research on contact fatigue life is of special interest to the members of the ISO-TC60 group.

The need for a national standard for gears does exist in China. There are several different standards in use today. The values of these standards provide good designs, but the values are not all interchangeable between the different standards. The gears manufactured from the new China materials and by new China processes are not all included in these other standards.

The technical interchange sponsored by ZRIIE is very healthy for the gear experts across the Nation as it multiplies their progress. The international activities of ZRIIE accomplishes the same result across the world.

6. CONSULTING ACTIVITIES:

Each lecture contained a period for questions. Also, in the following days, questions concerning the lecture and other projects were discussed.

Examples are:

1. The analysis of lateral vibrations per the
API 163 Standard
2. The activity in the U.S.A. on ductile iron gear
research

7. VISIT TO SICHUAN GEARBOX PLANT:

The purposes of the visit to the plant were to present lectures and training on the Computer Aided Design of Gears and on Standards and to gain a firsthand view of the state of gear manufacturing technology as it is practiced in China today. Due to the limited time, only one day of lecturing was presented on the topics of torsional vibrations and the AGMA 218.01 Standard. However, copies of all seven lectures were provided to them.

The Sichuan Gearbox Plant is a subsidiary of China State Shipbuilding Corporation. The products of this plant include gearboxes, clutches, couplings and dampers. The plant is located in Jiangjin on the Long River and has 1200 employees. The plant has eight shops, which include:

1. Gearbox manufacturing
2. Gearbox assembly testbeds
3. Heat treatment (carburize, induction, nitride)
4. Press shop
5. Forging and welding
6. Friction disk manufacture

The plant started in 1966. In 1978 - 1979 license agreements with Lomann & Stolterfoht and with Geislinger were made to manufacture marine gears and elastic damping couplings respectively. A tour of the facility showed that it is an excellent gear plant with the machines, testing equipment, quality control and personnel required to do the job correctly.

8. CONCLUSIONS:

The organization of ZRIIE and the Gear Division is well planned to advance the development of gears within the Nation. The high technology of gears and gear systems is a combination of art and science. The performance of a gear system depends on the nature of the parent material, the machining operations, the heat treating process, the gear design analysis, the system design, and the operating conditions. The Gear Division is organized to consider all of these factors. The interactions with industry, universities and other institutions is very beneficial to all.

The facilities at ZRIIE are adequate to perform Computer Aided Design of gears. However, the software and hardware are rapidly advancing and plans for regular upgrading should exist.

A solids modeling software package should be considered.

Improvements in transportation and communication systems within the Nation will aid in commercial developments in China's gear industry.

The UNIDO support for the computerized control of the carburizing heat treating process, will be very helpful.

The UNIBO Gear CAD project has provided a good exchange of ideas on computer aided design of gears and an increased understanding of the American Gear Manufacturer's Standards for gear design.

The rapid advances in gear technology, computer aided testing, computer aided manufacturing, and gear CAD in China and in the world present a need for a long range education and training program.

There is a need for a training facility at GRIME in order to provide effective training in modern gear technology such as hot processing methods, manufacturing methods, quality measurements, and computer aided design and analysis. The facility should be furnished with adequate computers and other equipment to allow the participants to receive personal training.

Perhaps 10 training stations would be appropriate.

(The 386 computers should be considered.)

Audio visual equipment is needed. It is recommended that these needs be considered.

APPENDIX

Participants in Lectures on Gear CAD In Zhengzhou, July, 1988

NAME	AGE	TECHNICAL TITLE	AFFILIATIONS
1. Chen Zegao	56	Senior Engineer	Shanghai Research Institute of Hoist
2. Mei Jianping	35	Teacher	East China Institute of Chemical Engineering
3. Jin Guopin	42	Teacher	Technologz College, Shanghai University
4. Leng Xiangzhu		Teacher	Xuzhou Gear Plant
5. Cheng Dahei	43	Engineer	Kaifeng Air Separator Factory
6. Yhang Qiankun		Assistqnt Engineer	Kaifeng Air Separator Factory
7. Yao Hongli			Ansan Tractor Research Institute
8. Yu Jiang			Ansan Tractor Research Institute
9. Wang Jianshe	30	Graduate	Changchun Research Institute of Optical Machine
10. Shen Qingzhu	24	Graduate	Changchun Research Institute of Optical Machine
11. Li Debao	40	Engineer	Dalian Research Institute of Hoist
12. Zhao Wei	30	Graduate	Northeastern Institute of Technology
13. Li Jingfeng	24	Graduate	"
14. Ding shichao		Graduate	"

15. Shen Tao	24	Engineer	Shenyang Blower Works
16. Wang yuhua	28	Engineer	"
17. Tong Rongchu	48	Engineer	Beijing Gear Company
18. Ma yuanjing	25	Assistant Engineer	"
19. Liu xitian	46	Engineer	Taiyuan Research Institute of Hoist
20. Jia Yi		Teacher	Gear Research Institute, Taiyuan University of Industry Technology
21. Tang zhengbao	53	Associate Professor	Central China University of Science and Technology
22. Zhong yifang	53	Associate professor	"
23. Che Hexiang	53	Associate professor	"
24. Yang Kaixiou	45	Teacher	"
25. Li Haixiang	49	Associate Professor	Wuhan Institute of Water Transportation Engineering
26. Fan Qi	26	Assistant	"
27. Xie Peilin	42	Teacher	Wuhan Institute of Navy Engineer
28. Zhou Jingyu	38	Technician	Hubei Vehicle Elements Factory
29. Yan shaomu	23	Technician	"
30. Li Rei	23	Assistant Engineer	"
31. Chen Lin		Assistant Engineer	"
32. Gao Xiangqun	49	Senior Engineer	Zhuzhou Research Institute No. 608

33. Wei Gang	26	Graduate	Zhuzhou Research Institute No. 608
34. Deng Dize	49	Senior Engineer	Changqing Vehicle Office
35. Yang Peilin	25	Assistant	Xian Jaotong University
36. Liu Geng	27	Assistant	Shanxi Institute of Mechanical Engineer
37. Wang Xiaoguang	31	Assistant	Northwestern University of Industry Technology
38. Liu Renxian	50	Professor	Xian Institute of Metallurgical Architecture Engineer
39. Wang Yuhang		Assistant Enginer	Xian Research Institute of Heavy-duty Machinery
40. Liang Botao		Graduate	Gear Research Section, Luoyang Institute of Technology
41. zhang Jianzhong		Assistant Engineer	Luoyang Mining Machinery Plant
42. Pei Jingning	30	Engineer	"
43. Liu Guoping	30	Engineer	"
44. Zhou Jiliang	54	Professor	Luoyang Tractor Research Institute
45. Sun Gongwei	48	Senior Engineer	"
46. An Lical	50	Engineer	"
47. Wu Xucheng		Engineer	"
48. Wang Luming	54	Senior Engineer	"
49. Wang Shiyan	30	Engineer	"
50. Zhao Kaotian	30	Engineer	"
51. Yu Reixi	45	Engineer	"

52. Li Shuping	25	Engineer	Luoyang Tractor Research Institute
53. Wang Xiaoling	35	Engineer	"
54. Zhou yu	35	Engineer	"
55. Zhou Xiaodong	25	Graduate	Beijing University of Science and Technology
56. Ai Chunting	35	Teacher	Wuhan University of Industry Technology
57. Yan Dinghong		Teacher	Shanghai University of Industry Technology.
58. Hu ziqiang		Assistant	"
59. Ou zonhying	52	Professor	Dalian University of science and Technology
60. Chang Keqin		Engineer	Zhengzhou Research Institute of Mechanical Engineer
61. Zhang Tingjian		Engineer	"
62. Liu Zhilei		Assistant Engineer	"
63. Li Xiouzhen		Engineer	"
64. Zhang Zhiwei		Assistant Engliener	"
65. Xia Yi		Engineer	"
66. Gao xinshu		Assistant Engineer	"
67. Jing Xian		Engineer	"
68. Zhu shiqing		Assistant Engineer	"
69. Xu Jiaoyao		Engineer	"
70. Liuo Shijun		Graduate	"
71. Cai Neng		Graduate	"
72. Wang Jifeng		Graduate	"

LECTURE 1

COMPUTER AIDED DESIGN :
Steady State and Kinematic Simulation

PREFACE

Seven lectures on the computer aided design of gears and gear systems are documented in this manuscript. These lectures were presented in a national meeting at the Zhengzhou Research Institute of Mechanical Engineering (ZRIME) in Zhengzhou, China. ZRIME is responsible for standards, research and development relative to the nation's gear industry and is part of the State Commission of Machinery Industry of the People's Republic of China.

The first three papers deal with the use of computers in the dynamic simulation of mechanical and gear systems and include torsional vibration studies. The fourth paper gives an introduction of the finite element method for computer analysis of stresses and deflections for non-prismatic shapes like gear teeth. The fifth paper discusses gear failures and outlines the Lewis and the Hertz equations for bending and compressive stresses in gear teeth. The sixth paper introduces the AGMA 218 Standard and shows how the Lewis and Hertz equations are modified for the American Gear Manufacturer's Standard on gear design. The last lecture introduces commercial software for computerized gear design.

The preparation, organization and management of this meeting by the Gear Division of ZRIME was exceptional. The personal care shown by each member of the staff is appreciated. The funding of this project by the United Nations Industrial Development Organization made this technology exchange possible. The technical competence of interpreters Jia Sun, Ding-Hong Yan, Zongying Ou and Mr. Mao added greatly to the presentations. The careful typing of the manuscripts by Mrs. Rook and Mrs. Yeatman was a significant contribution. Many of the examples and

research results are based on activities with Marine Gears, Inc. The efforts of my co-authors and of many graduate students are gratefully acknowledged. Carol's support made it possible for me to participate in this project.

E. William Jones

ABSTRACT:

Modern computers with low cost graphics are changing the scope of the mechanical designer's responsibilities and the way he performs his tasks. Some of the implications of Computer Aided Engineering are presented. The response of the engineer to the CAE environment is demonstrated by software for gear forces and for mechanism design.

1. INTRODUCTION:

The availability of low cost, fast computers with large memory and good graphics is producing a revolution in design departments. In the recent past computers were used primarily for engineering calculations which had extensive complexity or length. The major problems for the designer included digesting the voluminous output, summarizing the results briefly, accessibility of the computer, time required per run, learning to program, training and retraining to use new hardware and software. The access problem is rapidly disappearing with the changing price to performance index. The low cost of graphics is providing a visual solution to the problem of coping with the volumes of printed output. Modern software with considerations for human factors is much easier to use. The computer offers the potential to perform calculations at a fixed quality level by reducing the human variation. The level of quality control depends on the maturity of the software, and it is still vulnerable to human errors in the input data. The use of a common data base and the integration of Computer Aided Design with Computer Aided Manufacturing are important. The potential of today's computers to contribute to the design task is making significant improvements.

Engineering design is an iterative process, which produces a specification for a product, which will fill a human need. The quality of the product and the timeliness with which the design task is completed are significant factors in determining the value of the product.

Engineering management faces different questions as their task changes from managing people to managing a machine room with operators. The yearly fees for maintenance and software rental are a large part of the engineering budget. The changing CAE technology makes hardware and software technically obsolete rapidly, which requires upgrading of software and hardware and retraining of personnel. The lack of standardization and interchangeability of hardware and software have been major problems and are beginning to get some attention from the hardware and software suppliers. The Construction Industry Institute's Design Committee is currently studying the impact, implications and needs of CAE for the construction industry. Even though CAE is still in the evolutionary stage the engineering community needs to be involved with CAE so we will grow also.

The training required to practice engineering is changing. The designer with a workstation can perform a larger and more complex task in a shorter time span. This reduction in time span reduces the conscious and subconscious thought time which the designer applies to the task. This may reduce the designers creative responses during the design phase. Conversely, the computer may allow the designer to study more alternatives during the design phase since it can reduce the repetitive manual labor. The enlarged scope of the task argues that the designer's training and qualifications must be increased to match

his responsibilities. While the designer must have some computer skills, he must also understand the physics of the application, the constraints on how to design for manufacturability, servicability, safety and human factors, and he must have the mature judgement necessary to make decisions.

The benefits of CAD/CAE are still being debated. Some suggest that a benefit is in the reduced number of draftsmen on the task, however, the savings on the drafting expense is more than offset by the cost and maintenance of the computer and software. Much of the savings are outside of the design room. These savings include:

1. The reduced cost of rework during manufacturing.
2. The reduced loss due to scrap material.
3. The creation of a common data base for all.
4. Electronic transmission of drawings to remote sites.
5. The reduction in product development time.

A creative approach is required in the evaluation of CAE benefits because the task is usually redefined in the CAE environment. As an example, in 1975 Caterpillar Tractor Company evaluated the Finite Element Method. Some questions were:

1. Can the FEM reduce the time required between the initiation of design and the release for production?
2. What education and skills are required for use of the FEM?

Several engineers with different levels of education and experience were given different components of a new product, which had been designed by conventional methods. Since these engineers were learning the FEM, the time required for their solutions was not representative.

However, if the FEM could predict any major failures of these components prior to testing, then the component could be redesigned prior to the test. A failure of a component during the test of this high speed product would produce failures of other components also. A failure during the test would produce a delay of several months in the product release date because:

1. First, the failures must be analyzed to determine the "root cause."
2. Then, the component with the "root cause" must be redesigned.
3. The redesigned component must be manufactured. If the component is a forging or casting, the die or mold must be reworked.
4. The test must be rebuilt and restarted with zero credit for fatigue cycle testing.

Hence, the major gains from this CAE application were in the Proving Grounds Budget.

The results of this study showed a stress in a fillet of a forging to be above the endurance limit. A one inch fillet radius would have been satisfactory but the component drawing showed half of an inch. A review of the original layout showed a one inch radius in this transition region, but the draftsman's circle templet had a maximum hole size of one inch. Hence, the designer's intuition had been correct, but without calculations to reinforce this intuition an oversight was made. The drawing was changed. After this study, Caterpillar created a group for performing finite element analysis for their product design groups.

Some general purpose software packages have been developed and examples are given, but the list of examples is not intended to be complete.

- | | |
|---|------------------------------|
| 1. Computer Aided Design
and Drafting. | CADAM, AutoCAD |
| 2. Dynamic Simulation | ACSL, CSMP |
| 3. Mathematics, Statistics | MATHLIB, MATHCAD, TKSOLVER |
| 4. Word Processing | Word Perfect, Microsoft Word |
| 5. Finite Elements | ANSYS, MSC-NASTRAN |

Special purpose CAD software can be a good engineering aid.

First, there are small, homemade, special purpose CAD packages for personal tasks. Engineers should identify these tasks. Five examples are given below. The program INERTIA is typical of this class of programs. The program GEARFORC is for one area of technology, but it has a more general group of users since it is designed to evaluate the bearing reactions for all combinations of helical gears and pinions. The program FOURBAR is general for one area of technology and it uses graphics to help show the output. These three programs can analyze an existing configuration. The fourth example deals with the use of CAD in the synthesis (invention) of a configuration. The fifth example indicates the coupling of Computer Aided Design and Computer Aided Drafting software. The challenge for the mechanical designer is to identify tasks, which are repeated and require significant human efforts, and to develop software to perform these tasks.

2. EXAMPLE ONE: Inertia and Torsional Stiffness

The calculation of mass moments of inertia and torsional stiffnesses of members with circular cross-sections is an often repeated task in evaluating the mass-elastic characteristics of a gear train. Hence, a program to evaluate and add inertias and spring rates may be very useful even though it is elementary. Since the majority of errors in programs occur due to faulty input of the data, the program must print all input data on hard copy for future reference and quality control. The program INERTIA is listed in Appendix A and the output for the shafting section of Figure 2.1 is given in Table 2.1.

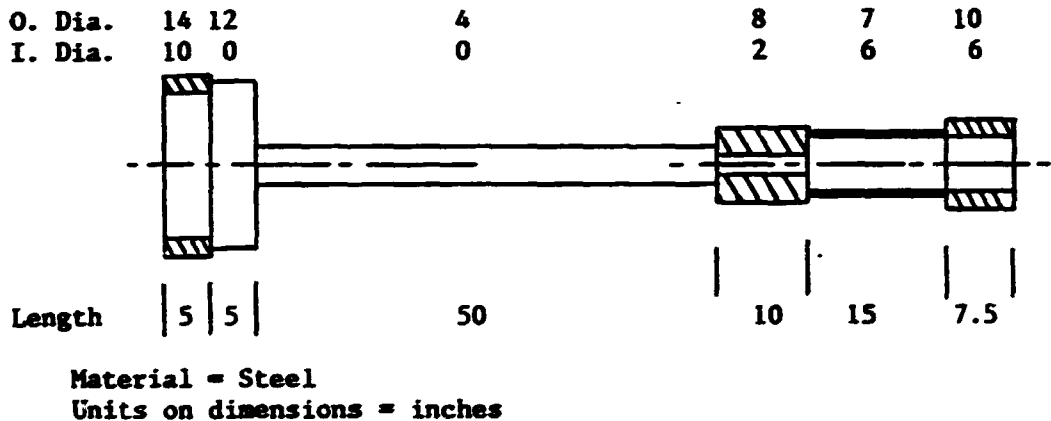


Figure 2.1 Shaft Section

3. EXAMPLE TWO: Generalized Bearing Reaction Program

The calculation of the bearing reaction forces on a shaft, which is supported by two bearings in a helical gear transmission, is a common task. A program for evaluating the bearing reactions, which allows for any number of gears on the shaft and for any number of pinions to be in mesh with each gear, is developed in this example.

TABLE 2.1 Output from Program: INERTIA

TORSIONAL STIFFNESS AND INERTIA
PROGRAM: INERTIA

MATERIAL DENSITY = .283 POUNDS/CUBIC INCH
NUMBER OF DISCS = 6

DISC NUMBER = 1
OUTSIDE DIAMETER = 14 INCHES
INSIDE DIAMETER = 10 INCHES
LENGTH OF DISC = 5 INCHES

DISC NUMBER = 2
OUTSIDE DIAMETER = 12 INCHES
INSIDE DIAMETER = 0 INCHES
LENGTH OF DISC = 5 INCHES

DISC NUMBER = 3
OUTSIDE DIAMETER = 4 INCHES
INSIDE DIAMETER = 0 INCHES
LENGTH OF DISC = 50 INCHES

DISC NUMBER = 4
OUTSIDE DIAMETER = 8 INCHES
INSIDE DIAMETER = 2 INCHES
LENGTH OF DISC = 10 INCHES

DISC NUMBER = 5
OUTSIDE DIAMETER = 7 INCHES
INSIDE DIAMETER = 6 INCHES
LENGTH OF DISC = 15 INCHES

DISC NUMBER = 6
OUTSIDE DIAMETER = 10 INCHES
INSIDE DIAMETER = 6 INCHES
LENGTH OF DISC = 7.5 INCHES

TORSIONAL STIFFNESS = 5310063 INCH POUNDS/RADIAN
SHAFT INERTIA = 27.43824 IN. LB. SEC. SEC.
TOTAL WEIGHT = 727.9261 POUNDS

(The word pinion normally refers to the smaller of the two mating gear elements, but in this example the word 'pinion' refers to the elements which are meshing with that element on the shaft whose bearing reactions are to be evaluated.)

A typical gear and shaft arrangement is shown in Figure 3.1. Bearing number 1 is chosen as the location of the origin of the right hand coordinate system. The positive z-axis is directed to the right along the centerline of the shaft. Distances to the left of the origin have negative values for the z-coordinate. The x-axis is horizontal and the y-axis is vertical. This figure shows two gears. Each gear has one mating 'pinion'. There is a force F_g in this figure and the sign of this force is positive, if the force is directed upward. If F_g is due to gravity, the numerical magnitude must have a negative sign. The angular orientation for each pinion is identified by the angle θ , which is the rotation about the z-axis. This angle is measured from the positive x-direction with the positive direction defined by the right hand rule and illustrated in Figure 3.2. The positive direction for the helix angle is selected as the right hand helix per Figure 3.3.

The tangential component of the tooth load is

$$W_T = P \times 396,000 / (2 \times \pi \times N \times d/2)$$

where,

P = Input power, horsepower

N = Speed of shaft under study (CCW is positive), RPM

d = Pitch diameter of gear with speed N, inches

$$d = N_T / (P_d \times \cos(\psi))$$

N_T = Number of teeth

P_d = Normal diametral pitch

ψ = Helix angle (right hand helix is positive), degrees

ϕ_n = Pressure angle in normal plane, degrees.

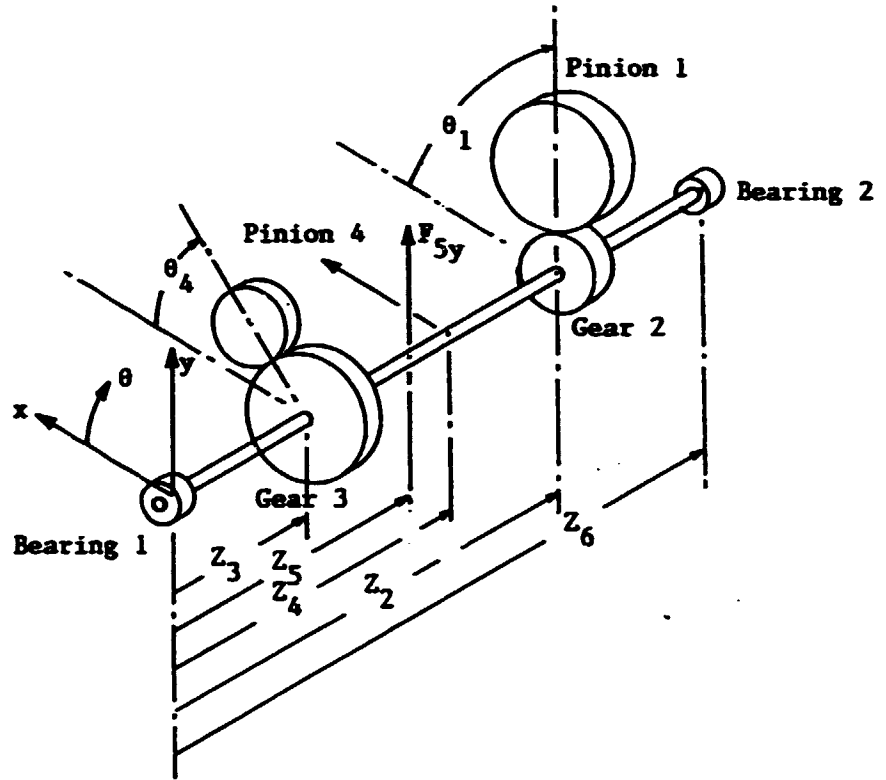


Figure 3.1 Transmission Gear, Shaft and Bearing Arrangement

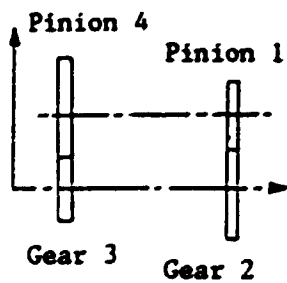


Figure 3.2 Sign Convention for Pinion Location

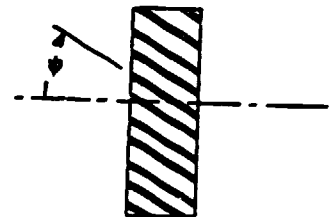
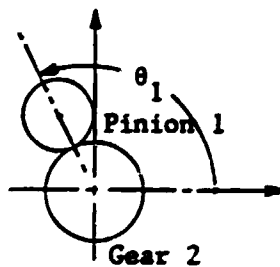


Figure 3.3 Sign Convention for Helix Angle

The components of the force of the pinion on the gear are illustrated in Figure 3.4 and the magnitudes are given in Table 3.1. The signs of these forces depend on whether the gear is driving or is being driven. The radial force on the gear is

$$WR(N,M) = ABS(WT) \times \tan\phi_n / \cos\psi$$

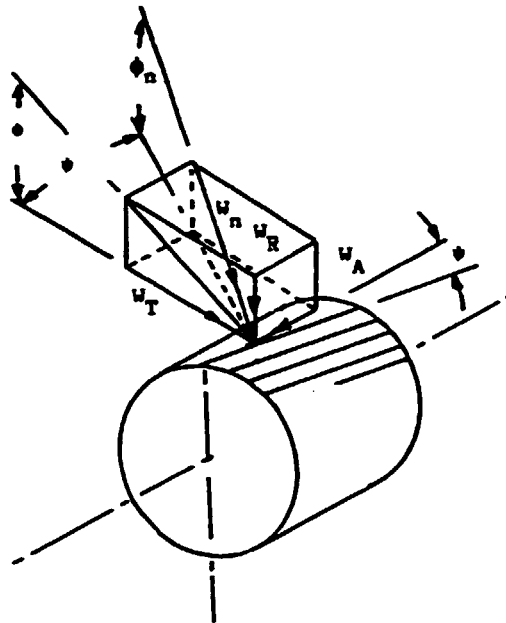


Figure 3.4 Helical Gear Forces

TABLE 3.1 Equations for Components of Forces Acting on Gear N due to Pinion M

Symbol for force component	When the gear is driven	When the gear is driving
WTY(N,M)	WT x Cosθ	-WT x Cosθ
WTX(N,M)	-WT x Sinθ	WT x Sinθ
WRX(N,M)	-WR x Cosθ	-WR x Cosθ
WRY(N,M)	-WR x Sinθ	-WR x Sinθ
WA(N,M)	-WT x Tanψ	WT x Tanψ

The sum of the moments may be used to evaluate the components of the forces at the bearings. The moment of force F is given by the mixed triple scalar product (1)¹ of the three vectors, λ , r and F .

$$M = \lambda \cdot (r \times F)$$

where,

λ = A unit vector parallel to the axis about which the moment is evaluated.

$$\lambda = i\lambda_x + j\lambda_y + k\lambda_z$$

λ_x , λ_y and λ_z are the direction cosines of the axis about which the moment is evaluated.

i , j and k = unit vectors along x , y and z axes respectively.

r = The position vector of the force relative to a point on the axis of rotation.

$$r = ix + jy + kz$$

F = The force vector

$$F = iF_x + jF_y + kF_z .$$

Hence,

$$M = \begin{vmatrix} \lambda_x & \lambda_y & \lambda_z \\ x & y & z \\ F_x & F_y & F_z \end{vmatrix}$$

Each pinion will produce a moment M due to tooth contact forces on the gear. If each external force, which is not produced by tooth contact, is divided into x and y components (F_x and F_y), then each component will also produce a moment M . For the gear and shaft arrangement of Figure 3.1 the sums of the moments about the x -axis, $\sum M_{x1}$, and about the y -axis, $\sum M_{y1}$, at bearing one are given below and the

¹Numbers in parentheses identify references.

equations for the y-component, R_{y2} , and the x-component, R_{x2} , of the reactions at bearing number two are derived from these moment equations.

$$\begin{aligned} \sum M_{x1} &= \begin{vmatrix} 1 & 0 & 0 \\ .5d_2 \cos \theta_1 & .5d_2 \sin \theta_1 & Z_2 \\ (W_{T2x} + W_{R2x}) & (W_{T2y} + W_{R2y}) & W_{A2} \end{vmatrix} \\ &+ \begin{vmatrix} 1 & 0 & 0 \\ .5d_3 \cos \theta_4 & .5d_3 \sin \theta_4 & Z_3 \\ (W_{T3x} + W_{R3x}) & (W_{T3y} + W_{R3y}) & W_{A3} \end{vmatrix} \\ &+ \begin{vmatrix} 1 & 0 & 0 \\ 0 & 0 & Z_5 \\ F_{5x} & F_{5y} & 0 \end{vmatrix} + \begin{vmatrix} 1 & 0 & 0 \\ 0 & 0 & Z_6 \\ R_x & R_y & R_z \end{vmatrix} = 0 \end{aligned}$$

$$R_{2y} = \{ [.5W_{A2}d_2 \sin \theta_1 - Z_2(W_{T2y} + W_{R2y})] + [(.5W_{A3}d_3 \sin \theta_4 - Z_3(W_{T3y} + W_{R3y})] + [0 - Z_5F_{5y}] \} / Z_6$$

$$\begin{aligned} \sum M_{y1} &= \begin{vmatrix} 0 & 1 & 0 \\ .5d_2 \cos \theta_1 & .5d_2 \sin \theta_1 & Z_2 \\ (W_{T2x} + W_{R2x}) & (W_{T2y} + W_{R2y}) & W_{A2} \end{vmatrix} \\ &+ \begin{vmatrix} 0 & 1 & 0 \\ .5d_3 \cos \theta_4 & .5d_3 \sin \theta_4 & Z_3 \\ (W_{T3x} + W_{R3x}) & (W_{T3y} + W_{R3y}) & W_{A3} \end{vmatrix} \end{aligned}$$

$$+ \begin{vmatrix} 0 & 1 & 0 \\ 0 & 0 & Z_5 \\ F_{5x} & F_{5y} & 0 \end{vmatrix} + \begin{vmatrix} 0 & 1 & 0 \\ 0 & 0 & Z_6 \\ R_{2x} & R_{2y} & R_{2z} \end{vmatrix} = 0$$

$$R_{2x} = \{ [(.5W_{A2}d_2 \cos\theta_1 - Z_2(W_{T2x} + W_{R2x})] + [.5d_3W_{A3} \cos\theta_4 - Z_3(W_{T3x} + W_{R3x})] - [Z_5F_{5x} - 0] \} / Z_6$$

The values of R_{2y} and R_{1y} only depend on four entries in the array for ΣM_{x1} : $MX1(2,2)$, $MX1(2,3)$, $MX1(3,2)$ and $MX1(3,3)$. The array for ΣM_{x1} may be represented for any general case by the following equation.

$$MX1 = \sum_{N=1}^{NOG} \sum_{M=1}^{NP} \begin{vmatrix} 1 & 0 & 0 \\ 0 & .5d(N)\sin(\theta(N,M)) & Z(N) \\ 0 & (W_{TX}(N,M) + W_{RX}(N,M)) & W_A(N,M) \end{vmatrix}$$

$$+ \sum_{n=1}^{NFY} \begin{vmatrix} 1 & 0 & 0 \\ 0 & 0 & FY(N,2) \\ 0 & FY(N,1) & 0 \end{vmatrix} = MX1(3, (3(NP + NFY)))$$

where,

NOG = Number of gears in system.

NP = Number of pinions meshing with the Nth gear.

NFY = Number of forces in the y-direction.

FY(N,1) = Magnitude of the Nth force in the y-direction, lb.

FY(N,2) = Distance along the z-axis from bearing number 1 to the Nth force in the y-direction, in.

For the general case, data for the evaluation of $MX1$ may be stored in an array with 3 rows and $3(NP + NFY)$ columns. The equation for $MX1$ may be rewritten with the noncontributing terms set equal to zero.

$$MX1 = \left[\begin{array}{ccc|ccc|ccc} 1 & 0 & 0 & 1 & 0 & 0 & 1 & 0 & 0 \\ 0 & MX1(2,3) & MX1(2,3) & 0 & MX1(2,5) & MX1(2,6) & 0 & MX1(2,8) & MX1(2,9) \\ 0 & MX1(3,2) & MX1(3,3) & 0 & MX1(3,5) & MX1(3,6) & 0 & MX1(3,8) & MX1(3,9) \end{array} \right]$$

Therefore, for one pinion in mesh with one gear:

$$MX1(2,2) = .5d_2 \sin \theta_1$$

$$MX1(2,3) = Z_2$$

$$MX1(3,2) = W_{T2y} + W_{R2y}$$

$$MX1(3,3) = W_{A2}$$

Each additional pinion in mesh with the gear adds three columns to the array. Each external force contributes three additional columns to the array. The values of elements of the array will be defined as follows for the case above.

$$MX1(2,8) = 0$$

$$MX1(2,9) = Z_5$$

$$MX1(3,8) = F_{5y}$$

$$MX1(3,9) = 0$$

With this definition of the array MX1, the following algorithm will evaluate the y-component of the bearing reaction at bearing number two,

R_{2y} :

C Initialize bearing reactions

$$R1Y = 0$$

$$R2Y = 0$$

C SX = Number of columns in arrays MX1 and MX2.

$$SX = 3*(NP + NFY)$$

For I = 2 to (SX-1) step 3

$$R2Y = R2Y + [MX1(2,I)*MX1(3,I+1)-MX1(2,I+1)*MX1(3,I)]/Z6$$

$$R1Y = R1Y + (MX2(2,I)*MX2(3,I+1)-MX2(2,I+1)*MX2(3,I))/Z6$$

Next I

The equation for R_{1y} is also evaluated in this algorithm. The terms of the equation for R_{1y} are the same as for R_{2y} except the distances along the z-axis. The array MX2 is defined as follows for each pinion:

$$MX2(2,2) = MX1(2,2)$$

$$MX2(2,3) = MX1(2,3) - Z6$$

$$MX2(3,2) = MX1(3,2)$$

$$MX2(3,3) = MX1(3,3)$$

The array MX2 is defined as follows for each force:

$$MX2(2,8) = MX1(2,8)$$

$$MX2(2,9) = MX1(2,9) - Z6$$

$$MX2(3,8) = MX1(3,8)$$

$$MX2(3,9) = MX1(3,9)$$

The form of the equation for R_{2x} is the same as for R_{2y} even though the terms differ. The terms in R_{2x} are from the first and third columns of the 3X3 arrays instead of from the second and third columns. The above algorithm would produce the value of R_{2x} , if values of the terms in the first column are transferred into the second column of array MY1 as follows:

$$MY1(2,2) = .5d_2 \cos \theta_1$$

$$MY1(2,3) = Z_2$$

$$MY1(3,2) = W_{T2x} + W_{R2x}$$

$$MY1(3,3) = W_{A2}$$

For the forces,

$$MY1(2,8) = 0$$

$$MY1(2,9) = Z_5$$

$$MY1(3,8) = F_{5x}$$

$$MY1(3,9) = 0 .$$

The number of columns in this array, MY1, will be

$$SY = 3*(NP + NFX)$$

Hence, the following algorithm will produce the bearing reaction forces, R1X and R2X, in the x-direction at bearings one and two respectively.

C Initialize bearing reactions

$$R1X = 0$$

$$R2X = 0$$

C SY = Number of columns in arrays MY1 and MY2.

$$SY = 3*(NP + NFX)$$

For I = 2 to (SY - 1) Step 3

$$R2X = R2X + [MY1(2,I)*MY1(3,I+1) - MY1(2,I+1)*MY1(3,I)]/Z6$$

$$R1X = R1X + [MY2(2,I)*MY2(3,I+1) - MY2(2,I+1)*MY2(3,I)]/Z6$$

Next I

The equation for R1X given is the algorithm depends on array MY2 which differs from array MY1 by the following definitions.

$$MY2(2,2) = MY1(2,2)$$

$$MY2(2,3) = MY1(2,3) - Z6$$

$$MY2(3,2) = MY1(3,2)$$

$$MY2(3,3) = MY1(3,3)$$

For each y force, the array MY2 is

$$MY2(2,8) = MY1(2,8)$$

$$MY2(2,9) = MY1(2,9) - Z6$$

$$MY2(3,8) = MY1(3,8)$$

$$MY2(3,9) = MY1(3,9)$$

A program listing for "GEAFORC", which uses this algorithm, is in Appendix B. The data of Table 3.2 represents an example problem. The program output for this problem is given in Table 3.3.

4. EXAMPLE THREE: Four-Bar Linkage Kinematics

The four-bar linkage is a commonly used mechanism which has a highly developed design methodology (2,3,4). The analysis of the four-bar linkage provides a good example for the application of computer aided design methods. First the logical progression of the analysis must be developed. After the analysis is complete, computer graphics may be applied to plot data or to illustrate the motion of the mechanism.

The analytical procedure for determining the positions, velocities and accelerations of a four-bar linkage has been often published (5) and the following equations follow the outline used by Professor Rezek of Purdue University. For reference, it is repeated in brief form. For one given position of the input crank, link R_2 , the four links may be assembled in the uncrossed configuration as illustrated in Figure 4.1 or in the crossed configuration of Figure 4.2. The first step in the analysis will be to identify the lengths, R_1 , R_2 , R_3 and R_4 , of the

TABLE 3.2 Input Data for "GEAFORC"

BEARING REACTIONS IN HELICAL GEAR TRANSMISSIONS

PROGRAM: GEARFORC

THE INPUT DATA :

THERE ARE 2 GEARS
THERE ARE A TOTAL OF 2 PINION(S)
NO GEAR HAS MORE THAN 1 PINION(S)
THE DISTANCE BETWEEN BEARINGS IS 58.142 INCHES
THE SHAFT SPEED IS -789.7 RPM

FOR GEAR NUMBER 1

GEAR NUMBER 1 HAS 1 PINION(S)
PRESSURE ANGLE = 20 DEGREES
HELIX ANGLE = -14.3615 DEGREES
DISTANCE FROM BRG. 1 TO GEAR 1 = 7.065 INCHES
DISTANCE FROM BRG. 2 TO GEAR 1 = -51.077 INCHES
PITCH DIAMETER = 25.35941 INCHES
THE NORMAL DIAMETRAL PITCH = 3.175 TEETH/IN.
NUMBER OF TEETH ON GEAR = 79

FOR PINION 1 ON GEAR 1

PINION NUMBER 1 IS A DRIVING PINION
ANGULAR POSITION = 90 DEGREES
INPUT POWER = 2000 HORSEPOWER

FOR GEAR NUMBER 2

GEAR NUMBER 2 HAS 1 PINION(S)
PRESSURE ANGLE = 20 DEGREES
HELIX ANGLE = -14.3615 DEGREES
DISTANCE FROM BRG. 1 TO GEAR 2 = 29.896 INCHES
DISTANCE FROM BRG. 2 TO GEAR 2 = -28.246 INCHES
PITCH DIAMETER = 22.1082 INCHES
THE NORMAL DIAMETRAL PITCH = 3.175 TEETH/IN.
NUMBER OF TEETH ON GEAR = 68

FOR PINION 1 ON GEAR 2

PINION NUMBER 2 IS A DRIVEN PINION
ANGULAR POSITION = 90 DEGREES
INPUT POWER = 2000 HORSEPOWER

THE EXTERNAL LOADS :

FX 1 = 0 POUNDS
FX 1 IS 0 INCHES FROM BRG 1
FX 1 IS -58.142 INCHES FROM BRG 2

FY 1 = 0 POUNDS
FY 1 IS 0 INCHES FROM BRG 1
FY 1 IS -58.142 INCHES FROM BRG 2

TABLE 3.3 Output from "GEAFORC" Program

RESULTS

GEAR TOOTH FORCES:

GEAR NUMBER 1
PINION NUMBER 1

THE TANGENTIAL TOOTH LOAD IS	=	-12589 POUNDS
THE X-COMP. OF THE TANG. TOOTH LOAD IS	=	12588 POUNDS
THE Y-COMP. OF THE TANG. TOOTH LOAD IS	=	0 POUNDS
THE RADIAL TOOTH LOAD IS	=	4729 POUNDS
THE X-COMP. OF THE RADIAL TOOTH LOAD IS	=	0 POUNDS
THE Y-COMP. OF THE RADIAL TOOTH LOAD IS	=	-4730 POUNDS
THE AXIAL (Z-COMPONENT) TOOTH LOAD IS	=	-3223.163 POUNDS

GEAR NUMBER 2
PINION NUMBER 1

THE TANGENTIAL TOOTH LOAD IS	=	-14440 POUNDS
THE X-COMP. OF THE TANG. TOOTH LOAD IS	=	-14440 POUNDS
THE Y-COMP. OF THE TANG. TOOTH LOAD IS	=	-1 POUNDS
THE RADIAL TOOTH LOAD IS	=	5425 POUNDS
THE X-COMP. OF THE RADIAL TOOTH LOAD IS	=	0 POUNDS
THE Y-COMP. OF THE RADIAL TOOTH LOAD IS	=	-5426 POUNDS
THE AXIAL (Z-COMPONENT) TOOTH LOAD IS	=	3697.157 POUNDS

BEARING REACTIONS:

FOR BEARING NUMBER 1:

R1	=	7903 POUNDS
R1Y	=	6790 POUNDS
R1X	=	-4044 POUNDS

FOR BEARING NUMBER 2:

R2	=	6787 POUNDS
R2Y	=	3364 POUNDS
R2X	=	5895 POUNDS

THE TOTAL AXIAL LOAD, WA = 473 POUNDS

four links and to determine the initial position of the input crank angle, θ_2 . The second step is to determine if these four links will be assembled in the crossed or uncrossed configuration.

The geometry of the triangle connecting points D, A and C of Figure 4.3 may be analyzed by the half angle equations.

$$S_1 = .5(AC + R_1 + R_2)$$

$$\alpha = 2 \tan^{-1} \left[\frac{(S_1 - AC)(S_1 - R_2)}{S_1(S_1 - R_1)} \right]^{.5}$$

$$\beta = 2 \tan^{-1} \left[\frac{(S_1 - AC)(S_1 - R_1)}{S_1(S_1 - R_2)} \right]^{.5}$$

The angle β may be determined from Figure 4.3 by evaluating the distances A_y and A_x and applying the tangent function.

$$A_x = R_1 - R_2 \cos \theta_2$$

$$A_y = R_2 \sin \theta_2$$

$$\beta = \tan^{-1}(A_y/A_x)$$

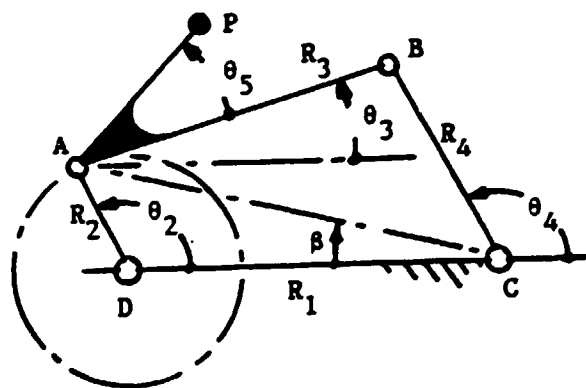


Figure 4.1 Uncrossed Configuration of Four-Bar Linkage

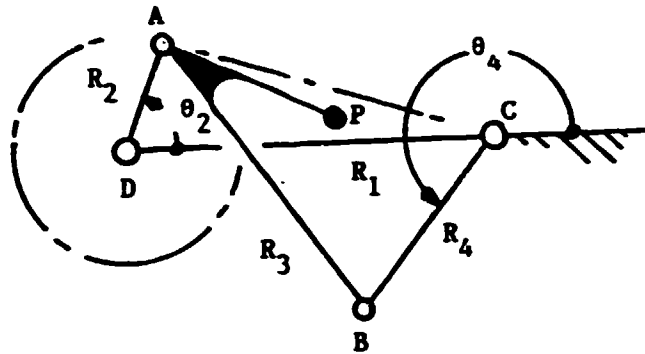


Figure 4.2 Crossed Configuration of Four-Bar Linkage

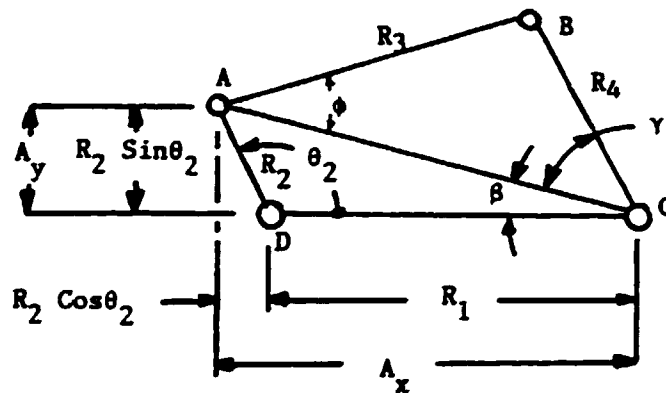


Figure 4.3 Geometry for Four-Bar Analysis

If the ATN function from BASIC is used to evaluate β , its value will only be correct if $A_x \geq 0$. The following logic makes the correction when $A_x < 0$.

$$\text{If } A_x < 0 \text{ then } \beta = \beta + \pi$$

The relationship between A_x and AC is

$$AC = A_x / \cos \beta$$

The half angle equations may be applied to triangle ABC to obtain γ .

$$S = .5(AC + R_3 + R_4)$$

$$\gamma = 2 \tan^{-1} \left[\frac{(S - AC)(S - R_4)}{S(S - R_3)} \right]^{-.5}$$

$$\phi = 2 \tan^{-1} \left[\frac{(S - AC)(S - R_3)}{S(S - R_4)} \right]^{-.5}$$

For the uncrossed configuration:

$$\theta_3 = \phi - \beta$$

$$\theta_4 = \pi - (\beta + \gamma)$$

For the crossed configuration:

$$\theta_3 = 2\pi - (\beta + \phi)$$

$$\theta_4 = \pi - \beta + \gamma$$

In order to plot the linkage in its various positions, the x-y coordinates of points A, B and P are specified below as a function of the input crank angle. Point P is a point on the coupler link.

$$X_A = R_2 \cos \theta_2$$

$$Y_A = R_2 \sin \theta_2$$

$$X_P = X_A + R_3 \cos(\theta_3 + \theta_5)$$

$$Y_P = Y_A + R_3 \sin(\theta_3 + \theta_5)$$

$$X_B = R_4 \cos \theta_4 + R_1$$

$$Y_B = R_4 \sin \theta_4$$

The positions and velocities for the uncrossed and crossed mechanisms in Figure 4.4 are given in Tables 4.1 and 4.2. The accelerations may be easily added using equations from (6).

TABLE 4.1

FOUR BAR LINKAGE POSITIONS AND VELOCITIES

THIS IS NOT A CROSSED TYPE LINKAGE.

LENGTH OF GROUND LINK R1 = 14
 LENGTH OF INPUT CRANK R2 = 9
 LENGTH OF COUPLER LINK R3 = 20
 LENGTH OF OUTPUT CRANK R4 = 12
 R5-DIST. FROM JOINT R2 AND R3 TO COUPLER POINT P = 10
 ANGLE BETWEEN R3 AND R5, DEGREES = 45
 ANGULAR VELOCITY OF INPUT CRANK, RAD/SEC = 1
 POSITION INCREMENT FOR INPUT CRANK, DEGREES = 10

THETA2 DEGREE	THETA3 DEGREE	THETA4 DEGREE	OMEGA3 RAD/S	OMEGA4 RAD/S	VEL-A IN/S	VEL-B IN/S	VEL-P IN/S	THETA P DEGREE
0	LINKAGE WILL NOT ASSEMBLE AT THIS POSITION.							
10	LINKAGE WILL NOT ASSEMBLE AT THIS POSITION.							
20	LINKAGE WILL NOT ASSEMBLE AT THIS POSITION.							
30	LINKAGE WILL NOT ASSEMBLE AT THIS POSITION.							
+40.0	-17.2	-0.6	+1.0268	+2.2095	+9.00	-26.51	+19.16	+123.5
+50.0	-9.9	+16.8	+0.5495	+1.4459	+9.00	+17.35	+14.33	+134.4
+60.0	-5.3	+29.8	+0.3945	+1.1864	+9.00	+14.24	+12.77	+143.9
+70.0	-1.7	+40.9	+0.3231	+1.0516	+9.00	+12.62	+11.97	+153.0
+80.0	+1.3	+51.0	+0.2866	+0.9630	+9.00	+11.58	+11.49	+162.1
+90.0	+4.1	+60.3	+0.2685	+0.9002	+9.00	+10.90	+11.17	+170.9
+100.0	+7.7	+69.0	+0.2618	+0.8453	+9.00	+10.15	+10.92	+179.7
+110.0	+11.3	+77.2	+0.2631	+0.7957	+9.00	+9.55	+10.71	+188.3
+120.0	+14.0	+84.9	+0.2706	+0.7462	+9.00	+8.95	+10.51	+196.7
+130.0	+17.7	+92.1	+0.2831	+0.6953	+9.00	+8.34	+10.31	+205.0
+140.0	+20.8	+98.8	+0.2999	+0.6414	+9.00	+7.70	+10.09	+213.1
+150.0	+24.1	+104.9	+0.3202	+0.5840	+9.00	+7.01	+9.85	+221.1
+160.0	+27.5	+110.5	+0.3430	+0.5229	+9.00	+6.27	+9.53	+229.0
+170.0	+30.7	+115.4	+0.3671	+0.4584	+9.00	+5.50	+9.27	+236.9
+180.0	+33.9	+119.9	+0.3913	+0.3913	+9.00	+4.70	+8.93	+244.8
+190.0	+37.1	+123.2	+0.4139	+0.3227	+9.00	+3.97	+8.56	+252.9
+200.0	+39.7	+125.1	+0.4332	+0.2533	+9.00	+3.24	+8.15	+261.3
+210.0	+42.1	+125.3	+0.4476	+0.1838	+9.00	+2.51	+7.72	+270.2
+220.0	+44.3	+123.8	+0.4554	+0.1139	+9.00	+1.77	+7.29	+279.3
+230.0	+46.2	+120.3	+0.4549	+0.0429	+9.00	+1.01	+6.85	+290.4
+240.0	+47.7	+115.6	+0.4441	+0.0316	+9.00	+0.38	+6.48	+302.3
+250.0	+48.9	+109.9	+0.4203	+0.1123	+9.00	-1.35	+6.19	+315.9
+260.0	+49.6	+103.3	+0.3797	+0.2043	+9.00	-2.45	+6.07	+331.2
+270.0	+49.9	+95.7	+0.3164	+0.3134	+9.00	-3.73	+6.25	+347.3
+280.0	+49.1	+87.5	+0.2204	+0.4580	+9.00	-5.50	+6.93	+4.6
+290.0	+47.8	+78.4	+0.0742	+0.6543	+9.00	-7.35	+8.27	+19.2
+300.0	+45.5	+68.5	+0.1561	+0.9480	+9.00	-11.38	+10.56	+29.8
+310.0	+42.1	+57.9	+0.5493	+1.4457	+9.00	-17.33	+14.33	+34.4
+320.0	+37.7	+46.7	+1.3966	+2.5792	+9.00	-30.95	+22.02	+29.3
330	LINKAGE WILL NOT ASSEMBLE AT THIS POSITION.							
340	LINKAGE WILL NOT ASSEMBLE AT THIS POSITION.							
350	LINKAGE WILL NOT ASSEMBLE AT THIS POSITION.							

TABLE 4.2

FOUR BAR LINKAGE POSITIONS AND VELOCITIES

THIS IS A CROSSED TYPE LINKAGE.

LENGTH OF GROUND LINK R1 = 14
 LENGTH OF INPUT CRANK R2 = 9
 LENGTH OF COUPLER LINK R3 = 20
 LENGTH OF OUTPUT CRANK R4 = 12
 R5-DIST. FROM JOINT R2 AND R3 TO COUPLER POINT P = 10
 ANGLE BETWEEN R3 AND R5, DEGREES = 45
 ANGULAR VELOCITY OF INPUT CRANK, RAD/SEC = 1
 POSITION INCREMENT FOR INPUT CRANK, DEGREES = 10

THETA2 DEGREE	THETA3 DEGREE	THETA4 DEGREE	OMEGA3 RAD/S	OMEGA4 RAD/S	VEL-A IN/S	VEL-B IN/S	VEL-P IN/S	THETA-P DEGREE
0	LINKAGE WILL NOT ASSEMBLE AT THIS POSITION.							
10	LINKAGE WILL NOT ASSEMBLE AT THIS POSITION.							
20	LINKAGE WILL NOT ASSEMBLE AT THIS POSITION.							
30	LINKAGE WILL NOT ASSEMBLE AT THIS POSITION.							
+40.0	+298.9	+292.3	-1.3966	-2.5793	+9.00	-30.95	+1.66	+214.0
+50.0	+289.9	+263.2	-0.5493	-1.4458	+9.00	-17.35	+9.91	+175.0
+60.0	+295.5	+251.9	-0.1561	-0.9480	+9.00	-11.38	+9.91	+159.9
+70.0	+286.2	+243.6	+0.0742	-0.6543	+9.00	-7.85	+9.91	+155.3
+80.0	+337.7	+233.1	+0.2204	-0.4589	+9.00	-5.55	+9.91	+151.1
+90.0	+290.5	+234.3	+0.3164	-0.3154	+9.00	-3.79	+9.91	+147.2
+100.0	+294.0	+231.7	+0.3797	-0.2043	+9.00	-2.65	+9.91	+143.5
+110.0	+298.0	+230.1	+0.4203	-0.1123	+9.00	-1.35	+9.91	+140.0
+120.0	+302.3	+229.4	+0.4441	-0.0315	+9.00	-0.33	+9.91	+136.4
+130.0	+306.6	+229.4	+0.4549	+0.0428	+9.00	+0.51	+9.91	+132.9
+140.0	+311.1	+230.2	+0.4554	+0.1133	+9.00	+1.37	+9.91	+129.4
+150.0	+315.9	+231.7	+0.4475	+0.1939	+9.00	+2.21	+9.91	+126.0
+160.0	+320.0	+233.3	+0.4332	+0.2933	+9.00	+3.04	+9.91	+122.6
+170.0	+323.3	+235.0	+0.4139	+0.4139	+9.00	+3.87	+9.91	+119.2
+180.0	+327.0	+240.4	+0.3913	+0.5524	+9.00	+4.70	+9.91	+115.8
+190.0	+330.3	+244.6	+0.3671	+0.7007	+9.00	+5.53	+9.91	+112.4
+200.0	+333.5	+249.5	+0.3430	+0.8592	+9.00	+6.36	+9.91	+109.0
+210.0	+336.9	+255.1	+0.3202	+1.0277	+9.00	+7.19	+9.91	+105.6
+220.0	+340.4	+261.2	+0.2999	+1.2062	+9.00	+8.01	+9.91	+102.2
+230.0	+344.0	+267.9	+0.2831	+1.3947	+9.00	+8.84	+9.91	+98.8
+240.0	+347.7	+275.1	+0.2706	+1.5932	+9.00	+9.67	+9.91	+95.4
+250.0	+351.1	+282.9	+0.2631	+1.8017	+9.00	+10.50	+9.91	+92.0
+260.0	+354.5	+291.1	+0.2599	+2.0202	+9.00	+11.33	+9.91	+88.6
+270.0	+358.0	+299.7	+0.2585	+2.2587	+9.00	+12.16	+9.91	+85.2
+280.0	+361.5	+309.0	+0.2866	+2.5172	+9.00	+13.00	+9.91	+81.8
+290.0	+365.0	+319.1	+0.3231	+2.7957	+9.00	+13.83	+9.91	+78.4
+300.0	+368.3	+330.2	+0.3693	+3.0942	+9.00	+14.67	+9.91	+75.0
+310.0	+371.9	+343.2	+0.5495	+3.4127	+9.00	+15.50	+9.91	+71.6

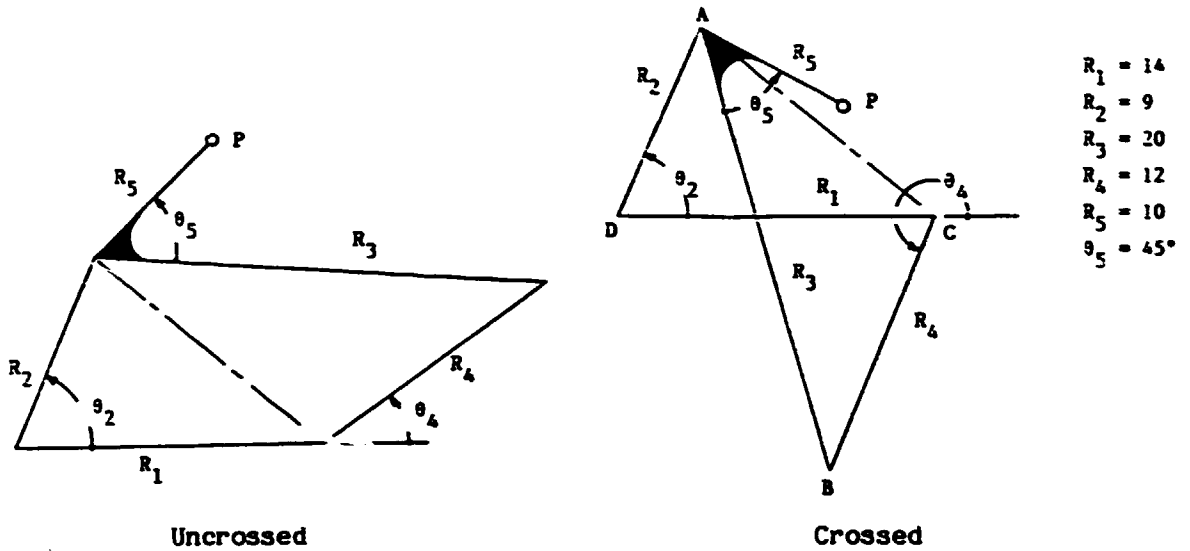


Figure 4.4 Four-Bar Linkages for Example Problem

The x-y coordinates of points A, B and P may now be plotted using the elementary graphics commands included in QuickBASIC. The commands used for this task are

CLS - Clears the screen on the monitor so a new graph may be started.

SCREEN 2 - Sets the specification to match the display screen with 640 x 200 pixels. Supports CGA, EGA, VGA and MCGA.

VIEW - Defines screen limits for graphical output.

WINDOW - Defines logical dimensions of current viewport.

LINE - Draws a line from one point to another.

CIRCLE - Draws a circle of specified radius around a specific center.

Before applying these commands, the size of the graph required must be determined. This is determined by performing a bubble sort on all x-dimensions and y-dimensions to determine the maximum and minimum

values of x and y required by the data for this problem. Since the data is in dimensioned arrays, this bubble sort is easily performed by a For-Next loop. After the maximum and minimum values of the x and y are determined, this information is combined with the information on Window size to obtain a scaling factor. Then all values of data are scaled to fit within the window. If screen width to height ratio is 4/3 and the ratio of y-pixels to x-pixels is 350/640, multiply x-dimensions by $(4/3)(350/640)$ to give true scale on plotter.

The graphical output for the mechanism is given in Figure 4.5. The computer program listing is given in Appendix C.

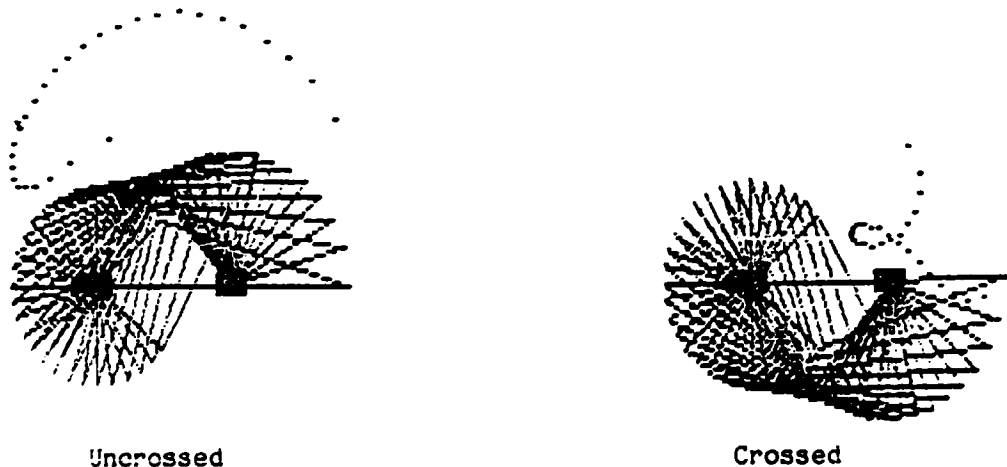


Figure 4.5 Graphical Output from FOURBAR Program

5. EXAMPLE FOUR: Synthesis

Synthesis is the process of "building up" a complex whole from simple elements. Synthesis is that creative step in the design process which invents a configuration for the solution to the previously defined problem. Analysis may be a sizing process, which may occur after the synthesis of the solution's configuration, to assure proper reliability and performance. However, analysis may become part of the

synthesis process. This example uses the design of a mechanism, which must produce a specific movement, to illustrate the use of synthesis in computer aided design. The dyad method used in this example is developed nicely by Sandor and Erdman in Reference 4.

The design problem is to synthesize a mechanism which will move a gear blank from position 1 to position 2 and then to position 3 for various manufacturing operations as shown in Figure 5.1. The design targets for the motion of this part are:

$\gamma_1 = 0$	$\delta_1 = 0$
$\gamma_2 = 40^\circ$	$\delta_2 = -2x + 6iy$
$\gamma_3 = 90^\circ$	$\delta_3 = -10x + 8iy$

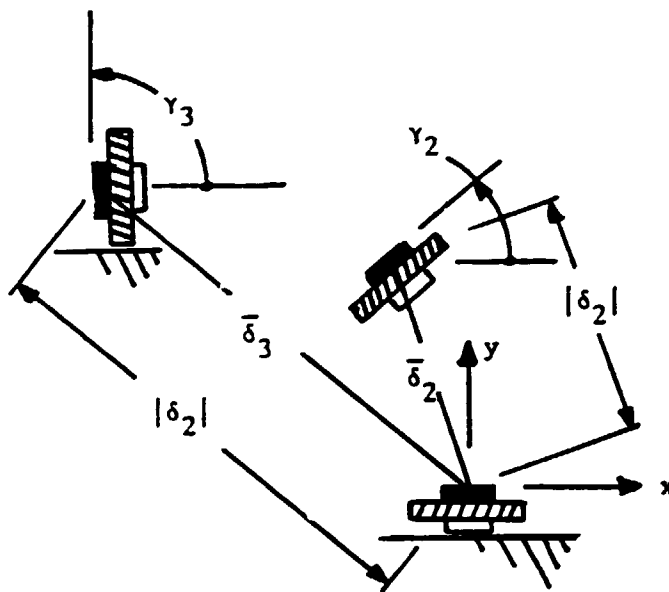


Figure 5.1 Gear Transport Problem Definition

If the solution is assumed to be in the form of a four bar mechanism, the lengths and positions for half of the mechanism may be synthesized by working with vectors \bar{W} and \bar{Z} to produce the desired displacements, $\bar{\delta}$, of P while the coupler link containing Z rotates through the desired angles γ . The vectors \bar{W} and \bar{Z} as shown in Figure 5.2 represent the original positions of the input crank, DA, and the line AP, respectively. The sum of \bar{W} plus \bar{Z} forms the vector pair, the dyad, for the initial position. This dyad is defined by the following vector equation

$$\bar{W} + \bar{Z} = W e^{i\theta_1} + Z e^{i\gamma_1}$$

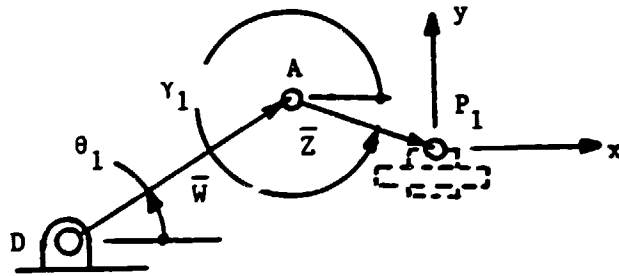


Figure 5.2 Dyad for Half of Four-Bar Mechanism

When the dyad moves to position 2, the displacement of P is $\bar{\delta}_2$ and the angle of rotation of the coupler link, which contains Z, is ξ_2 . Where,

$$\xi_2 = \gamma_2 - \gamma_1$$

The dyad in position 2 as illustrated in Figure 5.3 is given by the following vector equation.

$$\bar{w}_2 = We^{i(\theta_1 + \psi_2)} + Ze^{i(\gamma_1 + \epsilon_2)} = We^{i\theta_1} e^{i\psi_2} + Ze^{i\gamma_1} e^{i\epsilon_2}$$

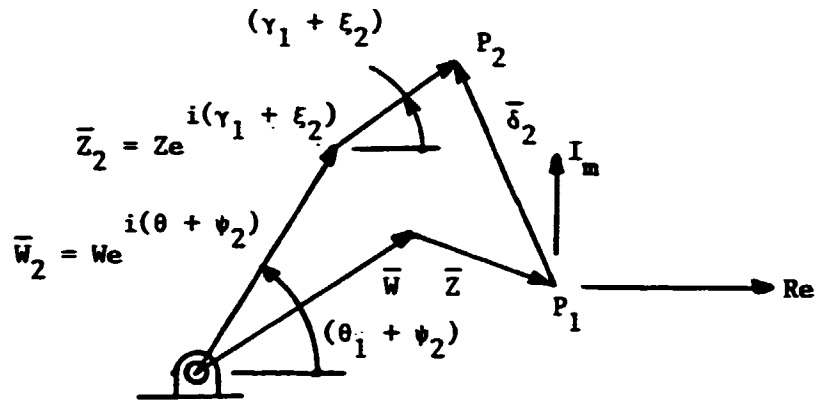


Figure 5.3 Dyad Moving from Position 1 to Position 2

The vector loop equation for positions 1 and 2 may be written as follows:

$$\bar{w}_2 = We^{i(\theta_1 + \psi_2)} + Ze^{i(\gamma_1 + \epsilon_2)} - We^{i\theta_1} - Ze^{i\gamma_1} = \bar{\delta}_2$$

or

$$\bar{w}(e^{i\psi_2} - 1) + \bar{z}(e^{i\epsilon_2} - 1) = \bar{\delta}_2$$

For the first and third positions the following equation may be written for the vector loop.

$$\bar{w}(e^{i\psi_3} - 1) + \bar{z}(e^{-i\epsilon_3} - 1) = \bar{\delta}_3$$

with,

$$\epsilon_3 = \gamma_3 - \gamma_1$$

These last two vector equations may be changed into four nonlinear algebraic equations by using the Euler's relationship from Figure 5.4.

The real or x component of the unit vector \bar{r} is Re and the imaginary or y component is I_m .

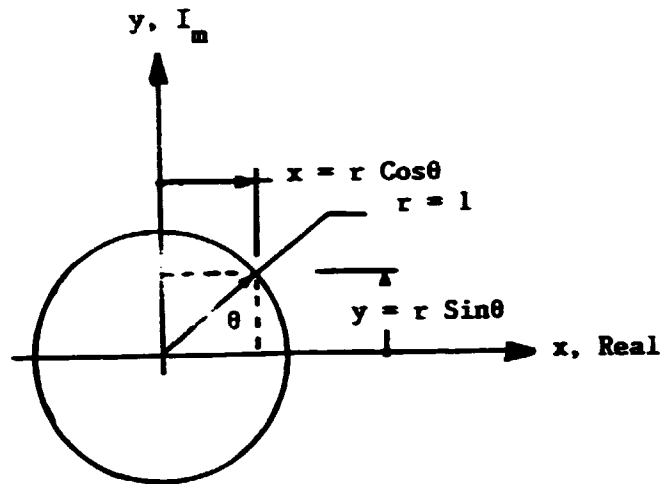


Figure 5.4 Unit Vector on Complex Plane

The two vector loop equations may be placed in matrix form.

$$\begin{vmatrix} (e^{i\psi_2} - 1) & (e^{i\xi_2} - 1) \\ (e^{i\psi_3} - 1) & (e^{i\xi_3} - 1) \end{vmatrix} \begin{vmatrix} \bar{W} \\ \bar{Z} \end{vmatrix} = \begin{vmatrix} \bar{\delta}_2 \\ \bar{\delta}_3 \end{vmatrix}$$

If the complex elements in the square matrix are expanded into real and imaginary components using Euler's relationship, this matrix equation becomes

$$\begin{vmatrix} (R_1 + iI_1) & (R_2 + iI_2) \\ (R_3 + iI_3) & (R_4 + iI_4) \end{vmatrix} \begin{vmatrix} \bar{W} \\ \bar{Z} \end{vmatrix} = \begin{vmatrix} \bar{\delta}_2 \\ \bar{\delta}_3 \end{vmatrix}$$

where,

$$\begin{aligned} R_1 &= \cos\psi_2 - 1 & I_1 &= \sin\psi_2 \\ R_2 &= \cos\xi_2 - 1 & I_2 &= \sin\xi_2 \\ R_3 &= \cos\psi_3 - 1 & I_3 &= \sin\psi_3 \\ R_4 &= \cos\xi_3 - 1 & I_4 &= \sin\xi_3 \end{aligned}$$

But, the other vectors may also be expanded into real and imaginary components.

$$\bar{W} = W_R + iW_I$$

$$\bar{Z} = Z_R + iZ_I$$

$$\bar{\delta}_2 = \delta_{2R} + i\delta_{2I}$$

$$\bar{\delta}_3 = \delta_{3R} + i\delta_{3I}$$

Substitution into the matrix of vector equations and separating the real and imaginary components produces the following matrix of four algebraic equations.

$$\begin{vmatrix} R_1 & -I_1 & R_2 & -I_2 \\ I_1 & R_1 & I_2 & R_2 \\ R_3 & -I_3 & R_4 & -I_4 \\ I_3 & R_3 & I_4 & R_4 \end{vmatrix} \begin{vmatrix} W_R \\ W_I \\ Z_R \\ Z_I \end{vmatrix} = \begin{vmatrix} \delta_{1R} \\ \delta_{1I} \\ \delta_{2R} \\ \delta_{2I} \end{vmatrix}$$

The above four algebraic equations contain the following unknowns:

$\psi_2, \psi_3, \xi_2, \xi_3, W_R, W_I, Z_R$ and Z_I . For the stated problem, values of rotation of the coupler link \bar{Z} are given:

$$\xi_2 = 40^\circ$$

$$\xi_3 = 90^\circ$$

Hence, there are four equations and six unknowns. In order to solve the equations, two of the remaining six variables must be defined. One method of solution would be to assume a value for each of the two angles, ψ_2 and ψ_3 . This changes the four equations from non-linear to linear equations and values for W_R, W_I, Z_R and Z_I may be obtained directly by Gauss elimination. The negatives of these values may be plotted from point P to locate the pivot point A and the ground pivot D.

The locations of all possible ground pivots, D, and their corresponding circle points, A, may be evaluated by performing the above procedure in a pair of nested do loops. The outer loop could vary ψ_3 through 360° in increments of perhaps 10° while the inner loop could

vary ψ_2 through 360° in similar increments. The two curves traced by these pairs of pivot point locations are Burmeister Curves and they define all possible design combinations which will perform the stated task. In order to manage the wide spread of data, a test of the values of W_R , W_I , Z_R and Z_I could be conducted and those values outside of the feasible region could be discarded prior to plotting the data.

6. EXAMPLE FIVE: Integration of Computer Aided Drafting with Computer Aided Design and Analysis

A program may calculate the sizes of four gears in a gear train configuration based on bending stress and contact stress. The data from the program may be transmitted to a Gear Generation Program, GGP. These two programs can be linked together by using the BASIC command CHAIN.

The GGP program formats the values of the dimensions of the gears so this information can be read by the computer aided drawing system, AutoCAD. The program generates the positions of the ends of each straight line section of the drawing, the positions of each arc section of the drawing, and the position and content of any text. Figure 6.1 identifies the positions of generic points on this standard drawing. The output is written to the Drawing Interchange File, otherwise known as the DXF file. The DXF file contains information needed by the AutoCAD software to create a drawing. (Other CAD systems may use IGES instead of DXF.)

The DXF file must be written in a specific arrangement, but many sections can be omitted for simplification. The file for this example is considered simple, since it uses only a few sections. The general file structure has five sections:

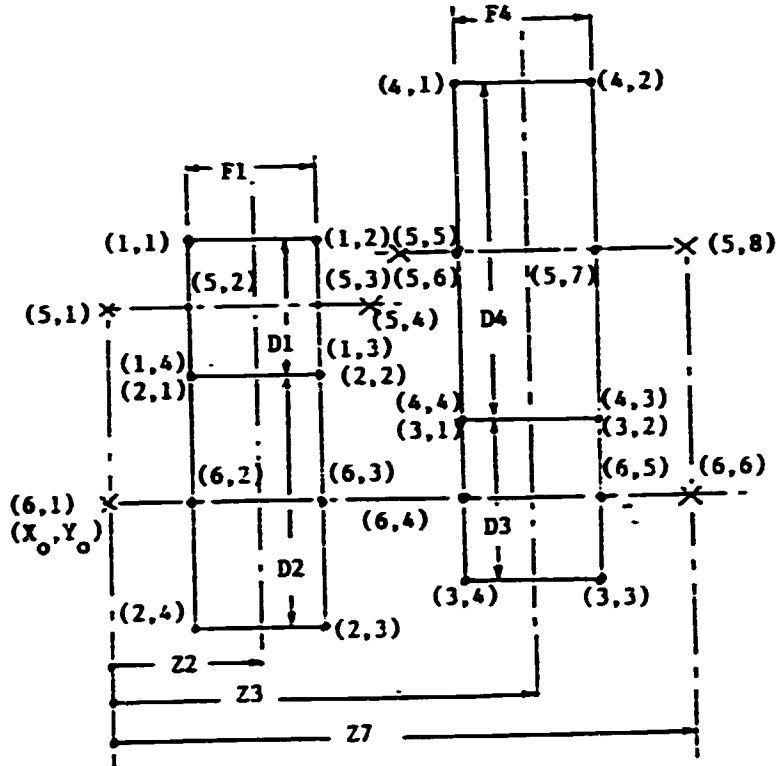


Figure 6.1 Generic Transmission with Coordinate Definition

A. HEADER section - General information about the drawing is found here. Each parameter of the HEADER section has a variable name and an associated value. This section may be omitted if no special settings are needed to complete the drawing.

B. TABLES section - This section defines named items such as line types, layers, text styles, and views. It may be omitted if not needed.

C. BLOCKS section - This section contains the entities for each block in the drawing. A block is a set of entities, such as lines, arcs, circles, and text, which when grouped together form a compound object. For example, a square can be drawn and be defined as a block called "square." Each time the block "square" is inserted into the drawing, the square appears. Usually blocks are much more complex and are used to eliminate repetitious drawing of components that are used frequently. The blocks section may also be omitted if no blocks are used.

D. ENTITIES section - This section contains the drawing entities, including any block references. The entity commands are as follows:

LINE	POINT	CIRCLE
ARC	SOLID	TEXT
INSERT	TRACE	

This is the main section of the program and in some instances the only section.

E. END OF FILE - This is the last section. It is the signal to AutoCAD that the file is complete. The program must end with this section.

DXF files are composed of multiple groups, each occupying two lines in the DXF file. The first line is a group code, which is a positive integer. The group value is the second line of the group. This value is in a format specified by the group code. The group codes are categorized in the following way:

<u>GROUP CODE RANGE</u>	<u>FOLLOWING VALUE</u>
0 - 9	String
10 - 59	Floating Point
60 - 79	Integer

After examining the outline of the DXF file, it is apparent that it has a definite pattern. After each "SECTION" is called, there is a 2 group code, which indicates that the name of the section follows. The Gear Generation Program in Appendix D shows that there is only one section, ENTITIES, plus the END OF FILE section that closes the program. On line 1300 a LINE INPUT statement is used to input a file name for the DXF file being created. In line 1400 the DXF file is opened and the following program can be written in the file. The command PRINT #1 must be used to write each bit of information to the DXF file.

The DXF file starts with a 0 group code, followed by SECTION. The section is then named by entering a 2 group code followed by the ENTITIES section name, so these are the first outputs of GGP. From line 1850 to line 2500, coordinates are calculated for the gear train using data calculated in the Gear Design program.

In lines 2800 through 3900, the outlines of the four gears are generated. The entity command LINE is used to accomplish this. The following commands are used in a subroutine to draw one line.

Definitions are to the right of each entry.

0	group code 0 precedes each entity
LINE	command to draw a line
8	group code for layer name
0	layer name for line (default)

10	group code for 1st x-coordinate
X1	1st x-coordinate
20	group code for 1st y-coordinate
Y1	1st y-coordinate
11	group code for 2nd x-coordinate
X2	2nd x-coordinate
21	group code for 2nd y-coordinate
Y2	2nd y-coordinate

The above group codes are always used in this manner. To draw a line, values would be assigned to X1, Y1, X2, and Y2. To draw a line connected to this first line, X2 and Y2 can be used as a first set of coordinates, then assign values to a set of new coordinates X3 and Y3. Lines 4000 through 6700 draw the axes of the gear train.

Calculations can be executed anywhere in the GGP program as long as they do not interfere with the order of commands in the DXF file.

Text is created in the file by using the following command series:

0	group code 0 precedes entity
TEXT	command to input text
8	layer group code
0	layer name (default)
10	group code for text start point (x-coord.)
X	x-coordinate start point
20	group code for text start point (y-coord.)
Y	y-coordinate start point
40	group code for text height
H	text height value

1 group code for text value

GEARS text value

At the end of the ENTITIES section and before END OF FILE, the DXF file must be closed. First, the section must be closed by another 0 group code followed by ENDSEC. The file is then closed by another 0 group code followed by EOF.

The listing of the DXF created by GGP is in Appendix E.

Figure 6.2 shows the drawing created by AutoCAD using a Gear Design Program and this Gear Generation Program.

Creating the DXF file by this method is complicated on personal computers. Larger mainframes have enhanced capability for graphical design.

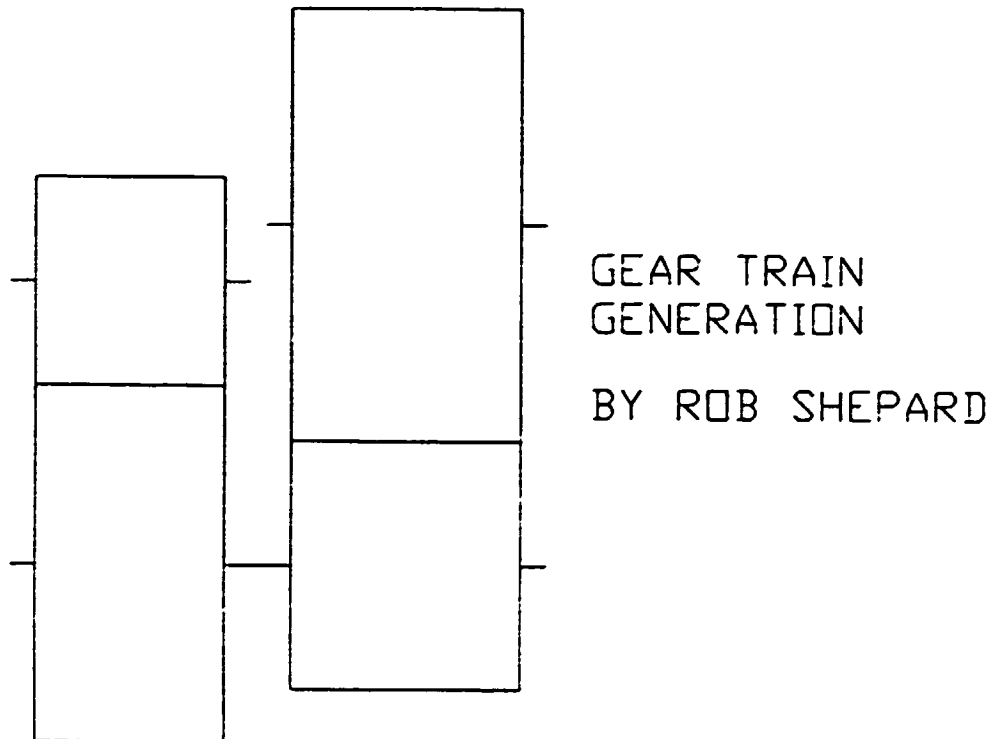


Figure 6.2 Four Gear Transmission Drawing from Automated Design Process

REFERENCE LIST

1. Beer, F. P. and Johnson, Jr., E. R., Vector Mechanics for Engineers: Statics, McGraw-Hill Book Co., 1972.
2. Hall, Jr., A. S., Kinematics and Linkage Design, BALT Publishers, West Lafayette, Indiana, 1966.
3. Paul, Burton, Kinematics and Dynamics of Planar Machinery, Prentice-Hall, Inc., Englewood Cliffs, New Jersey, 1979.
4. Sandor, G. N., and Erdman, A. G., Advanced Mechanism Design: Analysis and Synthesis, Vol. 2, Prentice-Hall, Inc., Englewood Cliffs, New Jersey, 1984.
5. Shigley, J. E., and Uicker, Jr., J. J., Theory of Machines and Mechanisms, McGraw-Hill Book Co., 1980.
6. Mable, H. H., Reinholtz, C. F., Mechanisms and Dynamics of Machinery, John Wiley and Sons, Inc., 1987.

APPENDIX A

PROGRAM : 'INERTIA'

```
1 LPRINT "                TORSIONAL STIFFNESS AND INERTIA"
2 LPRINT "                PROGRAM: INERTIA"
5 DIM K(40), I(40)
6 LPRINT
9 INPUT "TOTAL NUMBER OF DISCS": I2
10 WT = 0
11 K1 = 0
12 INERTIA = 0
14 INPUT "WEIGHT DENSITY OF MATERIAL, LB/IN3 (ENTER .293 FOR STEEL)= ": W1
16 LPRINT "                MATERIAL DENSITY = ": W1; " POUNDS/CUBIC INCH"
18 LPRINT "                NUMBER OF DISCS = ": I2
19 LPRINT

20 FOR I1 = 1 TO I2

21 LPRINT "                DISC NUMBER = ": I1
25 PRINT "DISK NUMBER =": I1

30 INPUT " OUTSIDE DIAMETER, IN =": D1
35 INPUT " INSIDE DIAMTER , IN =": D2
40 LPRINT "                OUTSIDE D'AMETER = ": D1; " INCHES"
50 LPRINT "                INSIDE DIAMETER = ": D2; " INCHES"
60 INPUT " LENGTH OF DISC , IN =": L
80 LPRINT "                LENGTH OF DISC = ": L; " INCHES"
82 W = 3.14159 * (D1 2 - D2 2) * L * W1 / 4
90 I(I1) = .5 * W1 * L * 3.1415 * ((D1 / 2) 4 - (D2 / 2) 4) / 386
100 INERTIA = INERTIA + I(I1)
102 K(I1) = 11500000 * 3.14159 * (D1 4 - D2 4) / (L * 32)
104 K1 = K1 + 1 / K(I1)
105 WT = WT + W
106 NEXT I1
107 K2 = 1 / K1
108 LPRINT "                TORSIONAL STIFFNESS = ": K2; " INCH POUNDS/RADIAN"
109 LPRINT "                SHAFT INERTIA = ": INERTIA; " IN. LB. SEC. SEC."
110 LPRINT "                TOTAL WEIGHT = ": WT; " POUNDS"
120 END
```

APPENDIX B

PROGRAM : "GEAFORC"

```

51 REM                                GENERALIZED BEARING REACTION PROGRAM
54 REM                                PROGRAM: "GEAFORC"
55 REM                                WRITTEN BY BRENT KNIGHT
56 REM                                MISSISSIPPI STATE UNIVERSITY
57 REM                                SPRING, 1988
59 REM
100 CLS
900 PI = 3.1415927#
910 PRINT "THIS PROGRAM CALCULATES THE REACTIONS AT THE TWO BEARINGS"
920 PRINT " WHICH SUPPORT A 'SHAFT' IN A HELICAL GEAR TRANSMISSION."
930 PRINT " THE WORD 'GEAR' REFERS TO THE GEAR ELEMENTS ON THIS 'SHAFT' AND"
940 PRINT " THE WORD 'PINION' REFERS TO THE ELEMENTS WHICH ARE IN MESH WITH"
950 PRINT " THE GEAR ELEMENTS ON THIS 'SHAFT'."
980 INPUT "SPEED OF 'SHAFT' (CCW IS POSITIVE), RPM          *"; SS
990 INPUT "TOTAL NUMBER OF 'PINIONS' MESHING WITH ALL 'GEARS' *"; NP
995 PRINT "BEARING 1 IS THE ORIGIN FOR THE RIGHT HAND"
996 PRINT " COORDINATE SYSTEM. THE DISTANCE FROM BEARING"
1000 PRINT " NUMBER 1 TO BEARING NUMBER 2 IS POSITIVE IF"
1006 PRINT " BEARING 2 IS TO THE RIGHT OF BEARING 1."
1007 INPUT "DISTANCE FROM BEARING 1 TO BEARING 2, IN          *"; DBB
1010 INPUT "TOTAL NUMBER OF 'GEARS' ON 'SHAFT'              *"; NOG
1020 INPUT "MAX NO. OF 'PINIONS' MESHING WITH ANY ONE 'GEAR' *"; MNP
1030 DIM THETA(NOG, MNP), GP(NOG), DG(NOG, MNP)
1035 CLS
1040 FOR N = 1 TO NOG: FOR M = 1 TO MNP: THETA(N, M) = 0: NEXT M: NEXT N
1050 FOR N = 1 TO NOG
1060 PRINT "GEAR NUMBER*"; N
1070 INPUT " NUMBER OF 'PINIONS' IN MESH WITH THIS GEAR*"; GP(N)
1075 PRINT "-----"
1080 FOR M = 1 TO GP(N)
1085 PRINT " PINION *"; M; "ON GEAR *"; N
1087 INPUT " IS THIS A DRIVEN PINION ? IF YES, THEN INPUT 1 ; IF NO, THEN INPUT
0"; DG(N, M): PRINT : PRINT
1090 INPUT " ANGULAR POSITION OF THE PINION"; THETA(N, M): THETA(N, M) = THETA(N
, M) * PI / 180
1100 NEXT M
1110 PRINT : PRINT : PRINT
1120 NEXT N
1130 DIM PA(NOG), HA(NOG), D(NOG, 2), N(NOG), P(NOG, MNP), PD(NOG), WTX(NOG, MNP
), WTY(NOG, MNP), WRX(NOG, MNP), WRY(NOG, MNP), WA(NOG, MNP), WT(NOG, MNP), WR(N
OG, MNP), NOTEETH(NOG), DPITCH(NOG)
1140 CLS
1150 FOR N = 1 TO NOG
1160 PRINT "FOR GEAR NUMBER"; N
1170 INPUT " PRESSURE ANGLE *"; PA(N)
1175 PA(N) = PA(N) * PI / 180
1190 INPUT " HELIX ANGLE *"; HA(N)
1195 HA(N) = HA(N) * PI / 180
1200 INPUT " DISTANCE FROM BEARING 1 TO GEAR CENTER*"; D(N, 1)
1205 D(N, 2) = D(N, 1) - DBB
1230 INPUT " DIAMETRAL PITCH*"; DPITCH(N)
1232 INPUT " NUMBER OF TEETH*"; NOTEETH(N)
1233 PRINT : PRINT
1235 PD(N) = NOTEETH(N) / (DPITCH(N) * COS(HA(N)))
1240 NEXT N
2000 FOR N = 1 TO NOG
2030 FOR M = 1 TO GP(N)
2035 PRINT " FOR PINION NUMBER"; M; "ON GEAR NUMBER"; N

```

```
2037 INPUT " INPUT HORSEPOWER.Hp =": P(N, M)
2040 WT(N, M) = P(N, M) * 33000 / (2 * PI * SS * PD(N) / 2)
2050 WR(N, M) = ABS(WT(N, M)) * TAN(PA(N)) / COS(HA(N))
2060 WTX(N, M) = -WT(N, M) * SIN(THETA(N, M))
2070 WTY(N, M) = WT(N, M) * COS(THETA(N, M))
2072 IF DG(N, M) = 1 THEN WTX(N, M) = -WTX(N, M): WTY(N, M) = -WTY(N, M)
2080 WRX(N, M) = -WR(N, M) * COS(THETA(N, M))
2090 WRY(N, M) = -WR(N, M) * SIN(THETA(N, M))
2110 WA(N, M) = -WT(N, M) * TAN(HA(N))
2115 IF DG(N, M) = 1 THEN WA(N, M) = -WA(N, M)
2120 NEXT M
2130 CLS
2140 NEXT N
3000 INPUT "NUMBER OF EXTERNAL LOADS IN THE X-DIR.=": NFX
3010 INPUT "NUMBER OF EXTERNAL LOADS IN THE Y-DIR.=": NFY
3030 DIM FX(NFX, 3), FY(NFY, 3)
3040 FOR N = 1 TO NFX
3045 PRINT "THE SIGN CONVENTION IS RIGHT HAND RULE WITH Z POSITIVE TO THE RIGHT"
3046 PRINT "AND Y POSITIVE UPWARD AND X POSITIVE INWARD. THE ORIGIN IS AT BEARING"
3047 PRINT
3050 PRINT "FOR FORCE FX": N
3060 INPUT " MAGNITUDE OF FORCE IN X DIRECTION (INWARD IS POSITIVE), LB=": FX(N, 1)
3070 INPUT " DISTANCE FROM BEARING #1 TO FORCE FX (TO THE RIGHT IS POS.), IN=":
FX(N, 2)
3075 FX(N, 3) = FX(N, 2) * DBB
3080 CLS
3090 NEXT N
3100 CLS
3110 FOR N = 1 TO NFY
3115 PRINT "IF A FORCE IS ACTING TO THE RIGHT OF THE SPECIFIED BEARING IT IS A P"
3120 PRINT "OSITIVE DISTANCE FROM THE BEARING.": PRINT : PRINT : PRINT
3120 PRINT "FOR FORCE FY": N
3130 INPUT " MAGNITUDE OF FORCE IN Y DIRECTION (DOWN IS NEGATIVE), LB=": FY(N, 1)
3140 INPUT " DISTANCE FROM BEARING #1 TO FORCE FY (TO THE RIGHT IS POS.), IN=":
FY(N, 2)
3145 FY(N, 3) = FY(N, 2) * DBB
3150 CLS
3160 NEXT N
3170 CLS
3750 SX = (NP * NFX) * 3: SY = (NP * NFY) * 3
3750 DIM MX1(3, SX), MY1(3, SY), MX2(3, SX), MY2(3, SY)
3900 FOR I = 1 TO 3: FOR II = 1 TO SX: MX1(I, II) = 0: NEXT II: NEXT I
3920 FOR I = 1 TO 3: FOR II = 1 TO SX: MX2(I, II) = 0: NEXT II: NEXT I
3640 FOR I = 1 TO 3: FOR II = 1 TO SY: MY1(I, II) = 0: NEXT II: NEXT I
3860 FOR I = 1 TO 3: FOR II = 1 TO SY: MY2(I, II) = 0: NEXT II: NEXT I
4020 II = -2
4030 FOR M = 1 TO NOG
4050 FOR NN = 1 TO GP(M)
4060 II = II + 3
4100 MX1(2, II + 1) = 1 / 2 * PD(M) * SIN(THETA(M, NN))
4103 MX1(2, II + 2) = D(M, 1)
4106 MX1(3, II + 1) = WTY(M, NN) * WRY(M, NN)
4109 MX1(3, II + 2) = WA(M, NN)
4112 REM
4115 MY1(2, II + 1) = 1 / 2 * PD(M) * COS(THETA(M, NN))
4118 MY1(2, II + 2) = D(M, 1)
4121 MY1(3, II + 1) = WTX(M, NN) * WRX(M, NN)
4124 MY1(3, II + 2) = WA(M, NN)
4127 REM
4130 MX2(2, II + 1) = 1 / 2 * PD(M) * SIN(THETA(M, NN))
4133 MX2(2, II + 2) = D(M, 2)
4135 MX2(3, II + 1) = WTY(M, NN) * WRY(M, NN)
4138 MX2(3, II + 2) = WA(M, NN)
```

```
4142 REM
4145 MY2(2, II - 1) = 1 / 2 * PD(M) * COS(THETA(M, NN))
4148 MY2(2, II - 2) = D(M, 2)
4151 MY2(3, II - 1) = WTX(M, NN) * WEX(M, NN)
4154 MY2(3, II - 2) = WA(M, NN)
4155 REM
4160 NEXT NN
4170 NEXT M
4172 REM
4175 JJ = II
4177 REM
4178 REM FORCES FOR SUM OF MOMENTS ABOUT BRG 1 AND BRG 2 IN THE X-DIR
4181 REM
4185 FOR M = 1 TO NFY
4190 II = II + 3
4250 MX1(2, II - 2) = FY(M, 2): MX2(2, II + 2) = FY(M, 3)
4270 MX1(3, II + 1) = FY(M, 1): MX2(3, II + 1) = FY(M, 1)
4290 NEXT M
4381 REM
4382 REM FORCES FOR SUM OF MOMENTS ABOUT BRG 1 AND BRG 2 IN THE Y-DIR
4384 REM
5000 FOR M = 1 TO NFX
5010 JJ = JJ + 3
5040 MY1(2, JJ - 2) = FX(M, 2): MY2(2, JJ + 2) = FX(M, 3)
5050 MY1(3, JJ + 1) = FX(M, 1): MY2(3, JJ + 1) = FX(M, 1)
5060 NEXT M
5993 REM
5994 REM CALCULATE THE BEARING REACTIONS BY MATRIX EXPANSION
5995 REM
5999 R1X = 0: R2X = 0: R2Y = 0: R1Y = 0
6000 FOR I = 2 TO SX - 1 STEP 3
6020 R2Y = MX1(2, I) * MX1(3, I + 1) - MX1(2, I + 1) * MX1(3, I) + R2Y
6025 R1Y = MX2(2, I) * MX2(3, I + 1) - MX2(2, I + 1) * MX2(3, I) + R1Y
6027 NEXT I
6029 FOR I = 2 TO SY - 1 STEP 3
6030 R2X = MY1(2, I) * MY1(3, I + 1) - MY1(2, I + 1) * MY1(3, I) + R2X
6035 R1X = MY2(2, I) * MY2(3, I + 1) - MY2(2, I + 1) * MY2(3, I) + R1X
6040 NEXT I
6060 R2Y = R2Y / DBB: R2X = R2X / DBB: R1Y = R1Y / -DBB: R1X = R1X / -DBB
6070 GOTO 9000
6072 LPRINT TAB(12): "FOR BEARING NUMBER 1:"
6075 R1 = INT(SQR(R1X2 + R1Y2)): LPRINT TAB(15): "R1 = ": R1: " POUNDS"
6080 R1Y = INT(R1Y): LPRINT TAB(17): "R1Y = ": R1Y: " POUNDS"
6085 R1X = INT(R1X): LPRINT TAB(17): "R1X = ": R1X: " POUNDS": LPRINT
6086 LPRINT TAB(12): "FOR BEARING NUMBER 2:"
6087 R2 = INT(SQR(R2X2 + R2Y2)): LPRINT TAB(15): "R2 = ": R2: " POUNDS"
6090 R2Y = INT(R2Y): LPRINT TAB(17): "R2Y = ": R2Y: " POUNDS"
6095 R2X = INT(R2X): LPRINT TAB(17): "R2X = ": R2X: " POUNDS": LPRINT
7000 FOR N = 1 TO NOG
7020 FOR M = 1 TO MNP
7040 WA = WA + WA(N, M): WA = INT(WA)
7060 NEXT M
7080 NEXT N
7100 LPRINT : LPRINT TAB(12): "THE TOTAL AXIAL LOAD, WA = ": WA: " POUNDS"
7200 END
7210 LPRINT
9000 LPRINT TAB(10): "BEARING REACTIONS IN HELICAL GEAR TRANSMISSIONS"
9005 LPRINT
9010 LPRINT TAB(24): "PROGRAM: GEARFORC": LPRINT
9015 LPRINT TAB(10): "THE INPUT DATA : "
9018 LPRINT
9020 LPRINT TAB(15): "THERE ARE": NOG: "GEARS"
9040 LPRINT TAB(15): "THERE ARE A TOTAL OF ": NP: "PINION(S)"
9060 LPRINT TAB(15): "NO GEAR HAS MORE THAN": MNP: "PINION(S)"
9080 LPRINT TAB(15): "THE DISTANCE BETWEEN BEARINGS IS": DBB: "INCHES"
9085 LPRINT TAB(15): "THE SHAFT SPEED IS ": SG: "RPM"
```

```

9150 LPRINT
9200 FOR N = 1 TO NOG
9210 LPRINT TAB(10): "FOR GEAR NUMBER": N
9215 LPRINT TAB(15): "GEAR NUMBER": N; "HAS": GP(N); "PINION(S)"
9260 LPRINT TAB(15): "PRESSURE ANGLE          =": PA(N) * 180 / PI; "DE
GREES"
9290 LPRINT TAB(15): "HELIX ANGLE          =": HA(N) * 180 / PI; "DE
GREES"
9300 LPRINT TAB(15): "DISTANCE FROM BRG. 1 TO GEAR": N; "= ": D(N, 1); "INCHES"
9310 LPRINT TAB(15): "DISTANCE FROM BRG. 2 TO GEAR": N; "= ": D(N, 2); "INCHES"
9320 LPRINT TAB(15): "PITCH DIAMETER          =": PD(N); "INCHES"
9322 LPRINT TAB(15): "THE NORMAL DIAMETRAL PITCH    =": DPITCH(N); "TEETH/IN.
"
9324 LPRINT TAB(15): "NUMBER OF TEETH ON GEAR      = ": NOTEETH(N)
9330 LPRINT
9350 REM NEXT N
9490 LPRINT
9500 REM FOR N=1 TO NOG
9520 FOR M = 1 TO GP(N)
9540 LPRINT TAB(13): "FOR PINION": M; "ON GEAR": N
9560 LPRINT
9565 IF DG(N, M) = 0 THEN AS = " DRIVING "
9570 IF DG(N, M) = 1 THEN AS = " DRIVEN "
9575 LPRINT TAB(15): "PINION NUMBER": N; "IS A": AS; "PINION"
9580 LPRINT TAB(15): "ANGULAR POSITION = ": THETA(N, M) * 180 / PI; "DEGREES"
9600 LPRINT TAB(15): "INPUT POWER          = ": P(N, M); "HORSEPOWER"
9620 NEXT M
9640 LPRINT
9660 NEXT N
9665 IF NFX > 0 THEN GOTO 9680
9667 IF NFY = 0 THEN GOTO 9780
9680 LPRINT
9700 LPRINT TAB(10): "THE EXTERNAL LOADS : "
9720 LPRINT
9730 FOR N = 1 TO NFX
9740 LPRINT TAB(15): "FX": N; " = ": FX(N, 1); "POUNDS"
9750 LPRINT TAB(15): "FX": N; "IS ": FX(N, 2); "INCHES FROM BRG 1"
9760 LPRINT TAB(15): "FX": N; "IS ": FX(N, 3); "INCHES FROM BRG 2"
9765 LPRINT
9770 NEXT N
9775 LPRINT
9780 FOR N = 1 TO NFY
9790 LPRINT TAB(15): "FY": N; " = ": FY(N, 1); "POUNDS"
9800 LPRINT TAB(15): "FY": N; "IS ": FY(N, 2); "INCHES FROM BRG 1"
9910 LPRINT TAB(15): "FY": N; "IS ": FY(N, 3); "INCHES FROM BRG 2"
9815 LPRINT
9820 NEXT N
9825 IF NFY = 0 THEN GOTO 10000
9850 REM -----
10000 LPRINT CHR$(12)
10001 LPRINT : LPRINT : LPRINT
10002 LPRINT TAB(10): "                                RESULTS": LPRINT
10005 LPRINT TAB(10): "                                GEAR TOOTH FORCES:"
10010 LPRINT
10020 FOR N = 1 TO NOG
10045 LPRINT TAB(12): "GEAR NUMBER": N
10060 FOR M = 1 TO GP(N)
10065 LPRINT TAB(12): " PINION NUMBER": M
10070 LPRINT
10075 WT(N, M) = INT(WT(N, M))
10080 WTX(N, M) = INT(WTX(N, M))
10085 WTY(N, M) = INT(WTY(N, M))
10090 WR(N, M) = INT(WR(N, M))
10095 WRX(N, M) = INT(WRX(N, M))
10097 WRY(N, M) = INT(WRY(N, M))
10100 LPRINT TAB(15): "THE TANGENTIAL TOOTH LOAD IS          = ": WT(N, M);

```



```
" POUNDS"
10120 LPRINT TAB(15); " THE X-COMP. OF THE TANG. TOOTH LOAD IS = ": WTX(N, M):
" POUNDS"
10140 LPRINT TAB(15); " THE Y-COMP. OF THE TANG. TOOTH LOAD IS = ": WTY(N, M):
" POUNDS"
10160 LPRINT TAB(15); "THE RADIAL TOOTH LOAD IS = ": WR(N, M):
" POUNDS"
10180 LPRINT TAB(15); " THE X-COMP. OF THE RADIAL TOOTH LOAD IS = ": WRX(N, M):
" POUNDS"
10200 LPRINT TAB(15); " THE Y-COMP. OF THE RADIAL TOOTH LOAD IS = ": WRY(N, M):
" POUNDS"
10210 LPRINT TAB(15); "THE AXIAL (Z-COMPONENT) TOOTH LOAD IS = ": WA(N, M):
" POUNDS"
10220 NEXT M
10240 LPRINT
10260 NEXT N
10400 LPRINT
10420 LPRINT TAB(10); " BEARING REACTIONS:"
10440 LPRINT
10450 LPRINT : GOTO 6072
10500 END
```


APPENDIX D

Program : " Gear Generation Program"

```
1000 REM
1100 REM GEAR TRAIN DRAWING GENERATOR
1200 REM
1250 DIM PTX(20,20),PTY(20,20)
1300 LINE INPUT "DRAWING (DXF) FILE NAME: ";A$
1400 OPEN "O".1,A$+"DXF"
1500 PRINT #1,C
1500 PRINT #1,"SECTION"
1700 PRINT #1, 2
1800 PRINT #1,"ENTITIES"
1850 X0=4:Y0=8
1900 PTX(1,1)= X0 + Z2 - F1/2
1910 PTY(1,1)= Y0 + D1 + D2/2
1920 PTX(1,2)= X0 + Z2 + F1/2
1930 PTY(1,2)= Y0 + D1 + D2/2
1940 PTX(1,3)= X0 + Z2 + F1/2
1950 PTY(1,3)= Y0 + D2/2
1960 PTX(1,4)= X0 + Z2 - F1/2
1970 PTY(1,4)= Y0 + D2/2
1975 PTX(1,5)= PTX(1,1)
1976 PTY(1,5)= PTY(1,1)
1980 PTX(2,1)= X0 + Z2 - F2/2
1990 PTY(2,1)= Y0 + D2/2
2000 PTX(2,2)= X0 + Z2 + F2/2
2010 PTY(2,2)= Y0 + D2/2
2020 PTX(2,3)= X0 + Z2 + F2/2
2030 PTY(2,3)= Y0 - D2/2
2040 PTX(2,4)= X0 + Z2 - F2/2
2050 PTY(2,4)= Y0 - D2/2
2055 PTX(2,5)= PTX(2,1)
2056 PTY(2,5)= PTY(2,1)
2060 PTX(3,1)= X0 + Z3 - F3/2
2070 PTY(3,1)= Y0 + D3/2
2080 PTX(3,2)= X0 + Z3 + F3/2
2090 PTY(3,2)= Y0 + D3/2
2100 PTX(3,3)= X0 + Z3 + F3/2
2110 PTY(3,3)= Y0 - D3/2
2120 PTX(3,4)= X0 + Z3 - F3/2
2130 PTY(3,4)= Y0 - D3/2
2135 PTX(3,5)=PTX(3,1)
2136 PTY(3,5)=PTY(3,1)
2140 PTX(4,1)= X0 + Z3 - F4/2
2150 PTY(4,1)= Y0 + D4 + D3/2
2160 PTX(4,2)= X0 + Z3 + F4/2
2170 PTY(4,2)= Y0 + D4 + D3/2
2180 PTX(4,3)= X0 + Z3 + F4/2
2190 PTY(4,3)= Y0 + D3/2
2200 PTX(4,4)= X0 + Z3 - F4/2
2210 PTY(4,4)= Y0 + D3/2
2215 PTX(4,5)=PTX(4,1)
2216 PTY(4,5)=PTY(4,1)
2220 PTX(5,1)= X0
2230 PTY(5,1)= Y0 + (D1 + D2)/2
2240 PTX(5,2)= X0 + Z2 - F1/2
2250 PTY(5,2)= PTY(5,1)
2260 PTX(5,3)= X0 + Z2 + F1/2
2270 PTY(5,3)= PTY(5,1)
2280 PTX(5,4)= X0 + Z + Z2
2290 PTY(5,4)= PTY(5,1)
2300 PTX(5,5)= X0 + Z2 - Z2
2310 PTY(5,5)= Y0 + (D3 + D4) / 2
2320 PTX(5,6)= X0 + Z2 - F4/2
2330 PTY(5,6)= PTY(5,5)
2340 PTX(5,7)= X0 + Z2 + F4/2
```

```
2350 PTY(5,7) = PTY(5,5)
2360 PTX(5,8) = X0 + Z7
2370 PTY(5,8) = PTY(5,5)
2380 PTX(6,1) = X0
2390 PTY(6,1) = Y0
2400 PTX(6,2) = X0 + Z2 - F2/2
2410 PTY(6,2) = Y0
2420 PTX(6,3) = X0 + Z2 + F2/2
2430 PTY(6,3) = Y0
2440 PTX(6,4) = X0 + Z3 - F3/2
2450 PTY(6,4) = Y0
2460 PTX(6,5) = X0 + Z3 + F3/2
2470 PTY(6,5) = Y0
2480 PTX(6,6) = X0 + Z7
2490 PTY(6,6) = Y0
```

```
2500 REM
2600 REM
2700 REM
```

```
2800 FOR I=1 TO 4
2850 FOR J=1 TO 4
2900 PRINT #1,0
3000 PRINT #1,"LINE"
3100 PRINT #1,8
3200 PRINT #1,"0"
3400 PRINT #1,10
3500 PRINT #1,PTX(I,J)
3600 PRINT #1,20
3700 PRINT #1,PTY(I,J)
3710 PRINT #1,11
3720 PRINT #1,PTX(I,J-1)
3730 PRINT #1,21
3740 PRINT #1,PTY(I,J-1)
3800 NEXT J
3900 NEXT I
```

This Draws Gears

```
4000 FOR J=1 TO 7 STEP 2
4100 PRINT #1,0
4200 PRINT #1,"LINE"
4300 PRINT #1,5
4400 PRINT #1,"0"
4500 PRINT #1,10
4600 PRINT #1,PTX(5,J)
4700 PRINT #1,20
4800 PRINT #1,PTY(5,J)
4900 PRINT #1,11
5000 PRINT #1,PTX(5,(J+1))
5100 PRINT #1,21
5200 PRINT #1,PTY(5,(J+1))
5300 NEXT J
```

This Draws Axis for Gears 1 & 4

```
5400 FOR J=1 TO 5 STEP 2
5500 PRINT #1,0
5600 PRINT #1,"LINE"
5700 PRINT #1,5
5800 PRINT #1,"0"
5900 PRINT #1,10
6000 PRINT #1,PTX(6,J)
6100 PRINT #1,20
6200 PRINT #1,PTY(6,J)
6300 PRINT #1,11
6400 PRINT #1,PTX(6,(J+1))
6500 PRINT #1,21
6600 PRINT #1,PTY(6,(J+1))
6700 NEXT J
6800 PRINT #1,0
6900 PRINT #1,"ENDSEC"
7000 PRINT #1,0
7100 PRINT #1,"EOF"
```

This Draws Axis of Shaft for Gears 2 & 3

```
7200 CLOSE 1
7300 END
```

APPENDIX E

File : "Drawing Interchange File"

0	8	11
SECTION	0	30.99147
2	10	21
ENTITIES	5.3	14.39639
0	20	0
LINE	17.19481	LINE
8	11	8
0	15.33833	0
10	21	10
5.3	17.19481	30.99147
20	0	20
27.98872	LINE	14.39639
11	8	11
15.33833	0	30.99147
21	10	21
27.98872	15.33833	1.60361
0	20	0
LINE	17.19481	LINE
8	11	8
0	15.33833	0
10	21	10
15.33833	-1.19481	30.99147
20	0	20
27.98872	LINE	1.60361
11	8	11
15.33833	0	18.83833
21	10	21
17.19481	15.33833	1.60361
0	20	0
LINE	-1.19481	LINE
8	11	8
0	5.3	0
10	21	10
15.33833	-1.19481	18.83833
20	0	20
17.19481	LINE	1.60361
11	8	11
5.3	0	18.83833
21	10	21
17.19481	5.3	14.39639
0	20	0
LINE	-1.19481	LINE
8	11	8
0	5.3	0
10	21	10
5.3	17.19481	18.83833
20	0	20
17.19481	LINE	36.78375
11	8	11
5.3	0	30.99147
21	10	21
27.98872	18.83833	36.78375
0	20	0
LINE	14.39639	LINE

8	11	9
0	16.87833	0
10	21	10
20.99147	22.59177	20.99147
20	0	20
26.78375	LINE	9
11	8	11
20.99147	0	32.29147
21	10	21
14.39639	17.50833	9
0	20	0
LINE	25.59007	TEXT
8	11	8
0	19.90833	0
10	21	10
20.99147	25.59007	24.79147
20	0	20
14.39639	LINE	22.59007
11	8	40
19.80833	0	1.5
21	10	1
14.39639	20.99147	GEAR TRAIN
0	20	0
LINE	25.59007	TEXT
8	11	8
0	22.29147	0
10	21	10
13.80833	25.59007	24.79147
20	0	20
14.39639	LINE	20.09007
11	8	40
18.30833	0	1.5
21	10	1
26.78375	4	GENERATION
0	20	0
LINE	9	TEXT
8	11	8
0	5.0	0
10	21	10
4	9	24.79147
20	0	20
22.59177	LINE	15.59007
11	8	40
5.0	0	1.5
21	10	1
22.59177	15.00833	BY ROB SHEPARD
0	20	0
LINE	8	ENDSEC
8	11	0
0	18.80833	EOF
10	21	02
15.00833	9	GENERATION
20	0	
22.59177	LINE	

LECTURE 2

Predicting the Performance of Dynamic Mechanical Systems

Abstract:

A mathematical model may be used to evaluate the performance of high speed machines. This model may be used to predict the contribution of various design variables to the required specifications. This paper reviews some aspects of dynamic systems: model formulation, solutions of equations, numerical integration, sensitivity studies, and optimization.

1. Introduction

Mathematical models are used to design dynamic systems which must meet specific performance criteria. For example, the performance of a vehicle with different design parameters may be predicted for a specific duty cycle. Or the displacement versus time characteristic of a variable speed mechanism may be evaluated. The model may be used to optimize the performance of the system and it may be used to quantify the sensitivity of the performance to changes in each design variable. However, the configuration of the machine is also constrained by considerations of economics, safety, aesthetics, manufacturability and standards. The accuracy of the model's predictions is an important consideration. The quest for the absolute model may lead the engineer through infinite difficulties according to Professor B. E. Quinn of Purdue University.

This paper gives a review of some fundamental concepts which are used in dynamic modeling of machines. The solution of algebraic and differential equations is discussed. The need for sensitivity studies is presented. An optimization program is described and illustrated.

2. Fundamental Concepts for Modeling

The dynamic model of a machine is the mathematical relationship between variables based on physical laws. The following tasks are included in the modeling activity:

- 2.1 Identification of the required output
- 2.2 Identification of the duty cycle
- 2.3 Definition of the system's mass, elastic and damping characteristics
- 2.4 Identification of the excitation and restraints
- 2.5 Specification of the design variables to be considered
- 2.6 Application of Newton's and Euler's equations of motion plus the equations of continuity and constraint to produce a system of equations which will predict the required output in terms of the specified design variables.

The output required from the model should be identified as the first step. If the model is to be used to design for improved performance, the variables which account for good performance must be identified. For example, good performance of a forklift truck may be related to the number of pallets moved per day. If the model is to be used to reduce cost, the energy consumption would be a significant variable. If the model is to be used to predict torsional vibrations, the combining of one inertia with an adjacent inertia will reduce the complexity of the problem, but it also eliminates one degree of freedom and its related mode of vibration from the solution. Hence, the desired output significantly affects the mathematics of the model.

The identification of a duty cycle for a machine is essential in order to predict performance. Several different duty cycles may be used if the application of the machine varies. For example, a forklift truck operating in a lumber yard has significantly different operating requirements than when operating in a warehouse per Figure 2.1. The duty cycle may require different configurations of the system. For example, the torsional vibration of a fishing vessel with a food processing plant (Figure 2.2) may have different duty cycles with different power outputs for the following drivetrain configurations:

Engine at idle speed and all clutches disengaged.

Engine at rated speed and clutch to generator engaged.

Engine at rated speed and clutches to generator and propeller engaged.

Engine not at rated speed, propeller engaged, and generator off line.

Shipping and Receiving Cycle

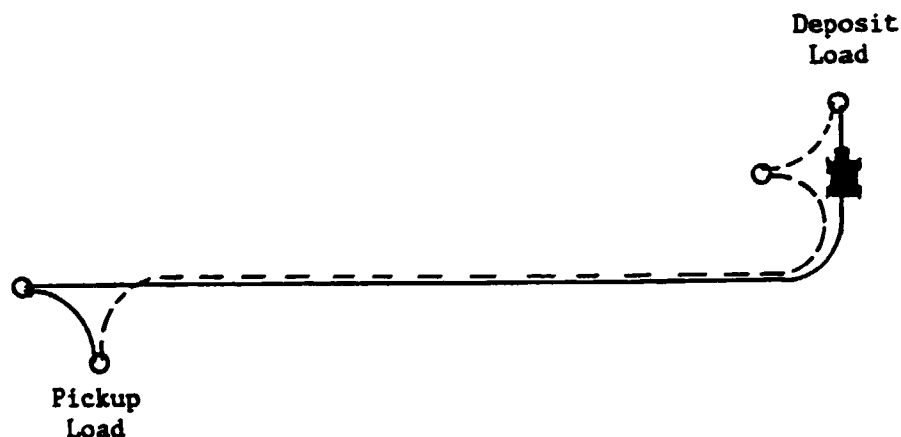


Figure 2.1 Forklift Truck Duty Cycles

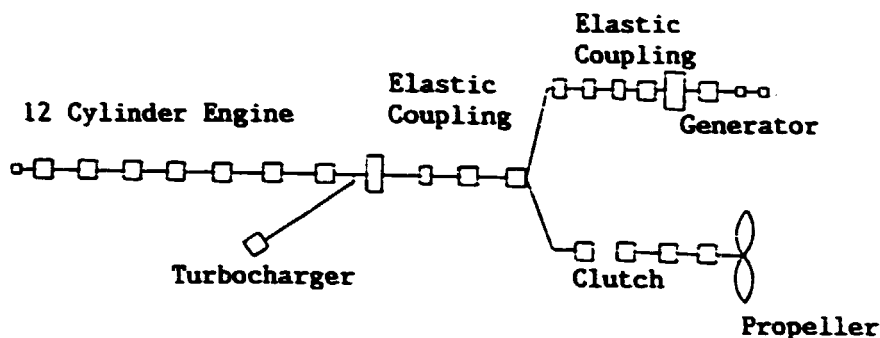


Figure 2.2 Factory Ship Power Train Mass-Elastic Diagram

The mass, elastic and dissipative characteristics of the machine are required for the equations of motion. Hence, the configuration of the machine must be developed before the model can be formulated. The mathematical model of the machine must be complex enough to produce the required output, but simple enough to allow completion of the analysis within the cost and time constraints. The number of equations in the model may be reduced by using equivalent masses, equivalent inertias, equivalent spring rates and equivalent damping. Careful judgement must be used when reducing the original system to these equivalent quantities in order to assure that the mathematical model will properly represent the original system.

Equivalent mass of a system may be determined by writing the different equations for the system and combining them into one differential equation with a single variable representing all of the mass and inertia terms. For the geared system of Figure 2.3, this procedure is as follows. The equations of motion for the pinion and for the gear are:

$$I_p \alpha_p = T_{in} + T_{Gp}$$

$$I_G \alpha_G = T_{pG} + T_{out}$$

The angular displacement relationship for pinion and gear is:

$$\theta_p = - \theta_G * \text{Ratio.}$$

The second derivative gives the angular acceleration relationship:

$$\alpha_p = - \alpha_G * \text{Ratio.}$$

A C.C.W. torque on the gear by the pinion will produce a C.C.W. torque on the pinion due to the reaction of the gear:

$$T_{pG} = + T_{Gp} * \text{Ratio.}$$

Substituting these equations into the differential equation for the gear gives:

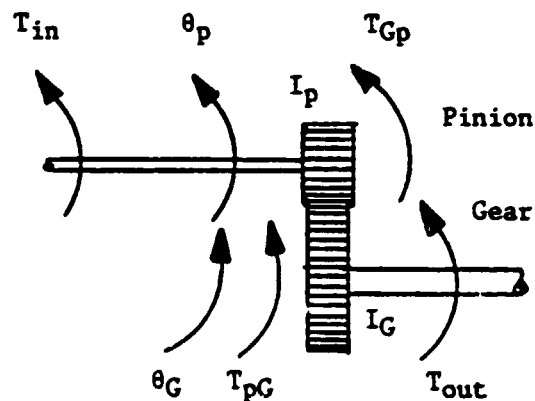
$$I_G(- \alpha_p/\text{Ratio}) = + T_{Gp} * \text{Ratio} + T_{out}$$

Divide by Ratio,

$$I_G \alpha_p/\text{Ratio}^2 = - T_{Gp} - T_{out}/\text{Ratio}$$

Add this latter differential equation to the first differential equation:

$$(I_p + I_G/\text{Ratio}^2)\alpha_p = T_{in} - T_{out}/\text{Ratio}$$



All variables are shown in the positive direction, CCW.

Figure 2.3 Original Mass-Elastic Diagram for Geared System

If the original system is replaced by an equivalent system as shown in Figure 2.4 in which all shafts rotate at engine speed, the sign of T_{out} is reversed and the differential equation for the gear pair would be:

$$I_{equiv} \alpha_p = T_{in} - T_{out}/Ratio$$

Comparison of this latter differential equation with the prior equation shows that the equivalent inertia is

$$I_{equiv} = I_p + I_G/Ratio^2.$$

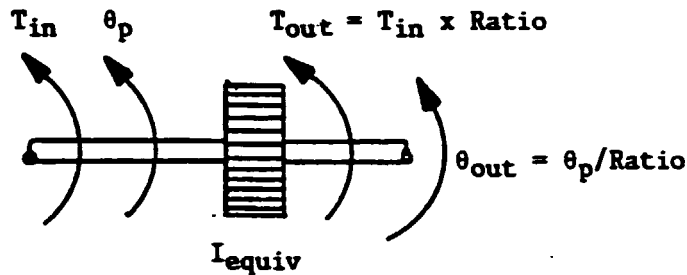


Figure 2.4 Equivalent Mass-Elastic System

An alternative method for obtaining the equivalent inertia is to equate the kinetic energy of the original system to the kinetic energy of the equivalent system per Reference 6. For this sample problem, the equivalent inertia of the gear pair referred to pinion speed may be obtained as follows:

$$KE_{original} = KE_{equivalent}$$

$$\frac{1}{2} I_p \omega_p^2 + \frac{1}{2} I_G \omega_G^2 = \frac{1}{2} I_{equiv} \omega_p^2$$

By cancelling the one half and using the relationship between the angular velocities,

$$\omega_G = -\omega_p / \text{Ratio},$$

The kinetic energy equation becomes

$$I_p \omega_p^2 + I_G (\omega_p / \text{Ratio})^2 = I_{\text{equiv}} \omega_p^2.$$

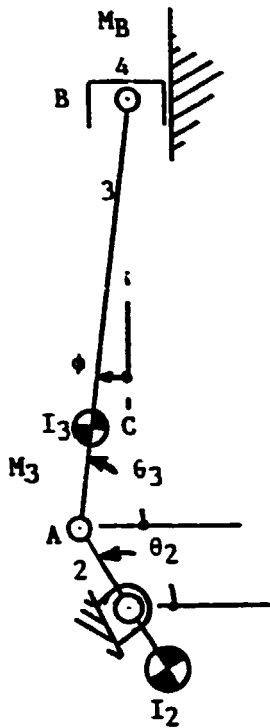
Solve this expression for I_{equiv} , which agrees with the former equation.

$$I_{\text{equiv}} = I_p + I_G / \text{Ratio}^2$$

A mechanical linkage has an equivalent inertia which changes in magnitude as the position changes. Consider the engine's slider crank mechanism of Figure 2.5. The angular velocity of each link and the linear velocity of the center of gravity of each link are evaluated for an input crank speed of 1 radian per second as illustrated in Figure 2.6. (This calculation was performed by a four-bar linkage program for a linkage with the output crank located at 90° from the path of the piston and for an "infinitely" long output crank.)

The inertia of the piston, connecting rod and crankshaft may be represented by an equivalent inertia, I_{EQ} , which has the speed of the crankshaft. I_{EQ} has a different value for each position of the crankshaft. The magnitude of I_{EQ} may be obtained by equating the kinetic energy of the original system to the kinetic energy of the equivalent system at each position:

$$\begin{aligned} .5 \times I_{EQ} \times \omega_2^2 &= .5 \times I_2 \times \omega_2^2 + .5 \times M_B \times V_4^2 \\ &+ .5 \times I_3 \times \omega_3^2 + .5 \times M_3 \times V_{CG3}^2 \\ I_{EQ} &= I_2 (\omega_2 / \omega_2)^2 + M_B (V_4 / \omega_2)^2 + I_3 (\omega_3 / \omega_2)^2 + M_3 (V_{CG3} / \omega_2)^2 \end{aligned}$$



- M_B = Piston assembly mass
- $M_B = 0.119 \text{ lb sec}^2/\text{in}$
- M_3 = Connecting rod weight
- $M_3 = 0.355 \text{ lb sec}^2/\text{in}$
- I_3 = Inertia of connecting rod about center of gravity
- $I_3 = 31.6 \text{ lb in sec}^2$
- I_2 = Inertia of crankshaft
- $I_2 = 30 \text{ lb in sec}^2$
- l = Length of connecting rod = 23 inches
- R = Radius of crank
- $R = 5.25 \text{ in}$
- AC = Distance from rod end to C.G. of rod
- $AC = 5 \text{ in}$

Figure 2.5 Schematic of Engine Piston and Crank Mechanism

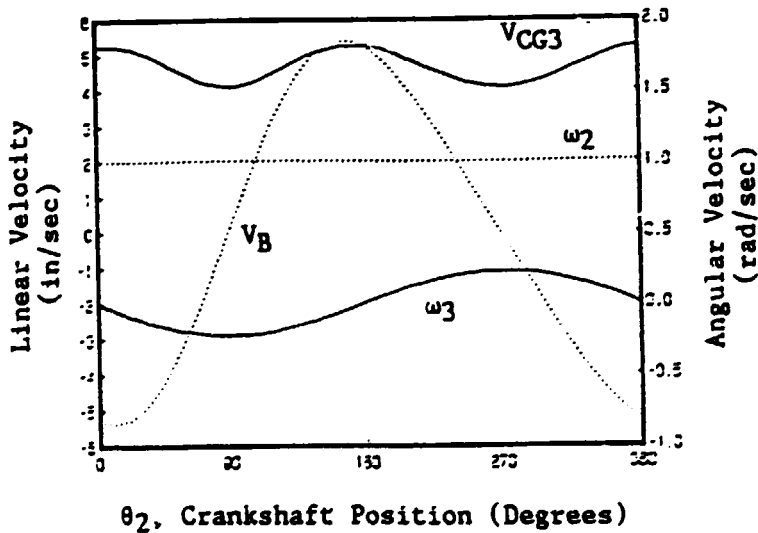


Figure 2.6 Velocities of Piston and Crank Mechanism

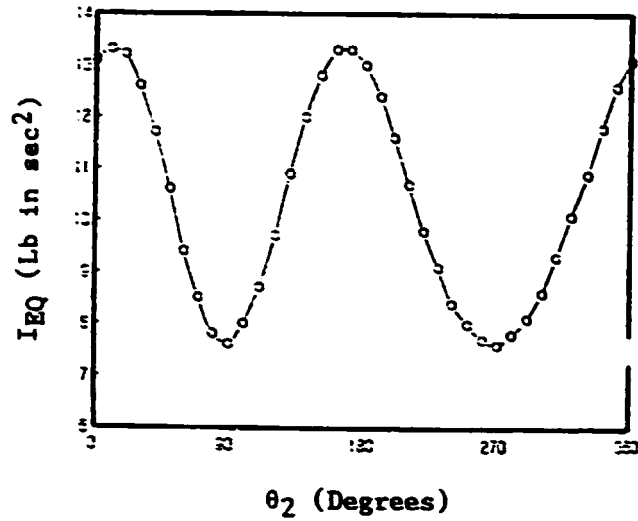
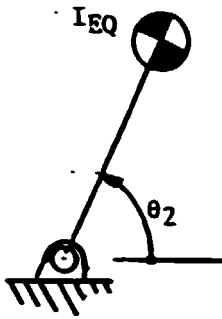


Figure 2.7 Equivalent Inertia as a Function of Crank Position

This latter equation shows that the equivalent inertia of a linkage is the sum of the products of velocity ratios times the mass and inertia values of the links. This ratio of velocities is independent of the actual speed of the linkage, since it is established by the position and configuration of the mechanism. The dependence of the velocity ratio on the mechanism position may be illustrated by considering the velocity polygon of a mechanism. The shape of the polygon is a function of position while the size is determined by the magnitude of the velocity. This is illustrated in Figure 2.8 showing the graphical solution to the velocity equation:

$$V_B = V_A + V_{B/A}$$

If V_A is doubled, the polygon will double in size but the ratio V_A/V_B will not change at this position.

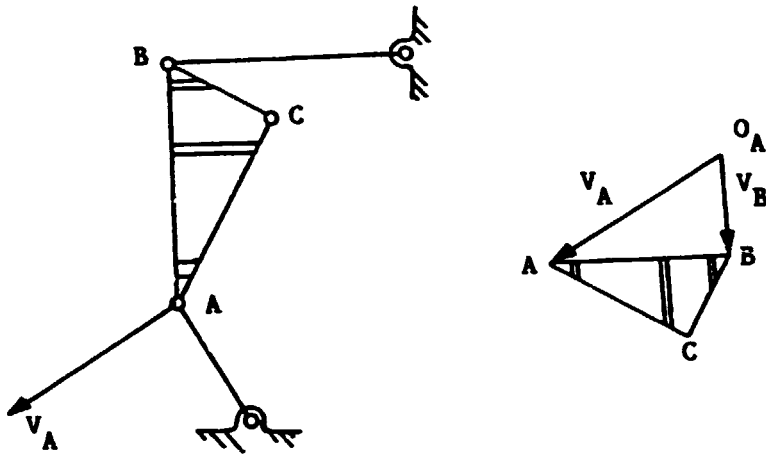


Figure 2.8 Velocity Polygon for Linkage

When a mass is supported by the free end of a spring, whose opposite end is stationary, portions of the spring's mass move with different velocities. The equivalent mass of the spring will be considered as that fraction of the spring's mass which moves with the velocity of the free end. The kinetic energy of the spring with one end fixed may be equated to the kinetic energy of a massless spring supporting an equivalent mass on its free end per Figure 2.9.

$$KE_{\text{original}} = KE_{\text{equivalent}}$$

$$\int_0^L .5 \times v^2 \times dm = .5 M_{\text{EQ}} v^2$$

- where,
- v = Velocity of particle of spring mass = $V \times X/L$
 - dm = Mass of particle of spring = $\rho \times A \times dX$
 - X = Distance from stationary end to particle of mass
 - V = Velocity of free end of spring
 - L = Length of spring
 - ρ = Mass density of spring

A = Area of spring normal to x-direction.

Hence,

$$M_{\text{spring}} = \int_0^L dm = \rho \times A \times L$$

$$M_{\text{EQ}} = \int_0^L (X/L)^2 (\rho \times A \times dX)$$

$$M_{\text{EQ}} = \rho \times A \times L/3 = M_{\text{spring}}/3$$

For a shaft in torsion with one end fixed and the other end supporting an inertia, J, (Figure 2.9) the equivalent inertia due to that part of the shaft which moves is obtained as follows

$$KE_{\text{original}} = KE_{\text{equivalent}}$$

$$\int d(KE) = .5 \times J_{\text{EQ}} \times \omega^2$$

$$.5 \int_0^L \omega_p^2 \times dJ_p = .5 \times J_{\text{EQ}} \times \omega^2$$

The angular velocity of the shaft varies from zero at the base to ω at the free end. So the angular velocity of a particle located a distance X from the free end is

$$\omega_p = \omega \times X/L$$

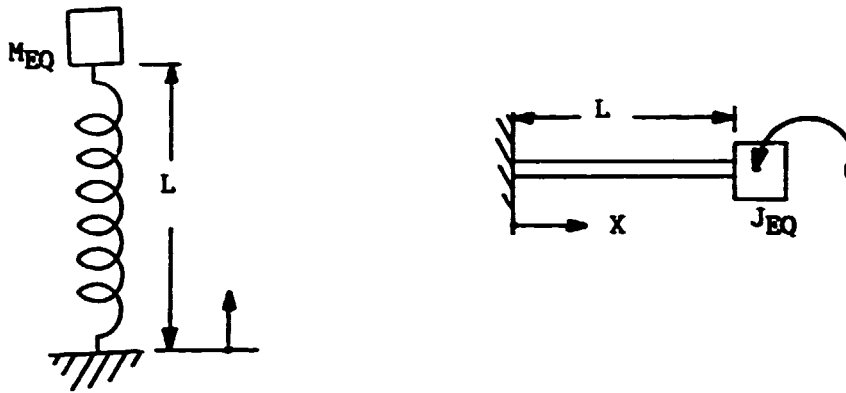
The mass moment of inertia of a particle with radius of gyration r is

$$dJ_p = \rho \times A \times r^2 \times dX$$

$$.5 \times \int_0^L \rho \times A \times r^2 \times (\omega \times X/L)^2 \times dX = .5 \times J_{\text{EQ}} \times \omega^2$$

$$J_{\text{EQ}} = \rho \times A \times L \times r^2/3 = M \times r^2/3 = J_{\text{shaft}}/3$$

Hence, the equivalent inertia of a shaft with one end stationary is equal to one third of the inertia of the total shaft. This equivalent inertia rotates at the speed of the free end of the shaft.



$$M_{EQ} = M_{spring}/3$$

M_{spring} = Mass of spring

$$J_{EQ} = J_{shaft}/3$$

J_{shaft} = Mass moment of inertia
of shaft

Figure 2.9 Equivalent Inertia of Fixed End Spring

The elastic properties of the machine must also be quantified in order to create a mathematical model of the dynamic system. The elastic deformations provide storage for the potential energy, which may be changed into kinetic energy at a later phase. The elastic properties may be characterized by spring constants. An example of a spring constant would be the ratio of the change in force on a gear tooth to the change in deflection of the tooth per Figure 2.10. An example of torsional stiffness would be the ratio of the change in shaft torque to the corresponding angular deflection.

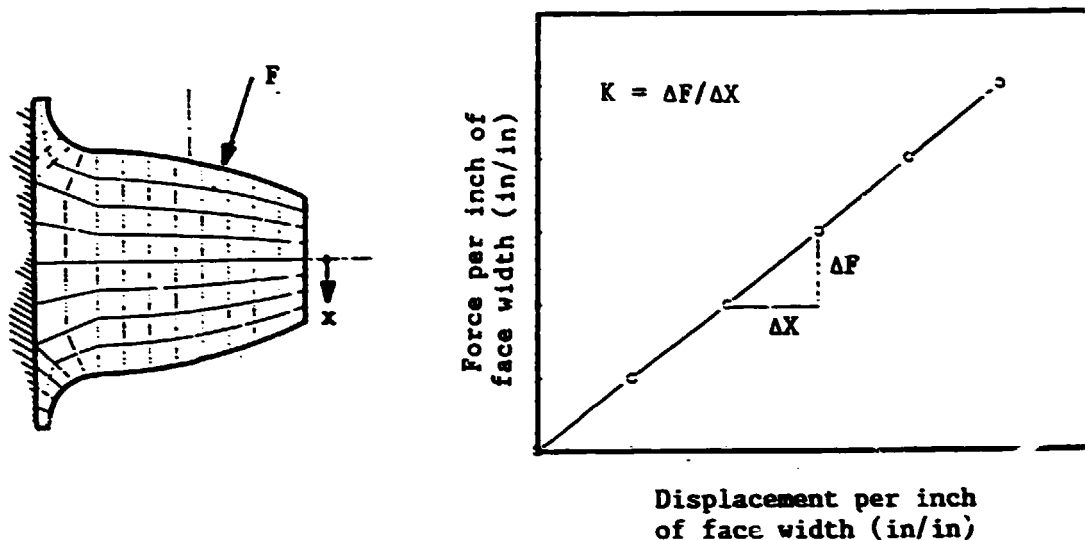


Figure 2.10 Gear Tooth Stiffness from Finite Element Analysis

The elastic characteristics of some machines are more complex than these two examples and equivalent spring constants may be used to simplify the model. If several springs are in parallel, as when more than one pair of teeth of a helical gear shares the load, this multiple spring system may be represented by an equivalent system with only one spring. This is illustrated in Figure 2.11 and the equivalent spring constant is evaluated as follows for the equivalent system. This expression is valid for parallel torsion springs also.

$$K_{EQ} = F/X = (F_1 + F_2 + F_3)/X = F_1/X + F_2/X + F_3/X = K_1 + K_2 + K_3$$

$$K_{EQ} = \sum_{i=1}^n K_i$$

where, F = Total force on all springs

X = Deflection of each spring

K_{EQ} = Equivalent spring constant, lb/in

n = Number of springs in parallel

K_i = Spring constant of original spring, lb/in

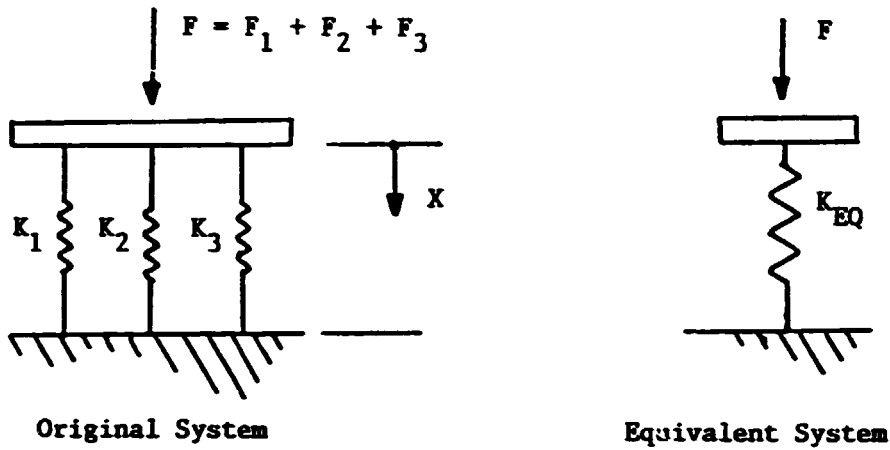


Figure 2.11 Springs in Parallel

If springs are in series, as the torsional spring constants of a stepped shaft, the equivalent system may be simplified. The total deflection at the end of the shaft is θ , which is made up of the sum of the deflections of the individual springs. The torque on each spring in series is the same.

$$\begin{aligned} \theta &= \theta_1 + \theta_2 + \theta_3 = T/K_1 + T/K_2 + T/K_3 \\ &= T(1/K_1 + 1/K_2 + 1/K_3) = T \times \sum_{i=1}^n (1/K_i) \end{aligned}$$

But, the equivalent system's spring constant is

$$K_{EQ} = T/\theta$$

so,

$$K_{EQ} = \sum_{i=1}^n (1/K_i)$$

K_{EQ} = Equivalent spring constant, lb in/radian

n = Number of springs in series

K_i = Spring constant for original spring, lb in/radian

This expression is valid for series extension springs also. A pair of gear teeth in mesh is another series spring arrangement (Reference 7) with each tooth having a stiffness, K_T , per Figure 2.12.

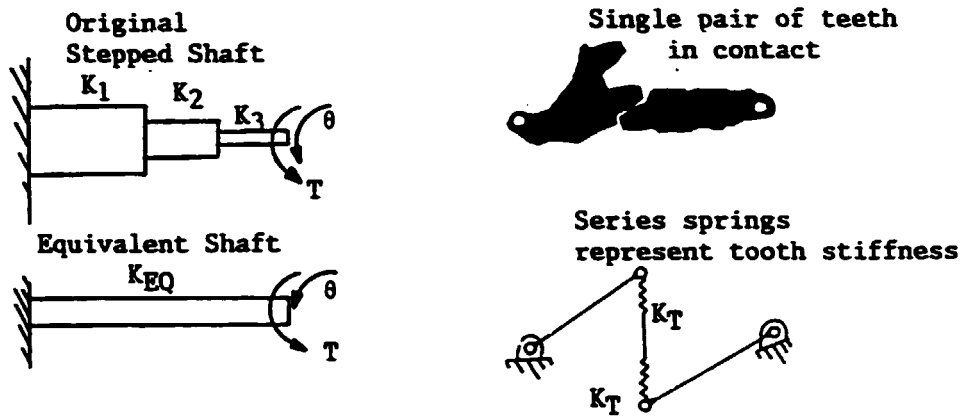


Figure 2.12 Springs in Series

The equivalent spring constant concept may be useful when nonlinear relationships exist between deflections and torque (or force). This nonlinearity may be a function of torque (or displacement) as in the elastic coupling illustrated in Figure 2.13. The equivalent spring constant is usually taken as the slope of the force (or torque) versus deflection curve at the operating point.

For systems with gears, the original system may be replaced by an equivalent system with all inertias operating at the same speed. The equivalent system must have an equivalent spring constant which will

allow it to store the same amount of potential energy as the original system, since the nature of a vibrating system is to transform kinetic energy into potential and then reverse this transformation. The

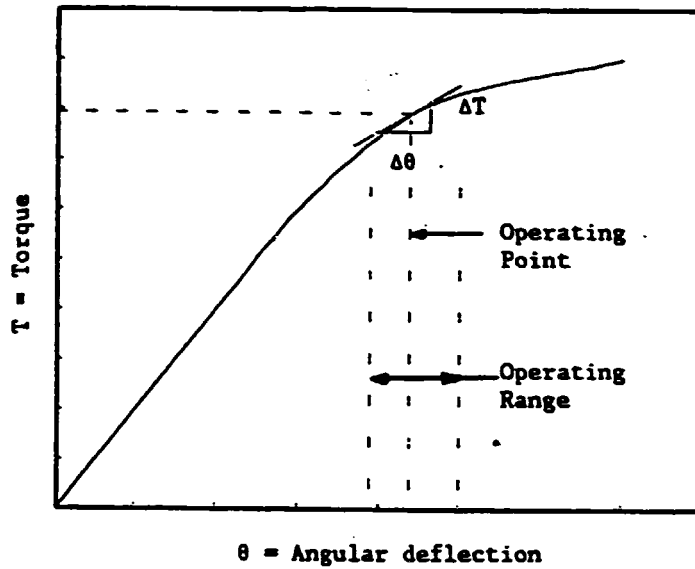


Figure 2.13 Nonlinear Springs

potential energy is stored in the springs as they deflect and is equal to the product of the average force times the displacement. Consider representing the original gear with the dual speed shaft system by an equivalent single speed system as in Figure 2.14. Equate the potential energies of these two systems to obtain the equivalent spring constant. In this sample, the

$$PE_{\text{original}} = PE_{\text{equivalent}}$$
$$.5 \times K_1 \times (\theta_2 - \theta_3)^2 = .5 \times K_{EQ} \times (\theta_2 \times \text{Ratio} - \theta_3 \times \text{Ratio})^2$$

Hence,

$$K_{EQ} = K_1 / \text{Ratio}^2 .$$

The equivalent inertias are also shown in the figure.

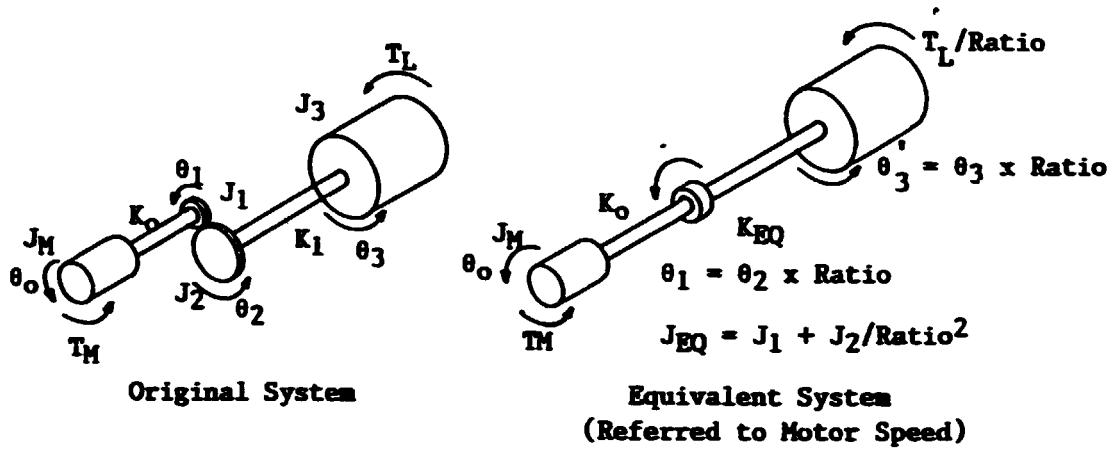


Figure 2.14 Equivalent Spring Constant

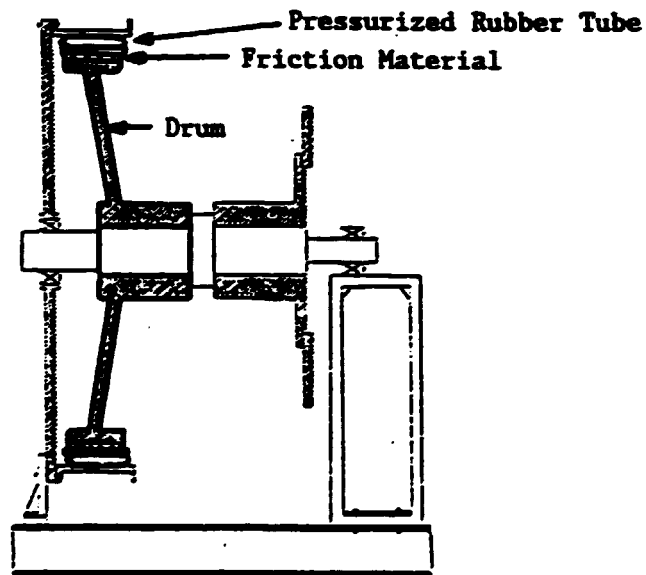


Figure 2.15 40 Inch Pneumatic Clutch in Test Stand

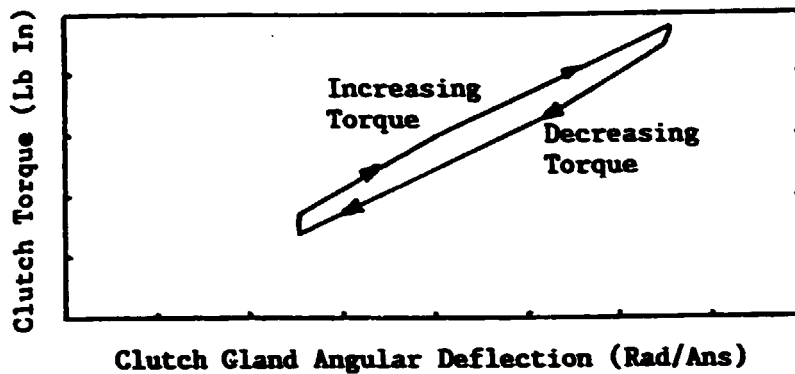


Figure 2.16 Torsional Deflection of 40 Inch Clutch

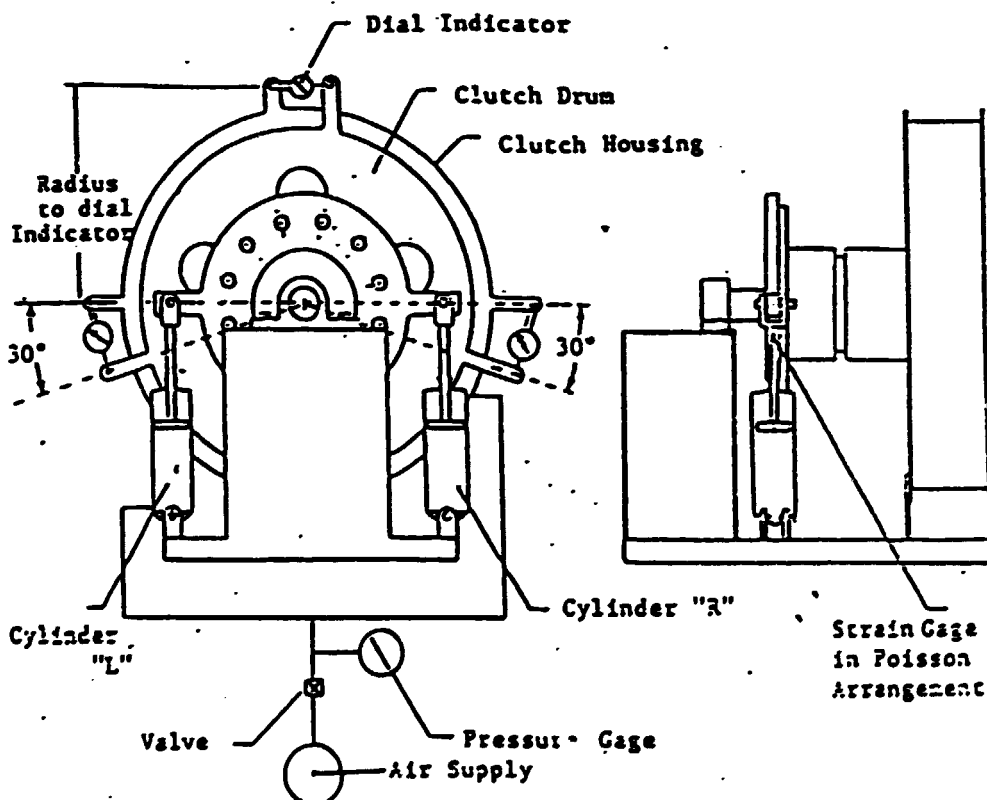


Figure 2.17 Device for Static Measurements of Torsional Clutch Stiffness and Damping

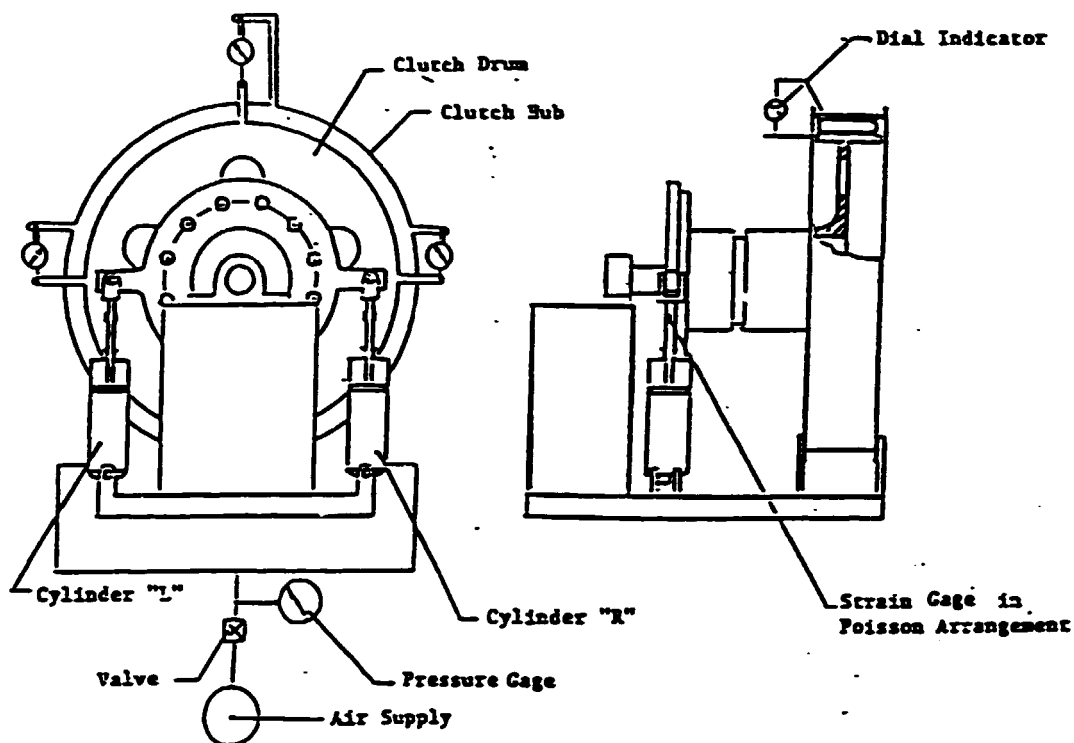


Figure 2.18 Device for Static Measurements of Radial Clutch Stiffness and Damping

The torsional stiffness of a pneumatically activated clutch as illustrated in Figure 2.15 may be evaluated as the mean slope of the torque deflection curve. Values of relative damping and torsional stiffness were measured in the zero frequency test device designed by Cardenas (Reference 8) in Figure 2.17. Typical load curves are shown in Figure 2.16. The results of tests by Elahi are in Table 2.1 (Reference 9). This work was supported by Marine Gears, Inc.

The radial stiffness of these clutches may also be evaluated by removing one bearing to allow the shaft to deflect radially and rerouting the hydraulic lines to cause both cylinders to move in the same direction. This test setup is shown in Figure 2.18. The radial stiffness results of tests by Elahi (Reference 9) are in Table 2.2. The test data in Figure 2.20 is typical for the 40 inch clutch.

Some pneumatic clutches do not allow the elastomer air bag to be deflected as the torque is transmitted by metal members. This results in a more rugged design, but the torsional stiffness is much higher and the energy dissipating capability of the elastomer is not available.

The damping characteristics of a system must be included in the dynamic model. The dissipation of energy by damping is one method for keeping the amplitudes of vibrating systems from reaching dangerous magnitudes. Damping may be achieved by viscous damping of a fluid, hysteresis damping in an elastic solid or coulomb friction damping between solids.

The viscous damper may be subjected to a harmonic excitation source,

$$P = P_0 \sin(\omega t + \phi) ,$$

which leads the displacement,

$$X = X_0 \sin(\omega t) ,$$

by a phase angle ϕ . The resulting work is

$$W = \pi P_0 X_0 \sin\phi$$

The damping force is

$$P_0 = c \times \omega \times X_0 .$$

P_0 is 90° out of phase with the displacement X_0 . Hence, the damping work per cycle is

$$W = \pi \times c \times \omega \times X_0^2 .$$

Damping by material hysteresis is due to internal friction which heats the material. Elastomer materials, such as rubber, have high hysteresis loss when strained. The elastomer material of the pressurized tube of the 40 inch clutch shown in Figure 2.15 provides damping. The area under the torque versus deflection curve for increasing torque is larger than the area under the curve traced as the clutch returns to the unloaded position per Figure 2.16. The hysteresis energy dissipated per cycle, W_d , is equal to the area between these two curves per Figure 2.19. The energy of a linear elastic deflection from the mean position to the maximum amplitude, X_{max} , is

$$W_e = .5 \times k \times X_{max}^2$$

Relative damping, ψ , is a term for characterizing hysteresis damping:

$$\psi = W_d/W_e$$

The relative damping for this 40 inch clutch with elastomer air bags was evaluated under static conditions and the values are given in Table 2.1.

The model of a system with hysteresis damping may be simplified by expressing the energy loss per cycle as a function of an equivalent viscous damping function. This is obtained by equating the energy dissipated per cycle for hysteresis damping to the energy dissipated per cycle by an equivalent viscous damper.

$$\psi \times W_e = \pi \times C_{EQ} \times \omega \times X_0^2$$

$$W_e = .5 \times K \times X_0^2$$

TABLE 2.1 Relative Damping and Torsional Stiffness of Clutches

Clutch Size (inch)	Maximum Torque (lb-in)	Minimum Torque (lb-in)	Mean Torque (lb-in)	$2\phi_v$ (Radian)	Torsional Stiffness (lb-in/rad)	Relative Damping
26	53,077	15,198	34,138	0.001531	24,741,346	0.8277
26	52,142	18,706	35,424	0.001358	24,621,502	1.0290
26	78,447	52,376	65,412	0.000962	27,100,832	0.9237
30	76,460	27,825	52,143	0.000905	53,734,394	0.8818
30	82,305	27,203	54,754	0.001062	51,870,470	0.8267
30	138,423	91,658	115,041	0.000878	53,263,098	0.6654
30	133,980	91,191	112,586	0.000840	50,933,222	1.1148
35	116,911	41,620	79,266	0.001960	38,413,776	0.7106
35	184,953	95,633	141,793	0.002554	36,147,220	0.9439
40	153,387	43,023	98,205	0.001537	71,804,815	0.9685
40	227,976	144,034	186,005	0.001342	62,549,926	0.7348
48	200,000	60,818	130,409	0.001217	114,299,509	1.3191
48	287,500	191,266	239,383	0.000637	151,073,784	1.5638

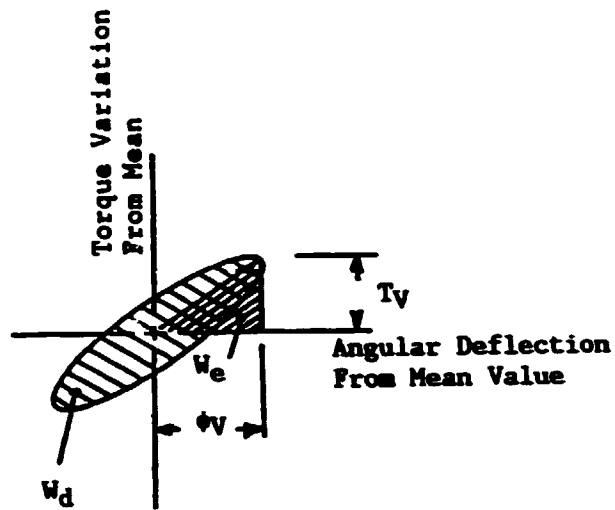


Figure 2.19 Hysteresis Damping Energy

Clutch Size (inch)	Maximum Radial Force (lb)	Radial Stiffness (lb/in)
26	3971	132,188
30	3420	87,710
30	3365	87,349
30	3456	87,592
30	5622	87,143
30	5049	88,182
35	2019	80,047
40	5889	143,298
48	5623	138,572

TABLE 2.2 Radial Stiffness of Pneumatic Clutches

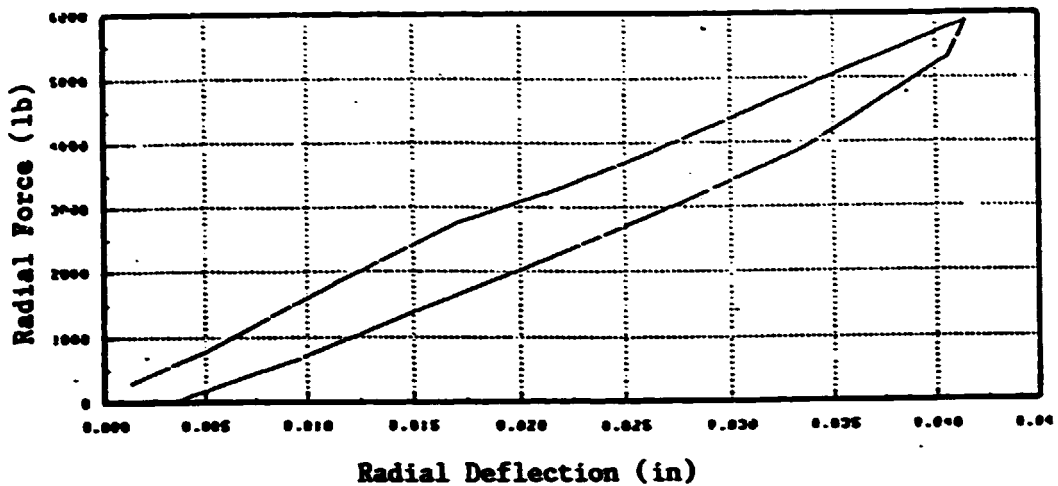


Figure 2.20 Radial Deflection of 40 Inch Clutch

Hence, the equivalent value of viscous damping is:

$$C_{EQ} = \frac{\psi}{2} \times K \times X_0^2 / (\pi \times \omega \times X_0)^2 = \frac{.5 \times K \times \psi}{\pi \times \omega}$$

Where,

K = Torsional stiffness of member with hysteresis

ω = Natural frequency of vibration.

3. Types of Excitation

The type of excitation for a mechanical system may be steady state, periodic, aperiodic or random. The method of analysis is different for each type.

For periodic excitation, the response of a linear system will also be periodic and the initial conditions will establish the amplitudes. The excitation of an internal combustion engine's gas pressure pulses

may be represented as a periodic excitation by a Fourier analysis of the gas pressure as shown in Figure 3.1. If the crankshaft speed, ω , is constant, the time, t , is a function of crank position, θ .

$$t = \theta/\omega$$

Hence, the period, T , for one cycle of a two stroke cycle engine with speed, ω , is

$$T = 2\pi/\omega$$

The Fourier expansion of the function is

$$x(t) = f(t) = f(k)$$

$$x(t) = X_{ave} + \sum_{n=1}^{\infty} B(n) \sin(n\omega t) + \sum_{n=1}^{\infty} C(n) \cos(n\omega t)$$

$$X_{ave} = \left(\sum_{k=1}^{NO} f(k) \Delta t \right) / T$$

NO = $T/\Delta t$ = Number of data sets in one period

$t = (k-.5)\Delta t$, for $k = 1, 2, 3, \dots, NO$

Δt = Time increment between data sets. (The first data set is at $t = \Delta t/2$ and the last set is at $t = T - \Delta t/2$)

X_{ave} = Average value of function over one period

N_T = Total number of harmonic components

n = Number of a harmonic. $1 \leq n \leq N_T$

The coefficients $B(n)$ and $C(n)$ must be evaluated for each value of n .

$$B(n) = (2/T) \sum_{k=1}^{NO} f(k) \times \sin((n \times 2 \times \pi/T) \times (k-.5)\Delta t)\Delta t$$

$$C(n) = (2/T) \sum_{k=1}^{NO} f(k) \times \cos((n \times 2 \times \pi/T) \times (k-.5)\Delta t)\Delta t$$

$B(n)$ = Amplitude of n th sine harmonic.

$C(n)$ = Amplitude of n th Cosine harmonic.

The phase angle between the harmonic components is

$$\phi(n) = \arctan (C(n)/B(n))$$

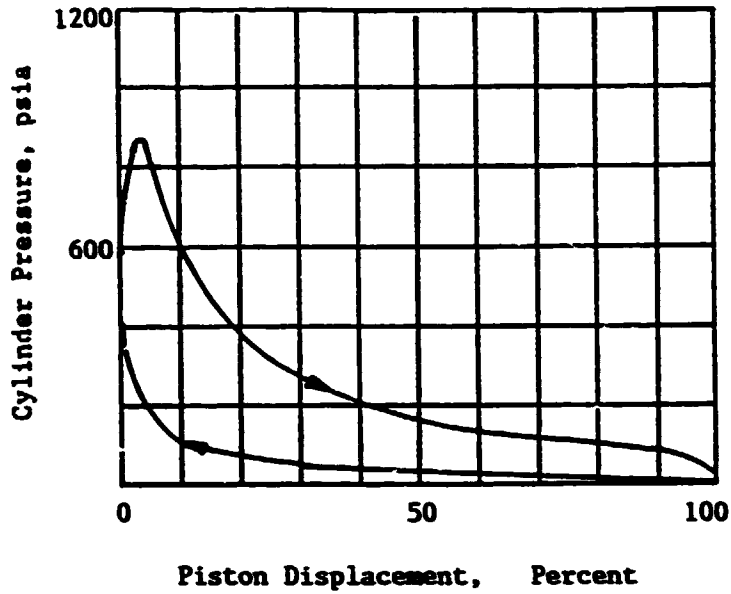


Figure 3.1 Engine Cylinder Pressure (Two Stroke Cycle)

INPUT DATA

ENGINE SPEED = 209.43 RAD/SEC
 NUMBER OF HARMONICS = 10
 TOTAL TIME PERIOD = .03 SEC

FOURIER SERIES COEFFICIENTS
 CONSTANT COEFFICIENT XBAR = 165.07

N	BN	CN
1	119.04	185.140
2	87.923	87.642
3	90.502	32.504
4	53.280	.010
5	44.167	-6.100
6	20.327	-18.589
7	13.113	-12.340
8	.305	-10.703
9	.407	-2.005
10	-5.023	-4.967

TABLE 3.2 Fourier Coefficients for Engine Gas Pressure

TIME (Seconds)	PRESSURE (PSI)	CRANKSHAFT POSITION (Degrees)
0	220	10
.001	640	12
.002	780	24
.003	580	36
.004	385	48
.005	280	60
.006	205	72
.007	175	84
.008	130	96
.009	106	108
.01	100	120
.011	98	132
.012	95	144
.013	90	156
.014	88	168
.015	10	180
.016	10	192
.017	10	204
.018	10	216
.019	12	228
.02	13	240
.021	10	252
.022	25	264
.023	30	276
.024	45	288
.025	50	300
.026	80	312
.027	100	324
.028	145	336
.029	210	348
.03	220	360

TABLE 3.1 Engine Gas Pressure Versus Time and Crankshaft Position.

Each harmonic component has a unique frequency, which is equal to the product of the engine speed and the harmonic number, n. At n = 2 a harmonic pressure, with a frequency of 418.8 rad/sec is produced by the engine. The magnitude of this pressure component is

$$P(t) = 165.07 + \sum_{n=1}^{N_T} 87.9 * \sin(2 * 209.4 * t) \\
 + \sum_{n=1}^{N_T} 87.6 \cos(2 * 209.4 * t)$$

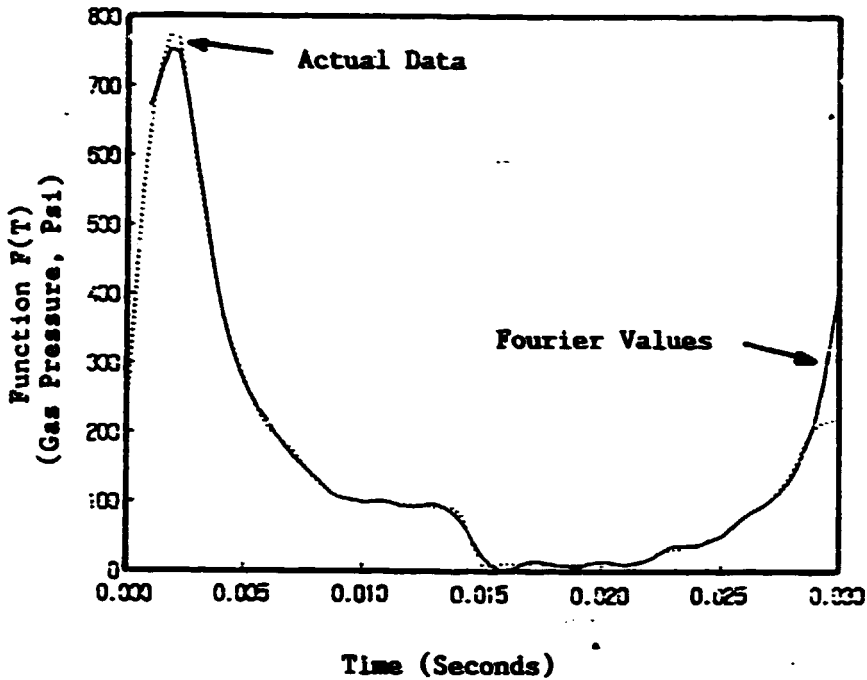


Figure 3.2 Graph of Fourier Representation of Engine Gas Pressure

This harmonically varying pressure produces forces which could excite a resonant vibration, if the system has a natural frequency of 418.8 radians/second. As the values of n increase above 11, the amplitudes decrease. This indicates that the energy of the higher harmonics will be too small to produce significant vibration amplitudes after overcoming the damping. These harmonic pressures also produce harmonic components of crankshaft torque. The response of a linear system may be obtained by summing the response for each of the harmonic components.

Aperiodic excitation is a nonrepeating pulse. The pulse is equivalent to the sum of numerous natural frequencies. The shape of the pulse determines its frequency content. For example, a step would contain high frequencies in order to define the sharp corner. The

Fourier Integral may be used to transform an aperiodic function, $f(t)$, from the time domain into an equivalent function, $g(\omega)$, in the frequency domain. In the frequency domain, the system response may then be characterized in terms of gain, the ratio of output to input. The Fourier Integral (10) may be expressed as

$$f(t) = \int_{-\infty}^{\infty} g(\omega) e^{i\omega t} d\omega$$

where,

$$g(\omega) = \frac{1}{2\pi} \int_{-\infty}^{\infty} f(s) e^{-i\omega s} ds$$

The dummy variable s may be replaced by the variable t and the following relationship may replace $e^{-i\omega t}$ in the expression for $g(\omega)$.

$$e^{-i\omega t} = \cos(\omega t) - i \sin(\omega t)$$

Hence,

$$g(\omega) = \frac{1}{2\pi} \int_{-\infty}^{\infty} f(t) \cos(\omega t) dt - \frac{i}{2\pi} \int_{-\infty}^{\infty} f(t) \sin(\omega t) dt$$

or,

$$g(\omega) = A - iB$$

where,

$$A = \frac{1}{2\pi} \int_{-\infty}^{\infty} f(t) \cos(\omega t) dt$$

$$B = \frac{1}{2\pi} \int_{-\infty}^{\infty} f(t) \sin(\omega t) dt$$

The absolute value of $g(\omega)$ is

$$|g(\omega)| = (A^2 + B^2)^{.5}$$

The phase angle for $g(\omega)$ is

$$\phi = \tan^{-1}(B/A) .$$

If the system gain, M, and the excitation are both expressed in the frequency domain, the system response at a frequency ω would be

$$E_{\text{output}} = M \times E_{\text{excitation}}$$

If the excitation of the system is random, it may be expressed in statistical terms as a power spectral density function, P_g . The power spectral density function is a function of frequency. The autocovariance function, $C(\tau)$, may also be used to locate periodic content of random functions (11 and 12). The following equation shows how $C(\tau)$ will have large values when the lag index corresponds to the period of a harmonic component of the data. However, if the relationship between the data, $Y(t)$ and $Y(t+\tau)$, is truly random, with values above and below zero, the value of $C(\tau)$ will approach zero.

$$C(\tau) = \lim_{T \rightarrow \infty} \left| \frac{1}{2T} \int_{-T}^T Y(t) \times Y(t + \tau) dt \right|$$

For numerical methods the following form is convenient.

$$C(R) = \frac{1}{n-R} \sum_{i=1}^{n-R} Y(i) \times Y(i+R)$$

where,

$C(R) = C(\tau)$ = the autocovariance function.

T = the time length of the data record.

t = time

τ = Lag value. (The maximum value of τ should not exceed 5 to 10% of the length of the data record.)

$\Delta\tau$ = Time interval between measured values of $Y(i)$.

$Y(i) = Y(t)$ = Variable under study (The data must be processed so

$Y(i)$ has a mean value of zero.

n = Total number of data points.

$M = \tau_{\max}/\Delta\tau$ = Total number of frequency bands.

$R = \tau/\Delta\tau$ = Lag index = 0, 1, 2, ..., M

The Fourier Transform of the autocovariance function is

$$g(\omega) = \frac{1}{2\pi} \int_{-\infty}^{\infty} C(\tau) \times e^{-i\omega\tau} d\tau$$

or

$$g(\omega) = \frac{1}{2\pi} \int_{-\infty}^{\infty} C(\tau) \cos(\omega\tau) d\tau - \frac{i}{2\pi} \int_{-\infty}^{\infty} C(\tau) \sin(\omega\tau) d\tau$$

Since $C(\tau)$ is an even function and $\sin(\omega\tau)$ is an odd function, this equation becomes:

$$g(\omega) = \frac{1}{2\pi} \int_{-\infty}^{\infty} C(\tau) \cos(\omega\tau) d\tau .$$

Power spectral density is

$$P(\omega) = 2g(\omega)$$

where,

$$0 \leq \omega \leq \omega_{\max}$$

$$g(\omega) = \frac{1}{2\pi} \int_0^{\omega_{\max}} C(\tau) \cos(\omega\tau) d\tau$$

The maximum frequency which can be identified by the data is

$$f_{\max} = 1/(2 \times \Delta t)$$

The frequency bands, M , divide this maximum frequency into increments Δf .

$$\Delta f = f_{\max}/M = 1/(2 \times M \times \Delta t)$$

Define H as an integer with the following relationship to frequency f_H :

$$f_H = H \times \Delta f$$

The values of H are taken as the values of R to establish the connection between $C(\tau)$ and $P(f_H)$. At $\tau = 0$ and $\tau = \infty$ the values of R are zero and M respectively. For numerical methods the following form is convenient

$$P(f_H) = (2/\pi) \int_{R=0}^{R=M} C(R) \times \cos(\pi HR/M) dR$$

The Fourier Transform will place the autocovariance function into the frequency domain. The area under the plot of $P(\omega)$ versus ω is the mean square value of the function $Y(t)$. Peaks in $P(\omega)$ identify frequencies, ω , of harmonics in $Y(t)$. The power spectral density function and the correlation function are very useful in signature analysis, which gives early warning of failures in bearings or gears by showing changes in the power spectrum of noise or acceleration signals.

A simple example of the use of the power spectral density function in signature analysis may be based on data for the acceleration of the driver of a vehicle (13). The rear shock absorbers were not active for the acceleration data in Figure 3.3. The power spectral density for this data is given as a function of frequency in Figure 3.4. The power spectral density function has its largest spike at 11 cps, which is near the natural frequency of wheel hop for the independently sprung front wheels. The next largest spike is 2 cps which is close to the body roll natural frequency of the vehicle.

For the condition with active rear shocks, the acceleration data is characterized as a probability density function in Figure 3.5. The probability density function gives a good indication of the magnitude scatter of the data. The probability of encountering loads in excess of one standard deviation (.035 g's) is 20%, when shocks are active.

This data for active shocks is given in the frequency domain in Figure 3.6. The signature of the machine shown in Figure 3.6 is similar to the signature of Figure 3.4 as the two dominant frequencies appear in both figures, however, the magnitudes are significantly different which indicates a significant change in the machine itself.

4. Integration of Equations of Motion

The predictive model must be based on the fundamental laws of physics, mathematical principles, the equations of continuity and constraint functions. The differential equations of motion, which define the relationships between forces and movement, will require numerical integration methods for most cases. The modified Euler predictor corrector method and the Runge-Kutta method are two popular integration methods. The fourth order accuracy Runge-Kutta method can provide a solution to the first order differential equation of the form

$$dx/dt = F(t,x) .$$

The solution at one time interval past k is

$$X_{k+1} = X_k + (a_1 + 2a_2 + 2a_3 + a_4)/6 ,$$

where,

$$a_1 = \Delta t \times F[(t), (X_k)]$$

$$a_2 = \Delta t \times F[(t + .5 \times \Delta t), (X_k + .5 \times a_1)]$$

$$a_3 = \Delta t \times F[(t + .5 \times \Delta t), (X_k + .5 \times a_2)]$$

$$a_4 = \Delta t \times F[(t + \Delta t), (X_k + a_3)] .$$

A computer algorithm for solving a system of differential equations is given by Singiresu S. Rao (1) and Charles M. Haberman (2) presents the theory.

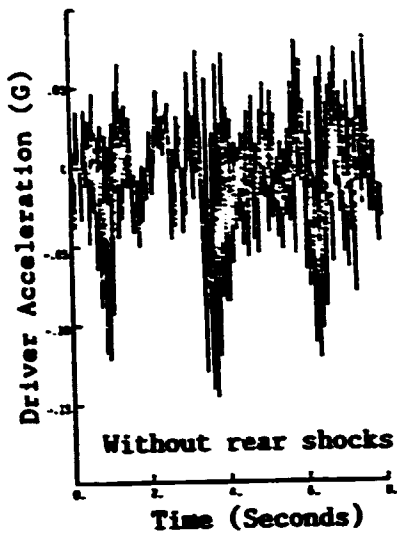


Figure 3.3 Vertical Driver Acceleration versus Time - U.S. 52 Highway

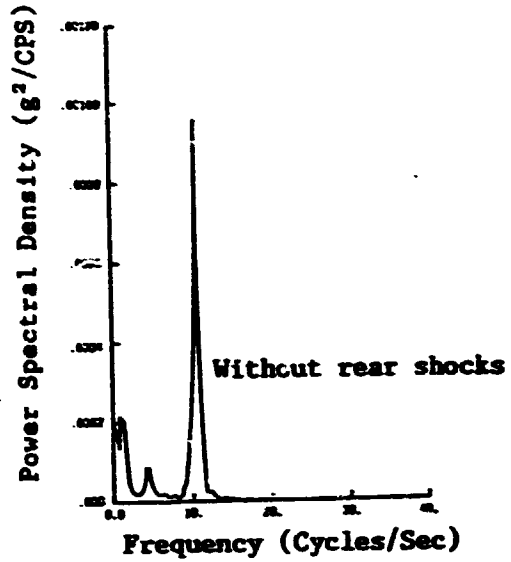


Figure 3.4 Power Spectrum of Driver Acceleration - U.S. 52

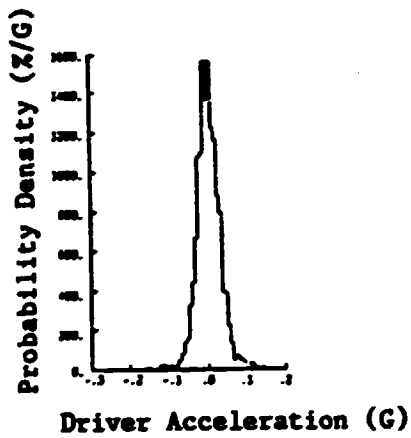


Figure 3.5 Probability Density of Driver Acceleration with Shocks - U.S. 52

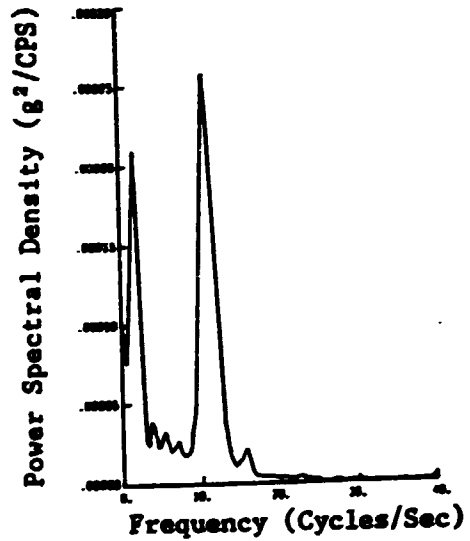


Figure 3.6 Power Spectrum of Driver Acceleration with Shocks - U.S. 52

A critical factor in the numerical integration is the choice the integration step size, Δt . If Δt is too small, the computer time will be excessive. If it is extremely small the computational accuracy of the computer may introduce errors. However, if Δt is too big, the solution will cease to be independent of the value of Δt . A practical suggestion for evaluating the size of Δt is to assign a value to Δt and perform the numerical integration over an interval with the maximum dynamic characteristics. The value of Δt is then plotted on the log scale of semi-log paper while the terminal value of the dependent variable is plotted on the other axis. Then change the value of Δt by a factor of 5 and repeat the prior procedure. The graph will show no variation in the value of the dependent variable for values of Δt which are small enough. The example in the next section will illustrate this technique.

5. Example: Vehicle Simulation

Suppose that it is desired to determine the change in the performance of a vehicle when different gear ratios are used in it's three speed transmission. The first step is to develop a predictive model for this vehicle. The duty cycle for this model requires the vehicle to start from rest and travel 1000 feet up a one degree slope. The output from the model is to be the time required to reach the end of this path. the data of Table 5.1 defines the problem and Figure 5.1 illustrates the original system.

The forces acting on this vehicle to produce its dynamic motion are described below. It is important to note that the force F_R depends on the actual mass and not on the equivalent mass.

W = Weight of vehicle, lb.

F_G = The resistance due to gravity as the vehicle moves up a slope of alpha, lb.

$$F_G = W \times \sin(\text{Alpha})$$

F_A' = Air drag resistance, lb.

$$F_A' = .0012 \times AF \times DC \times V^2$$

$$F_A = F_A' / V^2$$

AF = Projected frontal area of vehicle, ft^2 .

V = Velocity of vehicle, ft/sec.

DC = Drag coefficient

F_I = Inertia force

$$F_I = -M \times \ddot{X}$$

M = Actual mass of vehicle, $\text{lb sec}^2/\text{ft}$

$$M = W/g$$

FF = Moment about front tire contact point due to static weight only, lb ft.

$$FF = LF \times W \times \cos(\text{Alpha}) + H \times W \times \sin(\text{Alpha})$$

FR = Force normal to rear wheels due to static weight and dynamic loads, lb.

$$FR = (-F_I \times H + FF) / LT = (M \times \ddot{X} \times H + FF) / LT$$

$TENG$ = Torque produced by engine on crankshaft, lb ft. The following expression was obtained from a least squares fit of data for this engine.

$$TENG = .00197285 \times R^3 - .33022 \times R^2 + 13.456 \times R - 25.283$$

R = Engine speed, RPM, divided by 100.

Mu = Coefficient of traction between tire and road.

P = Thrust force of ground on tire, lb. The value of P depends on engine torque, gear ratio and wheel radius, but must not exceed P_{max} , which is the maximum slip force. Hence,

$$P \leq P_{max}$$

$$P = TENG \times GR(I) \times GRD \times EFF/RRW$$

GR(I) = Gear ratio in transmission.

GRD = Gear ratio in differential

EFF = Mechanical efficiency of transmission.

$$P_{max} = Mu \times FR$$

In order to simplify the differential equation of motion, the original system will be replaced by an equivalent system per Figure 5.2 with a translating mass, which has the same linear velocity as the vehicle. The equivalent mass is obtained by equating the kinetic energy of the original and equivalent systems.

$$KE_{original} = KE_{equivalent}$$

$$.5 \times (W/g) \times V^2 + .5(I_E + I_F + I_C) \times \omega_E^2 + .5(4 \times I_W) \times \omega_W^2 = .5 \times M_{EQ} V^2$$

But,

$$\omega_E = V \times GR(I) \times GRD/RRW$$

$$\omega_W = V/RRW$$

Combine these three equations to obtain:

$$M_{EQ} = (W/g) + (I_E + I_F + I_C) \times (GR(I) \times GRD/RRW)^2 + (4 \times I_W)/RRW^2$$

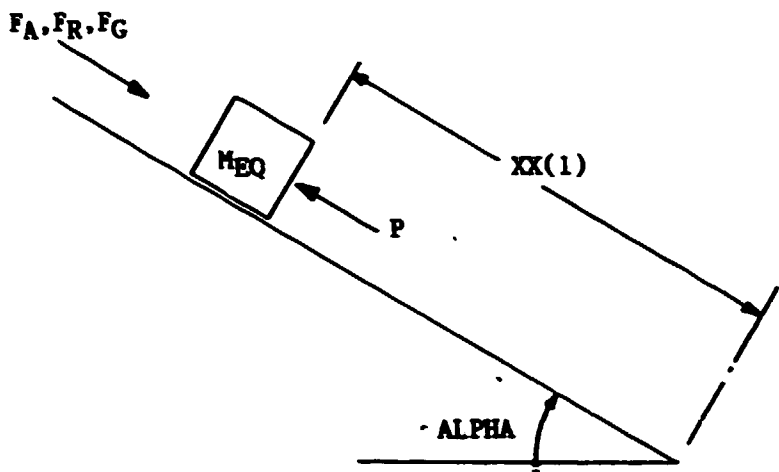


Figure 5.2 Equivalent System for Vehicle

The differential equation of motion for this vehicle is:

$$M_{EQ} \times \ddot{X} = P - F_G - F_R - F_A \times V^2$$

When the clutch is engaged,

$$P = TENG \times GR(I) \times GRD \times EFF/RRW$$

if, $P < P_{max}$.

So, $\ddot{X} = (P - F_G - F_R - F_A \times V^2)/M_{EG}$.

Otherwise, if $P > P_{max}$, set $P = P_{max}$ as follows.

$$P = P_{max} = \mu \times FR = \mu(M \times \ddot{X} \times H + FF)/LT$$

$$P = \mu \times \ddot{X} \times H \times M/LT - \mu(LF \times \cos(\alpha) + H \times \sin(\alpha))W/LT$$

For this latter case, the equation of motion is

$$\ddot{X} = \{ + \mu(LF \times \cos(\alpha) + H \times \sin(\alpha)) \times W + LT \times (- F_G - F_R - F_A \times V^2) \} / (M_{EQ} \times LT - \mu \times H \times M) .$$

When the clutch is disengaged,

$$P = 0$$

$$\ddot{X} = (- F_G - F_R - F_A \times V^2)/M_{EQ}$$

In order to use the Runge-Kutta method of integration, the variables will be redefined per standard practice as in Table 5.2.

TABLE 5.2 Variable Definitions for Vehicle

Old Variable Name	New Variable Name	Initial Value	Differential Equation
X	XX(1)	0	$F(1) = \dot{X} = XX(2) = \dot{XX}(1)$
$v = \dot{X}$	XX(2)	0	$F(2) = \ddot{X} = \Sigma F/M_{BQ} = \dot{XX}(2)$
\ddot{X}			

The size of the integration step, Δt , was varied from .001 to 0.5 seconds by factors of 5 while the distance traveled in 5 seconds was evaluated. This initial 5 seconds is associated with the maximum dynamic conditions for this problem. The results as shown in Figure 5.3 indicate that significant numerical error is created for this problem when Δt is greater than 0.10 seconds.

The displacement versus time and velocity versus time plots for this system's performance are shown in Figure 5.4 and 5.5.

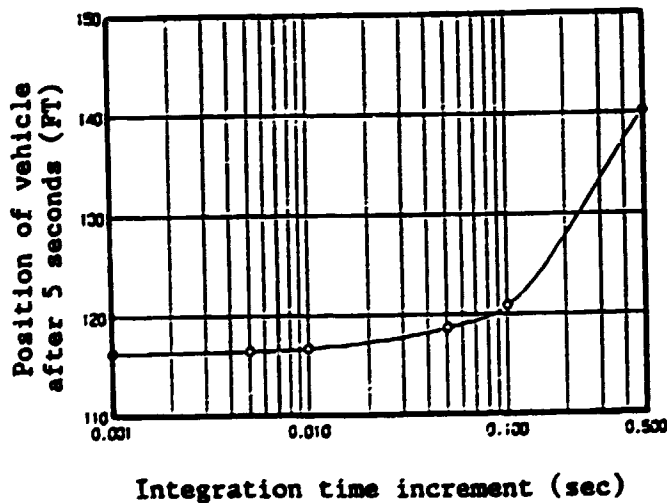


Figure 5.3 Investigation of Integration Step Size

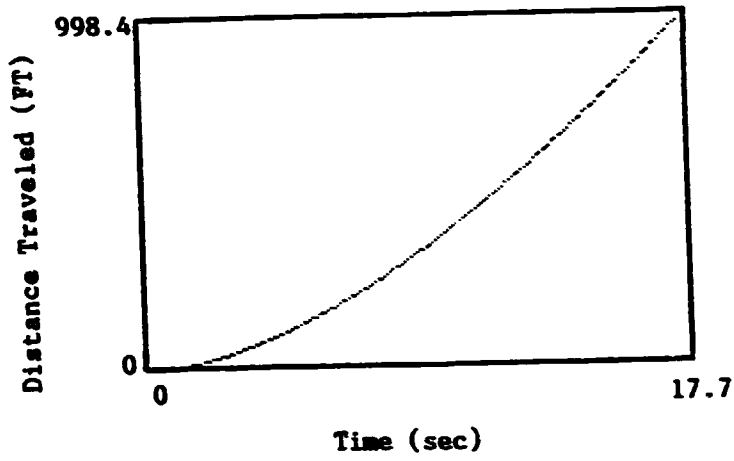


Figure 5.4 Vehicle Performance: Position versus Time

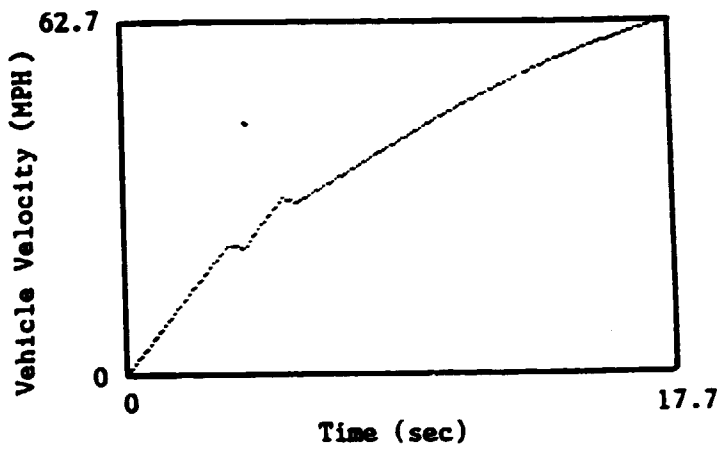


Figure 5.5 Vehicle Performance: Velocity versus Time

6. Solutions of Algebraic Equations

6.1 Solution of an Equation

The solution of a linear or nonlinear equation may be obtained by drawing a graph of the function to determine those values of the independent variable which reduce the function to zero. A nonlinear equation may have more than one root. Figure 6.1 illustrates how the function, $f(X)$, behave as X varies.

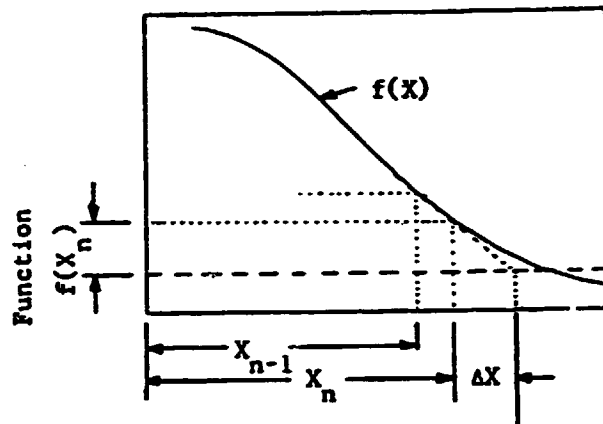


Figure 6.1 Solution to Function

The value of x which produces a zero value of the function, may be obtained by the Newton-Raphson numerical method. This method starts with the first two terms of the Taylor series expansion of the function $f(X)$ about the position x_n :

$$f(X_n + \Delta X) = f(X_n) + \Delta X \times f'(X_n)$$

$f'(X_n)$ is the slope of the function at $X = X_n$.

The small value ΔX which may be added to X_n to make $f(X_n + \Delta X)$ approach zero may be obtained by rearranging the Taylor series to solve for ΔX .

An initial trial value for X_n must be estimated.

$$f(X_n + \Delta X) = 0$$

$$f(X_n) + \Delta X \times f'(X_n) = 0$$

The slope may be approximated:

$$f'(X_n) = [f(X_n) - f(X_{n-1})] / (X_n - X_{n-1})$$

$$\Delta X = - f(X_n) \times (X_n - X_{n-1}) / [f(X_n) - f(X_{n-1})]$$

Add ΔX to X_n to bring X_n closer to the root as follows.

$$X_{n-1} = X_n$$

$$X_n = X_n + \Delta X$$

Repeat the above procedure of calculating the correction increment ΔX and modifying X_n and X_{n-1} . When $f(X_n)$ approaches zero, the solution has been obtained.

6.2 Solution of a System of Linear Equations

The Gaussian elimination method with pivot elements is a popular method for finding the roots of a system of linear equations.

Reference 3 gives a Fortran subroutine for this method. The following system of linear equations may be expressed in matrix form as indicated.

$$K_{11}X_1 + K_{12}X_2 + K_{13}X_3 = R_1$$

$$K_{21}X_1 + K_{22}X_2 + K_{23}X_3 = R_2$$

$$K_{31}X_1 + K_{32}X_2 + K_{33}X_3 = R_3$$

$$\begin{vmatrix} K_{11} & K_{12} & K_{13} \\ K_{21} & K_{22} & K_{23} \\ K_{31} & K_{32} & K_{33} \end{vmatrix} \begin{vmatrix} X_1 \\ X_2 \\ X_3 \end{vmatrix} = \begin{vmatrix} R_1 \\ R_2 \\ R_3 \end{vmatrix}$$

The Gaussian method uses the rules of algebra to modify the matrix equation until the diagonal of [K] has unity for each value and the entries in [K] below the diagonal are zero. The values of X_1 , X_2 and X_3 may then be obtained directly.

6.3 Solution of a System of Non-linear Equations

A non-linear system of equations may be solved by Newton's iterative method (Reference 4). The two equations below

$$f(X,y) = 0$$

$$g(X,y) = 0$$

may be satisfied if they are equal to zero when $X = X_0 + \Delta X$ and $y = y_0 + \Delta y$. The Taylor expansion about (X_0, y_0) is

$$f(X_0, y_0) + \Delta X \times \frac{\partial f(X_0, y_0)}{\partial X} + \Delta y \times \frac{\partial f(X_0, y_0)}{\partial y} = 0$$

$$g(X_0, y_0) + \Delta X \times \frac{\partial g(X_0, y_0)}{\partial X} + \Delta y \times \frac{\partial g(X_0, y_0)}{\partial y} = 0$$

Rearranging these two equations into matrix form produces the following.

$$\begin{vmatrix} \frac{\partial f(X_0, y_0)}{\partial X} & \frac{\partial f(X_0, y_0)}{\partial y} \\ \frac{\partial g(X_0, y_0)}{\partial X} & \frac{\partial g(X_0, y_0)}{\partial y} \end{vmatrix} \begin{vmatrix} \Delta X \\ \Delta y \end{vmatrix} = \begin{vmatrix} -f(X_0, y_0) \\ -g(X_0, y_0) \end{vmatrix}$$

Values of the partial derivatives provide the slope. The values of ΔX and Δy may then be evaluated as the changes in X and y which are required in order to approach the roots. Before repeating the above calculations, new values of X and y are needed.

$$X_1 = X_0 + \Delta X$$

$$y_1 = y_0 + \Delta y$$

This process is repeated until the functions approach zero.

The numerical values of the slopes $\partial f(X_0, y_0)/\partial X$, $\partial f(X_0, y_0)/\partial y$, $\partial g(X_0, y_0)/\partial X$ and $\partial g(X_0, y_0)/\partial y$ may be difficult to evaluate for some functions by taking the partial derivatives. An alternative is to estimate these slopes numerically over a small increment about the point X_0, y_0 . The size of the increment must be small so its size does not influence the magnitude of the slope.

7. Sensitivity Studies

Sensitivity studies quantify the relationship between the input parameters, which are independent design variables selected by the designer, and the output variable, which is the dependent variable representing value, performance or cost. The sensitivity study shows how the output variable responds to a change in the input variable, that is, it quantifies the amount of improvement in value (or the change in cost) for a specified change in a design variable.

Sensitivity studies help the engineer to develop a realistic model as it aids his visualization of the mathematical relationships between the variables. On the other hand, the optimization study normally determines the set of values of the input variables which will produce the "best" value of the output without regard to how the variables change in approaching this "best" value. Figure 7.1 illustrates a sensitivity study in which the current performance (cycles completed per shift) for the machine can be improved by 8.6 percent by an increase in vehicle rated speed of 25 percent while the performance can be improved an additional 5.5% by increasing the vehicle speed an additional 25%. The rate of change in performance is decreasing and

the safety of the operation is rapidly decreasing as the vehicle speed is increased. In the next section, which discusses optimization, the sensitivity study is applied to the "optimum" set of design variables to quantify the manner in which each variable approaches this optimum condition.

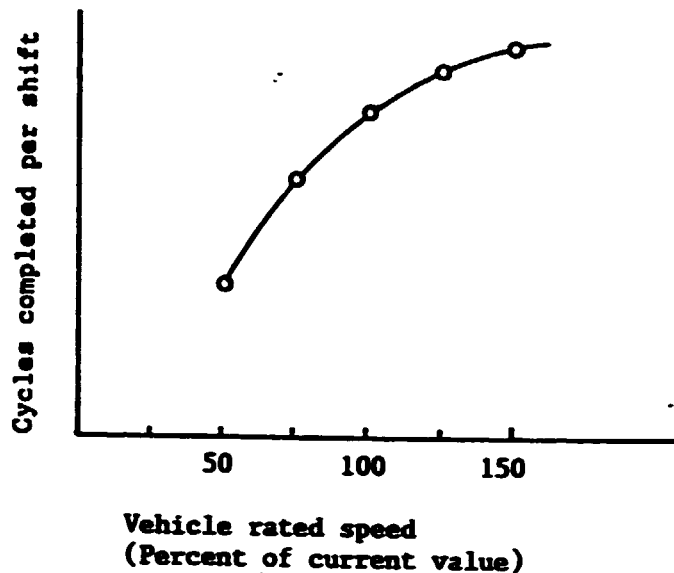


Figure 7.1 Sensitivity Study: Fork Lift Truck Performance

8. Optimization by the Complex Method

The Complex Method of optimization of a multivariable, nonlinear, constrained problem was studied by Dr. G. H. Michaud (5). This method finds the maximum or minimum value of a function.

To describe this method, consider a problem with n design variables. For a set of values for these n variables, the output of the system may be evaluated. Each set of n design variables locates a vertex in n -space. Each design variable is considered as one of the coordinates for the vertex in n space. Now consider k sets of these design variables from which k values of the output may be evaluated. If we select a problem with two independent design variables, n will be

equal to two. If we select k as equal to three times n , then $k = 5$. Michaud usually used $k = 2n$, but $3n$ may provide a more dynamic search. A plot of the six vertices in n -space is given in Figure 8.1. The six sets of design variables were scattered between upper and lower bounds for each of the independent variables. These sets of values may be randomly generated between these boundaries.

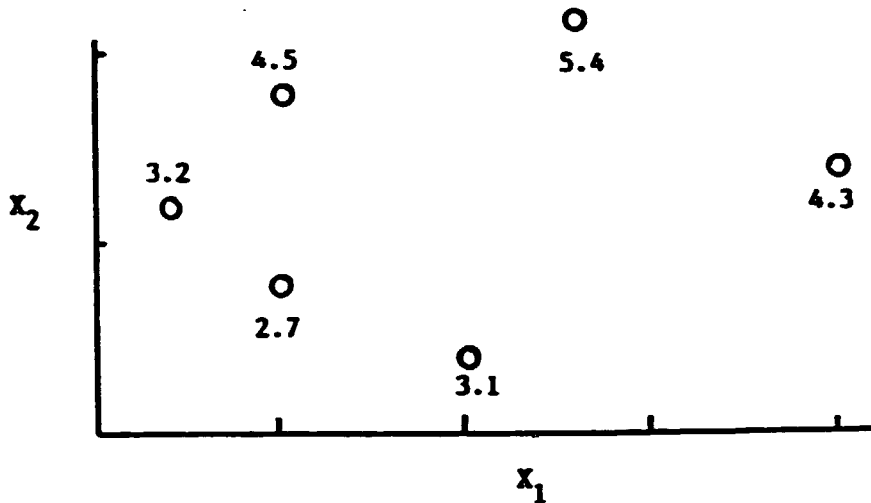


Figure 8.1 Complex for Two Space

The magnitude of the output parameter, which is to be optimized, is given beside each vertex in Figure 8.1. The output is to be maximized. The vertex with the lowest performance, has an output value of 2.7. This vertex with the lowest performance is removed and the centroid of the coordinates of the remaining vertexes is determined. Figure 8.1 shows the five remaining vertexes plus the centroid.

$$(X_1)_c = \frac{1}{k-1} \left[\sum_{j=1}^k (X_1)_j - (X_1)_R \right]$$

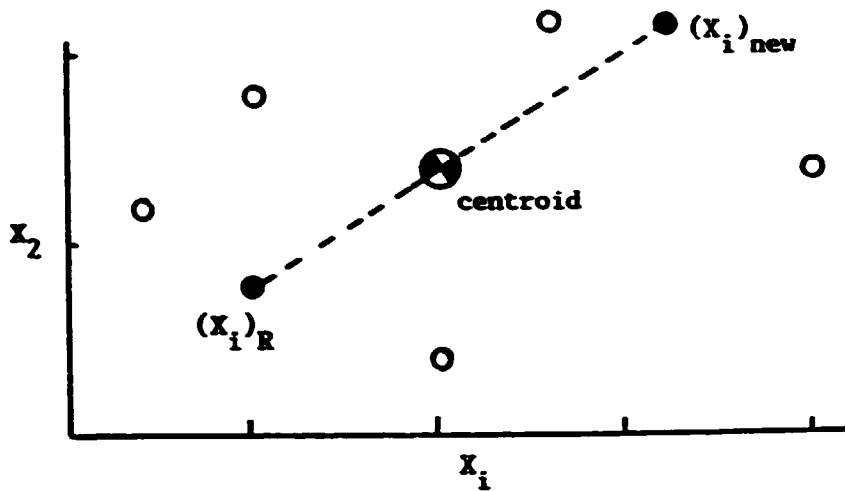


Figure 8.2 Complex Method Moving Strategy

The next step is to obtain an improved value of the independent variable by moving along a line from the rejected vertex, $(X_1)_R$, and through the centroid, $(X_1)_C$, to a new value $(X_1)_{new}$. The $(X_1)_{new}$ is a point beyond the centroid by α times the distance between the rejected vertex and the centroid. Box (3) used a value of $\alpha = 1.3$.

$$(X_1)_{new} = \alpha[(X_1)_C - (S_1)_R] + [X_1]_C$$

If this new point is within the bounds of the design space, the search continues with $(X_1)_{new}$ providing the one of the independent variables for a new vertex.

The value of the output parameter is evaluated for the set of values at $(X_1)_{new}$. The process is repeated by identifying the set of independent variables with the lowest performance and rejecting it. Then another new set of variables is obtained by marching from the rejected vertex through the centroid again.

If the new design point had been outside of the design space, a new trial value would have been located by moving in toward the centroid by the factor beta:

$$(X_i)_{\text{new}} = \beta[(X_i)_{\text{new}} - (X_i)_c] + (X_i)_c$$

One way to stop is to perform a certain number of iterations and observe the value of the output to determine if it is converging.

Dr. Michaud's Designer-Augmented Optimization Program requires the user to identify the output variable, which he calls the "objective function." He created a subroutine, OBJFUNK, which contains this function and the user must build this subroutine OBFUNK for each problem. His program also has a subroutine, TEST, which contains the upper and lower bounds for each independent design variable.

Subroutine TEST must also be rebuilt for each problem.

In order to combine some of the concepts of sensitivity studies with the concepts of optimization as described by Dr. Michaud, his optimization program was modified to produce sensitivity studies about the optimum design point. The sensitivity study keeps all design variables at their optimum values except one, which is allowed to vary while the output (performance) is evaluated. The results are presented in graphical form to aid in visualization of the sensitivity of the system's performance to changes in each particular design variable.

In order to demonstrate the use of this optimization/sensitivity program, the code from Example 1 for the vehicle with three speed transmission is inserted into subroutine OBFUNK, the output parameter, which is to be optimized, is chosen as the time required to travel 1000 feet. This is a minimization problem. The value of k is taken as 2n. The independent design parameters are the final drive gear ratio, the

transmission ratio in first gear and the transmission ratio in second gear. (The transmission ratio in third gear is 1 to 1.) The optimum gear ratios are

First Gear Ratio = 1.9

Second Gear Ratio = 1.4

Final Gear Ratio = 2.9

The sensitivity studies are shown in Figures 8.3, 8.4 and 8.5 for first, second and final drive ratios. The ratios in first and in the final drive are not very strong influences, if adequately large ratios are given to provide starting torque. However, second gear ratio has a much narrower band of desirable values in between the extremes of high and low values.

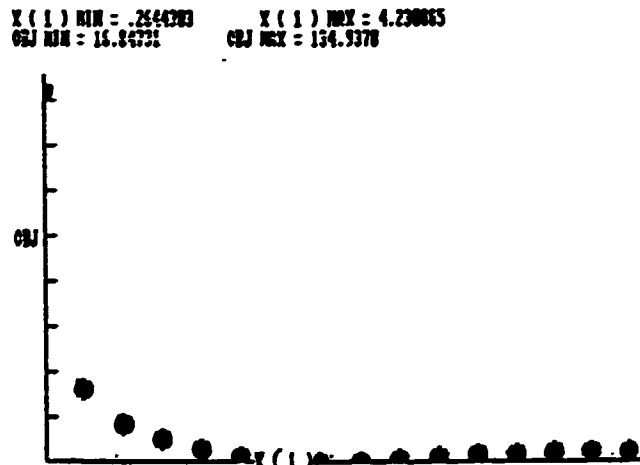


Figure 8.3 Vehicle Travel Time, OBJ, versus First Gear Ratio,
X(1)

X (2) MIN = .147685 X (2) MAX = 2.36312
OBJ MIN = 16.23679 OBJ MAX = 20.95851



Figure 8.4 Vehicle Travel Time, OBJ, versus Second Gear Ratio, X(2)

X (3) MIN = .2292498 X (3) MAX = 5.427897
OBJ MIN = 16.74777 OBJ MAX = 154.9578

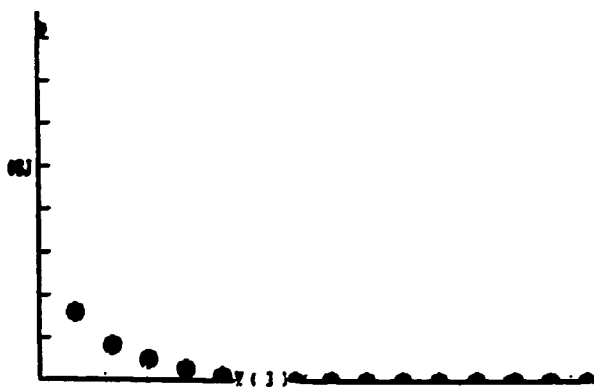


Figure 8.5 Vehicle Travel Time, OBJ, versus Final Drive Ratio, X(3)

REFERENCE LIST

1. Rao, Singiresu S., Mechanical Vibrations, Addison-Wesley Publishing Company, 1986.
2. Haberman, Charles M., Engineering Systems Analysis, Charles E. Merrell Books, Inc., Columbus, OH, 1965.
3. Tse, Francis S., et al, Mechanical Vibrations Theory and Applications, Allyn and Bacon, Inc., 1963.
4. Hildebrand, Francis B., Advanced Calculus for Applications, Prentice-Hall, Inc., 1962.
5. Michaud, G. H., "User's Manual I, A Designer-Augmented Optimization System," Ph.D. Thesis, Purdue University, 1974.
6. Harrison, H. L., Bollinger, J. G., Introduction to Automatic Controls, International Textbook Company, 1969.
7. Nestorides, E. J., A Handbook on Torsional Vibration, The British Internal Combustion Engine Research Association, Cambridge University Press, 1958.
8. Cardenas, Jaime, "Design of a Test Machine for Measuring Dynamical Properties of Torsional Elastomer Couplings," M.S. Thesis, Mississippi State University, 1982.
9. Elahi, Mehran, "Measurement of Static and Dynamic Characteristics of Elastomer Couplings Using Computerized Data Acquisition System," M. S. Thesis, Mississippi State University, 1985.
10. Wylie, Jr., C. R., Advanced Engineering Mathematics, McGraw-Hill, 1960.
11. Bendat, J. S., and Piersol, A. G., Random Data: Analysis and Measurement Procedures, Wiley-Interscience, New York, 1971.
12. Meirovitch, Leonard, Elements of Vibration Analysis, McGraw-Hill, 1986.
13. Jones, E. W., "Relating Pavement Roughness to Vehicle Behavior," Ph.D. Thesis, Purdue University, 1974.

LECTURE 3

TORSIONAL VIBRATIONS

ABSTRACT:

Torsional vibrations in geared systems may cause premature failures. Sensitivity studies, which show the change in torsional vibrations due to variations in the inertia, elastic and damping characteristics, are presented to illustrate how a system may be tuned to improve performance. A computational technique, based on the finite element method, that takes advantage of qualities unique to torsional systems is developed for analyzing the vibratory stresses in forced-damped torsional systems.

1. INTRODUCTION:

Torsional vibrations of power train systems may produce excessive vibratory stresses in the drive train and may cause 'hammering' of the gear teeth. The vibratory stresses may produce fatigue failure of the shafts. The gear tooth hammering, which is produced when the vibratory torque exceeds the mean torque, produces impact loads between the mating teeth which can be several times the vibratory torque in the gear shafts (1).¹

Torsional vibrations are produced by masses rotating out of a steady state position to twist the shaft. This rotation produces a restoring torque in the twisted shaft, which stores potential energy in the shaft. This stored potential energy accelerates the mass towards its steady-state position. However, due to the kinetic energy of the mass, it overshoots the steady state position. The repetition of this interchange from kinetic to potential energy and vice versa requires a

¹Numbers in parentheses refer to references.

spring and a mass and constitutes the natural frequency of vibration. At a given natural frequency, all of the masses are tuned to vibrate in unison (i.e., at the same number of vibrations per minute).

Each natural frequency has a unique shape (mode shape) for its deflection curve. The number of nodes (i.e., points with zero deflection) is one for the first natural frequency and increases by one for each higher frequency. (Counting the nodes is one way to determine if all natural frequencies have been located.) The zero mode has no nodes and represents the rigid body motion of the system. The mode shape is made up of the relative amplitudes of the angular displacements for each lump.

In order to maintain a torsional vibration, a periodic excitation torque must be applied to produce the vibratory motion and to overcome the continual energy loss of damping. Excitation torque may be produced by the internal combustion engine's gas pressure and reciprocating mechanism, by the propeller blades moving through differences in streamlines behind struts, by pump and compressor impeller blades or by reciprocating mechanisms of pumps and compressors. The magnitudes of these application torques are not usually adequate to produce damage; however, if the system has a natural frequency occurring at or near the frequency of an excitation torque, a resonant condition will occur and the application torque will be amplified.

The vibration excitation torque is normally divided into harmonic components to facilitate the analysis. (The alternate approach would be to use numerical integration to evaluate the response of the system to the total excitation torque.) This division of the excitation into single harmonics tends to focus the analysis on one natural frequency

at a time. The first and second harmonic components of the gas pressure curve for the engine curve of Figure 1.1 (8) are shown in Figure 1.2. (In order to transform the gas pressure into torque, the kinematics of the reciprocating slider crank mechanism must be considered.)

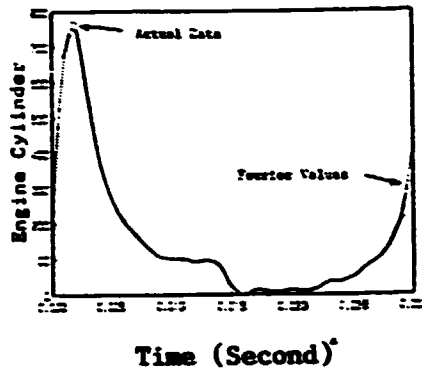


Figure 1.1 Engine Gas Pressure Curve for One 360° Cycle

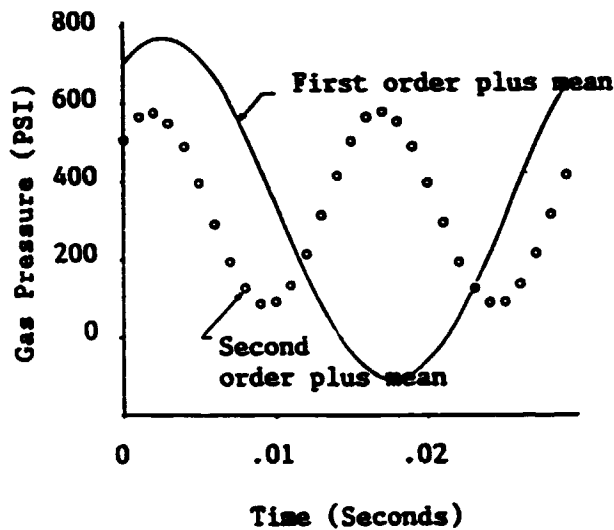


Figure 1.2 Gas Pressure Harmonics

The analysis of torsional vibrations is well defined in the literature. Den Hartog (3) describes the fundamentals of engine excitation, damping devices and the Holzer solution. Harrington (4) quantifies the energy sources and sinks for marine systems. Handbooks on torsional vibrations by the British Internal Combustion Engine

Research Association (5) and Ker Wilson (6) are available. The Underwriters for the Maritime industry have published Rules (7 and 8) for guidance of torsional vibration analysis.

The Holzer (11) method of analysis of free or forced, undamped torsional vibration systems has been popular because of the simple and repetitive nature of the calculations required. Holzer's table in these cases consists of real numbers. Hartog and Li (12) extended Holzer's method to include the analysis of free, damped torsional systems. Later, Spaetgens and Vancouver (13) further extended the method to solve the forced, damped torsional vibration problem. The arithmetic in this case involves complex numbers, which detracts from the 'simple calculations' advantage of the method. However, with the advent of computers, programs were written to carry out most of the tedious calculations. Wu and Chen (14) have written complete computer programs to analyze free or forced, undamped or damped single branch torsional systems. As indicated in their paper, some trial and error is required in the solution of the forced, damped torsional vibration problem. This is not desirable in computer methods as it could lead to considerable computer time and cost. Also the task of extending Holzer's method to analyze multi-branch, multi-junction, forced damped torsional systems does not appear to be easy.

TORVAP-A (15), a computer program for the torsional vibration analysis of multi-branch, multi-junction systems developed by BICERA (British Internal Combustion Engine Research Association) uses transfer matrices to arrive at a system of simultaneous equations for an equivalent torsional system with a reduced number of degrees of freedom. The other degrees of freedom are evaluated by working back

with the known degrees of freedom and appropriate transfer matrices. Thus the method essentially consists of two passes, with multiplication of transfer matrices required in each pass. The results of the intermediate stages are not stored. This reduces computer storage requirements but increases the number of calculations required. This program is reported to be faster and less expensive to use than the Holzer table method.

A method that reduces the number of calculations, while requiring little additional storage, would be an improvement over TORVAP-A. Such a method, based on the theory of finite elements, is presented in this paper.

One of the traditional methods currently in use for analyzing torsional systems assumes that the mode shape of the idealized free-undamped system is identical to the mode shape of the real forced-damped system (3). That is, the inertia forces are assumed to dominate the damping forces and excitation forces near resonant speeds. Conclusions drawn from results obtained by this traditional method have sometimes proved to be unsatisfactory because the damping forces and excitation forces may be large enough to distort the mode shape. Lloyd's Register of Shipping outlines the step by step method of analysis based on this traditional method and then comments that if it is unsatisfactory a forced, damped solution is to be used. However Lloyd's Register of Shipping does not outline the latter method of analysis or provide any guidance for the evaluation when the traditional method is unsatisfactory.

The effect of various design parameters (e.g., flywheel inertia, coupling torsional stiffness, etc.) on the torsional vibrations of a system may be used to tune the system for good torsional performance. Sensitivity studies which show this interaction are included in this paper.

2. COMPUTATIONAL TECHNIQUE BASED ON THE FINITE ELEMENT METHOD:

The theory for a torsional analysis method, which is based on the FEM, is presented in this section. The basic finite element for the torsional vibration system consists of one disk and one spring with an external and internal damper (Figure 2.1).

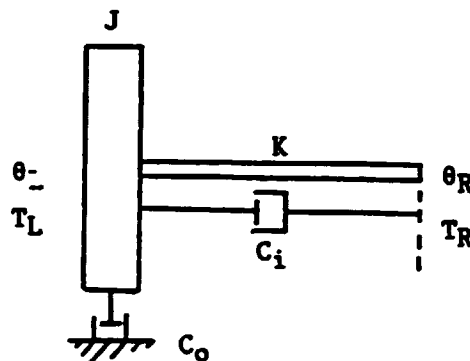


Figure 2.1 The Basic Finite Element

where

K = coefficient of stiffness of the spring

J = rotational mass moment of inertia of the disk about an axis through its center and perpendicular to the plane of the disk

C_i = internal damping coefficient

C_o = external damping coefficient

θ_L, θ_R = angular displacements at the left and right ends of the element respectively

T_L, T_R = torques at the left and right ends of the element respectively

From elementary theory of finite elements, the element stiffness matrix is [E]. The stiffness equation is:

$$[E] [\theta] = [T]$$

or, the expanded form of this equation is:

$$\begin{bmatrix} K - j^*w^*w + j^*w^*(C_0 + C_1) & -K - j^*w^*C_1 \\ -K - j^*w^*C_1 & K + j^*w^*C_1 \end{bmatrix} \begin{bmatrix} \theta_L \\ \theta_R \end{bmatrix} = \begin{bmatrix} T_L \\ T_R \end{bmatrix}$$

The values of θ_L, T_L, θ_R and T_R that satisfy the above equation, will satisfy the equations of motion. Note that, in general, θ and T are complex quantities, which have real and imaginary components.

The stiffness matrix can also be obtained by rearranging terms in the transfer matrix⁷.

Let the displacement vector be $\bar{\theta} = \theta * e^{i\omega t}$

and the exciting torque vector be $\bar{T} = -T * e^{i\omega t}$

$$\begin{bmatrix} \theta_R \\ T_R^* \end{bmatrix} = \begin{bmatrix} 1 & -1/(K + j^*w^*C_1) \\ 0 & 1 \end{bmatrix} \begin{bmatrix} 1 & 0 \\ w^*w^*J - j^*w^*C_0 & 1 \end{bmatrix} \begin{bmatrix} \theta_L \\ T_L \end{bmatrix}$$

$$= \begin{bmatrix} 1 - (w^*w^*J - j^*w^*C_0)/(K + j^*w^*C_1) & -1/(K + j^*w^*C_1) \\ w^*w^*J - j^*w^*C_0 & 1 \end{bmatrix} \begin{bmatrix} \theta_L \\ T_L \end{bmatrix}$$

Let $A = w^*w^*J - j^*w^*C_0$

and $B = K + j^*w^*C_1$

Then $\theta_R = (1 - A/B) * \theta_L - T_L/B$

which gives

$$T_L = -\theta_R * B + (B - A) * \theta_L$$

and $T_R^* = A * \theta_L + T_L$

which gives

$$T_R^* = B(\theta_L - \theta_R)$$

But $T_R^* = -T_R$ since T_R^* is the remainder torque which must be opposed by T for the element to satisfy the equations of motion.

Therefore,

$$T_R = -B(\theta_L - \theta_R) \quad 2$$

Equations 1 and 2 in the matrix form are:

$$\begin{bmatrix} T_L \\ T_R \end{bmatrix} = \begin{bmatrix} B - A & -B \\ -B & B \end{bmatrix} \begin{bmatrix} \theta_L \\ \theta_R \end{bmatrix}$$

$$= \begin{bmatrix} K - w^*w^*J + j^*w^*C_1 & -K - j^*w^*C_1 \\ -K - j^*w^*C_1 & K + j^*w^*C_1 \end{bmatrix} \begin{bmatrix} \theta_L \\ \theta_R \end{bmatrix}$$

or,

$$[T] = [E] [\theta]$$

The following example problem will illustrate the various steps in the finite element method (Figure 2.2). Assume consistent units for all quantities.

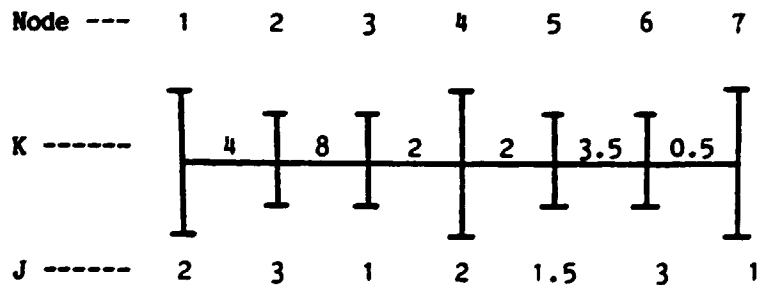


Figure 2.2 Illustrative Torsional System

Node	---	1	2	3	4	5	6	7
Applied Torques	---	8	8	-3	-1	8	8	-6

The harmonic frequency of the applied torque is two radians per second.

This problem may be solved as a one branch system, however, for illustrative purposes this solution considers the system to be made up of two branches with one junction.

Branch 1: This branch consists of nodes 4, 3, 2, 1. Node 4 is the junction node. The stiffness matrix of this branch [S], obtained by assembling the appropriate element stiffness matrices [E] as per the typical finite element procedure, is given below.

$$\begin{bmatrix} T_4 \\ T_3 \\ T_2 \\ T_1 \end{bmatrix} = [S] \begin{bmatrix} \theta_4 \\ \theta_3 \\ \theta_2 \\ \theta_2 \end{bmatrix}$$

where

$$[S] = \begin{bmatrix} 2-2*2^2 & -2 & 0 & 0 \\ -2 & 2+8-1*2^2 & -8 & 0 \\ 0 & -8 & 8+4-3*2^2 & -4 \\ 0 & 0 & -4 & 4-2*2^2 \end{bmatrix}$$

$$[S] = \begin{bmatrix} -6 & -2 & 0 & 0 \\ -2 & 6 & -8 & 0 \\ 0 & -8 & 0 & -4 \\ 0 & 0 & -4 & -4 \end{bmatrix}$$

The branch stiffness matrix is always tri-diagonal and symmetric. The off-diagonal elements are simply the negative of the diagonal value, -K, or it is -(+K+j*w*C_i) when internal damping is present. Therefore, from a computer storage point of view, it is only necessary to store the diagonal elements.

As other branches can be linked to this branch only at the extreme ends, only the two degrees of freedom at the ends of a branch need be retained to add to the system stiffness matrix. A super-element stiffness matrix, equivalent to the branch stiffness matrix, but with only two degrees of freedom can be obtained as follows.

The equations up to this point are:

Equation

$$\begin{array}{l}
 1 \\
 2 \\
 3 \\
 4
 \end{array}
 \begin{array}{c}
 \left| \begin{array}{cccc}
 -6 & -2 & 0 & 0 \\
 -2 & 6 & -8 & 0 \\
 0 & -8 & 0 & -4 \\
 0 & 0 & -4 & -4
 \end{array} \right|
 \end{array}
 \begin{array}{c}
 \left| \begin{array}{c}
 \theta_4 \\
 \theta_3 \\
 \theta_2 \\
 \theta_1
 \end{array} \right|
 \end{array}
 =
 \begin{array}{c}
 \left| \begin{array}{c}
 0 \\
 -3 \\
 8 \\
 0
 \end{array} \right|
 \end{array}$$

The values of T_4 and T_1 are omitted in the right hand vector. They will be added to the first and last entries of the right hand vector later as they should be added only once.

Eliminate θ_3 from equations 1 and 3 and retain equations 1, 3 and 4 by the following process, which forces column 2 of the above equation to be zero:

Multiply equation 2 by 1/3 and add to equation 1.

Multiply equation 2 by 8/6 and add to equation 3.

The resulting matrix equation is:

$$\begin{array}{l}
 1 \\
 3 \\
 4
 \end{array}
 \begin{array}{c}
 \left| \begin{array}{ccc}
 -20/3 & -8/3 & 0 \\
 -8/3 & -32/3 & -4 \\
 0 & -4 & -4
 \end{array} \right|
 \end{array}
 \begin{array}{c}
 \left| \begin{array}{c}
 \theta_4 \\
 \theta_2 \\
 \theta_1
 \end{array} \right|
 \end{array}
 =
 \begin{array}{c}
 \left| \begin{array}{c}
 -1 \\
 4 \\
 0
 \end{array} \right|
 \end{array}$$

Eliminate θ_2 from equations 1 and 4 and retain equations 1 and 4 which have the end nodes.

$$\begin{vmatrix} -6 & 1 \\ 1 & -5/2 \end{vmatrix} \begin{vmatrix} \theta_4 \\ \theta_1 \end{vmatrix} = \begin{vmatrix} -2 \\ -3/2 \end{vmatrix}$$

Branch 2: this branch consists of nodes 7, 6, 5, 4. Node 4 is the junction node.

The branch stiffness matrix is:

$$\begin{vmatrix} (.5-1*2^2) & -0.5 & 0 & 0 \\ -0.5 & (.5+3.5-3*2^2) & -3.5 & 0 \\ 0 & -3.5 & (3.5+2-1.5*2^2) & -2 \\ 0 & 0 & -2 & (2-0*2^2) \end{vmatrix} \begin{vmatrix} \theta_7 \\ \theta_6 \\ \theta_5 \\ \theta_4 \end{vmatrix} = \begin{vmatrix} 0 \\ 8 \\ 8 \\ 0 \end{vmatrix}$$

The values of T_7 and T_4 are omitted from the right hand vector as they will be added later. Also the value of J in the (4,4) position of the stiffness matrix is set to zero at this step as it was included in the matrix for branch one and should be added only once at the junction node.

The super-element stiffness matrix is reduced as follows by eliminating all displacement variables except at the ends of the branch.

$$\begin{vmatrix} -3.5 & -0.5 & 0 & 0 \\ -0.5 & -8 & -3.5 & 0 \\ 0 & -3.5 & -0.5 & -2 \\ 0 & 0 & -2 & 2 \end{vmatrix} \begin{vmatrix} \theta_7 \\ \theta_6 \\ \theta_5 \\ \theta_4 \end{vmatrix} = \begin{vmatrix} 0 \\ 8 \\ 8 \\ 0 \end{vmatrix}$$

$$\begin{vmatrix} -111/32 & 7/32 & 0 \\ 7/32 & 33/32 & -2 \\ 0 & -2 & 2 \end{vmatrix} \begin{vmatrix} \theta_7 \\ \theta_5 \\ \theta_4 \end{vmatrix} = \begin{vmatrix} -0.5 \\ 4.5 \\ 0 \end{vmatrix}$$

$$\begin{vmatrix} -3.5151515 & .4242424 \\ .4242424 & -1.8787878 \end{vmatrix} \begin{vmatrix} \theta_7 \\ \theta_4 \end{vmatrix} = \begin{vmatrix} -1.4545454 \\ 8.7272727 \end{vmatrix}$$

Assemble the super-element stiffness matrices to form the system stiffness equation. The values of T_4 , T_1 and T_7 are added to the right hand vector as shown below.

$$\begin{vmatrix} -6-1.8787878 & 1 & .4242424 \\ 1 & -2.5 & 0 \\ .4242424 & 0 & -3.5151515 \end{vmatrix} \begin{vmatrix} \theta_4 \\ \theta_1 \\ \theta_7 \end{vmatrix} = \begin{vmatrix} -2+8.7272727-1 \\ -1.5+8 \\ -1.4545454-6 \end{vmatrix}$$

$$\begin{vmatrix} -7.8787878 & 1 & .4242424 \\ 1 & -2.5 & 0 \\ .4242424 & 0 & -3.5151515 \end{vmatrix} \begin{vmatrix} \theta_4 \\ \theta_1 \\ \theta_7 \end{vmatrix} = \begin{vmatrix} 5.7272727 \\ 6.5 \\ -7.4545454 \end{vmatrix}$$

The system stiffness matrix, which is formed by the assembly of symmetric super-element stiffness matrices, is also symmetric.

The above system of equations can be solved to obtain the angular displacements of the super-element's degrees of freedom. (The super-element's degrees of freedom will be referred to as the 'master' degrees of freedom in the future.) The solutions are:

$$\theta_4 = -1$$

$$\theta_1 = -3$$

$$\theta_7 = 2$$

All of the stiffness matrices will be complex if damping is present in the system.

Let the degree of a junction node be defined as the number of junction nodes directly linked to it, ignoring intermediate nodes in the branches. All other master nodes (non-junction nodes at the termination of branches) are of degree zero. Only master nodes are assigned degrees.

As an example, consider the following system with 16 nodes and 8 branches as shown in Figure 2.3.

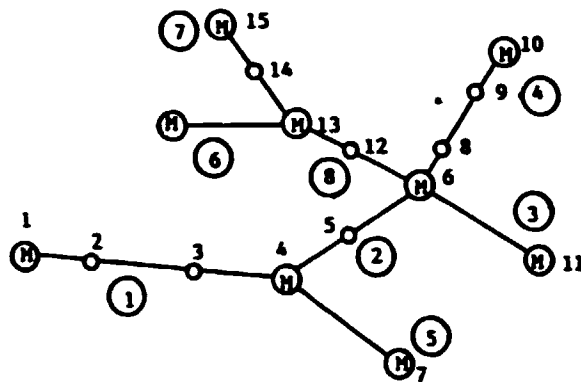


Figure 2.3 Torsional System to Illustrate Degree of Nodes

Node	- 1	4	6	7	10	11	13	15	16
Degree	- 0	1	2	0	0	0	1	0	0

All other master nodes are of degree 0.

Knowing the displacements at the master nodes, values at nodes adjacent to the master nodes may be calculated from equations obtained by adding together appropriate elements in the branch equilibrium equations. Displacements at all other nodes may be calculated directly from the branch equilibrium equations.

To ensure that no more than one unknown is present in an equation at any time during back substitution, nodes adjacent to the master nodes should be solved for in increasing degree of the master nodes. For example, in the above figure, displacements at the non-master nodes would be solved for in the following order:

<u>Branch</u>	<u>Direction (node to node)</u>	
1	(1 ---> 4)	
3	nodes (11 ---> 6)	
4	with (10 ---> 6)	First
5	degree (7 ---> 4)	pass
6	of zero (16 ---> 13)	
7	(15 ---> 13)	
2	nodes with (4 ---> 6)	Second
8	degree of one (13 ---> 6)	pass

In the first example problem, which was solved as a two branch system, nodes 1, 4 and 7 are of degree 0. Therefore displacements at all of the non-master nodes may be solved for in one pass.

The equilibrium equations for the whole system (without reduction to super-elements) are:

$$\begin{array}{ccccccc|c|c}
 -4 & -4 & 0 & 0 & 0 & 0 & 0 & \theta_1 & 8 \\
 -4 & 0 & -8 & 0 & 0 & 0 & 0 & \theta_2 & 8 \\
 0 & -8 & 6 & -2 & 0 & 0 & 0 & \theta_3 & -3 \\
 0 & 0 & -2 & -6+2 & -2 & 0 & 0 & \theta_4 & -1 \\
 0 & 0 & 0 & -2 & -.5 & -3.5 & 0 & \theta_5 & 8 \\
 0 & 0 & 0 & 0 & -3.5 & -8 & -.5 & \theta_6 & 8 \\
 0 & 0 & 0 & 0 & 0 & -.5 & -3.5 & \theta_7 & -6
 \end{array}$$

Having calculated the displacements at the master nodes 1, 4 and 7, the displacements at nodes 2, 3, 6 and 5 are calculated from equations 1, 2, 7 and 6 respectively.

From equation 1 : $\theta_2 = 1$

From equation 2 : $\theta_3 = .5$

From equation 7 : $\theta_6 = -2$

From equation 6 : $\theta_5 = 2$

The torque in a shaft can be calculated by the following formula:

$$[T_n] = K_n[\theta_{n-1} - \theta_n]$$

where (n-1) and n are the nodes on the shaft and K_n is the stiffness of the shaft.

The stress in the shaft can be calculated by the following formula:

$$\tau_n = T_n * c / J_n$$

where c is the radius of the shaft

and J_n is the polar moment of inertia of the shaft

The fundamental equations for the finite element of a shaft and mass with damping have been developed. A scheme which greatly reduces the numerical difficulties in the solution of a system which has many masses has been described. In order to implement these concepts in an efficient manner, a computer program must be designed to carry out these operations for a general system.

3. SATOV - A Computer Program for the Finite Element Method:

A computer program, SATOV (Stress Analysis for Torsional Vibrations), was written in Fortran for analyzing the vibratory stresses in a forced, damped, multi-branch torsional system(18). It is based on the procedure presented in the previous chapter.

Line M+1 - Complex torques applied at nodes in branch 1 (in the same order in which the nodes were specified for this branch)

Line M+2 - Complex torques applied at nodes in branch 2

Line M+NBRNCH - Complex torques applied at nodes in branch NBRNCH

For the case of engine excitation, data input is as follows:

Line 1 - IGOPR, IPLOT, 0 IGOPR = 0 printout suppressed
 = 1 printout activated
 IPLOT = 0 plots suppressed
 = 1 plots activated

Line 2 - IORD, ORD(1), TAMP(1), ORD(2), TAMP(2), ----, ORD(IORD),
 TAMP(IORD)

IORD = number of orders to be analyzed

ORD(I) = order number

TAMP(I) = excitation torque amplitude for order number ORD(I)

* NOTE * For a V - engine TAMP(I) = V * Torque amplitude
 where $V = 2 * \cos(\text{ORD}(I) * .5 * \text{ALPHA})$
 where $\text{ALPHA}/A = V$ angle of engine

Line 3 - FMIN, FMAX, FINC FMIN = minimum engine speed (rpm)
 FMAX = maximum engine speed (rpm)
 FINC = increment engine speed (rpm)

Line 4 - NBRNCH NBRNCH = number of branches in the system

Line 5 - NODMAX NODMAX = number of nodes in branch 1

Line 6 - NCYL, NSTKE NCYL = number of cylinders for the engine in
 this branch
 NSTKE = 2 for two stroke engine
 = 4 for four stroke engine

Line 7 - I(1), I(2), I(3), ---, I(NCYL) these are the firing orders
 according to the node numbers

* NOTE * In the case of a v - engine these are the firing orders in only one of the two banks. The V-factor, used in calculating the torque amplitude, takes into account the effect of the other bank of cylinders.

Line 8 - +NOD, +OJ, +OK) as explained for the case of externally
Line 9 - C₀, C₁) applied torques

repeat from line 5 for each branch of the system.

For the sample problem of chapter 2, the input data would be:

1,0,1
 2.,2.,1.
 2
 4
 -4,2.,2.
 3,1.,8.
 2,3.,4.
 1,2.,0.
 4
 7,1.,.5
 6,3.,3.5
 5,1.5,2.
 -4,2.,0.
 -1.,0.,-3.,0.,8.,0.,8.,0.
 -6.,0.,8.,0.,8.,0.,-1.,0.

The following problem gives an example of input data for the case of engine excitation.

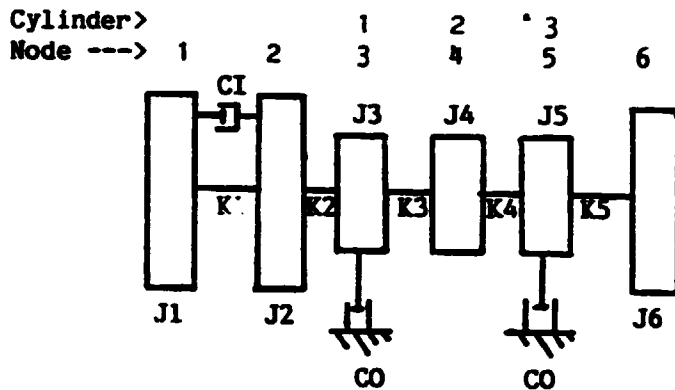


Figure 3.1 Example Problem with Engine Excitation

K1 = 1.5E6	J1 = 20.	CO = 2.E4
K2 = 13.05E6	J2 = 110.	CI = 1.E4
K3 = 16.5E6	J3 = 2.5	
K4 = 16.5E6	J4 = 2.5	
K5 = 12.7E6	J5 = 2.5	
	J6 = 110.	

Let the engine have the following characteristics:

3 cylinders, 4 stroke, 1-3-2 firing order.

Orders of excitation torque of interest are 1.5 and 4 with corresponding torque amplitudes of 7500. and 4000.

The range of engine speed, which is of interest is,

$$500 \text{ rpm} < n < 800 \text{ rpm}$$

Only vibratory torque plots are required for each shaft.

The data input would be:

0,1,0

2,1.5,7500., 4.,4000.

500., 800.,4.

1

6

3, 4

3, 5, 4

1, 20., -1.5E6

0.,1.E4

2,110., 13.05E6

3, -2.5, 16.5E6

2.E4, 0.

4, 2.5, 16.5E6

5, -2.5, 12.7E6

2.E4, 0.

6, 110., 0.

The output plot of this example is shown in Figure 3.2.

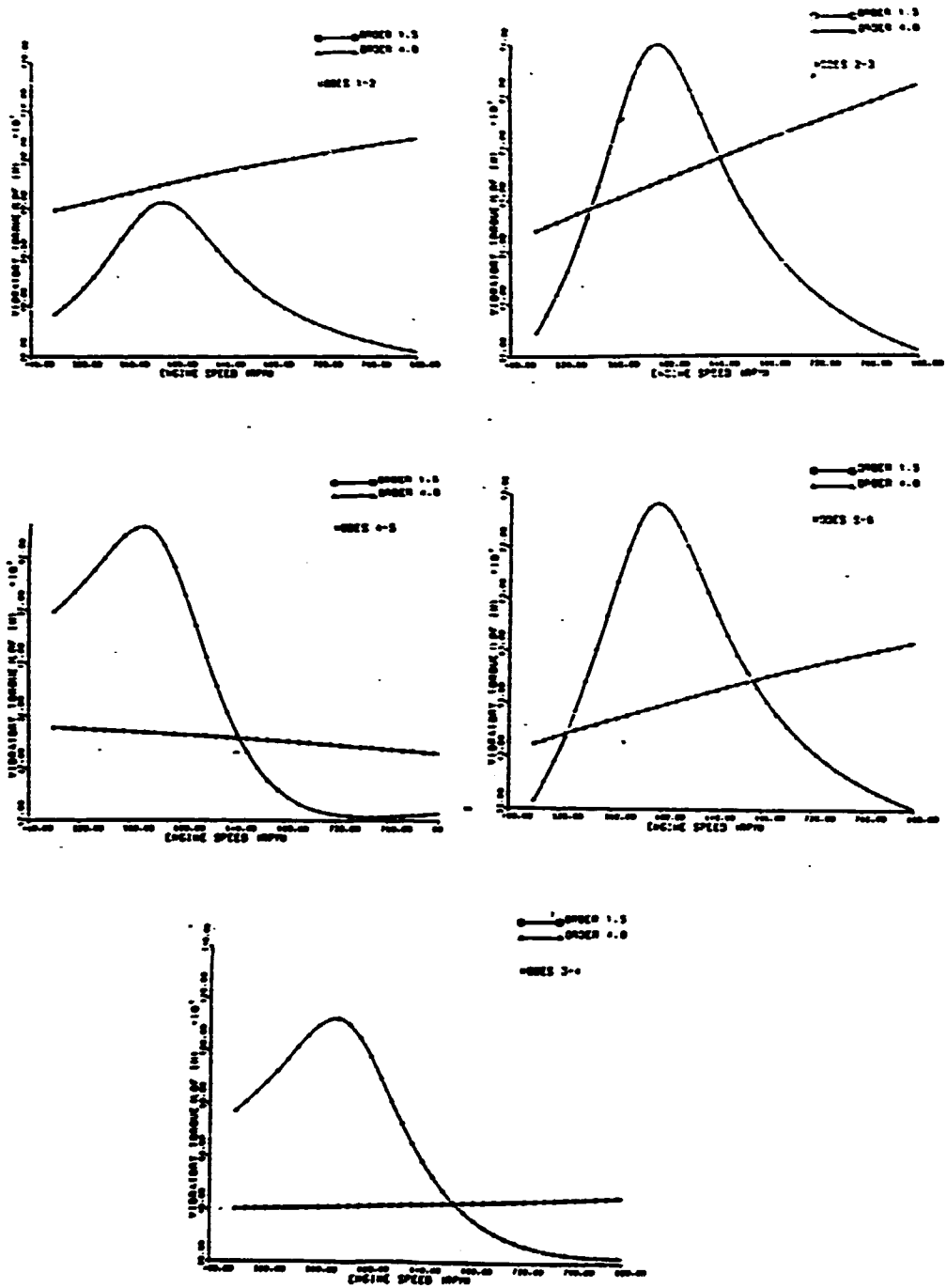


Figure 3.2

The program SATOV was used to evaluate the forced-damped response for the system illustrated in Figure 3.3, which encompasses almost all possible variations that could be encountered in a real torsional system. The data are given in Table 3.1. The results were compared with those obtained from the ANSYS* finite element software package. The frequency of the excitation torque is 800 rad./sec.

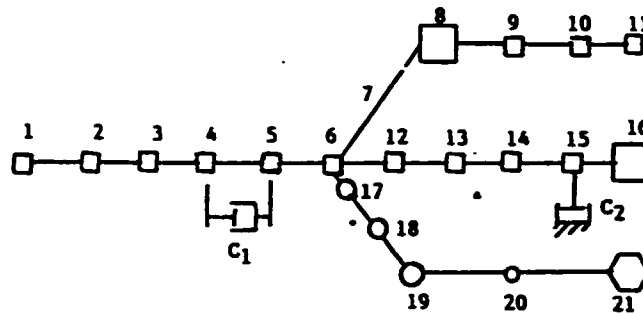


Figure 3.3 Torsional System for Testing the Program SATOV

TABLE 3.1 Mass-Elastic-Damping Data

INERTIA (lb.in.sec.)	TORSIONAL STIFFNESS (lb.in./rad.)
J1 = 40	K1,2 = 30.E6
J2 = 70	K2,3 = 40.E6
J3 = 20	K3,4 = 80.E6
J4 = 30	K4,5 = 20.E6
J5 = 50	K5,6 = 60.E6
J6 = 60	K6,7 = 40.E6
J7 = 20	K7,8 = 70.E6
J8 = 40	K8,9 = 60.E6
J9 = 70	K9,10 = 20.E6

J10 = 30	K10,11 = 60.E6
J11 = 10	K6,12 = 30.E6
J12 = 40	K12,13 = 40.E6
J13 = 20	K13,14 = 200.E6
J14 = 70	K14,15 = 150.E6
J15 = 30	K15,16 = 20.E6
J16 = 60	K6,17 = 40.E6
J17 = 10	K17,18 = 50.E6
J18 = 80	K18,19 = 300.E6
J19 = 40	K19,20 = 100.E6
J20 = 30	K20,21 = 80.E6
J21 = 60	

DAMPING COEFFICIENT

(lb.in.sec./rad.)

C1 = 10000.

C2 = 20000.

EXCITATION TORQUE

(lb.in.)

TAMP(I) = 0. + 0. i for I = 1 to 4

TAMP(5) = 5000 + 0 i

TAMP(I) = 0. + 0. i for I = 6 to 8

TAMP(9) = 8000 + 3000 i

TAMP(I) = 0. + 0. i for I = 10 to 15

TAMP(16) = 6000 + 0 i

TAMP(I) = 0. + 0. i for I = 17 to 21

DISPLACEMENTS

Node	SATOV		ANSYS	
	Real (radians)	Imaginary (radians)	Real (radians)	Imaginary (radians)
1	.339868E-3	.180836E-3	.339869E-3	.180837E-3
2	.498473E-4	.265226E-4	.498477E-4	.265229E-4
3	-.223497E-3	-.118918E-3	-.223498E-3	-.118919E-3
4	-.324410E-3	-.172611E-3	-.324411E-3	-.172612E-3
5	-.420827E-3	-.183111E-3	-.420829E-3	-.183112E-3
6	-.310458E-3	-.101807E-3	-.310460E-3	-.101808E-3
7	-.296527E-3	-.876311E-4	-.296529E-3	-.976326E-4
8	-.234344E-3	-.635064E-4	-.234346E-3	-.635079E-4
9	-.618107E-4	-.826484E-5	-.618115E-4	-.826573E-5
10	.194246E-3	.259731E-4	.194249E-3	-.259759E-4
11	.217439E-3	.290743E-4	.217443E-3	.290775E-4
12	.899598E-4	.106911E-3	.899604E-4	.106912E-3
13	.332699E-3	.195027E-3	.332701E-3	.195029E-3
14	.359954E-3	.200169E-3	.359956E-3	.200171E-3
15	.288788E-3	.147240E-3	.288790E-3	.147242E-3
16	-.639987E-3	-.160044E-3	-.639990E-3	-.160046E-3
17	-.161110E-3	-.528323E-4	-.161111E-3	-.528328E-4
18	-.210100E-4	-.688972E-5	-.210099E-4	-.688974E-5
19	.592580E-5	.194322E-5	.592595E-4	.194328E-5
20	.852161E-4	.279446E-4	.852166E-4	.279449E-4
21	.163877E-3	.537396E-4	.163878E-3	.537401E-4

Table 3.2 Comparison of Displacements from ANSYS and SATOV

The performance of the SATOV software is given credibility by the comparison of output from SATOV with output from the commercial software package ANSYS.² The results are almost identical. However, the cost of the large general purpose ANSYS package is several thousand dollars per month. A special purpose finite element package offers advantages in size and economy when a general purpose package is not otherwise needed.

4. SENSITIVITY STUDIES:

Sensitivity studies of the response of the torsional vibrations to a change in the size of a design variable can aide the analyst as the system is tuned. A plot of natural frequencies and excitation harmonics versus engine speed can indicate the proximity of a resonance condition for any engine speed. However, the sensitivity study can provide insight into the interaction of the variables which constitute the system.

The system of Figure 4.1 was analyzed and produced the ten natural frequencies identified on Figure 4.2 as f_1, f_2, \dots, f_{10} . The prime mover is a sixteen cylinder, two stroke, internal combustion engine which may be operated at different speeds between low idle and rated speed, when the generator is not producing 60 Hz current. The harmonic associated with a major critical speed (3) is the eighth order harmonic, which excites the system at a frequency equal to eight times the engine speed. The eighth harmonic is not close to resonance with any of the system's natural frequencies when the engine speed is operating at the rated speed, 900 RPM. However, the third order harmonic and the tenth harmonic are close to resonance with natural frequencies at this speed.

²ANSYS is the registered tradename of a finite element software package written and marketed by Swanson Analysis Systems, Inc.

It is more desirable to tune frequencies out of the operating speed range than to dampen the vibrations to acceptable levels. However, with fixed propeller systems, this is not practical.

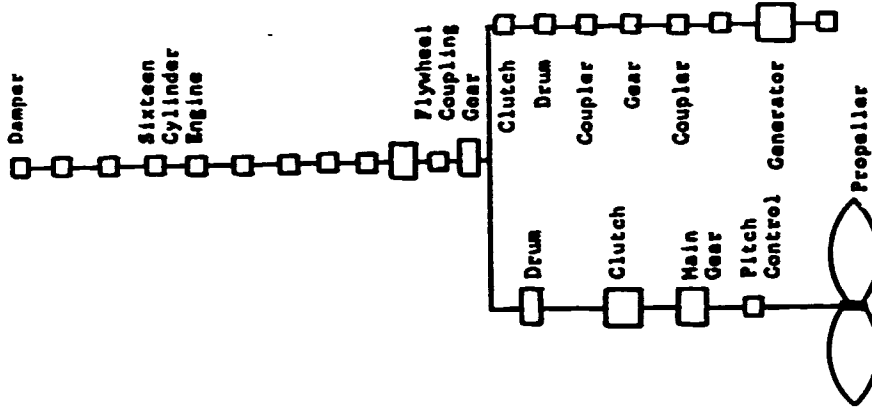


Figure 4.1

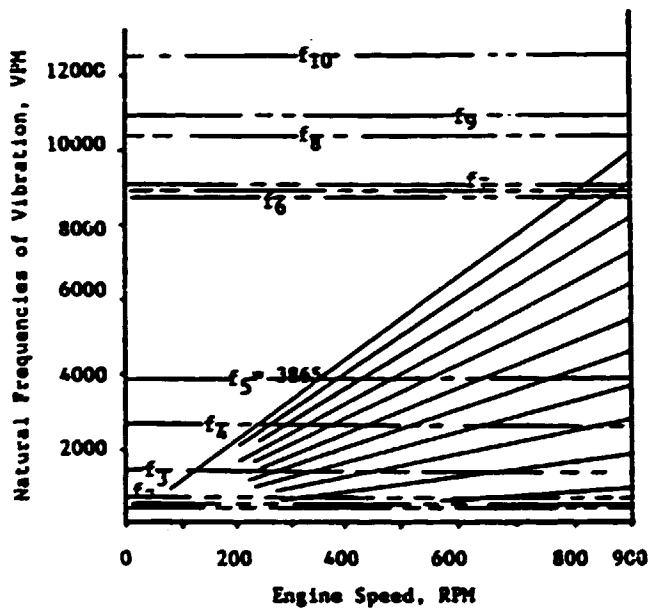


Figure 4.2

In order to conduct the sensitivity study to evaluate the changes needed to retune or dampen the system, a system model must be constructed. Even though the analysis process is well defined, the analyst must exercise his own judgement in order to obtain the desired results. The modeling of the system consists of dividing the inertias into lumps which are separated by spring constants. The damping may be distributed across the lumps of inertia if a damped natural frequency is to be evaluated. (If an undamped analysis is to be used, the damping appears in an energy balance equation which establishes an overall amplitude scaling factor (3). The undamped and unforced analysis assumes that damping torques and excitation torques are small and will not significantly change the relative amplitudes of the mode shape.) The natural frequencies and mode shapes may be obtained by the damped Holzer method or by the finite element method. The analyst must use an adequate number of inertia lumps which usually results in a branched mass-elastic diagram (10). The same mass-elastic diagram may be used for the finite element diagram as for the damped-branched Holzer method. The addition of entrained water to the propeller inertia value, the consideration of misfiring by an internal combustion engine, and the integration of nonlinear stiffness of an elastic coupling are some of the factors which the analyst must consider. If the number of lumped inertias is small, the time required to perform the analysis and evaluate the results is low; however, if the number is too small to represent the system, the results may contain errors.

In order to illustrate difficulties due to the lumping of inertias, consider Figure 4.3 which has a gear, coupling, propeller and two shafts. Most models would represent this system by three lumps of inertia, one made up of the gear plus half of shaft 1. A second lump consisting of the coupling plus half of shaft 1 and half of shaft 2. A third lump consisting of the propeller plus half of shaft 2. Now consider that the inertia of the coupling may be of the same magnitude as the inertia of half of the long shaft 2. This model is satisfactory for the propeller mode. However, in the coupling mode, the propeller and gear will move very little due to their large inertias while the coupling has high relative amplitudes. Hence, the two shafts tend to act like two springs each of which have one end fixed and the other end free. Therefore, for the coupling mode, the equivalent inertia of the second lump should be equal to the inertia of the coupling plus one third of the inertias of the two shafts. This does change the natural frequency. If the three lump system had been replaced with five or more lumps, the distribution of the inertias would have been more representative of the system for all modes of vibration.

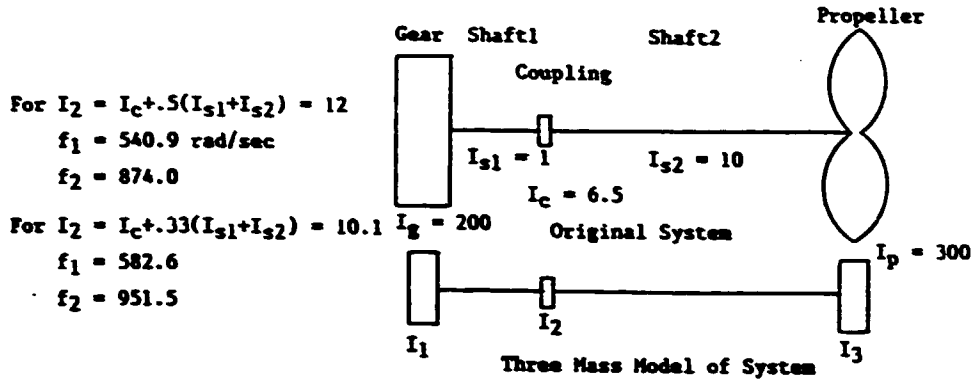


Figure 4.3 Three Mass System Comparison
 of Method for Evaluating I_2 .

The misfiring engine presents many different possibilities for the analysis (e.g., is partial firing occurring, which cylinder is misfiring, how many cylinders are misfiring?). One suggestion is to assume that compression of the air-gas mixture occurs without an ignition. This will establish some pressure harmonic components. Also, the variable torque due to the mass of the reciprocating slider-crank mechanism should be included. The location of the misfiring cylinder will influence the value of the phase vector sum of the piston displacements, §8.(3) It is suggested that the phase vector sums be evaluated for the engine with each cylinder misfiring and that only the worst case be used in the analysis.

The sensitivity study of the system shown in Figure 4.4 will be used as an example. The first natural frequency mode shape of Figure 4.5 shows the propeller swinging in opposition to the remainder of the system with the node located in the propeller shaft, which has low stiffness. The large stress is at the node since it experiences the full inertia torque.

This first mode can be excited by the first or second engine harmonic or by the 3 blade propeller when the engine speed is 584 RPM. The mode shape for the second natural frequency (Figure 4.6) shows the gear, G, and clutch, CD, swinging in opposition to the engine while the large propeller, which is on the end of the long propeller shaft, does not move appreciably from its steady state position. The third mode (Figure 4.7) shows the engine and gear swinging in opposition to the flywheel. This is a characteristic of this engine. The third mode (Figure 4.8) shows the engine damper swinging against the engine while the large flywheel is relatively stationary. The engine damper provides significant damping at vibrations of this frequency, which produces relative large deflections of the crankshaft.

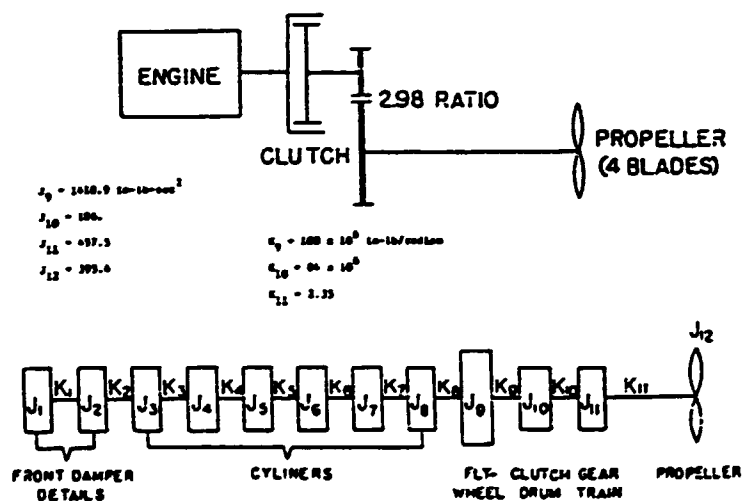


Figure 4.4 Marine Vessel Mass-Elastic Diagram

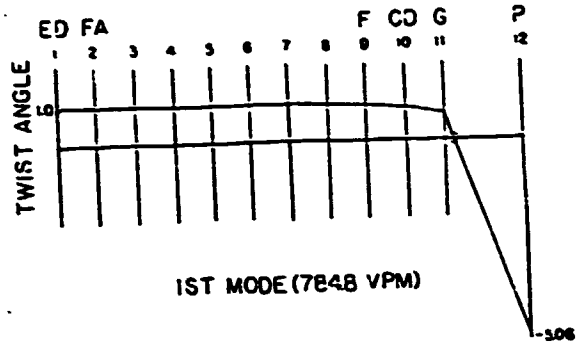


Figure 4.5 First Mode

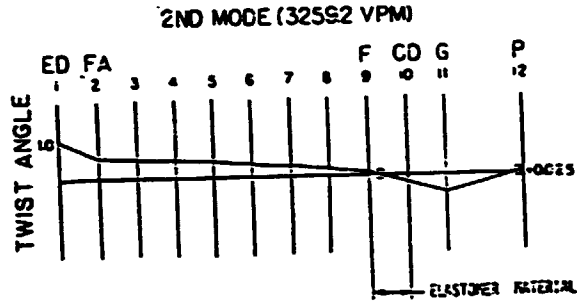


Figure 4.6 Second Mode

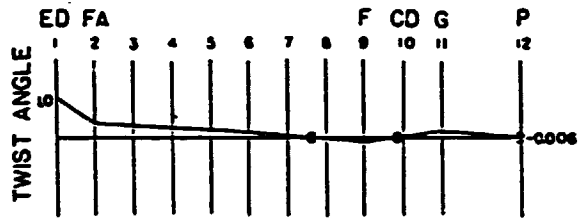


Figure 4.7 Third Mode

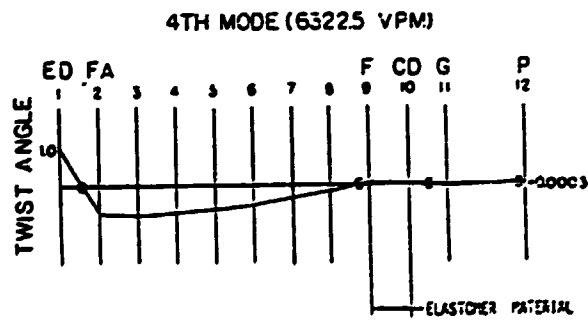


Figure 4.8 Fourth Mode

The sensitivity of the amplitude scaling factor (This is the factor which is multiplied times the mode shape amplitudes to change these relative amplitudes to absolute values.) as a function of engine damping is shown in Figure 4.9. The influence of flywheel inertia on the values of natural frequencies may be useful in retuning a system (Figure 4.10). The sensitivity of the mode shapes to flywheel inertia is indicated in Figure 4.11. The sensitivity of the natural frequencies to the stiffness of the elastic coupling, which is often changed to retune a system, is given in Figure 4.12. Since the elastic coupling has the node for the second frequency, the change in coupling stiffness has a maximum impact on mode 2. The sensitivity of natural frequencies to propeller shaft stiffness is used to retune the system (Figure 4.13). The sensitivity of mode shapes to changes in propeller inertia are shown in Figure 4.14. The sensitivity of natural frequencies to propeller inertia is shown in Figure 4.15.

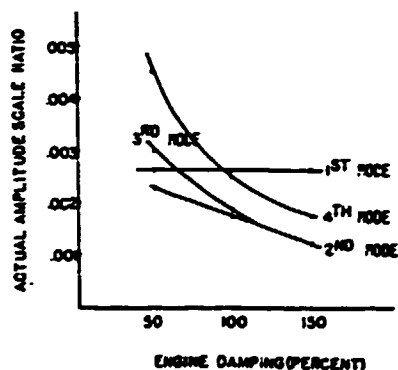


Figure 4.9 Sensitivity of Amplitude Scaling Factor to Engine Damping

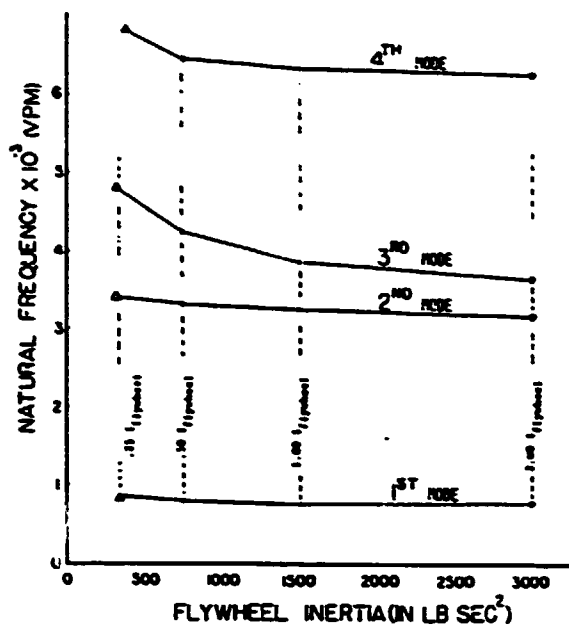


Figure 4.10 Sensitivity of Natural Frequencies to Flywheel Inertia

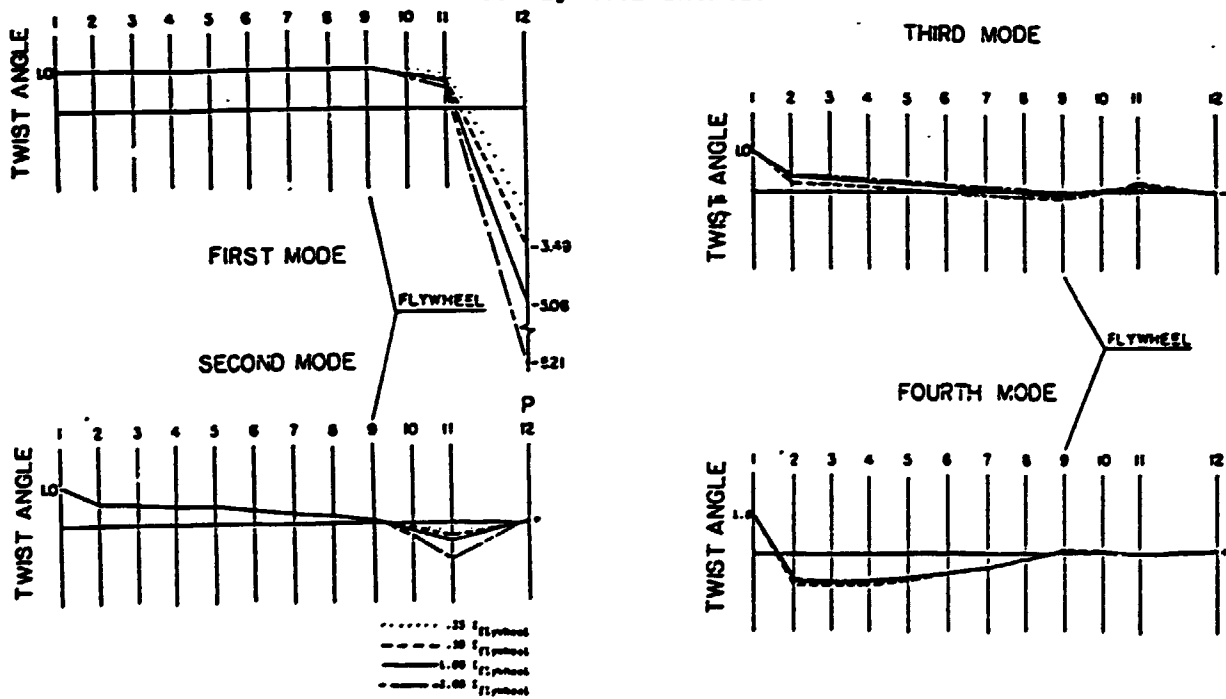


Figure 4.11 Sensitivity of Mode Shapes to Flywheel Inertia

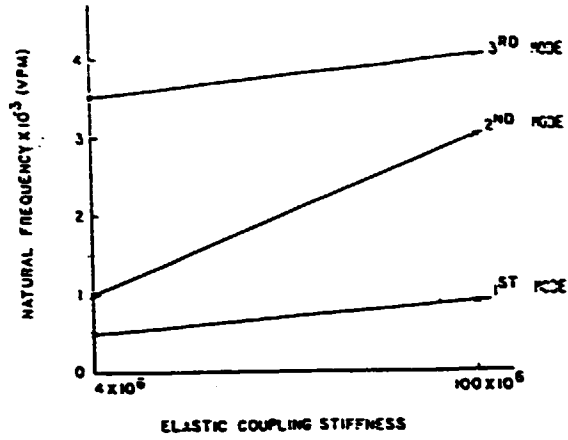


Figure 4.12 Sensitivity of Natural Frequencies to Elastic Coupling Stiffness

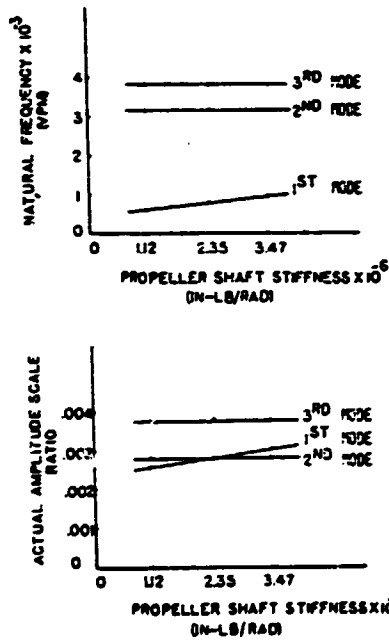


Figure 4.13 Sensitivity of Natural Frequencies to Propeller Shaft Stiffness

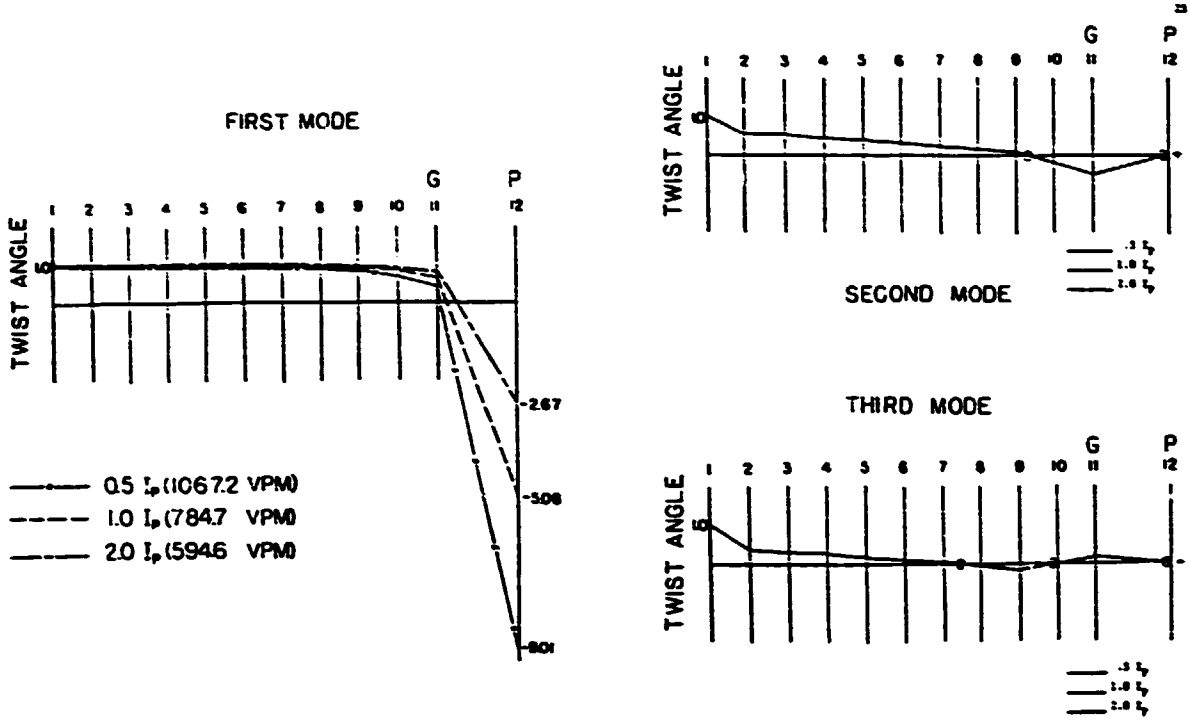


Figure 4.14 Sensitivity of Mode Shapes to Propeller Inertia

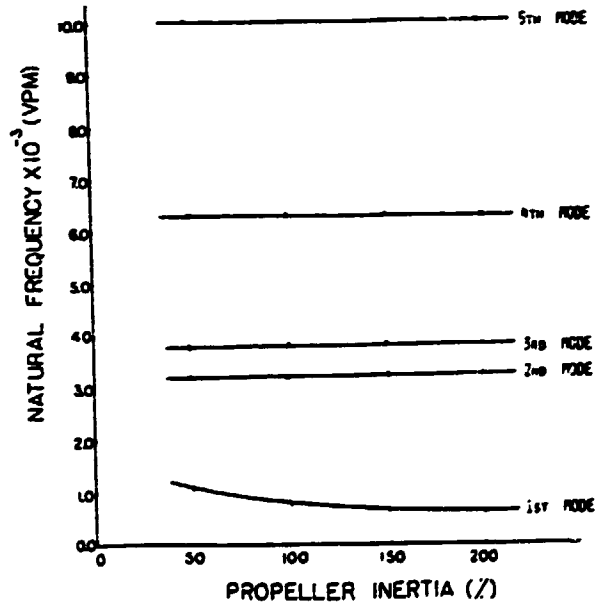


Figure 4.15 Sensitivity of Natural Frequencies to Propeller Inertia

APPENDIX A

Program : SATOV

HELIX LPP.FPOJL
ELIST 01/14/76 11:39:26
END ELIST 1 CARDS GENERATED.

SHDG.P ***** FPOJ2 *****

```

HELIX LPP.FPOJL
ELT 251 57421C 01/14/76 11:39:26 (42)
1.      *IMPLICIT COMPLEX (A-H,P-Z)
2.      DIMENSION A(30),B(12,15),T(30,4),CJ(30),CK(30),I(8(15),400(2))
3.      DIMENSION J(14),TNETA(30),NFIR(2),ORDB(6),OTAPP(5),DALPHA(2)
4.      DIMENSION OX(200),OY(200),OXA(100),ONOB(15),ITR(15),JMT(15,10)
5.      DIMENSION CJC(30),ORCC(30),AK(30),OPDAT(10,200)
6.
7.      READ IN OPTIONS DESIRED
8.      ICOPR = PRINTOUT OPTIONS
9.      NPLOT = PLOT OPTIONS
10.     PLOT = 1 - NO PLOTS GENERATED
11.     PLOT = 2 - PLOTS GENERATED
12.     INPT = ENGINE EXCITATION OR USER SPECIFIED TORQUES
13.     INPT = 0 - ENGINE EXCITATION
14.     INPT = 1 - USER SPECIFIED TORQUES
15.
16.     READ(5,*)ICOPP,PFLLT,INPT
17.
18.     IF(INPT.EQ.1) GO TO 102
19.     IF(ICOPP.EQ.1) WRITE(6,102)
20.     IF(ICOPP.EQ.1) WRITE(6,103)
21.     FORMAT(//,1X,'** RECIPROCATING ENGINE EXCITATION ***',//,1X,
22.     * 'ORDER',1X,'TORQUE AMPLITUDE')
23.
24.     READ IN NUMBER OF ORDERS, ORDER NUMBER AND CORRESPONDING
25.     TORQUE AMPLITUDE
26.
27.     READ(5,*)NORD,4*(ORD(I),OTAPP(I),I=1,NORD)
28.
29.     IF(ICOPP.EQ.1) WRITE(6,104)(ORD(I),OTAPP(I),I=1,NORD)
30.     FORMAT(//,1X,5(1X,F14.6))
31.
32.     READ IN MINIMUM FREQUENCY, "API" FREQUENCY, STEP FREQUENCY
33.
34.     READ(5,*)OMIN,OMAX,OSING
35.
36.     IF(INPT.EQ.0) GO TO 105
37.     NORDPT
38.     IF(ICOPR.EQ.1) WRITE(6,106)
39.     FORMAT(//,1X,5(1X,F14.6),1X,10(1X,F14.6),1X,1X)
40.     IF(ICOPR.EQ.1) WRITE(6,107)(OMIN,OMAX,OSING)
41.     FORMAT(//,1X,1X,1X,F14.7,1X,1X,1X,F14.7,
42.     * //,1X,1X,1X,F14.7)
43.     //,1X,1X,1X,F14.7)
44.
45.     READ IN NUMBER OF BRANCHES
46.
47.     READ(5,*)NBRACH
48.
49.     IF(ICOPR.EQ.1) WRITE(6,108)NBRACH
50.     FORMAT(//,1X,'NUMBER OF BRANCHES =',14)
51.     NBRACH
52.     DO 3 INI,NBRACH
53.     READ(5,*)NCPNAX
54.     IF(ICOPR.EQ.1) WRITE(6,109)NCPNAX
55.     FORMAT(//,1X,'BRANCH =',14,/,1X,' NUMBER OF NODES =',14,/)
56.     IF(INPT.EQ.1) GO TO 103
57.     READ(5,*)NCTV,NSTPE
58.     IF(ICOPR.EQ.1) WRITE(6,110)NCTV,NSTPE
59.     FORMAT(//,1X,14,' CYCLE ENGINE IN BRANCH',13,' WAS',
60.     * '13' CYLINDERS',//,1X,' FILING ORDER',/)
61.     READ(5,*)NFR(13),NCTV
62.     IF(ICOPR.EQ.1) WRITE(6,111)(NFR(I),I=1,13),NCTV)
63.     FORMAT(//,1X,13(1X,F14.7),1X,1X,F14.7)
64.     NCTV
65.     OPDATA(I) = FDATA(NSTPE) * FDATA(NSTPE) * 3.141592654 / FLDPT(NCTV)
66.     DO 4 J=1,NCTV
67.     UJC(IP,TR) = 0.
68.     UJC(IP,TR) = 0.
69.     UJC(IP,TR) = 0.
70.     UJC(IP,TR) = 0.
71.     READ(5,*)NCPNTR(13),CJ(IPNTR),CK(IPNTR)

```


***** PFOJZ *****

CONTINUE
BACK SUBSTITUTION OF ZERO DEGREE NODES (OPEN ENDED BRANCHES)

```

JPH=0
DO 71 J=1,NBRNCH
IF(IND(I).EQ.IND(I-1)-2) GO TO 71
IF(IND(I).EQ.IND(I-1)-1) GO TO 70
JPH=JPH+1
GO TO 71
70 IF(MOD(IND(I)),LT.0) GO TO 72
THETA(MOD(IND(I))-1)=THETA(MOD(IND(I))-1)+THETA(MOD(IND(I))-1)
*MOD(IND(I))/AK(IND(I))
*MOD(IND(I))/AK(IND(I))
IF(IND(I)-2.GT.IND(I-1)-2) GO TO 71
DO 71 J=IND(I)-2,IND(I)-1
THETA(MOD(J))-1=THETA(MOD(J))-1+THETA(MOD(J))-1
*AK(J-1)=THETA(MOD(J-1))/AK(J-1)
GO TO 71
72 THETA(MOD(IND(I)-1)-2)=-(THETA(MOD(IND(I)-1)-1.L)-AK(IND(I)-1)-1)
*THETA(MOD(IND(I)-1)-1))/AK(IND(I)-1)
IF(IND(I)-1.GT.IND(I-1)-1) GO TO 71
DO 71 J=IND(I)-1,IND(I)-1,-1
THETA(MOD(J))=-(THETA(MOD(J-1))+AK(J-1)*THETA(MOD(J-2)))
*AK(J)-1=THETA(MOD(J-1))/AK(J-1)
71 CONTINUE
IF(JPH.EQ.0) GO TO 74

COLLECT DATA ABOUT JUNCTION NODES IN 'JNT' ARRAY.
SUBSCRIPT-1 IS THE JUNCTION NODE COUNTED.
SUBSCRIPT-2
1 - NUMBER OF ADJACENT NODES INCLUDING THE JUNCTION NODE
2 - JUNCTION NODE (IS ALWAYS NEGATIVE)
3 - LOCATION OF FIRST ADJACENT NODE IN 'IND' ARRAY.
EXAMPLE - IF JNT(1,3)=7 THEN NDC(IND(7)) IS THE
ADJACENT NODE.
4 - LOCATION OF SECOND ADJACENT NODE IN 'IND' ARRAY.
5 - UPTO JNT(1,5)
(JNT(1,1)+1) - DEGREE OF JUNCTION NODE.

NDEGEX=1
JPH=0
DO 61 J=1,NJP
IF(MOD(I).GT.0) GO TO 61
JPH=JPH+1
NDEG=0
KAT=2
JNT(J,2)=PHOD(I)
DO 62 J=1,NBRNCH
IF(MOD(IND(J)).EQ.PHOD(I).CR.MOD(IND(J+1)-1).EQ.PHOD(I))
* GO TO 61
* GO TO 62
61 IF(IND(J).LE.IND(J+1)-2) GO TO 130
GO TO 131
130 IF(MOD(IND(J))=MOD(IND(J+1)-1).GT.0) NDEG=NDEG+1
131 IF(MOD(IND(J)).EQ.PHOD(I)) GO TO 64
KAT=KAT+1
JNT(J,KAT)=IND(J)-2
GO TO 62
KAT=KAT+1
JNT(J,KAT)=IND(J+1)
62 CONTINUE
IF(NDEGEX.LT.NDEG) NDEGEX=NDEG
JNT(J,1)=KAT
JNT(J,KAT)=NDEG
61 CONTINUE

JPH - IS NOW EQUAL TO THE NUMBER OF JUNCTION NODES.
NDEGEX - IS NOW EQUAL TO THE MAXIMUM DEGREE OF A JUNCTION NODE
IN THE WHOLE SYSTEM.

BACK SUBSTITUTION FOR HIGHER DEGREE NODES (NDEG > 0)
DO 72 J=1,NDEGEX
DO 75 I=1,N
NPDY(I,1)
IF(JNT(I,NPDY+1).LE.J) GO TO 75
D=0
ICND=0
DO 111 K=1,JNT(I,1)
IF(ABS(THETA(IND(IND(J+1)+K)))>.01) GO TO 111

```

***** SP022 *****

DATE C11426

PAGE

111
112
113
114
115
116
117
118
119
120
121
122
123
124
125
126
127
128
129
130
131
132
133
134
135
136
137
138
139
140
141
142
143
144
145
146
147
148
149
150
151
152
153
154
155
156
157
158
159
160
161
162
163
164
165
166
167
168
169
170
171
172
173
174
175
176
177
178
179
180
181
182
183
184
185
186
187
188
189
190
191
192
193
194
195
196
197
198
199
200

```

APR JNT(2,1)
C=C*1
111  IF(C=1) GO TO 75
112  IF(C=2) GO TO 112
113  IF(C=3) GO TO 112
114  IF(C=4) GO TO 112
115  IF(C=5) GO TO 112
116  IF(C=6) GO TO 112
117  IF(C=7) GO TO 112
118  IF(C=8) GO TO 112
119  IF(C=9) GO TO 112
120  IF(C=10) GO TO 112
121  IF(C=11) GO TO 112
122  IF(C=12) GO TO 112
123  IF(C=13) GO TO 112
124  IF(C=14) GO TO 112
125  IF(C=15) GO TO 112
126  IF(C=16) GO TO 112
127  IF(C=17) GO TO 112
128  IF(C=18) GO TO 112
129  IF(C=19) GO TO 112
130  IF(C=20) GO TO 112
131  IF(C=21) GO TO 112
132  IF(C=22) GO TO 112
133  IF(C=23) GO TO 112
134  IF(C=24) GO TO 112
135  IF(C=25) GO TO 112
136  IF(C=26) GO TO 112
137  IF(C=27) GO TO 112
138  IF(C=28) GO TO 112
139  IF(C=29) GO TO 112
140  IF(C=30) GO TO 112
141  IF(C=31) GO TO 112
142  IF(C=32) GO TO 112
143  IF(C=33) GO TO 112
144  IF(C=34) GO TO 112
145  IF(C=35) GO TO 112
146  IF(C=36) GO TO 112
147  IF(C=37) GO TO 112
148  IF(C=38) GO TO 112
149  IF(C=39) GO TO 112
150  IF(C=40) GO TO 112
151  IF(C=41) GO TO 112
152  IF(C=42) GO TO 112
153  IF(C=43) GO TO 112
154  IF(C=44) GO TO 112
155  IF(C=45) GO TO 112
156  IF(C=46) GO TO 112
157  IF(C=47) GO TO 112
158  IF(C=48) GO TO 112
159  IF(C=49) GO TO 112
160  IF(C=50) GO TO 112
161  IF(C=51) GO TO 112
162  IF(C=52) GO TO 112
163  IF(C=53) GO TO 112
164  IF(C=54) GO TO 112
165  IF(C=55) GO TO 112
166  IF(C=56) GO TO 112
167  IF(C=57) GO TO 112
168  IF(C=58) GO TO 112
169  IF(C=59) GO TO 112
170  IF(C=60) GO TO 112
171  IF(C=61) GO TO 112
172  IF(C=62) GO TO 112
173  IF(C=63) GO TO 112
174  IF(C=64) GO TO 112
175  IF(C=65) GO TO 112
176  IF(C=66) GO TO 112
177  IF(C=67) GO TO 112
178  IF(C=68) GO TO 112
179  IF(C=69) GO TO 112
180  IF(C=70) GO TO 112
181  IF(C=71) GO TO 112
182  IF(C=72) GO TO 112
183  IF(C=73) GO TO 112
184  IF(C=74) GO TO 112
185  IF(C=75) GO TO 112
186  IF(C=76) GO TO 112
187  IF(C=77) GO TO 112
188  IF(C=78) GO TO 112
189  IF(C=79) GO TO 112
190  IF(C=80) GO TO 112
191  IF(C=81) GO TO 112
192  IF(C=82) GO TO 112
193  IF(C=83) GO TO 112
194  IF(C=84) GO TO 112
195  IF(C=85) GO TO 112
196  IF(C=86) GO TO 112
197  IF(C=87) GO TO 112
198  IF(C=88) GO TO 112
199  IF(C=89) GO TO 112
200  IF(C=90) GO TO 112

```


REFERENCE LIST

1. A.G.M.A., AGMA Information Sheet Systems Considerations for Critical Service Gear Drives Manufacturers Association.
2. Jones, E. W., Peng, C. H., and Pan, C. T., Torsional Vibrations in Work Boat Power Trains From the Designer's Point of View, presented at the Work Boat Show, New Orleans, LA, Jan. 1982.
3. Den Hartog, J. P., Mechanical Vibrations, McGraw Hill Book Co., New York, 1956.
4. Harrington, Roy L., Marine Engineering, Society of Naval Architects and Marine Engineers, New York, NY, 1971.
5. Nestorides, E. J., A Handbook of Torsional Vibrations, British Internal Combustion Engine Research Association, University Press, Cambridge, 1958.
6. Wilson, Ker W., Practical Solution of Torsional Vibration Problems, Volumes 1-5, Third Edition, Chapman & Hall Ltd., 11 New Fetter Lane, London EC4.
7. Lloyd's, Rules and Regulations for the Construction and Classification of Steel Ships, Lloyd's Register of Shipping, West Sussex, RH10 2QN, England, 1976.
8. A.B.S., Rules for Building and Classing Steel Vessels, American Bureau of Shipping, 45 Broad Street, New York, NY, 1977.
9. Jones, E. W., Buchholz, F. J., Predicting the Performance of Dynamic Mechanical Systems, Zhengzhou Research Institute of Mechanical Engineering, Zhengzhou, PRC, 1988.
10. Tse, F. A., Morse, I. E., Hinkle, R. T., Mechanical Vibrations Theory and Applications, Allyn and Bacon, Inc., Boston, 1963.
11. Holzer, H., 'Analysis of Torsional Vibration', Springer, Berlin, 1921.
12. Hartog, J. P. and Li, J. P., 'Forced Torsional Vibrations with Damping: An Extension of Holzer's Method', Journal of Applied Mechanics, Trans. ASME, Vol. 68, 1946, p. A-276.
13. Spaetgens, T. W. and Vancouver, B. C., 'Holzer Method for Forced-Damped Torsional Vibrations', Journal of Applied Mechanics, Vol. 17, 1950, pp. 53-63.
14. Jong-Shyong Wu and Wen-Hsiang Chen, 'Computer Method for Forced Torsional Vibration of Propulsive Shafting Systems of Marine Engine With or Without Damping', Journal of Ship Research, Vol. 26, No. 3, Sept. 1982, pp. 176-189.

15. Edwards, A. J., 'TORVAP-A : A Computer Program for the Torsional Vibration Analysis of Multi-junction, Multi-branch Systems', Computer Aided Design, Vol. 5, No. 3, July 1973.
16. William T. Thomson, 'Vibration Theory and Applications', Prentice Hall, New Jersey, 1965.
17. Robert D. Cook, 'Concepts and Applications of Finite Element Analysis', Second Edition, John Wiley and Scns, New York, 1981.
18. Bangalore, Kumar N., Comparison of a Forced-Damped Finite Element Method with a Method Using Free-Undamped Vibration Mode Shapes for Torsional Vibration Analysis, Master of Mechanical Engineering Thesis, Mississippi State University, 1985.

LECTURE 4 : AN INTRODUCTION TO THE FINITE ELEMENT METHOD

ABSTRACT:

The Finite Element Method allows the mechanical designer to analyze complex shapes for stresses, deflections, vibrations, and thermal distributions. This paper gives an introduction to the Finite Element Method.

1. INTRODUCTION:

The mechanical designer tends to optimize function and minimize the material in a design. This often results in components with complex geometry which can not be analyzed by the equations from strength of materials because of their simplified assumptions (e.g., the shape is a long prismatic member). (On the other hand, the Civil Engineer tends to design structures using long prismatic members, which can be analyzed.) Two approaches were available to size these components with irregular shapes prior to the 1960's: the Theory of Elasticity Method and the Experimental Method.

The Theory of Elasticity Method with its elegant mathematics is not well suited to the needs of the practicing engineer. However, it is an excellent research method and has been used in many thesis dissertations to obtain the solutions of special case geometry and loading combinations. Professor R. J. Roark recognized the value of these solutions to practicing engineers and published a book, Formulas for Stress and Strain, containing many of these solutions (1)¹. This book has been regularly updated and serves the intended purpose well, however, the research has not covered all of the cases required by the practicing engineer.

¹1. Numbers in parentheses identify references.

The Experimental Method presents many options for sizing components and some of these options are listed below.

1. Manufacture the component, load it and observe any failures which occur. The load may be a static load or it may be a repeating load, which will produce fatigue.
2. Coat the component with a brittle coating (4), which has a low strain threshold. Load the part and observe the crack patterns in the coating to identify areas of high tensile strains.
3. Make a replica of the part from a birefringent material. Strain this replica in a polariscope to identify the differences in the principal stresses over the part.
4. Apply strain gages to the surface of the part and measure strains on the surface.

One reason for the wide acceptance of the Experimental Method is because it reduces the number of assumptions. On the other hand, before the Experimental Method can be applied, the component (or its replica) must be manufactured and the designer does not have a rational method for sizing the part for the initial drawing.

The analysis of frames, which are assembled from uniform prismatic members, was accelerated by the availability of the computer in the 1950's. By modeling the elastic deflection of a redundant frame using matrix methods, the forces and deflections could be analyzed.

Practicing engineers began to use the Finite Element Method, FEM, for the analysis of stresses and deflections of complex geometric shapes in the 1960's. This method provided an analytical method as an alternative to the Experimental Method. The idea of the FEM is to

divide the solution domain into a finite number of subdomains, which are called elements. These elements are connected only at their node points and on the element boundaries (2). By using small elements of material, whose force and deflection characteristics are known, a model of a complex shape can be constructed mathematically and the resulting equations can be solved.

Two types of finite elements are discussed in this paper: (a) "natural" elements and (b) elements based on assumed modes of displacement.

2. NATURAL ELEMENTS: Bar Element:

The finite element method may be based on the stiffness method to define the relationship between displacements, d , stiffness, k , and forces, r . The stiffness equation for a finite element is

$$[k]\{d\} = \{r\}$$

The bar type of finite element illustrated in Figure 2.1 is a uniform prismatic member which is aligned with the x-axis and subjected to axial loads. The ends of the bar element have nodes, which are labeled i or j . Other elements may be attached to these nodes. Forces may be applied at the nodes. The matrix quantities k , d and r for this element are:

$$[k] = \frac{AE}{L} \begin{vmatrix} 1 & -1 \\ -1 & 1 \end{vmatrix}$$

$$\{d\} = \begin{Bmatrix} u_i \\ u_j \end{Bmatrix}$$

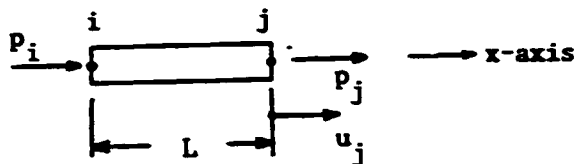
$$\{r\} = \begin{Bmatrix} P_i \\ P_j \end{Bmatrix}$$

Expansion of the stiffness equation into two linear equations by matrix multiplication yields the expected results:

$$u_i - u_j = p_i L/AE$$

$$-u_i + u_j = p_j L/AE$$

- A = Cross sectional area
- E = Modulus of Elasticity
- L = Length
- u_i = Displacement of ith node
- u_j = Displacement at jth node
- p_i = Axial force applied to i node
- p_j = Axial force applied to j node



NOTE: All forces are shown in the positive directions to illustrate the sign convention.

Figure 2.1 One Dimensional Bar Element

A two dimensional bar element is illustrated in Figure 2.2. It can have x and y displacements at each node and x and y components of forces may be applied at each node. The input data will be the initial positions of each node $[(x_i, y_i)$ and $(x_j, y_j)]$, the force components at each node $[(p_i, q_i)$ and $(p_j, q_j)]$, the cross sectional area (A), and the modulus of elasticity (E). The element length (L) is calculated.

$$L = [(x_j - x_i)^2 + (y_j - y_i)^2]^{.5}$$

The sines and cosines of the element's position angle are

$$S = \sin \beta = (y_j - y_i)/L$$

$$C = \cos \beta = (x_j - x_i)/L$$

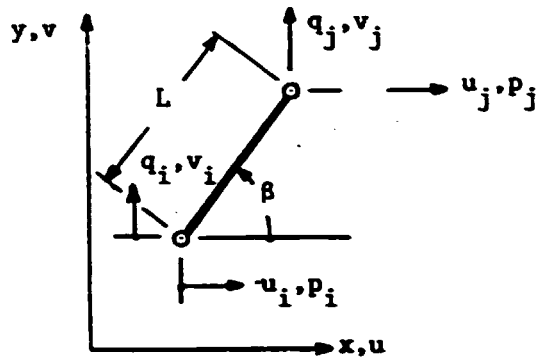


Figure 2.2 Two Dimensional Bar Element

The stiffness equation for this two dimensional element has the following form since it has two degrees of freedom at each node.

$$[k] \{d\} = \{r\}$$

$$[k_{\text{BAR}}] = \begin{vmatrix} k_{1,1} & k_{1,2} & k_{1,3} & k_{1,4} \\ k_{2,1} & k_{2,2} & k_{2,3} & k_{2,4} \\ k_{3,1} & k_{3,2} & k_{3,3} & k_{3,4} \\ k_{4,1} & k_{4,2} & k_{4,3} & k_{4,4} \end{vmatrix}$$

$$\{d\} = \begin{vmatrix} u_i \\ v_i \\ u_j \\ v_j \end{vmatrix}$$

$$\{r\} = \begin{vmatrix} p_i \\ q_i \\ p_j \\ q_j \end{vmatrix}$$

The values of any column in k may be obtained by setting all displacements equal to zero except for the one displacement, which is multiplied by this column. Figure 2.3 illustrates a bar element with all displacements fixed except u_i . Using these values for displacements, the forces obtained will be equal to the stiffness, since spring rate is defined as the force required to produce a unit deflection. Substitute the following value of d into the stiffness equation.

$$\{d\} = \begin{Bmatrix} 1 \\ 0 \\ 0 \\ 0 \end{Bmatrix}$$

The result is:

$$\begin{Bmatrix} k_{1,1} \\ k_{1,2} \\ k_{1,3} \\ k_{1,4} \end{Bmatrix} = \begin{Bmatrix} p_i \\ q_i \\ p_j \\ q_j \end{Bmatrix}$$

Values of these force components may be obtained by using the equation for axial deflection (Δ) of a uniform bar subjected to an axial load (P).

$$\Delta = PL/AE$$

$$\Delta = \cos \beta u_i = C x l$$

$$P = \Delta AE/L = C AE/L = p_i/C$$

Hence,

$$p_i = C^2 AE/L.$$

From static equilibrium requirements,

$$p_j = -p_i = -C^2 AE/L$$

And for the vertical component v_i ,

$$\Delta = \cos \beta u_i = C$$

$$P = \Delta AE/L = CAE/L = q_i/\sin \beta = q_i/S$$

Hence,

$$q_i = CS AE/L = -q_j$$

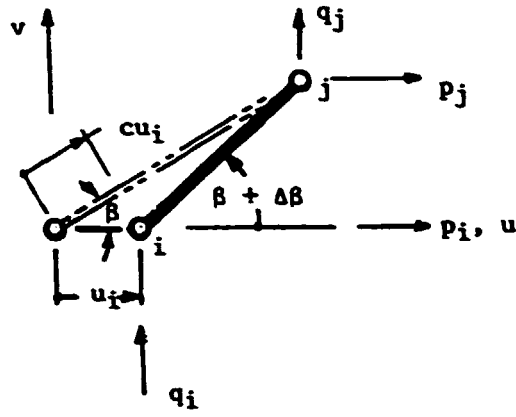


Figure 2.3 Bar Element with $u_i = 1$, and $u_j = v_i = v_j = 0$.

Values for the second column may be obtained by assuming the following values for displacements: $v_i = 1$ and $u_i = u_j = v_j = 0$.

$$\{d\} = \begin{Bmatrix} 0 \\ 1 \\ 0 \\ 0 \end{Bmatrix}$$

The axial deflection of the bar is

$$\Delta = S v_i = S \times 1$$

and

$$P = \Delta AE/L = S AE/L = q_i/S.$$

Hence,

$$q_i = S^2 AE/L = -q_j$$

and,

$$p_i = CS AE/L = -p_j.$$

Substitute into the stiffness equation to obtain values for column 2 of the k matrix.

$$\begin{Bmatrix} k_{1,1} & k_{1,2} & k_{1,3} & k_{1,4} \\ k_{2,1} & k_{2,2} & k_{2,3} & k_{2,4} \\ k_{3,1} & k_{3,2} & k_{3,3} & k_{3,4} \\ k_{4,1} & k_{4,2} & k_{4,3} & k_{4,4} \end{Bmatrix} \begin{Bmatrix} 0 \\ 1 \\ 0 \\ 0 \end{Bmatrix} = \begin{Bmatrix} CS AE/L \\ S^2 AE/L \\ -CS AE/L \\ -S^2 AE/L \end{Bmatrix}$$

Hence,

$$\begin{bmatrix} k_{1,2} \\ k_{2,2} \\ k_{3,2} \\ k_{4,2} \end{bmatrix} = \begin{bmatrix} CS & AE/L \\ S^2 & AE/L \\ -CS & AE/L \\ -S^2 & AE/L \end{bmatrix}$$

This process may be continued until the following stiffness equation for the bar element is obtained for two dimensional space.

$$\frac{AE}{L} \begin{bmatrix} c^2 & CS & -c^2 & -CS \\ CS & S^2 & -CS & -S^2 \\ -c^2 & -CS & c^2 & CS \\ -CS & -S^2 & CS & S^2 \end{bmatrix} \begin{bmatrix} u_i \\ v_i \\ u_j \\ v_j \end{bmatrix} = \begin{bmatrix} P_i \\ q_i \\ P_j \\ q_j \end{bmatrix}$$

If a structure contains more than one element, the stiffness equation of all of the elements can be combined into a single matrix equation, which can easily be evaluated for the unknown displacements and reactions. Each element stiffness equation may be expanded to structure size to allow the matrix addition. The structure of Figure 2.4 has two elements. The stiffness equation for each element after expansion to structure size is shown below. The number of degrees of freedom for the structure is 6, so the K matrix must be 6 x 6.

	DATA	
	Element 1	Element 2
Nodes	1,2	2,3
Stiffness	k_1	k_2
Length	L_1	L_2
Area	A_1	A_2
Displacements	$u_i = u_1 = 0$ $v_i = v_1 = 0$ $u_j = u_2$ $v_j = v_2$	$u_i = u_2$ $v_i = v_2$ $u_j = u_3 = 0$ $v_j = v_3 = 0$
Forces	$P_i = P_1$ $q_i = q_1$ $P_j = P_2 = F \cos \theta$ $q_j = q_2 = -F \sin \theta$ $\theta = 270^\circ$ $c = 0$ $s = -1$	$P_i = P_2 = F \cos \theta$ $q_i = q_2 = -F \sin \theta$ $P_j = P_3$ $q_j = q_3$ $\theta = 180^\circ$ $c = -1$ $s = 0$

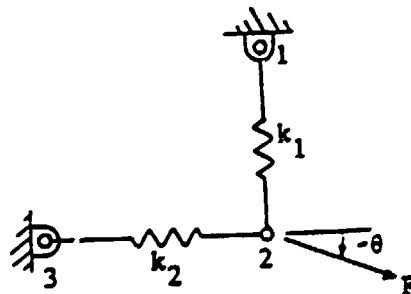


Figure 2.4 Structure FE Model

For element 1:

$$[k_1] = \frac{A_1 E_1}{L_1} \begin{vmatrix} 0 & 0 & 0 & 0 \\ 0 & 1 & 0 & -1 \\ 0 & 0 & 0 & 0 \\ 0 & -1 & 0 & 1 \end{vmatrix} \begin{vmatrix} u_1 \\ v_1 \\ u_2 \\ v_2 \end{vmatrix} = \begin{vmatrix} p_1 \\ q_1 \\ p_2 \\ q_2 \end{vmatrix}$$

For element 2:

$$[k_2] = \frac{A_2 E_2}{L_2} \begin{vmatrix} 1 & 0 & 1 & 0 \\ 0 & 0 & 0 & 0 \\ -1 & 0 & 1 & 0 \\ 0 & 0 & 0 & 0 \end{vmatrix} \begin{vmatrix} u_2 \\ v_2 \\ u_3 \\ v_3 \end{vmatrix} = \begin{vmatrix} p_2 \\ q_2 \\ p_3 \\ q_3 \end{vmatrix}$$

Element 1 must have rows 5 and 6 and columns 5 and 6 added to k_1 in order to accommodate the degrees of freedom u_3 and v_3 . Element 2 must have rows 1 and 2 and columns 1 and 2 added to k_2 to accommodate degrees of freedom u_1 and v_1 . If zeros are placed in k_1 and k_2 in these added rows and columns as shown below, then their addition will not modify the force-deflection contribution by these two elements.

$$\frac{A_1 E_1}{L_1} \begin{vmatrix} 0 & 0 & 0 & 0 & 0 & 0 \\ 0 & 1 & 0 & -1 & 0 & 0 \\ 0 & 0 & 0 & 0 & 0 & 0 \\ 0 & -1 & 0 & 1 & 0 & 0 \\ 0 & 0 & 0 & 0 & 0 & 0 \\ 0 & 0 & 0 & 0 & 0 & 0 \end{vmatrix} \begin{vmatrix} u_1 \\ v_1 \\ u_2 \\ v_2 \\ u_3 \\ v_3 \end{vmatrix} = \begin{vmatrix} p_1 \\ q_1 \\ p_2 \\ q_2 \\ p_3 \\ q_3 \end{vmatrix}$$

The stiffness equation for the structure is the sum of the element stiffness equations. For this structure the stiffness equation with the external forces and the displacement boundary conditions is

$$\begin{array}{cccccc|c|c|c}
 0 & 0 & 0 & 0 & 0 & 0 & 0 & P_1 \\
 0 & \frac{A_1 E_1}{L_1} & 0 & \frac{-A_1 E_1}{L_1} & 0 & 0 & 0 & q_1 \\
 0 & 0 & \frac{A_2 E_2}{L_2} & 0 & \frac{-A_2 E_2}{L_2} & 0 & u_2 & F \cos \beta \\
 0 & \frac{-A_1 E_1}{L_1} & 0 & \frac{A_1 E_1}{L_1} & 0 & 0 & v_2 & F \sin \beta \\
 0 & 0 & \frac{-A_2 E_2}{L_2} & 0 & \frac{A_2 E_2}{L_2} & 0 & 0 & p_3 \\
 0 & 0 & 0 & 0 & 0 & 0 & 0 & q_3
 \end{array}$$

This structure stiffness equation may be solved by Gaussian methods for the unknown displacements (u_2 and v_2), since F , β , A , E and L are known. After u_2 and v_2 are evaluated, their values may be substituted into the structure stiffness equation to obtain the ground reactions, p_1 , q_1 , p_3 and q_3 .

3. NATURAL ELEMENTS: Beam Elements

The beam element is based on elastic beam theory. The beam element has one node at each end and each node has two degrees of freedom: transverse deflection, w , and slope, θ . The displacement vector is

$$\{d\} = \begin{Bmatrix} w_i \\ \theta_i \\ w_j \\ \theta_j \end{Bmatrix}$$

Each node may have a moment, m , or a transverse force, q . Hence, the loading vector is

$$\{r\} = \begin{Bmatrix} q_1 \\ m_1 \\ q_j \\ m_j \end{Bmatrix}$$

The stiffness equation is

$$[k] \{d\} = \{r\}.$$

The values of the entries in $[k]$ may be obtained by assigning a displacement of unity to one degree of freedom and a value of zero to the other three displacements. For example, a displacement

$$\{d\} = \begin{Bmatrix} 1 \\ 0 \\ 0 \\ 0 \end{Bmatrix},$$

gives the following from the stiffness equation.

$$\begin{Bmatrix} k_{1,1} \\ k_{2,1} \\ k_{3,1} \\ k_{4,1} \end{Bmatrix} = \begin{Bmatrix} q_1 \\ m_1 \\ q_j \\ m_j \end{Bmatrix}$$

Figure 3.1 shows a beam element which matches the example displacement.

Castigliano's Theorem may be applied with the above equation to evaluate the stiffness values.

$$v_1 = \frac{\partial U}{\partial q_1} = \frac{\partial}{\partial q_1} \int_0^L \frac{M^2}{2EI} dx = \int_0^L \frac{\partial}{\partial q_1} \frac{(q_1 x - m_1)^2}{2EI} dx$$

$$v_1 = 1 = \int_0^L (q_1 x^2 - m_1 x) / (EI) dx$$

$$1 = (q_1 \frac{L^3}{3} - \frac{m_1 L^2}{2}) / (EI)$$

Substitute, $q_1 = k_{1,1}$ and $M_1 = k_{2,1}$ from above into this latter equation.

$$EI = k_{1,1}L^3/3 - k_{2,1}L^2/2$$

Repeating this calculation for other unit displacements will yield the other equations and the stiffness matrix k_{BEAM} may be obtained for the beam element.

$$[k_{\text{BEAM}}] = \frac{EI}{L^3} \begin{vmatrix} 12 & 6L & -12 & 6L \\ 6L & 4L^2 & -6L & 2L^2 \\ -12 & -6L & 12 & -6L \\ 6L & 2L^2 & -6L & 4L^2 \end{vmatrix}$$

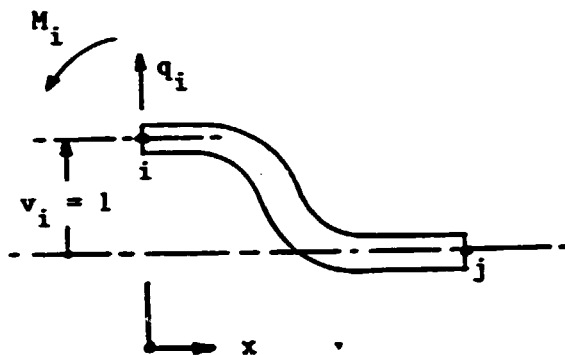


Figure 3.1 Beam Element with
Displacements: $v_i = 1, \theta_i = v_j = \theta_j = 0$

4. NATURAL ELEMENTS: Frame Element

The Beam element and the Bar element give the same values of displacement and stress as obtained by strength of materials methods. These two elements may be expanded to six degrees of freedom and K_{Bar} added to K_{BEAM} to create the Frame element with three degrees of freedom per node: axial deflection, transverse deflection, and slope. The resulting stiffness equation is (2):

$$[K] \{d\} = \{r\}$$

$$\begin{bmatrix} F & G & H & -F & -G & H \\ G & P & Q & -G & -P & Q \\ H & Q & T & -H & -Q & B \\ -F & -G & -H & F & G & -H \\ -G & -P & -Q & G & P & -Q \\ H & Q & B & -H & -Q & T \end{bmatrix} \begin{bmatrix} u_i \\ w_i \\ \theta_i \\ u_j \\ w_j \\ \theta_j \end{bmatrix} = \begin{bmatrix} P_i \\ Q_i \\ M_i \\ P_j \\ Q_j \\ M_j \end{bmatrix}$$

where,

$$L = [(x_j - x_i)^2 + (y_j - y_i)^2]^{.5}$$

$$C = (x_j - x_i)/L \quad S = (y_j - y_i)/L$$

$$S_1 = AE/L \quad C_1 = 6EI/L^2 \quad G = S_1 SC - DSC$$

$$T = 4 EI/L \quad D = 12 EI/L^3 \quad H = -C_1 S$$

$$B = 2 EI/L \quad F = S_1 C^2 + D S^2 \quad P = S_1 S^2 + DC^2$$

$$Q = C_1 C$$

A finite element program, FRAME, which uses the Frame element is given in appendix A. This program evaluates the deflections and reactions of a structure. This program is used to evaluate the bending moment reactions and the deflection of a wall of the transmission housing in Figure 4.1. The thrust wall supports the thrust bearing for the propeller force. The thrust wall is shown in Figure 4.2.

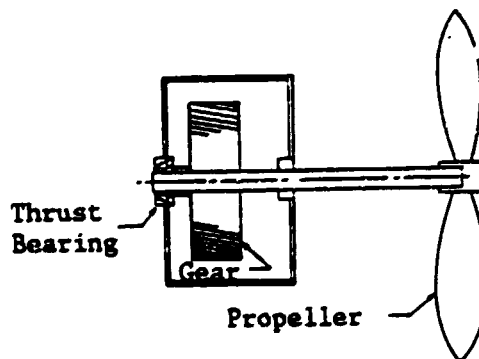


Figure 4.1 Transmission

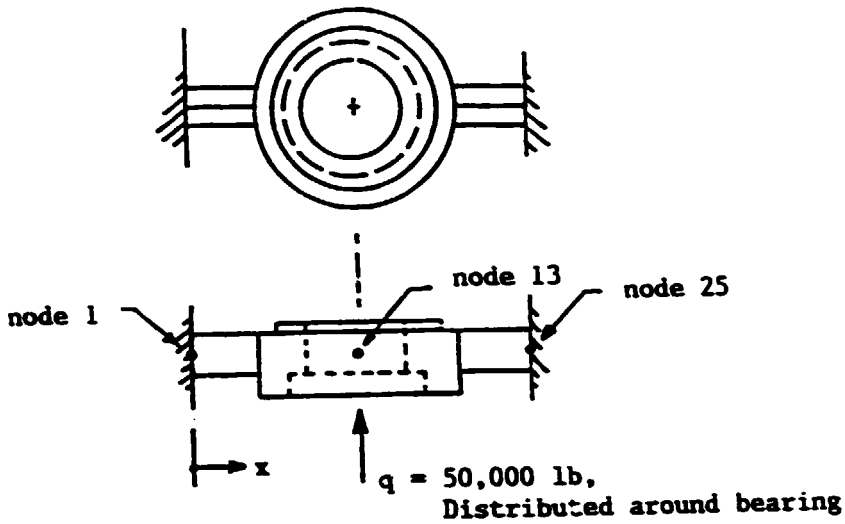


Figure 4.2 Thrust Wall of Transmission Housing

The moments of inertia vary from one end of the wall to the other. The values of location, area, section width (SW_1, SW_2, SW_3) and inertia are given for the midpoints of each section of the wall in Table 4.1.

TABLE 4.1 Data for Transmission Wall

Node	Location (inches)	Area (inches ²)	Inertia (inches ⁴)	Force (lb)	Moment (lb-in)
1	0.00	45	42.0	0	0
2	4.00	47	42.0	0	0
3	7.50	54	140.0	0	0
4	8.23	64	245.0	0	0
5	9.00	74	315.0	0	0
6	9.69	95	345.0	0	0
7	10.39	98	157.5	2083	0
8	10.69	82	141.0	4167	0
9	11.49	69	107.5	4167	0
10	12.79	45	87.5	4167	0
11	14.29	25	80.0	4167	0
12	16.20	25	76.5	4167	0
13	18.00			4167	0

The forces, moments and deflections evaluated by this program are given in Table 4.2. The lack of visual aids to illustrate the output is a significant handicap for this type of program. However, the cost of the program is sometimes a limiting factor.

TABLE 4.2

DEFLECTION OF NODES

NODE NUMBER 1		NODE NUMBER 14	
X-DEFLECTION	= 0	X-DEFLECTION	= 0
Y-DEFLECTION	= 0	Y-DEFLECTION	= 5.297454E-03
ANGULAR DEFLECTION	= 0	ANGULAR DEFLECTION	= -1.29659E-04
NODE NUMBER 2		NODE NUMBER 15	
X-DEFLECTION	= 0	X-DEFLECTION	= 0
Y-DEFLECTION	= 8.543822E-04	Y-DEFLECTION	= 4.929388E-03
ANGULAR DEFLECTION	= 3.735071E-04	ANGULAR DEFLECTION	= -2.549617E-04
NODE NUMBER 3		NODE NUMBER 16	
X-DEFLECTION	= 0	X-DEFLECTION	= 0
Y-DEFLECTION	= 2.343122E-03	Y-DEFLECTION	= 4.483418E-03
ANGULAR DEFLECTION	= 4.360998E-04	ANGULAR DEFLECTION	= -3.368382E-04
NODE NUMBER 4		NODE NUMBER 17	
X-DEFLECTION	= 0	X-DEFLECTION	= 0
Y-DEFLECTION	= 2.66831E-03	Y-DEFLECTION	= 4.011703E-03
ANGULAR DEFLECTION	= 4.305017E-04	ANGULAR DEFLECTION	= -3.975969E-04
NODE NUMBER 5		NODE NUMBER 18	
X-DEFLECTION	= 0	X-DEFLECTION	= 0
Y-DEFLECTION	= 2.98938E-03	Y-DEFLECTION	= 3.693199E-03
ANGULAR DEFLECTION	= 4.253601E-04	ANGULAR DEFLECTION	= -4.081899E-04
NODE NUMBER 6		NODE NUMBER 19	
X-DEFLECTION	= 0	X-DEFLECTION	= 0
Y-DEFLECTION	= 3.281223E-03	Y-DEFLECTION	= 3.569798E-03
ANGULAR DEFLECTION	= 4.203481E-04	ANGULAR DEFLECTION	= -4.14057E-04
NODE NUMBER 7		NODE NUMBER 20	
X-DEFLECTION	= 0	X-DEFLECTION	= 0
Y-DEFLECTION	= 3.571494E-03	Y-DEFLECTION	= 3.277611E-03
ANGULAR DEFLECTION	= 4.145141E-04	ANGULAR DEFLECTION	= -4.202098E-04
NODE NUMBER 8		NODE NUMBER 21	
X-DEFLECTION	= 0	X-DEFLECTION	= 0
Y-DEFLECTION	= 3.59692E-03	Y-DEFLECTION	= 2.995876E-03
ANGULAR DEFLECTION	= 4.082514E-04	ANGULAR DEFLECTION	= -4.251897E-04
NODE NUMBER 9		NODE NUMBER 22	
X-DEFLECTION	= 0	X-DEFLECTION	= 0
Y-DEFLECTION	= 4.01542E-03	Y-DEFLECTION	= 2.664949E-03
ANGULAR DEFLECTION	= 3.875264E-04	ANGULAR DEFLECTION	= -4.30295E-04
NODE NUMBER 10		NODE NUMBER 23	
X-DEFLECTION	= 0	X-DEFLECTION	= 0
Y-DEFLECTION	= 4.486879E-03	Y-DEFLECTION	= 2.339934E-03
ANGULAR DEFLECTION	= 3.365273E-04	ANGULAR DEFLECTION	= -4.358452E-04
NODE NUMBER 11		NODE NUMBER 24	
X-DEFLECTION	= 0	X-DEFLECTION	= 0
Y-DEFLECTION	= 4.971584E-03	Y-DEFLECTION	= 8.528827E-04
ANGULAR DEFLECTION	= 2.543982E-04	ANGULAR DEFLECTION	= -3.729167E-04
NODE NUMBER 12		NODE NUMBER 25	
X-DEFLECTION	= 0	X-DEFLECTION	= 0
Y-DEFLECTION	= 5.298942E-03	Y-DEFLECTION	= 0
ANGULAR DEFLECTION	= 1.291188E-04	ANGULAR DEFLECTION	= 0
NODE NUMBER 13			
X-DEFLECTION	= 0		
Y-DEFLECTION	= 5.415197E-03		
ANGULAR DEFLECTION	= 4.250251E-07		

5. ELEMENTS BASED ON ASSUMED DISPLACEMENT FIELDS:

A more general finite element is based on the Rayleigh-Ritz solution of a variational problem (6). The displacement (or the temperature for a thermal element) within the element is assumed to be adequately described by a simple polynomial. The coefficients of the polynomial define the shape of the displacements across the element. The equations of equilibrium for this "general element" may be obtained by the "principle of minimum potential energy" (2): "Among all admissible configurations of a conservative system, those that satisfy the equations of equilibrium make the potential energy stationary with respect to small variations in displacement. If the stationary condition is a minimum, the equilibrium state is stable." The locations of the minimums for the Potential Function, π_p , may be determined by setting the partial derivatives of π_p with respect to each variable equal to zero. If the displacement variables are a_1 , a_2 and a_3 , the following three equations will be equations of equilibrium.

$$\partial \pi_p / \partial a_1 = 0$$

$$\partial \pi_p / \partial a_2 = 0$$

$$\partial \pi_p / \partial a_3 = 0$$

In order to illustrate this concept, consider a bar with two elements as shown in Figure 5.1. Assume the displacements, u , of points along the bar vary in a linear manner as defined by the following displacement function.

$$v = a_1 + a_2 s \quad \text{for } 0 \leq y \leq L$$

$$v = a_3 + a_4 s \quad \text{for } L \leq y \leq 2L$$

where,

$$0 \leq s \leq L$$

Since the polynomial coefficients (a_1 through a_4) have little physical meaning, it is desirable to replace these coefficients with other variables which do have physical significance such as the displacements of the nodes: v_1 , v_2 and v_3 .

$$\{D\} = \begin{Bmatrix} v_1 \\ v_2 \\ v_3 \end{Bmatrix}$$

Substitution of boundary conditions at the nodes into the displacement function for element 1-2 gives:

$$v_1 = a_1 + a_2s = a_1 \quad \text{at } s = 0$$

$$v_2 = a_1 + a_2s = a_1 + a_2L \quad \text{at } s = L$$

These two equations may be placed in matrix form:

$$\begin{Bmatrix} v_1 \\ v_2 \end{Bmatrix} = \begin{bmatrix} 1 & 0 \\ 1 & L \end{bmatrix} \begin{Bmatrix} a_1 \\ a_2 \end{Bmatrix}$$

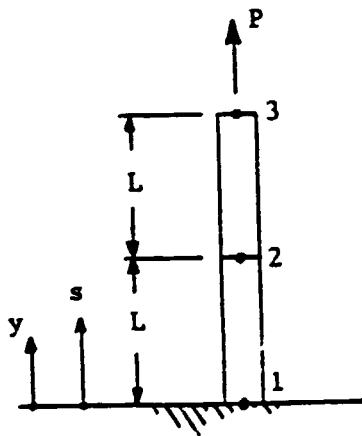


Figure 5.1 Structure with Two Elements

or, the inverse yields

$$\begin{Bmatrix} a_1 \\ a_2 \end{Bmatrix} = \begin{bmatrix} 1 & 0 \\ -1/L & 1/L \end{bmatrix} \begin{Bmatrix} v_1 \\ v_2 \end{Bmatrix}$$

Hence,

$$v = a_1 + a_2 s = [1 + s] \begin{Bmatrix} a_1 \\ a_2 \end{Bmatrix}$$

Combine these equations to replace the coefficients a_1 and a_2 with the nodal displacements v_1 and v_2 .

$$v = [1 + s] \begin{bmatrix} 1 & 0 \\ -1/L & 1/L \end{bmatrix} \begin{Bmatrix} v_1 \\ v_2 \end{Bmatrix}$$

The shape function N , which gives the relationship between displacements at any point in an element and the displacements at the nodes is

$$[N] = [1 + s] \begin{bmatrix} 1 & 0 \\ -1/L & 1/L \end{bmatrix} = [(1 - s/L) \quad (s/L)]$$

Hence,

$$v = [N] \begin{Bmatrix} v_1 \\ v_2 \end{Bmatrix} = [N] \{d\}$$

For element 2-3,

$$v = [N] \begin{Bmatrix} v_2 \\ v_3 \end{Bmatrix}$$

If this element is not subjected to initial strains, the strain energy per unit volume of material due to applied loads is

$$U_0 = .5 [\epsilon_y]^T E [\epsilon_y]$$

where,

E = Modulus of elasticity

ϵ_y = Strain in y-direction

For plane problems, the relationship between strain, ϵ_y , and displacement in the y-direction, v , is:

$$\epsilon_y = \partial v / \partial y = \partial v / \partial s = \partial / \partial s ([N] \{d\}) = [-1/L \quad 1/L] \{d\}$$

Therefore, the total strain energy in elements 1 and 2 is given by U_1 .

$$U_1 = \int_0^{L_1} .5 \begin{vmatrix} v_1 \\ v_2 \end{vmatrix}^T \begin{vmatrix} -1/L \\ 1/L \end{vmatrix} E_1 \begin{bmatrix} -1/L & 1/L \end{bmatrix} \begin{vmatrix} v_1 \\ v_2 \end{vmatrix} A_1 ds$$

$$+ \int_0^{L_2} .5 \begin{vmatrix} v_2 \\ v_3 \end{vmatrix}^T \begin{vmatrix} -1/L \\ 1/L \end{vmatrix} E_2 \begin{bmatrix} -1/L & 1/L \end{bmatrix} \begin{vmatrix} v_2 \\ v_3 \end{vmatrix} A_2 ds$$

$$U_1 = .5 \begin{vmatrix} v_1 \\ v_2 \end{vmatrix}^T \int_0^{L_1} E_1 A_1 \begin{vmatrix} 1/L^2 & -1/L^2 \\ -1/L^2 & 1/L^2 \end{vmatrix} ds \begin{vmatrix} v_1 \\ v_2 \end{vmatrix}$$

$$+ .5 \begin{vmatrix} v_2 \\ v_3 \end{vmatrix}^T \int_0^{L_2} E_2 A_2 \begin{vmatrix} 1/L^2 & -1/L^2 \\ -1/L^2 & -1/L^2 \end{vmatrix} ds \begin{vmatrix} v_2 \\ v_3 \end{vmatrix}$$

$$U_1 = .5 \begin{vmatrix} v_1 \\ v_2 \end{vmatrix}^T \begin{vmatrix} \frac{E_1 A_1}{L_1} & & \\ & 1 & -1 \\ & -1 & 1 \end{vmatrix} \begin{vmatrix} v_1 \\ v_2 \end{vmatrix}$$

$$+ .5 \begin{vmatrix} v_2 \\ v_3 \end{vmatrix}^T \begin{vmatrix} \frac{E_2 A_2}{L_2} & & \\ & 1 & -1 \\ & -1 & 1 \end{vmatrix} \begin{vmatrix} v_2 \\ v_3 \end{vmatrix}$$

The potential for the force R to do work during displacement D is U_2 , where R and D represent all forces on the structure and their nodal displacements.

$$U_2 = - [D]^T [R] = - [v_1 \ v_2 \ v_3] \begin{Bmatrix} R_1 \\ R_2 \\ R_3 \end{Bmatrix}$$

Hence, the total potential function is

$$\pi_p = U_1 + U_2 = .5 [D]^T [k_1] [D] + .5 [D]^T [k_2] [D] - [D]^T [R]$$

where, the stiffness matrices are expanded to structure size by adding rows and columns of zeros:

$$[k_1] = A_1 E_1 / L_1 \begin{vmatrix} 1 & 1 & 0 \\ -1 & 1 & 0 \\ 0 & 0 & 0 \end{vmatrix} \quad [k_2] = A_2 E_2 / L_2 \begin{vmatrix} 0 & 0 & 0 \\ 0 & 1 & -1 \\ 0 & -1 & 1 \end{vmatrix}$$

Applying the principal of minimum potential energy will yield the equations of equilibrium for this structure based on nodal displacements.

$$\partial \pi_p / \partial D = [K_1][D] + [K_2][D] - [R] = 0$$

or,

$$\frac{A_1 E_1}{L_1} \begin{vmatrix} 1 & -1 & 0 \\ -1 & 1 & 0 \\ 0 & 0 & 0 \end{vmatrix} \begin{vmatrix} v_1 \\ v_2 \\ v_3 \end{vmatrix} + \frac{A_2 E_2}{L_2} \begin{vmatrix} 0 & 0 & 0 \\ 0 & 1 & -1 \\ 0 & -1 & 1 \end{vmatrix} \begin{vmatrix} v_1 \\ v_2 \\ v_3 \end{vmatrix} - \begin{vmatrix} r_1 \\ r_2 \\ r_3 \end{vmatrix} = 0$$

The boundary conditions to be applied to this matrix equation are

$$[D] = \begin{vmatrix} v_1 \\ v_2 \\ v_3 \end{vmatrix} = \begin{vmatrix} 0 \\ v_2 \\ v_3 \end{vmatrix}$$

$$[R] = \begin{vmatrix} r_1 \\ r_2 \\ r_3 \end{vmatrix} = \begin{vmatrix} r_1 \\ 0 \\ p \end{vmatrix}$$

The matrix equation of equilibrium may be solved to yield nodal displacements and nodal reactions. The strain may be evaluated at any point, y , in the element by the relationship

$$\epsilon_y = \partial v / \partial s$$

since,

$$dy = ds$$

where,

v is the assumed displacement function, which is dependent on the nodal displacements:

$$v = [N] \begin{vmatrix} v_1 \\ v_2 \end{vmatrix}$$

$$v = [N] \begin{vmatrix} v_2 \\ v_3 \end{vmatrix}$$

The stress may be evaluated from Hook's law using these strains.

$$\{\sigma\} = [E] \{\epsilon\}$$

The Raleigh Ritz method may also be used to develop the isoparametric element.

6. ISOPARAMETRIC ELEMENTS:

The isoparametric element may be used to model general shapes because its sides may be curved and the element may be nonrectangular. Body fixed coordinates ξ and η are used for this element, with magnitudes ranging from +1 to -1 as shown in Figure 6.1. Assumed displacement function, u , for the two-dimensional isoparametric solid element, STIF42, in the ANSYS (2) finite element software is given below in terms of the element's coordinates ξ and η . The last two terms may be omitted. The Rayleigh Ritz method is used to set up the solution.

$$U = .25 \left((1 - \xi)(1 + \eta)U_1 + (1 + \xi)(1 - \eta)U_j + (1 + \xi)(1 + \eta)U_k + (1 - \xi)(1 - \eta)U_l \right) + U_1(1 - \xi^2) + U_2(1 - \eta^2)$$

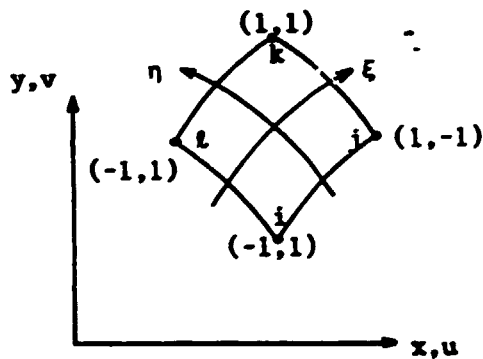


Figure 6.1 Two-Dimensional Isoparametric Element

7. EXAMPLE: Comparison of Beam Element and Isoparametric Element.

The isoparametric element may be used to model components with high strain gradients or complex geometries which do not match the assumptions for the beam element (e.g. the root of a gear tooth). On the other hand, if a beam element can be used, the efficiency and accuracy of the solution should be improved.

The analysis of the cantilever beam (Figure 7.1) for stress and deflection using one beam element is compared to the analysis when using various combinations of the ANSYS (3) isoparametric element STIF42. The correct answer per strength of materials theory may be obtained by using only one beam element. Figure 7.2 shows the element model and the deflected model, which gives the maximum deflection of .00667 inches. The stress at the wall is

$$S_x = MC/I = 3,000 \text{ psi.}$$

(3) Note: ANSYS is a registered tradename of a Finite Element Software package by Swanson Analysis, Inc. Some of the examples in this paper were completed using the PC/ED and PC/Linear versions of ANSYS.

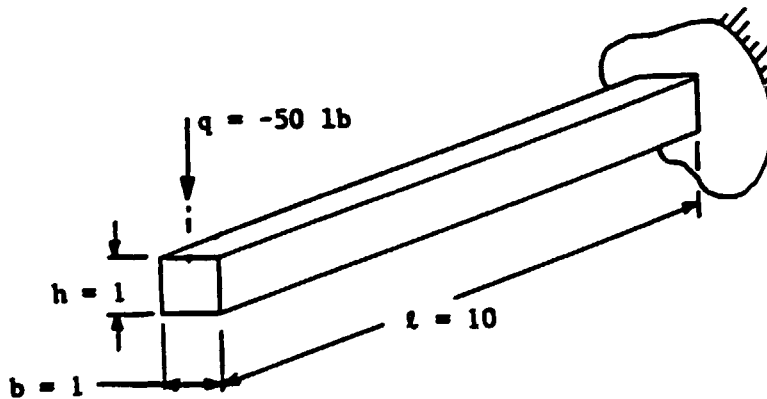
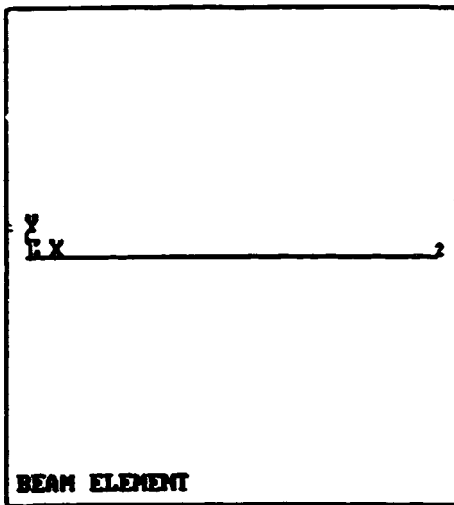
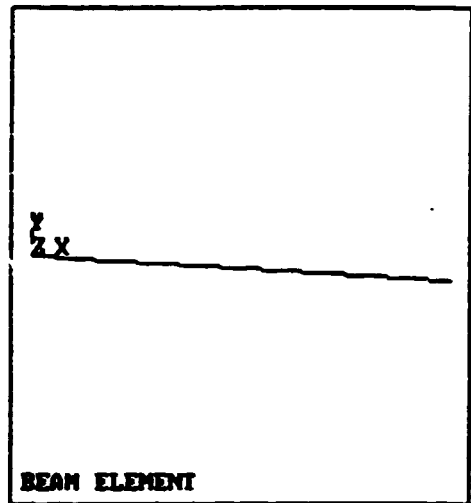


Figure 7.1 Cantilever Beam



F. E. Model



Deflected Shape

Figure 7.2 Cantilever Beam Model
Using One Beam Element.

The analysis of the cantilever beam using one isoparametric element gives a maximum deflection of .00507 inches, as indicated in the deflection plot of Figure 7.3. However, the plot of the stress in the x-direction (S_x), which is along the axis of the beam, indicates that stress is not changing as the distance from the load is increased (i.e. S_x is not a function of bending moment). Hence, the stress calculations are not valid for this model. (The one isoparametric element model gives a value of stress at the wall of $S_x = 1500$ psi). (The input code for ANSYS is in Appendix B.)

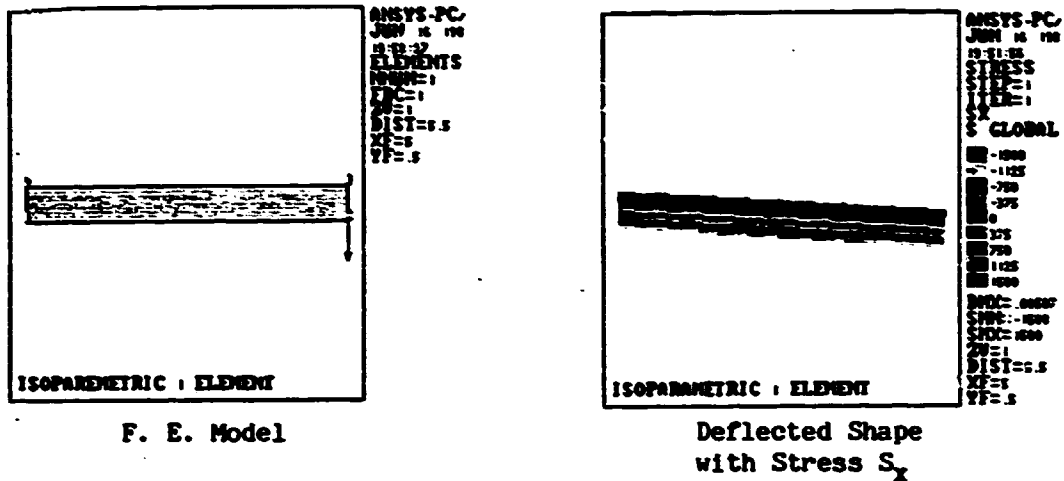


Figure 7.3 Cantilever Beam Model Using One Isoparametric Element

The analysis of the cantilever beam using four isoparametric elements with an aspect ratio of 10 per Figure 7.4 gives a maximum deflection of .00615 inches. The distribution of the stress S_x is significantly improved and at the wall $S_x = 2226$ psi.

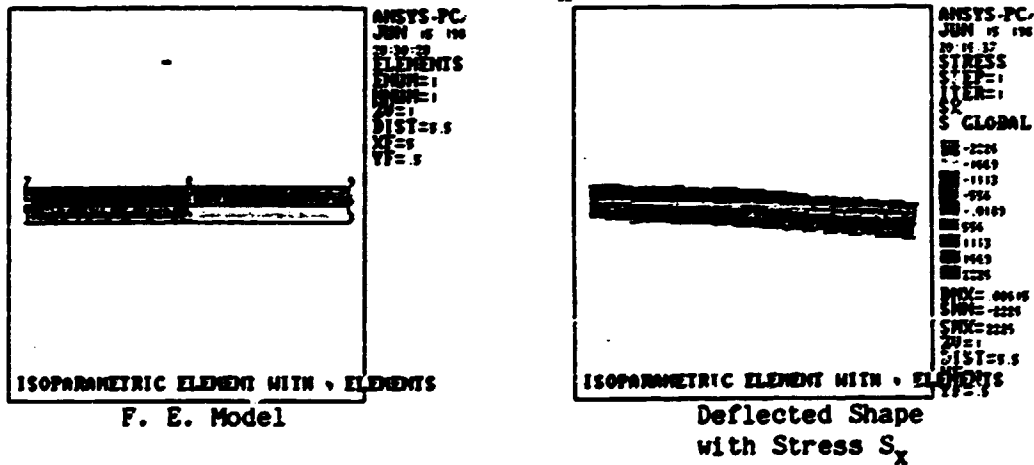
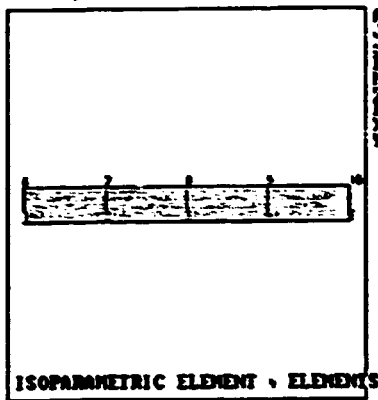
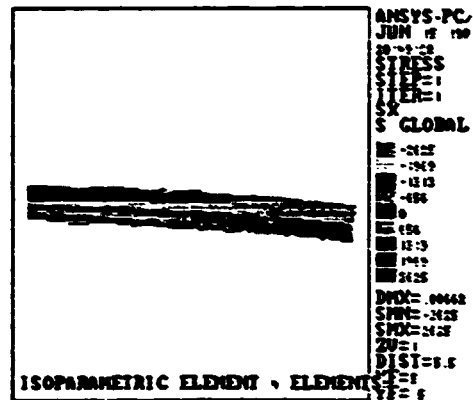


Figure 7.4 Cantilever Beam Model Using Four Isoparametric Elements

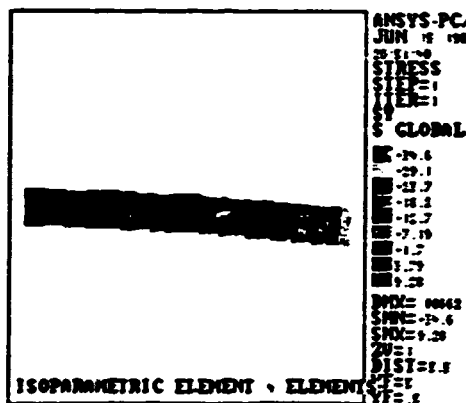
The analysis of the cantilever beam was repeated with the four elements arranged in a manner to produce an aspect ratio (the ratio of length over width) of 2.5 per Figure 7.5. The maximum deflection is .00662 and at the wall the stress S_x is 2,625 psi. The vertical stress S_y is shown in the figure and the values are negligible.



F. E. Model



Deflected Shape with Stress S_x



Deflected Shape with Stress S_y

Figure 7.5 Cantilever Beam Model Using Four Parallel Isoparametric Elements

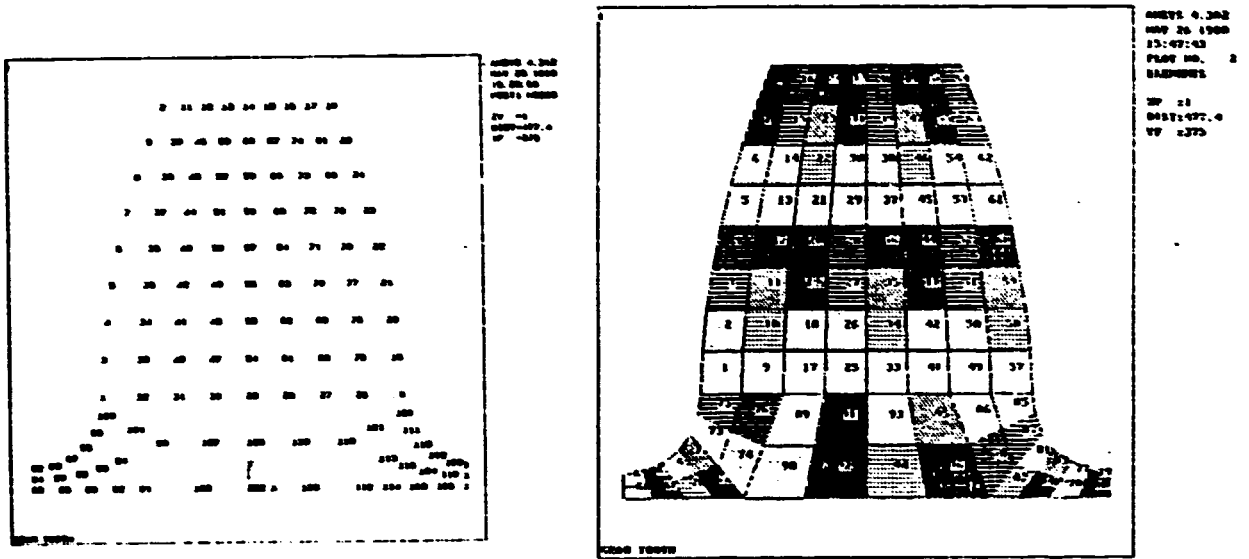
The conclusions from this comparison are:

1. For bending of prismatic bars, the beam element is the most accurate and efficient.
2. The density of the isoparametric elements over the area of a strain gradient will significantly affect the accuracy.
3. The values of deflection are generally more reliable than the values for stress.
4. The arrangement of the elements and the aspect ratio will significantly affect the accuracy.
5. As the number of elements is increased in an area, the stresses and deflections should converge toward the true answer.

8. EXAMPLE: Gear Teeth

The FEM has been used extensively to evaluate the stress and deflection of gear teeth. The value of the stress concentration factor used in the International Standards Organization (ISO) method for rating tooth strength (8) is evaluated by the FEM. The distribution of the load across the face of the tooth due to deflections of the elastic system must be evaluated in order to determine the amount of helix modification required. The end of the pinion adjacent to the powered shaft has the highest torque so this end of the pinion should have the largest deflection. The FEM may be used to evaluate this load-deflection condition (9).

The stiffness of a single tooth may be evaluated by the FEM. The node numbers and the subsequent elements are shown in Figure 8.1. ANSYS PC/Linear software plus the Solids Modeling package produced this model. The entire load is applied to node 7 which produces the gross tooth deflection with local distortion due to the point load per Figure 8.2. The transverse deflection (u_x) of the tooth is shown in Figure 8.3. The vertical component of stress, s_y , is shown in Figure 8.4 and illustrates the influence of the radial load, W_r , on the bending stress of the tooth. The compressive stresses add on the side opposite to the point of load application.



Node Numbers

Element Numbers

Figure 8.1 Finite Element Model of Gear Tooth

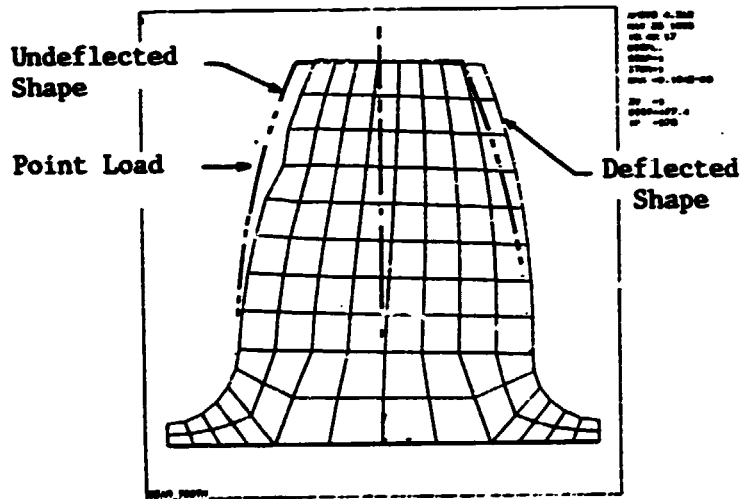


Figure 8.2 Tooth Deflection

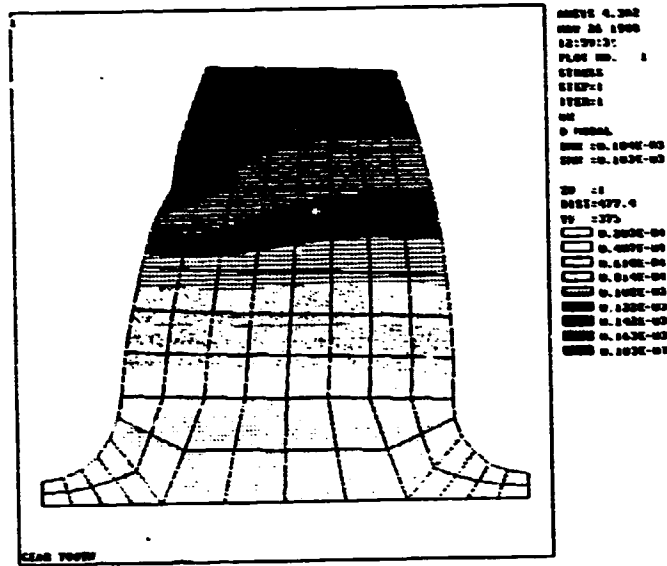


Figure 8.3 Transverse Displacement of Tooth

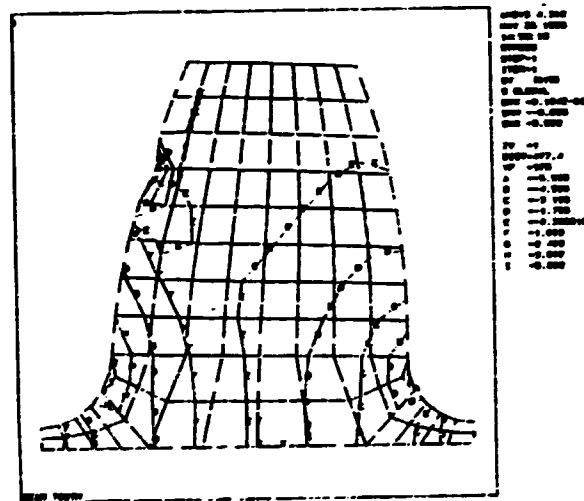


Figure 8.4 Vertical (sy) Component of Tooth Stress

9. EXAMPLE: Transverse Vibration

The transverse vibration and longitudinal vibrations in geared systems may be of critical importance even though they receive less attention than the more subtle torsional vibration. The natural

frequencies for the transverse vibration of the shaft and gears of Figure 9.1 are given in Table 9.1 and the first mode shape is plotted in Figure 9.2.

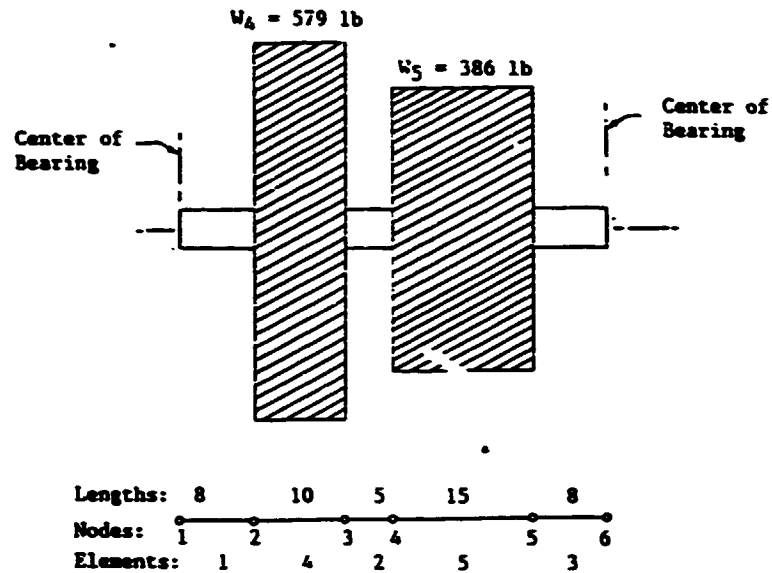


Figure 9.1 Counter Shaft Vibration in Transmission

TABLE 9.1
NATURAL FREQUENCIES FOR
TRANSMISSION SHAFT

MODE	FREQUENCY (VPM)
1	116.2
2	517.5
3	829.1
4	2717.

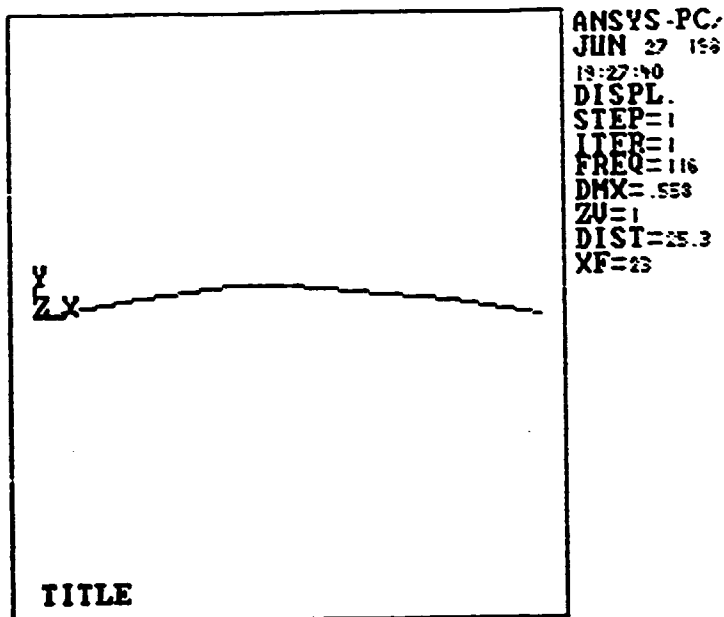


Figure 9.2 First Mode Transverse Vibration of Transmission Shaft

10. CONCLUSIONS

The Finite Element Method provides a tool, which allows the mechanical designer to analyze complex geometric shapes with complex loading for stress, deflection and temperature distributions. The FEM uses a numerical procedure to solve the system of equations, so an answer is produced even though it may not be representative of the physical system. The successful use of the FEM requires the designer to have a deep understanding of stress and strain in addition to understanding the performance and limitations of the various types of elements. The FEM has not eliminated the need for the Experimental Method, but it has reduced the lost time spent in testing various faulty configurations for a component. The Experimental Method still provides for overall quality control. The FEM helps create an optimum design.

REFERENCE LIST

1. Roark, R. J., and Young, W. C., Formulas for Stress and Strain, McGraw Hill Book Co., 1975.
2. Cook, Robert D., Concepts and Applications of Finite Element Analysis, John Wiley and Sons, Inc., 1981.
3. Boresi, A. P., and Sidebottom, O. M., Advanced Mechanics of Materials, John Wiley and Sons, Inc., 1985.
4. Dally, J. W., and Riley, W. F., Experimental Stress Analysis, McGraw Hill Book Co., 1978.
5. Huebner, K. H., and Thornton, E. A., The Finite Element Method for Engineers, John Wiley & Sons, 1982.
6. Bathe, Klaus-Jurgen, Finite Element Procedures in Engineering Analysis, Prentice-Hall, 1982.
7. Kohnke, P. C., ANSYS Engineering Analysis Systems Theoretical Manual, Swanson Analysis Systems, Inc., Houston, PA, 15342, 1983.
8. Dudley, D. W., Handbook of Practical Gear Design, McGraw Hill Book Co., 1984.
9. Brownridge, C., and Hollingworth, D., Advanced Gearbox Technology in Small Turbo Propeller Engines, Gears and Power Transmission Systems for Helicopters and Turboprops, AGARD Conference Proceedings No. 369, Advisory Group For Aerospace Research and Development, North Atlantic Treaty Organization.


```
510 S = (YJ - YI) / L
520 S1 = A * E / L: T = 4 * E - I / L: B = 2 * E - I / L
525 C1 = 6 * E - I / L: 2: D = 12 * E - I / L: 3
530 F = S1 * C - 2 * D * S: 2: G = S1 * C - S - D - S - C
535 H = -C1 * S: P = S1 * S - 2 * D * C: 2: Q = C1 * C
540 SE(1, 1) = F: SE(1, 2) = G: SE(1, 3) = H: SE(1, 4) = -F
545 SE(1, 5) = -G: SE(1, 6) = H
550 SE(2, 1) = G: SE(2, 2) = P: SE(2, 3) = Q: SE(2, 4) = -G
555 SE(2, 5) = -P: SE(2, 6) = Q
560 SE(3, 1) = H: SE(3, 2) = Q: SE(3, 3) = T: SE(3, 4) = -H
565 SE(3, 5) = -Q: SE(3, 6) = B
570 SE(4, 1) = -F: SE(4, 2) = -G: SE(4, 3) = -H: SE(4, 4) = F
575 SE(4, 5) = G: SE(4, 6) = -H
580 SE(5, 1) = -G: SE(5, 2) = -P: SE(5, 3) = -Q: SE(5, 4) = G
585 SE(5, 5) = P: SE(5, 6) = -Q
590 SE(6, 1) = H: SE(6, 2) = Q: SE(6, 3) = B: SE(6, 4) = -H
595 SE(6, 5) = -Q: SE(6, 6) = T
600 RETURN
610 .....
611 ' ARRAY ID .....
612 .....
613 ' UNBANDED .....
623 NEQ = NUMNP * 3
630 ..... BANDED .....
659 FOR N = 1 TO NUMNP
660 FOR J = 1 TO 3
661 ID(J, N) = 0
662 IF J > 1 THEN GOTO 666
663 PRINT "IS X-d.o.f. FOR NODE"; N; " FIXED (Y/N)": INPUT ; ANSW$
664 IF ANSW$ = "Y" OR ANSW$ = "y" THEN ID(J, N) = 1
665 GOTO 673
666 IF J > 2 THEN GOTO 670
667 PRINT "IS Y-d.o.f. FOR NODE"; N; " FIXED (Y/N)": INPUT ; ANSW$
668 IF ANSW$ = "Y" OR ANSW$ = "y" THEN ID(J, N) = 1
669 GOTO 673
670 PRINT "IS THETA-d.o.f. FOR NODE"; N; " FIXED(Y/N)": INPUT ; ANSW$
671 IF ANSW$ = "Y" OR ANSW$ = "y" THEN ID(J, N) = 1
672 GOTO 673
673 PRINT
674 PRINT "ID("; J; ", "; N; ") = "; ID(J, N)
680 NEXT J
690 NEXT N
700 NEQ = 0
710 FOR N = 1 TO NUMNP
720 FOR J = 1 TO 3
730 IF ID(J, N) > 0 THEN GOTO 770
740 NEQ = NEQ + 1
750 ID(J, N) = NEQ
760 GOTO 780
770 ID(J, N) = 0
780 NEXT J
790 NEXT N
800 RETURN
810 .....
820 ' BANDED MATRIX ROUTINE .....
830 .....
832 L = 0
834 MBAND = 0
836 FOR N = 1 TO NUMEL
840 PRINT "ELEMENT NUMBER: "; N
844 INPUT " LOWEST NODE NUMBER = "; NOD(1, N)
848 INPUT " HIGHEST NODE NUMBER = "; NOD(2, N)
850 PRINT
852 I = NOD(1, N)
856 J = NOD(2, N)
860 KK(1) = ID(1, I)
```

```
862 KK(2) = ID(2, I)
866 KK(3) = ID(3, I)
968 KK(4) = ID(1, J)
870 KK(5) = ID(2, J)
874 KK(6) = ID(3, J)
876 FOR I = 1 TO 6
880 IF KK(I) <= 0 THEN GOTO 910
884 K = KK(I)
888 FOR J = 1 TO 6
892 IF KK(J) < K THEN GOTO 906
894 L = KK(J) - K + 1
900 IF MBAND < L THEN MBAND = L
906 NEXT J
910 NEXT I
912 NEXT N
1090 RETURN
1100 .....
1110 STRUCTURAL STIFFNESS MATRIX IN BANDED AND UNBANDED FORM:
1120 .....
1125 IF SKIP = 1 GOTO 1136
1130 DIM S(NEQ, MBAND), RE(6), R(NEQ2), P(NEQ2), RS(NEQ)
1135 DIM DEFLEC(NEQ2), STIF(NEQ2, NEQ2), R2(NEQ2)
1136 .....
1140 FOR N = 1 TO NUMEL
1150 GOSUB 260
1160 I = MOD(1, N)
1170 J = MOD(2, N)
1180 KK(1) = ID(1, I)
1190 KK(2) = ID(2, I)
1200 KK(3) = ID(3, I)
1210 KK(4) = ID(1, J)
1220 KK(5) = ID(2, J)
1230 KK(6) = ID(3, J)
1231 KK2(6) = 3 - MOD(2, N)
1232 KK2(3) = 3 - MOD(1, N)
1233 KK2(5) = KK2(6) - 1
1234 KK2(4) = KK2(6) - 2
1235 KK2(2) = KK2(3) - 1
1236 KK2(1) = KK2(3) - 2
1240 FOR I = 1 TO 6
1250 IF KK(I) <= 0 THEN GOTO 1303
1260 K = KK(I)
1270 R(K) = R(K) + RE(I)
1280 FOR J = 1 TO 6
1290 IF KK(J) < K THEN GOTO 1302
1300 L = KK(J) - K + 1
1301 S(K, L) = S(K, L) + SE(I, J)          *BANDED STIFFNESS MATRIX.
1302 NEXT J
1303 NEXT I
1305 FOR I = 1 TO 6
1308 K = KK2(I)
1310 R2(K) = R2(K) + RE(I)
1315 FOR J = 1 TO 6
1325 L2 = KK2(J)
1330 STIF(K, L2) = STIF(K, L2) + SE(I, J)    *UNBANDED STIFFNESS MATRIX.
1335 NEXT J
1338 NEXT I
1345 NEXT N
1350 RETURN
1360 .....
1370 PRINTS STIFFNESS MATRIX IN BANDED FORM
1380 .....
1390 IF ANSW6 = "N" OR ANSW5 = "N" GOTO 1480
1400 LPRINT
1410 LPRINT "          STIFFNESS MATRIX IN BANDED FORM"
1420 LPRINT
```

```
1430 FOR J = 1 TO NEQ
1440 FOR K = 1 TO MBAND
1450 LPRINT "          S("; J; ";"; K; ")="; S(J, K)
1460 NEXT K
1470 NEXT J
1480 .....
1490 EXTERNAL FORCES APPLIED
1500 .....
1505 LPRINT
1510 LPRINT "          EXTERNAL FORCES APPLIED TO THE STRUCTURE"
1520 FOR N = 1 TO NUMNP
1540 FOR J = 1 TO 3
1560 IF ID(J, N) = 0 GOTO 1610
1570 PRINT "NODE NUMBER": N
1580 IF J = 1 THEN INPUT "FORCE IN X-DIRECTION "; RS(ID(J, N))
1590 IF J = 2 THEN INPUT "FORCE IN Y-DIRECTION "; RS(ID(J, N))
1600 IF J = 3 THEN INPUT "MOMENT ABOUT THE Z-AXIS": RS(ID(J, N))
1610 NEXT J
1620 NEXT N
1625 LPRINT
1630 FOR I = 1 TO NEQ
1640 R(I) = RS(I)
1650 LPRINT "          R("; I; ")="; RS(I)
1660 NEXT I
1670 LPRINT
1680 RETURN
1690 .....
1700 GAUSS ELIMINATION SOLVER
1710 .....
1720 IF MBAND > 1 GOTO 1770
1730 FOR N = 1 TO NEQ
1740 R(N) = R(N) / S(N, 1)
1750 NEXT N
1760 RETURN
1770 ON IFLAG GOTO 1790, 1930
1780 REDUCTION OF COEFFICIENT MATRIX
1790 FOR N = 1 TO NEQ
1800 FOR L = 2 TO MBAND
1810 IF S(N, L) = 0 GOTO 1900
1820 I = N + L - 1
1830 C = S(N, L) / S(N, 1)
1840 J = 0
1850 FOR K = L TO MBAND
1860 J = J + 1
1870 S(I, J) = S(I, J) - C * S(N, K)
1880 NEXT K
1890 S(N, L) = C
1900 NEXT L
1910 NEXT N
1920 FORWARD REDUCTION OF VECTOR CONSTANT.
1930 FOR N = 1 TO NEQ
1940 FOR L = 2 TO MBAND
1950 IF S(N, L) = 0 GOTO 1980
1960 I = N + L - 1
1970 R(I) = R(I) - S(N, L) * R(N)
1980 NEXT L
1990 R(N) = R(N) / S(N, 1)
2000 NEXT N
2010 SOLVING UNKNOWNNS BY BACK SUBSTITUTION.
2020 FOR M = 2 TO NEQ
2030 N = NEQ + 1 - M
2040 FOR L = 2 TO MBAND
2050 IF S(N, L) = 0 GOTO 2080
2060 K = N + L - 1
2070 R(N) = R(N) - S(N, L) * R(K)
2080 NEXT L
```



```
2090 NEXT M
2100 RETURN
2110 .....
2120 DEFLECTION RESULTS
2130 .....
2135 LPRINT
2140 LPRINT "          DEFLECTION OF NODES"
2145 COUNT = 0
2150 FOR N = 1 TO NUMNP
2160 LPRINT
2170 LPRINT "          NODE NUMBER": N
2180 FOR J = 1 TO 3
2185 COUNT = COUNT + 1
2190 IF ID(J, N) = 0 GOTO 2240
2200 IF J = 1 THEN LPRINT "          X-DEFLECTION      = "; R(ID(J, N))
2201 IF J = 1 THEN DEFLEC(COUNT) = R(ID(J, N))
2210 IF J = 2 THEN LPRINT "          Y-DEFLECTION      = "; R(ID(J, N))
2211 IF J = 2 THEN DEFLEC(COUNT) = R(ID(J, N))
2220 IF J = 3 THEN LPRINT "          ANGULAR DEFLECTION = "; R(ID(J, N))
2221 IF J = 3 THEN DEFLEC(COUNT) = R(ID(J, N))
2230 GOTO 2264
2240 IF J = 1 THEN LPRINT "          X-DEFLECTION      = 0"
2241 IF J = 1 THEN DEFLEC(COUNT) = 0
2250 IF J = 2 THEN LPRINT "          Y-DEFLECTION      = 0"
2251 IF J = 2 THEN DEFLEC(COUNT) = 0
2260 IF J = 3 THEN LPRINT "          ANGULAR DEFLECTION = 0"
2261 IF J = 3 THEN DEFLEC(COUNT) = 0
2264 NEXT J
2274 NEXT N
2275 ..... RESULTANT FORCE VECTOR .....
2276 LPRINT
2277 LPRINT "          ..... RESULTANT FORCE VECTOR ....."
2278 PRINT
2279 PRINT "FORCES AND REACTIONS VECTOR FOR STRUCTURE:"
2281 FOR ROW = 1 TO NUMNP - 3
2282 SUM = 0
2283 FOR COL = 1 TO NUMNP - 3
2284 SUM = STIF(ROW, COL) * DEFLEC(COL) + SUM
2285 NEXT COL
2287 P(ROW) = SUM
2291 PRINT "P( "; ROW; ") = "; P(ROW)
2293 LPRINT "          P( "; ROW; ") = "; P(ROW)
2294 NEXT ROW
2295 INPUT "DO YOU WISH THE PROGRAM TO RUN ANOTHER EXTERNAL FORCE (Y/N)"; REPLY$
2300 IF REPLY$ = "Y" OR REPLY$ = "y" THEN GOSUB 1510: IFLAG = 2: GOSUB 1690: GOS
UB 2110
2330 END
```

APPENDIX B
ANSYS . INPUT

```
/TITLE,ISOPARAMETRIC 1 ELEMENT
KAN,0
/COM KIND OF ANALYSIS (STATIC)
ET,1,42,0,0,3
/COM ELEMENT TYPE:STIF 42. KEYOPT (3) = 3
R,1,1
/COM REAL CONSTANT 1 IS = 1" (THICKNESS)
EX,1,30E6
/COM MODULUS OF ELASTICITY OF STEEL
DENS,1,.00073
/COM MASS DENSITY OF MATERIAL
NUXY,1,.29
/COM POISSON RATIO
GXY,1,12E6
/COM TORSIONAL MODULUS
/COM ENTER FOUR NODES AND THEIR COORDINATES:
N,1,0,0
N,2,10,0
N,3,10,1
N,4,0,1
/COM GENERATE ELEMENT BY CCW ENTRY OF NODE NUMBERS
E,1,2,3,4
/COM SPECIFY FIXED DEGREES OF FREEDOM:
D,1,UX
D,1,UY
D,4,UX
D,4,UY
/COM ENTER FOR AT NODE 3 IN THE Y-DIRECTION:
F,3,FY,-50
/COM NUMBER NODES ON PLOT:
NNUM,1
/COM PLOT OF ELEMENTS:
EPLOT
/COM SHOW FORCE ON PLOT:
FBC,1
/COM SHOW COORDINATE SYSTEM ON NODE PLOT:
CSPLT,1
NPLOT,1
/COM WRITE ANALYSIS FILE:
SFWRIT
/COM TERMINATE PREPROCESSING ACTIVITY:
FINISH
```

/TITLE.COUNTER SHAFT VIBRATION

KAN.2

ET.1.3

KAY.2.1

EX.1.3GE6

DENS.1..00073

R.1.12.56,12.56.4

R.2.100,1000.40

R.3.100,1000.30

N.1.0.0

N.2.8.0

N.3.18.0

N.4.23.0

N.5.38.0

N.6.46.0

REAL.1

E.1.2

E.3.4

E.5.6

REAL.2

E.2.3

REAL.3

E.4.5

M.2.UY.5

D.1.UY

D.1.UX

D.6.UY

D.6.UX

ACEL..1

SVTYP.3

FREQ..1.10

SV...44...44

SEWRIT

FINISH

LECTURE 5

METAL FAILURES IN TRANSMISSIONS

ABSTRACT :

Failures in transmissions may occur in shafts, bearings or gears. Analysis for stress and deflection is used to size parts to prevent failures and to determine the root cause of failures which have occurred.

1. INTRODUCTION:

The transmission designer must postulate the potential scenarios by which the system may fail and apply analysis to size the components properly. The analysis is based on physical properties of materials, the nature of the loading and environment and stress-strain relationships. This paper reviews these concepts. The gear design standards are based on these fundamental ideas.

2. FAILURES TYPES AND CHARACTERISTICS:

Component failures of transmissions may produce failure of the system. Different types of gear failures are illustrated in the American Gear Manufacturers Association publication AGMA-110.03 and Shipley's "Gear Failures", (1 and 6)¹.

- a. Wear of tooth contact surfaces
- b. Pitting of teeth at pitch line
- c. Breaking of teeth under static load
- d. Breaking of teeth under repeated load
- e. Scoring of teeth
- f. Involute interference of teeth
- g. Bearing failures
- h. Shaft fatigue
- i. Fretting of shaft in hub
- j. Excessive deflection
- k. Abrasive wear
- l. Low cycle crack propagation

¹Numbers in parentheses designate references.

Material tests show characteristics of different types of failures:

2.1 A uniaxial tensile test of a ductile bar produced the failure of Figure 2.1. The necking down of the test specimen in the area of failure is typical ductile behavior. The ductile material failed in shear as indicated by the 45° failure line. Mohr's circle for the uniaxial test specimen is given in Figure 2.2 and shows the maximum shear to be at an angle of $2\theta = 90^\circ$ from the principal axis, which is $\theta = 45^\circ$ on the part.

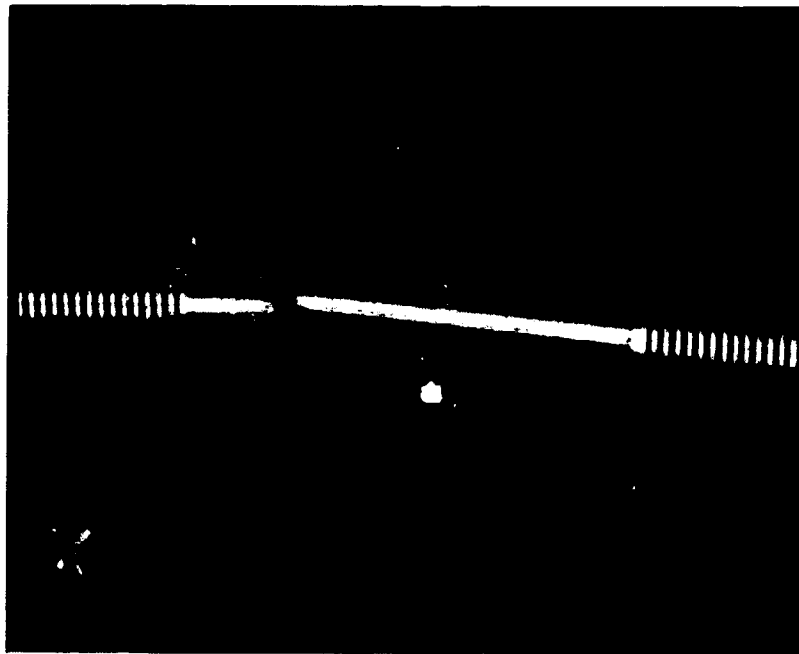


Figure 2.1 Aluminium Tensile Test Specimen Failure

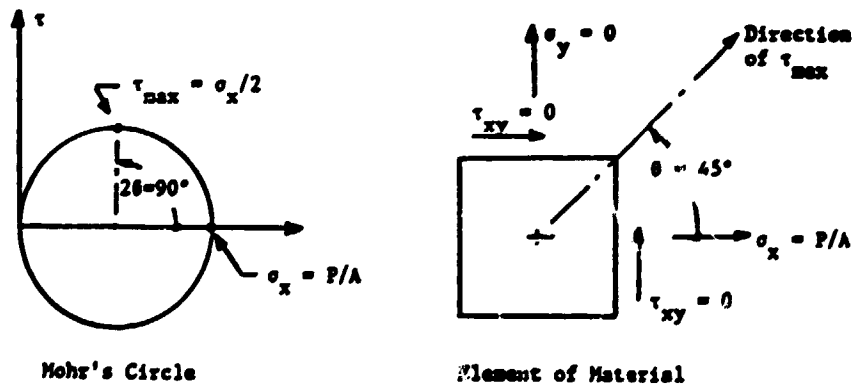


Figure 2.2 Element of Material From Surface of Tensile Test Bar with Stress Calculations

2.2 A torsion test of a brittle rod produced the failure of Figure 2.3. No necking due to yielding is apparent. The brittle material failed in tension as indicated by the 45° failure lines. Mohr's circle for this torsion test is shown in Figure 2.4 and indicates that the maximum normal stress occurs at $2\theta = 90^\circ$ from the principal axis.

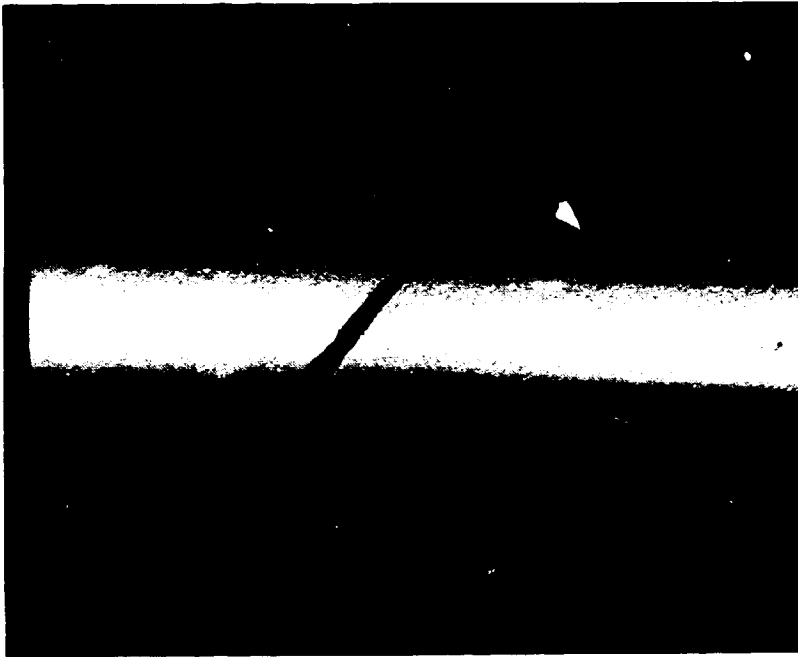


Figure 2.3 Brittle Rod Torsion Test Failure

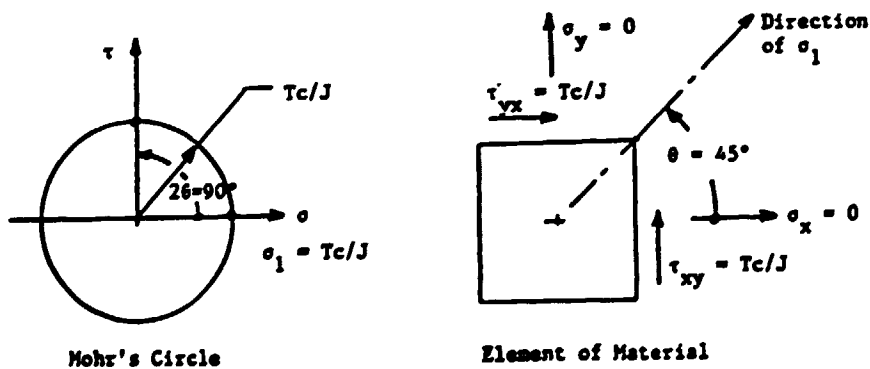


Figure 2.4 Element of Material From Surface of Brittle Chalk Torsion Test with Stress Calculations

2.3 A fatigue failure (1) is shown in Figure 2.5. The beach marks, which appear like the ridges of sand on the ocean beach, indicate the progression of the crack as it moved from the crack initiation site and across the material as the variable stress cycles were applied.

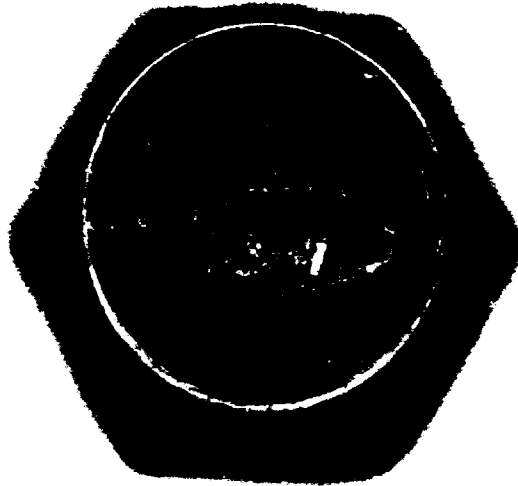


Figure 2.5 Fatigue Failure

2.4 Steady state overload is shown by the case hardened gear tooth failure of Figure 2.6. The granular nature of the entire failure area does not indicate any of the stress variations, which smooth the crack area, as shown in the fatigue failure.



Figure 2.6 Steady State Overload Failure of Gear Tooth

2.5 Direct shear under steady state loading of a shear pin is shown in Figure 2.7. The texture of the entire cross section is the same.

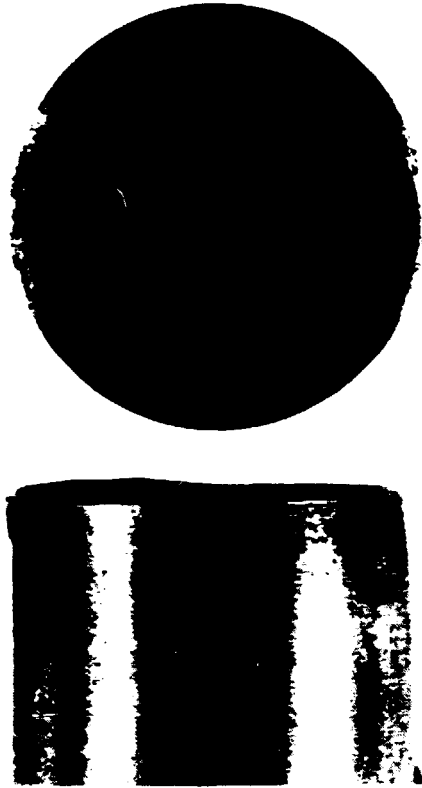


Figure 2.7 Shear Pin Failure

2.6 Fretting (2) is a failure mode which may occur in a shaft which is press fitted into a hub. The fretting is caused by relative motion between the rotating shaft as it bends and rubs against the more rigid hub. A brown powder from the oxidized wear products may appear between these rubbing surfaces. The fretting action of one surface rubbing on the other may develop small cracks which may propagate through the part as a fatigue failure.

2.7 Pitting failure (1) of a gear tooth may occur due to the compressive contact force. Hertz's equations give the surface compressive stress and the distribution of shear stress below the surface for contacting arcs such as gear teeth and roller bearings. The pitting crack may be initiated below the surface by a shear stress. The crack subsequently grows upward to the surface to free the particle of metal and create the pit. Pressures of the lubricant, which is trapped in the crack may assist this action. (Non-destructive pitting may occur due to poor contact between teeth to redistribute the loading evenly across the tooth

face. This nondestructive pitting does not produce failure of the tooth as in severe pitting and may be acceptable for some applications.)

2.8 Abrasive wear (6) of gear teeth may be produced by hard foreign particles in the lubricant. Grooves appear on the tooth surface as the hard particles slide over the teeth.

2.9 Involute interference may be produced by the tip of one tooth digging into the flank of the mating tooth. This is due to incorrect geometry such as too few teeth in the pinion. (3)

2.10 Impact loading (2) is due to the application of loads at a rate which is less than the longest natural period of the structure. The impact load may produce stresses which are several times higher than this same load would produce if applied during a time equal to or greater than three times the longest natural frequency.

2.11 Initial cracks in a component may propagate through the part to produce a failure by fracture. The initial cracks may be due to grinding or welding. This type of fracture progresses because of the high stress at the crack tip.

3. FAILURE PREDICTION:

The relationships between failures of materials, the loading on the material, and the properties of the material are used by the designer to size new components. This section reviews some of these relationships.

An abnormal load may produce a general yielding type of failure in a ductile material. The large deformations due to yielding may serve as a warning to the operator. The ductile material may allow enough stress redistribution at the tip of a crack to inhibit its growth. However, if the load is applied rapidly, time may not allow yielding. The impact resistance of materials also decreases when hardness increases as indicated by the fracture toughness and Charpy values.

3.1 For ductile materials, such as unhardened steel, failure under static loads has a good correlation with the distortion energy and the octahedral shearing stress theories (5). The octahedral shearing stress is

$$\tau_{oct} = (\sigma_{xx} + \sigma_{yy} + \sigma_{zz})/3.$$

For a uniaxial tensile test specimen with cross-sectional area, A , and load, P , the octahedral shearing stress at failure is

$$\tau_{oct}' = (P/A + 0 + 0)/3 = S_y/3$$

where,

$$\sigma_{xx}' = P/A = S_y = \text{yield stress}$$

$$\sigma_{yy}' = 0$$

$$\sigma_{zz}' = 0.$$

Hence, the factor of safety, FS , is

$$FS = \tau_{oct}'/\tau_{oct} = S_y/(\sigma_{xx} + \sigma_{yy} + \sigma_{zz})$$

3.2 For high cycle fatigue (4), both brittle and ductile materials fail by fracture instead of by general yielding at stresses well below the yield stress. The fatigue failure is initiated by a small crack and as the stress cycles continue, the crack elongates and forms the beach marks on the fracture surface.

The endurance limit, S_e , for steel is the maximum value of alternating stress which may be applied without producing a fatigue failure. The endurance limit, S_e' , for an actual component may be evaluated from the endurance limit, S_e , obtained from a reversed bending test of a standard test bar. To obtain S_e' , multiply S_e by factors which compensate for the differences between the actual component and the standard test bar.

$$S_e' = S_e k_a k_b k_c k_d k_e k_f$$

where,

k_a is the surface finish factor

k_b is the size factor

k_c is the reliability factor

k_d is the temperature factor

k_e is the modifying factor for stress concentration

k_f is the modifying factor for other effects (e.g., non reversed bending)

The material properties for fatigue may be represented by the Modified Goodman line, which lies at the bottom of the fatigue data scatter on a plot of alternating versus mean stress. For combined stress states, the distortion energy theory may be applied to obtain representative values for alternating, σ_a' , and mean, σ_m' , stress components, which establish a state of stress by the load line whose slope is σ_a' over σ_m' per Figure 3.1.

$$\sigma_a' = [\sigma_{xa}^2 - \sigma_{xa}\sigma_{ya} + \sigma_{ya}^2 + 3\tau_{xya}^2]^{.5}$$

$$\sigma_m' = [\sigma_{xm}^2 - \sigma_{xm}\sigma_{ym} + \sigma_{ym}^2 + 3\tau_{xym}^2]^{.5}$$

The factor of safety is evaluated using the allowable value of alternating stress, S_a .

$$FS = S_a / \sigma_a'$$

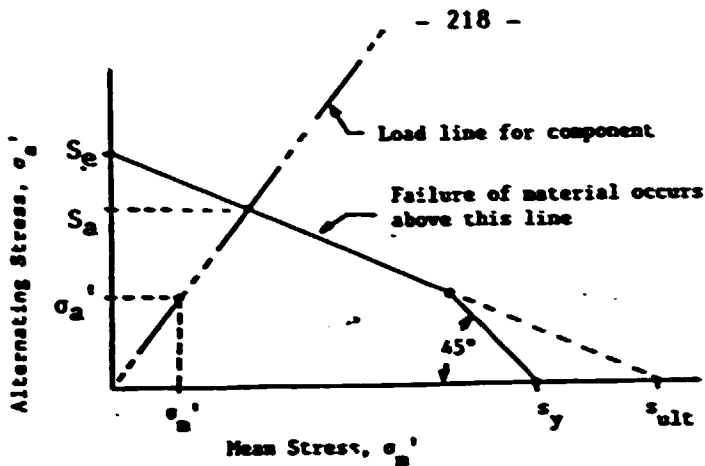


Figure 3.1 Modified Goodman Diagram

3.3 For contacting surfaces, which transmit forces, the compressive stress at the area of contact and the shear stresses below the contact surface are based on Hertz's equations (5). The contact area is formed by the elastic deformation of the two bodies. The analysis may be applied to two elliptical bodies, with each body having two different radii of curvature at the contact point like crowned gear teeth or per Figure 3.2. The theory may be simplified if the two contacting bodies are cylindrical (4). In this latter case, the area of contact has a half width b .

$$b = \{2P \left[\frac{(1-\nu_1^2)/E_1}{\pi l} + \frac{(1-\nu_2^2)/E_2}{\pi l} \right] \left(\frac{1}{d_{1c}} + \frac{1}{d_{2c}} \right) \}^{.5}$$

where,

P is the normal force between the two bodies

ν_1 and ν_2 are Poisson's ratios for cylinder 1 and cylinder 2

E_1 and E_2 are the compressive moduli of elasticity for cylinder 1 and cylinder 2

d_{1c} and d_{2c} are the diameters of cylinder 1 and cylinder 2

l is the length of the contact area

π is 3.14159

The maximum pressure value, which is the compressive stress, over the width $2b$ is

$$p = -2P/(\pi bl).$$

The maximum shear stress occurs below the contact surface a distance, z .

$$z = .7861 \times b$$

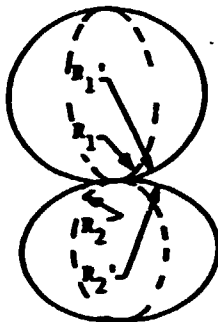


Figure 3.2 Contacting Elliptical Shaped Bodies

The rolling action of uncrowned gear teeth is like two cylinders with diameters defined by the tooth surfaces at the point of contact (7). The radius of the contacting cylinder, ρ , is defined by the involute function as illustrated in Figure 4. At the pitch circle, the value of ρ is

$$\rho = d_{1c}/2 = (d/2) \sin \phi$$

where,

d is the pitch diameter of pinion

ϕ is the involute angle

At any other diameter, d_1 , the radius is

$$\rho = (d_1/2) \sin \phi_1$$

The diameter of the larger contacting cylinder, which represents the gear tooth surface, is

$$d_{2c} = d_G \sin \phi = m_G d \sin \phi$$

where,

d_G is the pitch diameter of gear

m_G is the ratio of gear teeth divided by pinion teeth,

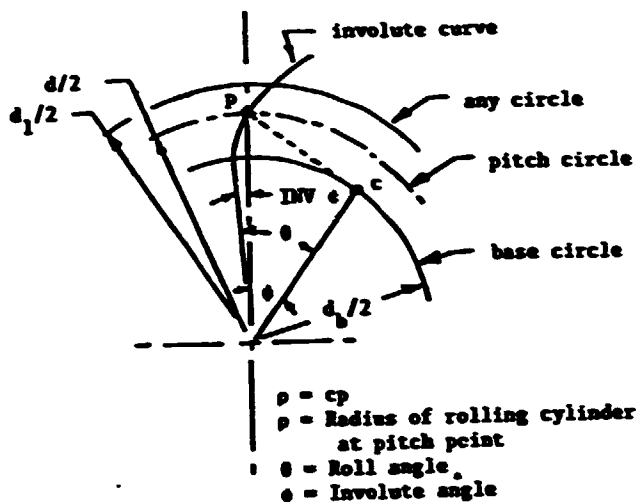


Figure 3.3 Diameter of Rolling Cylinders Representing Involute Tooth Contact

For helical gears, the radii of the contacting cylinders is in the section normal to the pitch helix. This section has a pitch ellipse instead of a pitch circle like the spur gear pair (7). Using the equation of an ellipse, the diameters of contacting cylinders are

$$d_{1c} = d \sin \phi_n / \cos^2 \psi$$

$$d_{2c} = m_G d_{1c}$$

where,

ψ is the helix angle

The compressive stress, σ_c , of external helical gear and pinion teeth is obtained by substitution of the latter two equations into the equation for p . The average length, l , of teeth sharing the load is a function of face width, F , and contact ratio.

$$l = F \times (\text{Contact Ratio}) / \cos \psi$$

The force normal to the tooth is

$$P = W_t / (\cos \psi \cos \phi_n)$$

where,

W_t is the tangential load in the transverse plane

ϕ_n is the normal pressure angle.

$$\sigma_c = p = \left\{ \frac{2P [d_{2c} + d_{1c}]/[d_{1c}d_{2c}]}{\pi d [(1-\nu_1^2)/E_1 + (1-\nu_2^2)/E_2]} \right\}^{.5}$$

$$\sigma_c = \left\{ \frac{2W_t}{\pi F[\text{Contact Ratio}]d} \frac{\cos^2\psi}{\sin\phi_n \cos\phi_n} \frac{[M_G + 1]}{M_G} \frac{1}{(1-\nu^2)(1/E_1 + 1/E_2)} \right\}^{.5}$$

Define an elastic constant (8), C_p , as

$$C_p = \left\{ 1/[\pi(1-\nu^2)(1/E_1 + 1/E_2)] \right\}^{.5}$$

Define a curvature factor (8), C_c , as

$$C_c = (\sin\phi_n \cos\phi_n / \cos^2\psi) [M_g / (M_g + 1)]^{.5}$$

Hence, the equation for compressive stress at the pitch line is

$$\sigma_c = C_p \left\{ \frac{W_t}{F d C_c [\text{Contact Ratio}]} \right\}^{.5}$$

3.4 Components which contain cracks may be analyzed by fracture mechanics principles to determine if the crack will propagate or remain dormant. For example, a weld area may contain cracks. An inspection of the weld may identify all cracks in excess of a threshold length, which is below the detection capability of the instrument. Hence, the analyst may postulate that cracks as long as the threshold length still exist in the component. For a Mode I crack, the "stress intensity factor", K_I , is (5)

$$K_I = \sigma (\pi a)^{.5} f(\lambda)$$

where,

σ = stress normal to crack

a = crack length or half length

$f(\lambda)$ = a function of crack and component sizes

A critical value of the stress intensity factor is defined as the "Fracture Toughness", K_{IC} . The values of K_{IC} are highly dependent on temperature. Similar steels may have significantly different values of K_{IC} at 30°F. When K_I exceeds K_{IC} , the crack will continue to grow even though the load is constant.

3.5 Breaking of gear teeth is normally associated with the bending loading of the tooth. Lewis proposed that a gear tooth could be modeled as a parabola, which is inscribed in the tooth, shaped beam with the apex located at the intersection of the tooth load and the centerline of the tooth. This beam would have a constant bending stress since the thickness, t , of the beam would vary as the square of the distance, l , from the apex. The location of the point of tangency of the parabola with the tooth surface identifies the position, a , of maximum bending stress, S_t . The load is shown in Figure 3.4. The bending stress for a rectangular cross section is:

$$S_t = Mc/I = W_t l^3 / (F t^2)$$

The distance x and the 90° inscribed triangle may be used to identify the location of the maximum bending stress, "a". By similar triangles,

$$\tan \alpha = \tan \alpha$$

$$(t/2)/x = l/(t/2)$$

so,

$$t^2 = 4lx$$

Hence, the thickness can be eliminated from the stress equation.

$$S_t = W_t l^3 / (4xF)$$

Divide the numerator and denominator by the circular pitch, p , and define y , which depends on the point of load application, as follows:

$$y = 2x/3p$$

Hence,

$$S_t = W_t 3p / (2x F p) = W_t / (F p y)$$

Define a tooth form factor, Y ,

$$y = Y/\pi$$

and substitute the diametral pitch, P_d , into the equation.

$$p = \pi/P_d$$

$$S_t = W_t P_d / (F Y).$$

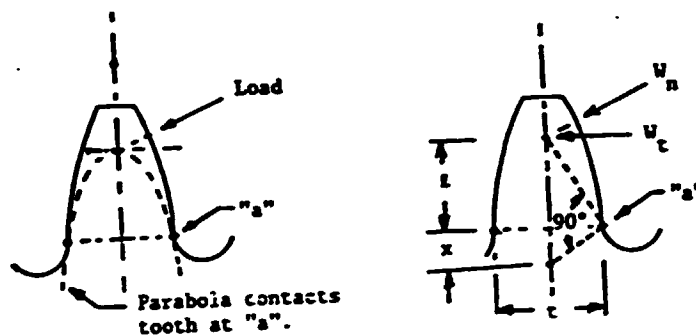


Figure 3.4 Tooth With Lewis Parabola Inscribed

The stress field at the root of the tooth will be amplified due to the changing cross section and fillet radii. The fatigue strength of the tooth may be adversely affected by the surface finish, tooth size, etc. Hence, for fatigue analysis, the value of S_t should be modified by a stress concentration factor, K_f .

The load sharing capability due to the contact ratio allows more than one tooth to share the load. Hence, the value of S_t should be modified due to the contact ratio.

These factors result in the following relationship for bending stress.

$$S_t = W_t P_d K_f / [\text{Contact Ratio}(F Y)]$$

4. Conclusions:

The design and manufacture of gears represents an advanced combination of art and science. The fundamental equations for compressive stress and bending stress of gear teeth as presented in this paper provide the basis for the AGMA 218.01 Standard (8); however, modifying factors (9) are added in the Standard to adapt these equations to the real world environment.

REFERENCE LIST

1. A.G.M.A., American Standard Nomenclature of Gear-Tooth Wear and Failure, AGMA 110.03 published by American Gear Manufacturers Association, Alexandria, VA, 1964.
2. Collins, J. A., Failure of Materials in Mechanical Design, Analysis, Prediction, Prevention, John Wiley & Sons, 1981.
3. Mabie, H. M. and Reinholtz, C. F., Mechanisms and Dynamics of Machinery, John Wiley, 1987.
4. Shigley, J. E. and Mitchell, L. D., Mechanical Engineering Design, McGraw Hill Book Co., 1983.
5. Boresi, A. P. and Sidebottom, O. M., Advanced Mechanics of Materials, John Wiley & Sons, 1985.
6. Shipley, E. E., Gear Failures, Reprint from Machine Design December 7, 1967, The Penton Publishing Co., Cleveland, OH.
7. Dudley, D. W., Practical Gear Design, McGraw Hill Book Co., Inc., 1954.
8. A.G.M.A., AGMA Standard for Rating the Pitting Resistance and Bending Strength of Spur and Helical Involute Gear Teeth, AGMA Standard 218.01, Dec. 1982, published by American Gear Manufacturers Association, Alexandria, VA.
9. Dudley, D. W., Handbook of Practical Gear Design, McGraw Hill Book Co., Inc., 1984.

A REVIEW OF AGMA 218.01, AGMA STANDARD FOR RATING THE PITTING RESISTANCE
AND BENDING STRENGTH OF SPUR AND HELICAL INVOLUTE GEAR TEETH

ABSTRACT:

The AGMA 218.01 Standard for rating the pitting and bending strength of spur and helical gears is reviewed in this paper.

1. INTRODUCTION:

The American Gear Manufacturer's Standard, AGMA 218.01, for Rating the Pitting Resistance and Bending Strength of Spur and Helical Involute Gear Teeth was introduced by the AGMA Committee for Gear Rating in 1982. "The purpose of this Standard is to establish a common base for rating various types of gears for different applications and to encourage the maximum practical degree of uniformity and consistency between rating practices within the gear industry. It provides the basis from which more detailed "AGMA Application Standards" are developed and provides a basis for calculating approximate ratings in the absence of such standards." (1)¹

The Standard includes those factors which influence the life and operation of the gear set. This standard is based on fundamental principles: Hertz's equation for compression and Lewis's equation for bending. When these equations are developed for members shaped like gear teeth, they take the following form per reference (2).

$$\text{Eq. 1 Compressive Stress: } S_c = c_p \left\{ \frac{W_t}{F_d C_c [\text{Contact Ratio}]} \right\}^{.5}$$

$$\text{Eq. 2 Bending Stress: } S_t = \frac{W_t P_d K_f}{[\text{Contact Ratio (F Y)}]}$$

The difficulties in adapting the Lewis equation to gear tooth stress are reviewed by Wellauer (3) and include:

¹Numbers in parentheses identify references.

1. The distribution of load across the face width and over the tooth profile, which vary with accuracy, tolerances, wear and deflection.
2. Stress concentration at root.
3. Size effect on fatigue life.
4. The variation in load position on the tooth as the gear rotates.
5. The compressive stress due to the radial component of load.

The modification of the Lewis equation to the gear environment is discussed by Dudley (3). He comments on four modifying factors:

K_o , the overload factor, which accounts for the roughness of the driving and driven apparatus.

K_s , the size factor, which reflects the experimental results showing lower endurance limits in components with larger cross sectional areas.

K_m , the load distribution factor, which depends on misalignment of axes of rotation, alignment errors due to tooth inaccuracies, and elastic deflections of shafts and bearings under load.

K_v , the dynamic factor, which is determined by the pitch line velocity, mass-elastic characteristics of teeth and gears, and accuracy of teeth.

The comments of Wellauer and Dudley were made for a standard which preceded AGMA 218.01, but most of these comments do apply to AGMA 218.01. The bending strength equation in AGMA 218.01 is:

$$\text{Eq. 3} \quad S_t = \frac{W_t K_a P_d K_s K_m}{K_v F J}$$

where,

S_t is the bending stress number

K_a is the application factor for bending strength

K_s is the size factor for bending strength

K_m is the load distribution factor for bending strength

K_v is the dynamic factor for bending strength

J is the geometry factor for bending strength

P_d is the diametral pitch, nominal, in the plane of rotation

$$P_d = P_{nd} \cos \psi_s$$

P_{nd} is the normal diametral pitch

ψ_s is the helix angle at standard pitch diameter.

The geometry factor, J , (1) is defined by the equation:

$$J = Y C_\psi / (K_f m_N)$$

where,

Y is the tooth form factor

K_f is the stress concentration factor

m_N is the load sharing ratio, which depends on the transverse

contact ratio m_p , and the face contact ratio m_F .

For Normal Helical Gears with $m_F > 1.0$:

$$m_N = F / L_{\min}$$

where,

L_{\min} is the minimum value of the total length of lines of

contact in the contact zone.

For most helical gears with $m_F \geq 2.0$ a conservative approximation

for m_N is:

$$m_N = P_N / (.95 Z)$$

where,

$$P_N = \text{Normal base pitch} = (\pi \cos \phi_c) / P_{nd}$$

ϕ_c = The normal profile angle of the equivalent standard rack cutter.

$$P_{nd} = \text{Normal diametral pitch}$$

Z = Length of line of action in transverse plane.

The profile contact ratio, m_p , (4) is

$$m_p = Z N_p / (\pi d \cos \phi_t)$$

where,

d = Operating pitch diameter of pinion

N_p = Number of teeth on pinion

ϕ_t = Operating transverse pressure angle

C_ψ is the helical factor and is unity for spur gears and helical gears with $m_F > 1.0$.

The geometry factor may be substituted into equation 2, if the helical factor is added, to obtain:

$$\text{Eq. 4} \quad S_t = W_t \frac{P_d}{F} \frac{1}{J}$$

This equation may be modified to reflect total load. The load W_t is the mean value of the tangential load and is evaluated from the maximum horsepower rating. However, the total load includes a dynamic component due to internally generated tooth loads, which are induced by non-conjugate meshing action of the teeth. This dynamic component is represented by the dynamic factor K_v . Also, the total load contains a variable component due to externally applied loads which are in excess of W_t (1). The application factor, K_a , makes allowance for any externally applied loads.

The equation may be modified to show the non-uniform distribution of load along the lines of contact due to cutting accuracy, alignment, elastic deflection, clearances, thermal expansion, crowning, and centrifugal deflections by the load distribution factor K_m .

The equation may be modified for the size of the tooth by the size factor, K_s .

Apply these four factors to Equation 4 to obtain Equation 3 for the bending stress number, S_t .

The allowable magnitude for this bending stress number is determined by material properties and the desired life as defined by the following equation:

$$S_t \leq S_{at} K_L / (K_t K_R)$$

where,

S_{at} = allowable bending stress number which is based on the statistical probability of one percent failures occurring after 10^7 cycles.

K_L = life factor for bending strength, which depends on the number of cycles required.

K_T = temperature factor for bending strength

K_R = reliability factor for bending strength, which accounts for the normal statistical distribution of failures found in materials tested in a laboratory when evaluating S_{at} . (For 1 failure per 100, after 10^7 cycles, $K_R = 1$.)

As experience is gained and as analytical methods are advanced, the values used for the factors like K_a , K_m , K_s , and K_v will improve. This will reduce the need for large values for factors of safety, because the unknowns will be reduced. This is a major area for future research.

The application factor K_a makes allowances for all externally applied loads in excess of the nominal tangential load W_t . The prime mover and the driven load are the major contributors to the variations in the externally applied loads. System vibration, acceleration torques, overspeeds, variation in system operation, and changes in process load conditions are sources of external loads.

The values of the life factors K_L and C_L for various materials could benefit from more test results. The wear of the gear teeth due to compressive stress presents a fatigue condition similar to that of roller bearings.

The factor of safety is not explicitly mentioned in AGMA 218.01. The implicit statement that

$$(S_t) \leq S_{at} K_L / (K_T K_R)$$

allows the designer to select a factor of safety.

Service factors, K_{SF} , have been used which included the application factor, K_a , and which sometimes included the reliability factor and life factor. If only K_a is included, the value of K_{SF} may be taken as K_a . However, if K_R and K_L are also included in K_{SF} , then the following relationship should be used:

$$K_{SF} = K_a K_R / K_L .$$

These comments have been primarily limited to the bending strength, however, a similar rationale would lead from Equation 1 to the AGMA 218.01 equation for the compressive stress number, S_c .

The AGMA 218.01 Standard is a general standard which provides the basis from which more detailed "AGMA Application Standards" may be developed. These "AGMA Application Standards" may provide appropriate values for Service Factors, K_{SF} and C_{SF} .

The AGMA 218.01 Standard is providing a good design guide, which improves product uniformity and helps the gear industry in the U.S.A. achieve a standard method for evaluating different gear designs.

The art and science of gearing is a legacy which modern man enjoys. I express appreciation to all of those who have contributed to this knowledge. Figure 1 is a sketch of an early contribution from China (5).

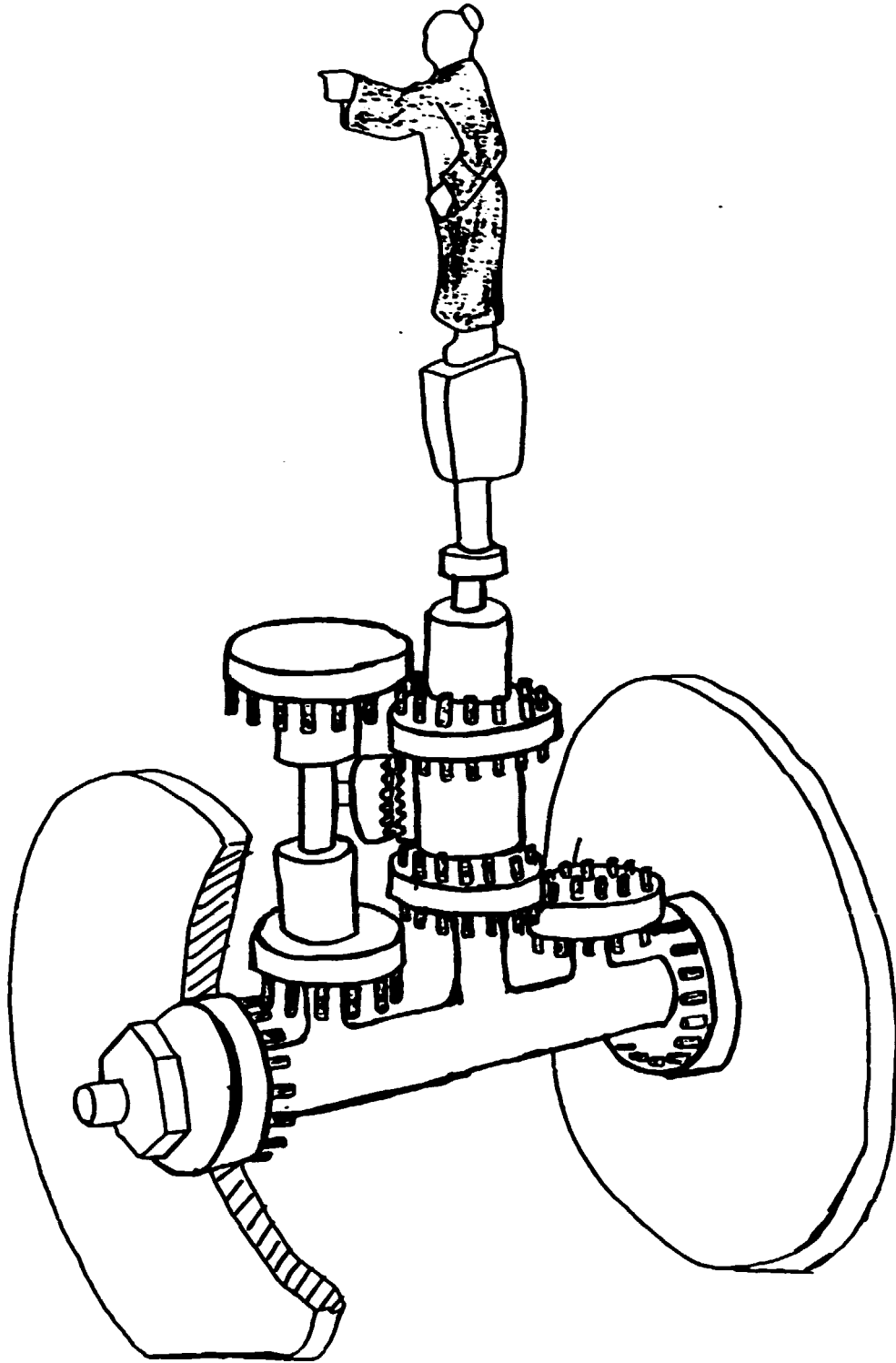


Figure 1. Sketch of South Pointing Chariot with Pin Gearing of Chinese Origin, circa 2600 B.C., displayed by Smithsonian Institution, Washington, D.C. and Referred to by Dudley in his Comments on the History of Gearing (5).

REFERENCE LIST

1. A.G.M.A., AGMA Standard for Rating the Pitting Resistance and Bending Strength of Spur and Helical Involute Gear Teeth, AGMA 218.01, published by American Gear Manufacturers Association, Alexandria, VA, 1982.
2. Jones, E. W., Metal Failures in Transmissions, Zhengzhou Research Institute of Mechanical Engineering, Zhengzhou, China, 1988.
3. Wellauer, E. J., Coordinated Rating for the Strength of Gear Teeth, AGMA 229.03, June, 1956, published by American Gear Manufacturers Association, Alexandria, VA, 1956.
4. Dudley, D., Practical Gear Design, McGraw Hill Book Co., Inc., 1954.
5. Dudley, D. W., The Evolution of the Gear Art, published by American Gear Manufacturers Association, Alexandria, VA, 1969.

LECTURE 7

GEAR CAD

ABSTRACT:

The use of computers for the design and manufacture of gears has been a fruitful endeavor. This paper gives brief examples of some computer aided design software for gears.

INTRODUCTION:

The application of the computer to the tasks of engineering, drawing and manufacturing gears has been rewarding.

Computer aided drafting provides the capability to see different views quickly, to enlarge or reduce sections easily, to reproduce similar designs using the old database and to check for interferences. The countershaft of a dredge pump gear, which was drawn by AutoCAD, is shown in Figure 1.1. The economic impact of computer aided drafting is

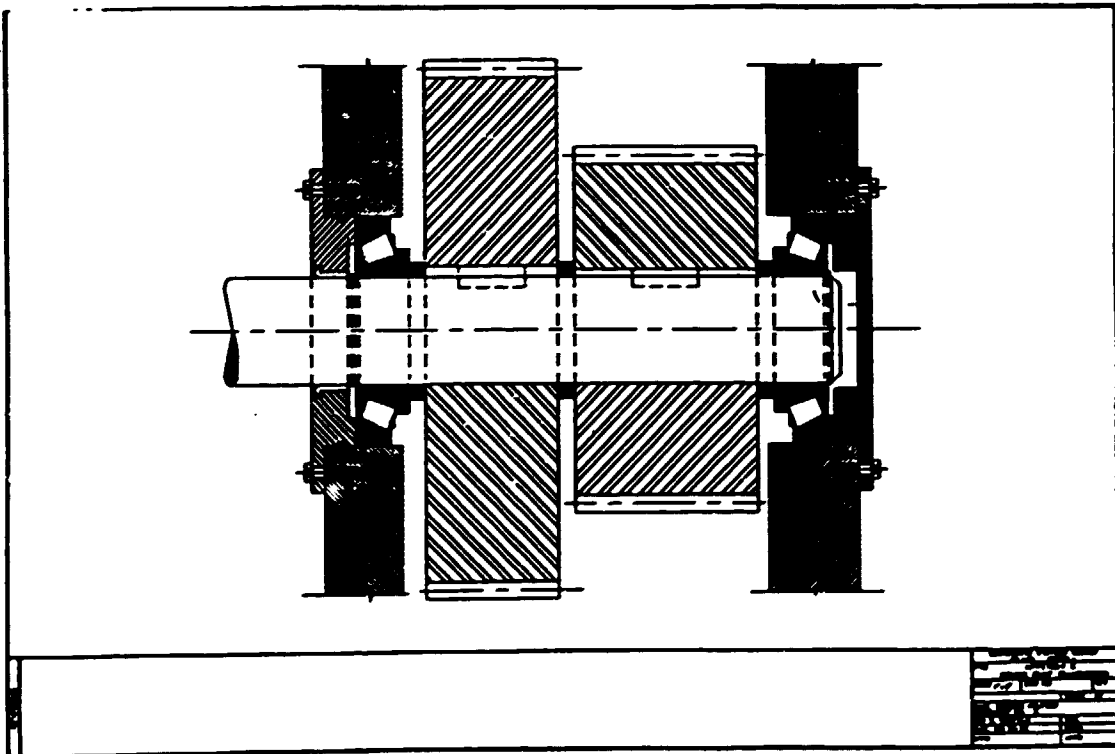


Figure 1.1 Gears for Dredge Pump

probably not significant in terms of the reduced number of draftsmen required, because of the added cost of equipment, maintenance, software, and machine operators. However, the economy of the total engineering and manufacturing activities may be greatly improved due to better quality control and the reduction of time.

The availability of computers for the engineering design function has resulted in many design software packages. The finite element software allows the engineer to analyze the stresses and deflections of parts having complex geometry. Programs which design gear sets are common. This software often uses data from the cutting hobs as input values. Other programs may be used in manufacturing to select change gears or cutting tools.

An example of commercial software for gear design, GEARTECH Software, Inc. offers three basic packages:

AGMA218

SCORING+

GEARCALC.

Appendix A gives some features of these packages. You may use a demonstration package for this software while you are here at the Zhengzhou Research Institute. If you desire copies of this demonstration disk or if you wish to purchase the actual software, contact

GEARTECH Software, Inc.

1017 Pomona Ave.

Albany, CA 94706

U. S. A.

A second example is software by Universal Technical Systems, Inc. The options of their gear design program #500 are given in appendix B. UTS also developed the mathematical modeling software, TK Solver/plus, which solves equations. You may use a demonstration package for TK Solver while you are here at the Zhengzhou Research Institute. We are prohibited from copying this software. If you desire copies of TK Solver/plus or the Gear Program #500, contact

Universal Technical Systems, Inc.

1220 Rock Street

Rockford, IL 61101

U. S. A.

APPENDIX A

GEARCALC

GEARCALC replaces the outmoded cut and try method of gear design which requires infinite patience and frequently results in less than optimum gear designs. GEARCALC uses an efficient closed-form algorithm to solve the surface durability and bending strength criteria simultaneously. This means that GEARCALC is fast, saving your valuable time while helping you to explore the possibilities for optimum gear design.

GEARCALC was designed to be the friendliest, most powerful gear design program you can buy. Within minutes of entering pressure angle, helix angle and gear ratio along with material/heat-treatment data, load data and required life, you have designed a maximum capacity gearset that has minimum volume and weight. You may choose to balance pitting and bending fatigue lives or assign extra capacity to either criteria. Change any one or two of the variables: pinion diameter, face width or diametral pitch, and GEARCALC instantly recalculates the gearset geometry to maintain the life balance.

With GEARCALC, you can design the addendum modifications to maximize pitting and wear resistance, scoring resistance or bending strength.

GEARCALC is integrated with programs AGMA218 and SCORING+ and automatically transfers common data including all the gear/tool geometry required by these programs.

GEARCALC features include:

- Material strengths based on latest values given in AGMA 218.01 Standard
- Balanced pitting and bending fatigue lives
- Addendum modification optimized for maximum: pitting and wear resistance, scoring resistance or bending strength
- Tooth combinations selected to achieve user specified tolerance on gear ratio
- Tooth combinations selected to achieve hunting or non-hunting ratios
- User controls face width/pinion diameter (F/d) ratio
- User controls operating pressure angle
- User controls operating center distance
- Calculates full gear/tool geometry required by AGMA218 and SCORING+ programs
- Output includes screen, hard-copy or disk reports

Minimum Hardware Requirements

IBM PC/XT, AT or compatible computer with 256K RAM, 1 double sided diskette drive, monochrome or CGA* card, printer and PC/MS-DOS 2.0 or higher operating system.

Optional:

- 2 floppy disks or hard disk
- 8047 math coprocessor
- Enhanced graphics
- IBM graphics printer (or equivalent, for SCORING+ hard copy graphics) such as: Epson FX series, Okidata 92, 93, 192, 193

*NOTE: CGA or EGA or equivalent required for SCORING+ graphics.
IBM is a registered trademark of International Business Machines.

If you have any questions, please call us at

(415) 524-0668

and talk to our gear experts and computer programming specialists. We are here to help.

FREE! demo diskettes can be obtained by contacting:

GEARTECH
Software, Inc.

1017 POMONA AVENUE
ALBANY, CALIFORNIA 94706

(415) 524-0668

GEARTECH

Software, Inc.

PRODUCT CATALOG

AGMA218 SCORING+ GEARCALC

GEARTECH Software, Inc. offers an integrated system of gear design/analysis programs.

GSI specializes in high-quality, user-friendly software for gear engineers. All programs are designed to work independently or together as an integrated system. You move from one module to the next with a single keystroke — without losing any common data.

The system provides an on-line database that gives you fast access to your previously analyzed gearsets. This provides you with automatic documentation of your gear designs and allows you to return to work-in-progress without having to re-key input data — just a few keystrokes retrieves your record from disk. If a new job is similar to an old one, you can retrieve the old record, alter a few values to create the new record, and be ready to run in seconds.

The interactive, menu-driven command structure features full screen editing that permits you to enter or modify data quickly and efficiently. All input data is automatically checked to ensure that it has the proper numeric format and is within the range of reasonable values. Format and out-of-range errors are highlighted and error messages are displayed to help you correct the errant data. Built-in geometry audit routines prevent costly errors by catching design errors (interference, excessive undercut and many more).

All programs are capable of analyzing spur and helical, external and internal gearsets with either standard or non-standard geometry. Algorithms are optimized for fast program execution to help you perform accurate, sophisticated analyses in a fraction of the time required using manual methods.

Flexible, logically organized reports make documentation of your work a pleasure. You may select reports in summary or extended form, in any order you wish. The Input Data Summary gives you an exact record of program input including all your analysis decisions. Never again wonder how you obtained a particular result or have difficulty repeating program runs.

All GSI programs are supplied with a User's Manual that explains every aspect of installation and operation of each program. Program capabilities are fully described and tutorial examples are provided to guide you through a program's operation. Each User's Manual includes an extensive theoretical section which explains the basis of all analyses performed.

GSI programs are the friendliest, most powerful gear design and analysis software you can buy.

AGMA218

Introduced in 1984, AGMA218 is rapidly becoming the industry standard program for rating spur and helical gearing. It rates gears exactly as intended by the American Gear Manufacturers Association Standard:

"AGMA STANDARD For Rating the Pitting Resistance and Bending Strength of Spur and Helical Involute Gear Teeth, AGMA 218.01, Dec 1982".

This is the AGMA's most up-to-date standard for rating parallel-axis gearsets. As this standard is updated by the AGMA, GSI revises AGMA218 to keep it current with the latest technological advances. With AGMA218, you can rate a gearset in a few minutes rather than spend hours with frustrating, error-prone hand calculations.

AGMA218 performs two basic types of analyses:

Life Rating — given the transmitted power and pinion speed, the pitting life and bending fatigue lives are calculated for a single load and speed, or for an entire spectrum of loads with the resultant life determined from Miner's Rule.

Power Rating — given the pinion speed and a required design life, the allowable transmitted power based on gear tooth pitting and bending fatigue are calculated for both the pinion and gear. The allowable power rating of the gearset is the minimum of the four power capacities.

AGMA218 is integrated with and automatically transfers common data to SCORING+.

AGMA218 features include:

- Analyzes all materials and heat-treatments covered in the AGMA Standard 218.01
- Considers effects of addendum modification, tooth thinning for backlash, stock allowance for finishing and complete tool geometry
- Calculates full gear geometry including I and J factors, loads, derating factors, strengths, stresses and life or power ratings
- Uses Miner's Rule to analyze up to 50 discrete loads with an on-line data base for storing up to 100 load arrays
- Calculates the dynamic factor and load distribution factor if not input by the user
- Considers number of contacts per revolution and uni-directional or reverse bending loads
- Output includes screen, hard-copy or disc reports

SCORING+

SCORING+ performs a complete analysis of the tribology of spur and helical gears. It considers all the known parameters which control the pitting, scoring (scuffing) and wear of gear teeth. SCORING+ gives you the analytical power you need to make important decisions concerning gear geometry, tooth modification, surface roughness, and lubricant and material properties. You can integrate SCORING+ with our program AGMA218 (pitting and bending fatigue lives) and have a complete set of tools for analyzing all the common gear failure modes.

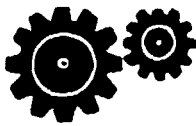
SCORING+ calculates the EHD film thickness using the Dowson and Higginson equation and the flash temperature using Blok's critical temperature theory. The specific film thickness helps you determine whether the gearset is operating in the full or partial EHD regime or is boundary lubricated, and gives you the data you need to assess the probability of wear-related distress. The flash temperature is your best criterion for predicting the probability of scoring (scuffing).

SCORING+ performs a complete kinematic analysis of the gear tooth velocities so you can quickly see how changes in pitch or addendum modification affect specific sliding ratios, and approach versus recess action. The Hertzian contact stress is calculated at each point of contact so you can see exactly where the maximum stress occurs. SCORING+ provides graphical plots of EHD film thickness, flash temperature, specific sliding and Hertzian stress. This is an extremely useful capability, allowing you to instantly review the results of a SCORING+ analysis.

SCORING+ features include:

- Calculates EHD film thickness and probability of wear
- Calculates flash temperature and probability of scoring
- Calculates rolling, sliding and entraining velocities, and specific sliding (slide/roll) ratios
- Calculates Hertzian contact stress
- Provides options for constant or variable coefficient of friction
- Provides single-key entry of default values for tool geometry and MIL-L-7808 lubricant
- Provides complete gear geometry calculation, audit and report
- Provides screen or hard-copy plots of EHD film thickness, flash temperature, specific sliding and Hertzian stress
- Output includes screen, hard-copy or disk reports

APPENDIX B



- 242 -
Price List for Gear Software

(Revised May 1988)

Universal Technical Systems, Inc.
1220 Rock Street, Rockford, IL 61101
Phone: (815) 963-2220, 800-435-7887

Program	Description	Price \$
#500	This Spur and Helical Gear Analysis Software Program uses an Expert Systems approach to design gear tooth profile and the cutting edge geometry of the tooling. (You need to purchase Option 1,2, or 3 before any of the other options can be added.)	
	Option	
1	Optimum tooth profile and tooling design when gears are hobbed	1950
2	Optimum tooth profile and tooling design when gears are shaped	1950
3	Combination of options 1 and 2	3150
4	Analysis of tooth profile when gears are shaved. This option also includes the design of shaving cutter	700
5	Specific sliding ratios (includes calculation and plotting)	500
6	Profile modification using Tip relief, topping, or semi topping hobs	1500
7	J-Factor balancing (balances strength of gear and pinion)	1700
8	Root fillet Grinding (includes design of grinding wheel)	1500
34	Almen - Straub stress factor calculation	700
40	UTS Data file Access This option is used to connect output of UTS Gear Analysis programs to other programs such as CAD/CAM, tooling database, etc.	500
50	Integrated Tooling Database This option is used to design a cutting tool, automatically search for the closest tool available in your database and re-run program 500 with the new data.	1500
#540	Load Rating of Gear Sets Using AGMA Standard 218.01 (see program numbers 60-5401, 5402, 5405 for other load rating programs)	1200
#550	Load Rating of Gear Sets Using AGMA Standards 210.02, 211.02, 220.02, 420.04, 421.06	700
#580	Minimum Weight Gearbox Design	1500

Computer System Requirement

IBM-PC family (PC, XT, AT, PS/2) or a 100% compatible with the following configuration:

- PC DOS 2.1 or Higher
- minimum memory 640K RAM
- one floppy and one hard drive
- color monitor with graphics card preferred
- HP series plotter with RS232C interface (optional for program #500)

Versions for HP 200 and 300 series are also available, please call for details.

All prices subject to change without notice